

CARBON-HETEROATOM REDUCTIVE ELIMINATION AND CATALYSIS
UTILIZING (POCOP)RH AND (POCOP)CO COMPLEXES

A Dissertation

by

SAMUEL DAVID TIMPA

Submitted to the Office of Graduate and Professional Studies of
Texas A&M University
in partial fulfillment of the requirements for the degree of

DOCTOR OF PHILOSOPHY

| | |
|---------------------|-------------------------|
| Chair of Committee, | Oleg V. Ozerov |
| Committee Members, | Michael B. Hall |
| | Marcetta Y. Darensbourg |
| | Samuel F. Noynaert |
| Head of Department, | David H. Russell |

August 2014

Major Subject: Chemistry

Copyright 2014 Samuel David Timpa

ABSTRACT

Transition metal catalyzed cross-coupling reactions of aryl halides have revolutionized the synthesis of organic molecules. These reactions, which are commonly catalyzed by group 10 metals, have found applications including natural product synthesis, pharmaceuticals, and agrochemicals. Pd catalyzed cross-coupling reactions have undergone the greatest development due to their wide applicability, high efficiency, and selectivity. The success of Pd is attributed to its ability to readily traverse between Pd(0) and Pd(II) oxidation states, which is essential to the mechanistic steps oxidative addition and reductive elimination.

The utility of transition metals outside of group 10 has largely been limited to Cu, but more recently several examples of Rh catalyzed cross-coupling reactions have been described. These examples propose a Rh(I)/Rh(III) cycle analogous to the Pd(0)/Pd(II) catalytic cycle involving aryl halide oxidative addition, transmetallation, and product forming reductive elimination; however, there has been little experimental evidence to support these claims. Examples of aryl halide oxidative addition to Rh(I) have been reported, but examples of reductive elimination from Rh(III) are less prevalent.

Pincer ligands, tridentate ligands that typically coordinate in a meridional fashion, provide an excellent scaffold for the examination of both oxidative addition and reductive elimination at Rh due to their ability to access to three-coordinate Rh(I) and stable five-coordinate Rh(III) complexes. The ability of the (PNP)Rh center to undergo

each of the stoichiometric reactions of catalytic C-C coupling reactions, including aryl halide oxidative addition and C-C reductive elimination, has been established.

This dissertation describes the ability of the (POCOP)Rh system to catalytically form C-C as well as C-N and C-S bonds. Several proposed catalytic intermediates have been isolated and their reactivity examined to gain insight into the mechanism of these catalytic transformations. C-N and C-S reductive elimination from Rh(III) have been closely examined, with results providing insight to their respective steric and electronic properties. In addition, the potential for (POCOP)Rh systems to undergo C-F reductive elimination were also examined both theoretically and experimentally. Finally, early investigations into the synthesis of (POCOP)Co complexes will be described, with an emphasis on demonstrating the aptitude for this system to experience concerted reductive elimination. Numerous (POCOP)Co complexes were isolated and characterized, including Co(II) and stable Co(III) compounds.

DEDICATION

*For my parents,
for everything you taught me*

ACKNOWLEDGEMENTS

I would like to thank my committee chair and research advisor, Prof. Oleg Ozerov for his guidance over the past five years and also during my summer research at Brandeis University in 2008. I appreciate his time and direction in my development to become a successful chemist. I would also like to thank my committee members, Prof. Michael Hall, Prof. Marcetta Darensbourg, and Prof. Samuel Noynaert.

Thanks also to the Ozerov research group members, both during my time at Brandeis University and at Texas A&M. I would particularly like to acknowledge Dr. Yanjun Zhu, who served as my mentor since my time at Brandeis. Her excitement about chemistry and dedication to research provided an excellent model that helped me realize the chemist that I hoped to become. I would also like to thank Jillian Davidson, Chun-I Lee, and Jessica DeMott for their constant entertainment and willingness to discuss topics not always related to chemistry. In addition, thanks to all of the Ozerov group members I had the experience to work with: Dr. Claudia Fafard, Dr. Weixing Gu, Dr. Deborah Bacciu, Dr. Dan Smith, Dr. David Herbert, Dr. Jia Zhou, Dr. Morgan MacInnis, Dr. Rafael Huacuja, Dr. Laura Gerber, Dan Graham, Rodrigo Ramirez, Billy McCulloch, Loren Press, Chandra Mouli Palit, Christopher Pell, and Wei-Chun Shih.

Finally, thanks to my parents and my sister for their encouragement and support from day one. I could not have done this without you.

NOMENCLATURE

| | |
|----------------------------------|--|
| OA | oxidative addition |
| RE | reductive elimination |
| ⁱ Pr | <i>iso</i> -propyl |
| ^t Bu | <i>tert</i> -butyl |
| dppf | bis(diphenylphosphino)ferrocene |
| tolyl | C ₆ H ₄ Me |
| PFc ^t Bu ₂ | ferrocenyl-di- <i>tert</i> -butylphosphine |
| NHC | N-heterocyclic carbene |
| COE | cyclooctene |
| COD | cyclooctadiene |
| dppp | bis(diphenylphosphino)propane |
| ⁱ Bu | <i>iso</i> -butyl |
| ⁿ Pr | <i>n</i> -propyl |
| TBE | <i>tert</i> -butylethylene |
| S ⁱ Pr ₂ | diisopropylsulfide |
| Ph | phenyl |
| Ar | aryl |
| py | pyridine |
| NCMe | acetonitrile |
| OAc | acetate |

| | |
|------------------|------------------------------|
| L | ligand |
| BHE | β -hydride elimination |
| THF | tetrahydrofuran |
| OEt ₂ | diethylether |
| DMAP | dimethylaminopyridine |
| NCS | N-chlorosuccinimide |
| OPiv | pivalate |
| solv | solvent |

TABLE OF CONTENTS

| | Page |
|---|------|
| ABSTRACT | ii |
| DEDICATION | iv |
| ACKNOWLEDGEMENTS | v |
| NOMENCLATURE | vi |
| TABLE OF CONTENTS | viii |
| LIST OF FIGURES | xi |
| LIST OF SCHEMES | xvii |
| LIST OF TABLES | xxi |
| CHAPTER I INTRODUCTION AND LITERATURE REVIEW | 1 |
| 1.1 Introduction | 1 |
| 1.2 Mechanism of Pd Catalyzed Cross-Coupling Reactions..... | 5 |
| 1.3 Rhodium Catalyzed Cross-Coupling Reactions..... | 10 |
| 1.4 Mechanism of Rh Catalyzed Cross-Coupling Reactions | 13 |
| 1.5 Utility of Pincer Ligands for Examination of OA and RE at Rh | 16 |
| CHAPTER II CATALYSIS OF KUMADA-TAMAO-CORRIU COUPLING BY A (POCOP)RH PINCER COMPLEX | 22 |
| 2.1 Introduction | 22 |
| 2.2 Results and Discussion..... | 24 |
| 2.2.1 Synthesis of (POCOP)Rh(H)(Cl) | 24 |
| 2.2.1.1 Determination of Reaction Impurities from Direct Synthesis..... | 26 |
| 2.2.2 Catalysis | 30 |
| 2.2.2.1 Role of Impurities in Catalysis..... | 33 |
| 2.2.3 Isolation of (POCOP)Rh(Ar)(X) | 34 |
| 2.3 Conclusion..... | 35 |
| 2.4 Experimental | 36 |
| 2.4.1 General Considerations | 36 |
| 2.4.2 Stoichiometric Reactions..... | 37 |
| 2.4.3 Catalytic Reactions..... | 43 |
| 2.4.4 X-ray Crystallography | 50 |

| | |
|---|-----|
| CHAPTER III THE FATE OF ARYL/AMIDO COMPLEXES OF RH(III) SUPPORTED BY A POCOP PINCER LIGAND: C-N REDUCTIVE ELIMINATION AND BETA-HYDROGEN ELIMINATION | 53 |
| 3.1 Introduction | 53 |
| 3.2 Results and Discussion..... | 55 |
| 3.2.1 Synthesis of (POCOP)Rh(Ar)(anilido) Complexes | 55 |
| 3.2.2 Reactivity of Alkyl Amines..... | 59 |
| 3.2.3 Concerted C-N Reductive Elimination..... | 63 |
| 3.2.4 Catalytic C-N Coupling with (POCOP)Rh(H)(Cl) | 67 |
| 3.3 Conclusion..... | 69 |
| 3.4 Experimental | 69 |
| 3.4.1 General Considerations | 69 |
| 3.4.2 Stoichiometric Reactions..... | 70 |
| 3.4.3 Kinetic Studies | 86 |
| 3.4.4 Catalytic Reactions..... | 89 |
| 3.4.5 X-ray Crystallography | 93 |
| CHAPTER IV A WELL DEFINED (POCOP)RH CATALYST FOR THE COUPLING OF ARYL HALIDES WITH THIOLS | 95 |
| 4.1 Introduction | 95 |
| 4.2 Results and Discussion..... | 97 |
| 4.2.1 Catalytic C-S Coupling | 97 |
| 4.2.1.1 Catalyst Screening..... | 97 |
| 4.2.1.2 Scope of C-S Coupling..... | 100 |
| 4.2.2 Synthesis of Intermediates..... | 103 |
| 4.2.3 Mechanism | 105 |
| 4.2.4 Additional Reactivity | 112 |
| 4.3 Conclusion..... | 115 |
| 4.4 Experimental | 116 |
| 4.4.1 General Considerations | 116 |
| 4.4.2 Isolated Compounds and Stoichiometric Reactions..... | 116 |
| 4.4.3 Catalytic Reactions..... | 132 |
| 4.4.3.1 Examination of Various Catalysts..... | 132 |
| 4.4.3.2 Solvent Optimization..... | 133 |
| 4.4.3.3 Base Optimization | 134 |
| 4.4.3.4 General Procedure for Catalytic C-S Coupling Reactions | 135 |
| 4.4.3.5 Maximizing the Turnover Number | 138 |
| 4.4.3.6 Effect of Excess Aryl Halide on Catalysis | 139 |
| 4.4.4 X-ray Crystallography | 139 |
| CHAPTER V TOWARDS CARBON-FLUORINE REDUCTIVE ELIMINATION WITH PINCER RHODIUM: A THEORETICAL AND EXPERIMENTAL STUDY | 143 |

| | |
|--|-----|
| 5.1 Introduction | 143 |
| 5.2 Results and Discussion..... | 146 |
| 5.2.1 Theoretical Analysis..... | 146 |
| 5.2.2 Synthesis of Model Compounds..... | 149 |
| 5.2.2.1 Attempted Synthesis of (POCOP)Rh(CHCH ₂)(X) Compounds | 149 |
| 5.2.2.2 Synthesis of (^t BuPOCOP)Rh Complexes. | 151 |
| 5.2.3 Attempted C-O Bond Formation..... | 153 |
| 5.3 Conclusion..... | 155 |
| 5.4 Experimental | 156 |
| 5.4.1 General Considerations | 156 |
| 5.4.2 Synthesis and Reactivity of Model Compounds | 156 |
| 5.4.3 X-ray Crystallography | 170 |
| CHAPTER VI SYNTHESIS AND REACTIVITY OF (POCOP)CO COMPLEXES .. | 174 |
| 6.1 Introduction..... | 174 |
| 6.2 Results and Discussion..... | 178 |
| 6.2.1 Synthesis of (POCOP)Co ^{II} Complexes | 178 |
| 6.2.1.1 Synthesis of (POCOP)Co(X) (X = halide) Compounds..... | 178 |
| 6.2.1.2 Synthesis of (POCOP)Co(R) Compounds | 181 |
| 6.2.1.3 Attempts towards (POCOP)Co(H)..... | 183 |
| 6.2.2 Synthesis of (POCOP)Co ^{III} Compounds | 186 |
| 6.2.3 Towards (POCOP)Co(R)(R') Complexes..... | 190 |
| 6.3 Conclusion..... | 191 |
| 6.4 Experimental | 191 |
| 6.4.1 General Considerations | 191 |
| 6.4.2 Synthesis of (POCOP)Co Complexes | 192 |
| 6.4.3 X-Ray Crystallography..... | 216 |
| CHAPTER VII SUMMARY | 218 |
| REFERENCES..... | 221 |
| APPENDIX A X-RAY STRUCTURES SUBMITTED TO CAMBRIDGE CRYSTALLOGRAPHIC DATA CENTER | 233 |

LIST OF FIGURES

| | Page |
|---|------|
| Figure 1-1. Successful ligand scaffolds for Pd catalyzed cross-coupling reactions..... | 10 |
| Figure 1-2. Common pincer ligand frameworks. | 17 |
| Figure 2-1. ORTEP drawing (50% thermal ellipsoids) of (POCOP)Rh(H)(Cl) (205). ⁸⁴ Selected atom labeling. Hydrogen atoms are omitted for clarity except for Rh-H. Selected bond distances (Å) and angles (deg): Rh1-P1, 2.2786(8); Rh1-C1, 2.3840(9); Rh1-C11, 1.987(2); Rh1-H1, 1.51(2); P1-Rh1-P2, 160.59(2); C1-Rh1-C11, 168.97(5); C1-Rh1-H1, 75.2(9). | 25 |
| Figure 2-2. ³¹ P{ ¹ H} NMR spectra of selected complexes collected in C ₆ D ₆ . (a) Synthesis of (POCOP)Rh(H)(Cl) (205) by a direct route. Small resonance at 157.9 ppm not shown. (b) Reaction of 205 with 0.60 eq. of 204 at RT. The singlet resonance representing the uncoordinated phosphine at 151.8 ppm is not shown. (c) Reaction of 205 with 0.53 eq. of 204 after thermolysis at 125 °C. (d) Reaction of 205 with 1.0 eq. of PhOP ⁱ Pr ₂ at RT. (e) Reaction of 205 with 1.0 eq. of PhOP ⁱ Pr ₂ after thermolysis at 125 °C. | 29 |
| Figure 2-3. ² H NMR spectra of deuterium exchange reactions. (collected in 1,4-dioxane) (a) Exchange of 205 with D ₂ O to give (POCOP)Rh(D)(Cl) (215). (b) 0.53 eq of 204 added to 215 to give 216. (c) After overnight thermolysis of 215 at 115 °C to give 216. | 30 |
| Figure 2-4. ORTEP drawing (50% thermal ellipsoids) of (POCOP)Rh(Ph)(I) (221). ⁸⁴ Selected atom labeling. Hydrogen atoms are omitted for clarity. Selected bond distances (Å) and angles (deg): Rh1-P1, 2.341(3); Rh1-P2, 2.334(3); Rh1-C6, 2.037(9); Rh1-C7, 2.072(8); Rh1-I1, 2.792(2); P1-Rh1-P2, 159.33(10); C6-Rh1-I1, 159.8(2); C6-Rh1-C7, 87.1(4). | 35 |
| Figure 3-1. ORTEP drawing (50% probability ellipsoids) of (POCOP)Rh(<i>p</i> -C ₆ H ₄ F)(NHPH) (305). ⁸⁴ Shown with selected atom labeling. Hydrogen atoms are omitted with the exception of the NH. Selected bond distances (Å) and angles (deg) for 305 follow: Rh1-P1, 2.3218(6); Rh1-P2, 2.2891(6); Rh1-C1, 2.019(2); Rh1-C7, 2.012(2); Rh1-N1, 2.076(2); P1-Rh1-P2, 157.79(2); C1-Rh1-N1, 162.38(7); Rh1-N1-C13, 135.3(1). | 59 |
| Figure 3-2. ORTEP drawings (50% probability ellipsoids) of (POCOP)Rh(NPh(CH ₂)) (308). ⁸⁴ Shown with selected atom labeling. Hydrogen atoms are omitted with the exception of the CH ₂ . Selected bond distances (Å) and angles (deg) for 308 follow: Rh1-P1, 2.245(1); | |

| | |
|---|----|
| Rh1-N1, 2.166(3); Rh1-C8, 1.993(3); N1-C1, 1.272(3); N1-C2, 1.440(3); P1-Rh1-P2, 158.40(2); C8-Rh1-N1, 176.13(9); C1-N1-C2, 119.9(2)..... | 61 |
| Figure 3-3. Calculated reaction coordinate diagram (Gibbs free energy, B3LYP, <i>MO6</i>) for the formation of 308. | 62 |
| Figure 3-4. Calculated reaction coordinate diagram (Gibbs free energy, B3LYP, <i>MO6</i>) for the formation of 309. | 63 |
| Figure 3-5. Plot of ln[304] vs. time for C-N RE from 304 in the presence of <i>p</i> - CF ₃ C ₆ H ₄ Br in various concentrations..... | 65 |
| Figure 3-6. Calculated reaction barrier for C-N RE from 304 at 103 °C. All of the geometries were fully optimized in toluene solvent <i>via</i> the PCM ¹⁰⁷ model at the M06 ¹⁰⁸ level of theory. Overlay of the calculated ground-state structure of 304 (gray) and the transition state (red) showing the aryl rotation that occurs prior to RE. | 66 |
| Figure 3-7. Left; Eyring plot for C-N RE from 304 in the 65 – 105 °C temperature range. Right; Plot of ln[304] vs. time for C-N reductive elimination from 304 in the 65 – 105 °C temperature range. | 67 |
| Figure 3-8. ¹ H NMR spectrum of (POCOP)Rh(<i>p</i> -C ₆ H ₄ CF ₃)(Br) (301) in C ₆ D ₆ . Minor residual pentane present..... | 71 |
| Figure 3-9. ¹ H NMR spectrum of (POCOP)Rh(<i>p</i> -C ₆ H ₄ CF ₃)(Cl) (302) in C ₆ D ₆ . Minor residual pentane present..... | 73 |
| Figure 3-10. ¹ H NMR spectrum of (POCOP)Rh(<i>p</i> -C ₆ H ₄ F)(Br) (303) in C ₆ D ₆ . Minor residual pentane and toluene present. | 74 |
| Figure 3-11. ¹ H NMR spectrum of (POCOP)Rh(<i>p</i> -C ₆ H ₄ CF ₃)(<i>p</i> -NH(C ₆ H ₄ Me)) (304) in C ₆ D ₆ . Minor residual pentane present..... | 76 |
| Figure 3-12. ¹ H NMR spectrum of (POCOP)Rh(<i>p</i> -C ₆ H ₄ F)(NPh) (305) in C ₆ D ₆ . Minor residual pentane present..... | 78 |
| Figure 3-13. ¹ H NMR spectrum of (POCOP)Rh(<i>p</i> -C ₆ H ₄ CF ₃)(O(CH ₃) ₃) (306) in C ₆ D ₆ . Resonances corresponding to <i>p</i> -C ₆ H ₄ CF ₃ protons are broad in the baseline. | 80 |
| Figure 3-14. ¹ H NMR spectrum of (POCOP)Rh(<i>p</i> -C ₆ H ₄ F)(NPh ₂) (307) in C ₆ D ₆ . Minor residual pentane and toluene present. Also, minor residual NaO ^t Bu (1.34 ppm) present. | 82 |

| | |
|---|-----|
| Figure 3-15. ^1H NMR spectrum of (POCOP)Rh(N(Ph)CH ₂) (308) in C ₆ D ₆ . Minor residual pentane present..... | 84 |
| Figure 3-16. ^1H NMR spectrum of (POCOP)Rh(C ₄ H ₇ N) (309) in C ₆ D ₆ | 86 |
| Figure 4-1. Scope of C-S coupling with (POCOP)Rh(H)(Cl) 205. | 101 |
| Figure 4-2. ORTEP drawings (50% probability ellipsoids) of (POCOP)Rh(Ph)(SPh) (406) (left) and (POCOP)Rh(SPh) ₂ (407) (right). ⁸⁴ Selected atom labeling. Hydrogen atoms are omitted for clarity. Selected bond distances (Å) and angles (deg) for 406 follow: Rh1-S1, 2.366(1); S1-C1, 1.774(5); Rh1-C7, 2.3852(8), Rh1-S1-C1, 114.7(2); C13-Rh1-S1, 154.6(1); C13-Rh-C7, 87.7(1); C7-Rh1-S1, 116.2(1). Selected bond distances (Å) and angles (deg) for 407 follow: Rh1-S1, 2.3266(6); S1-C1, 1.786(2); S1-C7, 1.797(2); Rh1-S1-C1, 116.93(8); Rh1-S1-C7, 118.00(7); C13-Rh1-S1, 166.90(6); C1-S1-C7, 99.8(1). | 105 |
| Figure 4-3. ORTEP drawings (50% probability ellipsoids) of (POCOP)Rh(H)(Ph)(SPh) (418) and (POCOP)Rh(NaSPH) (421). ⁸⁴ Selected atom labeling. Hydrogen atoms are omitted for clarity. Selected bond distances (Å) and angles (deg) for 418 follow: Rh1-S1, 2.323(3); S1-C1, 1.78(1); Rh1-S1-C1, 113.8(8), C7-Rh1-S1, 157.7(3). Selected bond distances (Å) and angles (deg) for 421 follow: Rh1-S1, 2.3852(8); S1-C1, 1.790(3); S1-Na1, 2.751(2); Rh1-S1-C1, 112.60(8); Rh1-S1-Na1, 132.70(4); Na1-S1-C1, 87.59(8); C7-Rh1-S1, 174.45(7)(3). The extended crystal packing of 421 (bottom) showing selected atom labelling. Hydrogen atoms and isopropyl methyl groups are omitted for clarity. The extended crystal packing structure of 421 shows sodium interactions with sulfur (Na-S, 2.751(2) Å), neighboring rhodium centers (Na---Rh, 2.8958(13) Å), and the chelating aryl-carbon of the pincer framework (Na---C, 2.881(3) Å). | 114 |
| Figure 4-4. $^{31}\text{P}\{^1\text{H}\}$ NMR spectra for the thermolysis of 406 in the presence of C ₆ H ₅ Br in C ₆ D ₆ | 122 |
| Figure 4-5. $^{31}\text{P}\{^1\text{H}\}$ NMR spectra for the thermolysis of 406 in the presence of C ₆ H ₅ Cl in C ₆ D ₆ | 123 |
| Figure 4-6. $^{31}\text{P}\{^1\text{H}\}$ NMR spectra in C ₆ D ₆ for the thermolysis of 407 in the presence of <i>o</i> -MeC ₆ H ₄ Br. | 127 |
| Figure 4-7. $^{31}\text{P}\{^1\text{H}\}$ NMR spectra for the thermolysis of 418 in d ₈ -toluene. The presence of [(POCOP)Rh(H)(SPh)] ₂ (420) is indicated by the new doublet formed starting at -60 °C. | 129 |

| | |
|---|-----|
| Figure 4-8. ^1H NMR spectra for the thermolysis of 418 in d_8 -toluene. The methine resonance for 418 begins to split at $-40\text{ }^\circ\text{C}$ and two new methine resonances occur for $[(\text{POCOP})\text{Rh}(\text{H})(\text{SPh})]_2$ (420) at $-60\text{ }^\circ\text{C}$. The resonances corresponding to 418 are marked with red (*) and the resonances corresponding to 420 are marked with blue (*) in the spectrum at $-80\text{ }^\circ\text{C}$. | 130 |
| Figure 4-9. Hydride region of the ^1H NMR spectra for the thermolysis of 418 in d_8 -toluene. The hydride for $[(\text{POCOP})\text{Rh}(\text{H})(\text{SPh})]_2$ (420) occurs at -16.9 ppm beginning at $-40\text{ }^\circ\text{C}$. The downfield hydride chemical shift indicates the hydride is not trans to an open coordination site. | 131 |
| Figure 5-1. Potential energy surface of C(vinyl)-F RE and C(vinyl)-C(aryl) RE from $(\text{POCOP})\text{Rh}(\text{CHCH}_2)(\text{F})$ (502). | 149 |
| Figure 5-2. X-ray crystal structure of 513 and 515. | 155 |
| Figure 5-3. ^1H NMR spectrum of 506 in CD_2Cl_2 . Minor residual pentane and toluene present. | 158 |
| Figure 5-4. ^1H NMR spectrum of $(^t\text{BuPOCOP})\text{H}$ (507) in C_6D_6 . | 159 |
| Figure 5-5. ^1H NMR spectrum of $(^t\text{BuPOCOP})\text{Rh}(\text{H})(\text{Cl})$ (508) in C_6D_6 . | 161 |
| Figure 5-6. ^1H NMR spectrum of $(^t\text{BuPOCOP})\text{Rh}(\text{S}^i\text{Pr}_2)$ (509) in C_6D_6 . Minor residual NaO^tBu present. | 162 |
| Figure 5-7. ^1H NMR spectrum of $(^t\text{BuPOCOP})\text{Rh}(\text{CHCH}_2)(\text{I})$ (510) in C_6D_6 . | 163 |
| Figure 5-8. ^1H NMR spectrum of $(^t\text{BuPOCOP})\text{Rh}(\text{CHCH}_2)(\text{OTf})$ (511) in C_6D_6 . Minor residual pentane present. | 165 |
| Figure 5-9. ^1H NMR spectrum of $(^t\text{BuPOCOP})\text{Rh}(\text{CHCH}_2)(\text{O}^t\text{Bu})$ (513) in C_6D_6 . Minor residual pentane present. | 167 |
| Figure 5-10. ^1H NMR spectrum of $(^t\text{BuPOCOP})\text{Rh}(\text{CHCH}_2)(p\text{-OC}_6\text{H}_4\text{F})$ (514) in C_6D_6 . Minor residual pentane present. | 169 |
| Figure 6-1. Examples of isolated five-coordinate Co(III) complexes. | 178 |
| Figure 6-2. ^1H NMR spectrum of $(\text{POCOP})\text{Co}(\text{Cl})$ (602), $(\text{POCOP})\text{Co}(\text{Br})$ (603), $(\text{POCOP})\text{Co}(\text{I})$ (604), and $(\text{POCOP})\text{Co}(\text{OTf})$ (605). The values below the spectra correspond to the peak integration. | 180 |
| Figure 6-3. ORTEP drawing (50% probability ellipsoids) of $(\text{POCOP})\text{Co}(\text{BH}_4)$ (616). ⁸⁴ Select atom labeling. Hydrogen atoms are omitted for clarity | |

| | |
|--|-----|
| with the exception of B-H hydrogen atoms. Selected bond distances (Å) and angles (deg) for 616 follow: Co1-H1, 1.70(3); Co1-H2, 1.57(2); Co1-C1, 1.922(2), C1-Co1-H1, 133.9(9); C1-Co1-H2, 157.7(9); P1-Co1-P2, 162.30(3). | 185 |
| Figure 6-4. ¹ H NMR spectrum of (POCOP)CoCl (602) in C ₆ D ₆ . Minor residual pentane present. | 193 |
| Figure 6-5. ¹ H NMR spectrum of (POCOP)Co(Br) (603) in C ₆ D ₆ . Minor residual pentane present. | 194 |
| Figure 6-6. ¹ H NMR spectrum of (POCOP)Co(I) (604) in C ₆ D ₆ . Minor residual pentane and Me ₃ SiI present. | 195 |
| Figure 6-7. ¹ H NMR spectrum of (POCOP)Co(OTf) (605) in C ₆ D ₆ . Minor residual pentane present. | 196 |
| Figure 6-8. ¹ H NMR spectrum of (POCOP)Co(F) (606) in C ₆ D ₆ . Minor residual pentane and grease present. | 197 |
| Figure 6-9. ¹ H NMR of (POCOP)Co(Ph) (607) in C ₆ D ₆ . Minor residual pentane, toluene, and grease present. | 198 |
| Figure 6-10. ¹ H NMR spectrum of (POCOP)Co(CH ₂ Ph) (608) in C ₆ D ₆ . Minor residual pentane present. | 199 |
| Figure 6-11. ¹ H NMR spectrum of (POCOP)Co(CCH) (609) in C ₆ D ₆ . Minor impurities including pentane and toluene present. | 200 |
| Figure 6-12. ¹ H NMR spectrum of isolated green solid from the reaction between 602 with excess (CH ₂ CH)MgCl in C ₆ D ₆ | 202 |
| Figure 6-13. ¹ H NMR spectrum of (POCOP)Co(CO) (610) in C ₆ D ₆ . Non-integrated signals between 4.8 and 6.3 ppm correspond to free 1,3-butadiene. | 203 |
| Figure 6-14. ¹ H NMR spectrum of (POCOP)Co(CF ₃) (613) in C ₆ D ₆ | 204 |
| Figure 6-15. ¹ H NMR spectrum of (POCOP)Co(O ^t Bu) (611) in C ₆ D ₆ . Minor residual pentane present. | 205 |
| Figure 6-16. ¹ H NMR spectrum of (POCOP)Co(NHPh) (612) in C ₆ D ₆ . Minor residual pentane and toluene present. | 206 |
| Figure 6-17. ¹ H NMR spectrum of (POCOP)Co(O ⁱ Pr) (615) in C ₆ D ₆ . Minor residual pentane present. | 207 |

| | |
|---|-----|
| Figure 6-18. ^1H NMR spectrum of $(\text{POCOP})\text{Co}(\text{Cl})_2$ (618) in C_6D_6 . Minor residual pentane and toluene present. | 209 |
| Figure 6-19. ^1H NMR of $(\text{POCOP})\text{Co}(\text{Cl})_2(\text{PMe}_3)$ (619) in C_6D_6 . Minor residual pentane and toluene present. | 210 |
| Figure 6-20. ^1H NMR spectrum of $(\text{POCOP})\text{Co}(\text{Ph})(\text{Cl})$ (620) in C_6D_6 . Large amount of residual pentane present. | 212 |
| Figure 6-21. ^1H NMR spectrum of $(\text{POCOP})\text{Co}(\text{Ph})(\text{OAc})$ (621) in C_6D_6 . Minor residual pentane and toluene present. | 213 |
| Figure 6-22. ^1H NMR spectrum of $(\text{POCOP})\text{Co}(\text{CF}_3)(\text{Cl})$ (622) in C_6D_6 | 214 |
| Figure 6-23. ^1H NMR spectrum of $(\text{POCOP})\text{Co}(\text{CF}_3)(\text{OTf})$ (623) in C_6D_6 . Minor residual pentane and toluene present. | 215 |

LIST OF SCHEMES

| | Page |
|--|------|
| Scheme 1-1. Examples of Pd catalyzed C-C cross-coupling reactions. | 3 |
| Scheme 1-2. Examples of Pd catalyzed C-heteroatom cross-coupling reactions. | 5 |
| Scheme 1-3. General cycles for Pd catalyzed cross-coupling. (a) Catalytic cycle for Pd catalyzed C-C and C-heteroatom coupling. (b) Catalytic cycle for Pd catalyzed Heck coupling. | 6 |
| Scheme 1-4. General reaction scheme for oxidative addition (OA) and reductive elimination (RE). | 7 |
| Scheme 1-5. Comparison of monodentate and bidentate phosphine ligands for Pd catalyzed cross-coupling. | 8 |
| Scheme 1-6. Pd catalyzed Suzuki coupling with aryl chlorides. | 8 |
| Scheme 1-7. Rh catalyzed C-C cross-coupling reactions. (a) Rh catalyzed Suzuki type coupling reaction. (b) Rh catalyzed Heck type coupling reaction. | 11 |
| Scheme 1-8. Rh catalyzed C-C bond forming reactions involving the direct functionalization of C-H bonds. | 12 |
| Scheme 1-9. Catalytic C-heteroatom cross-coupling with Rh. | 13 |
| Scheme 1-10. Rh catalyzed arylation of indoles with aryl iodides. | 14 |
| Scheme 1-11. Examples of OA to Rh(I). | 15 |
| Scheme 1-12. Comparison of frontier orbitals interactions for RE from six- and five-coordinate Rh. *Figure adapted from J. F. Hartwig, <i>Organotransition Metal Chemistry: From Bonding to Catalysis</i> ; University Science Books: Sausalito, 2009; Ch. 8. | 16 |
| Scheme 1-13. Oxidative addition reactions involving (pincer)Rh. | 18 |
| Scheme 1-14. Aryl halide OA to (PNP)Rh. (a) OA to (PNP)Rh ^I stabilized by weakly coordinating bulky dative ligands. (b) OA competition experiment between PhBr and PhCl. | 19 |
| Scheme 1-15. C-C RE from (PNP)Rh(Ph) ₂ | 20 |

| | |
|---|-----|
| Scheme 1-16. Comparison of ground states structure between d^6 Rh and d^8 Pd complexes prior to RE. | 21 |
| Scheme 2-1. C-C reductive elimination (RE) from (PNP)Rh center. | 23 |
| Scheme 2-2. Direct and indirect routes to the synthesis of (POCOP)Rh(H)(Cl) (205). | 25 |
| Scheme 2-3. Synthesis of (POCOP)Rh(H)(Cl) (205) via (POCOP)Rh(H)(OAc) (208). | 26 |
| Scheme 2-4. Independent synthesis of compounds 209 – 217. | 28 |
| Scheme 2-5. Net reaction and proposed mechanism for Rh-catalyzed C–C coupling. | 31 |
| Scheme 2-6. Synthesis of (POCOP)Rh(Ar)(I). | 35 |
| Scheme 3-1. General Pd(0)/Pd(II) and Rh(I)/Rh(III) cycle for catalytic C-N coupling reactions. | 55 |
| Scheme 3-2. Synthetic pathways to (POCOP)Rh aryl/anylido complexes. | 57 |
| Scheme 3-3. Synthesis and reactivity of (POCOP)Rh(C ₆ H ₄ F)(NPh ₂) (307). | 58 |
| Scheme 3-4. Formation of (POCOP)Rh(imine) complexes with alkyl substituted amines. | 60 |
| Scheme 3-5. C-N reductive elimination from 304 in the presence of an aryl halide trap. | 64 |
| Scheme 4-1. General Pd(0)/Pd(II) and Rh(I)/Rh(III) cycle for catalytic C-S coupling reactions. | 96 |
| Scheme 4-2. (Pincer)Rh catalyst screening for C-S coupling. a. Synthesis of (^{Napt} POCOP)H 404 and (^{Napt} POCOP)Rh(H)(Cl) 403; b. Catalyst screening for the coupling of p-CF ₃ C ₆ H ₄ Br with cyclohexanethiol and HS(<i>p</i> -C ₆ H ₄ Me). | 98 |
| Scheme 4-3. Synthesis of complexes 405–411. | 103 |
| Scheme 4-4. Proposed catalytic cycle for the coupling of aryl halides with thiols using 205 as the catalyst. | 106 |
| Scheme 4-5. Rate constants for reductive coupling, thioether dissociation, and OA. ... | 107 |

| | |
|---|-----|
| Scheme 4-6. For C(aryl)-S reductive coupling to occur, the aryl group must rotate to be face-on with the thiolate substituent. Increased steric bulk raises the barrier for this rotation..... | 110 |
| Scheme 4-7. Formation of (POCOP)Rh(H)(SPh) (418) and (POCOP)Rh(NaSPh) (421)..... | 113 |
| Scheme 5-1. Mechanism for nucleophilic C-F bond formation <i>via</i> Pd(0)/Pd(II) cycle..... | 144 |
| Scheme 5-2. Calculated ΔG and ΔG^\ddagger for C-F RE from (POCOP)Rh(Ph)(F) (501) and (POCOP)Rh(CHCH ₂)(F) (502)..... | 147 |
| Scheme 5-3. Transition state rotation for C-F RE from (POCOP)Rh(Ph)(F) (501). | 148 |
| Scheme 5-4. Reactivity of vinyl iodide with (POCOP)Rh(S ⁱ Pr ₂) (505). | 150 |
| Scheme 5-5. Reactivity of (^t BuPOCOP)Rh in the direction of a rhodium vinyl fluoride complex..... | 152 |
| Scheme 5-6. Reactivity of (^t BuPOCOP)Rh(CHCH ₂)(OR) complexes..... | 154 |
| Scheme 6-1. General M ⁿ /M ⁿ⁺² for transition metal catalyzed coupling reactions between aryl halides with nucleophiles. | 174 |
| Scheme 6-2. (a) Oxidative addition of H ₂ to (PN ^{Si} P ^t Bu)Co. (b) Formation of (PN ^{Py} P)Co(H) ₂ (BPin). | 176 |
| Scheme 6-3. (a) Active core of the vitamin B12. (b) Radical elimination from (PN ^{Si} P ^{Ph})Co(R)(Cl). (c) Concerted C-C reductive elimination from (PMe ₃) ₃ Co(I)(Me) ₂ | 177 |
| Scheme 6-4. Synthesis of (POCOP)Co(X) (X = Cl, Br, I, OTf, F) complexes..... | 179 |
| Scheme 6-5. Synthesis of (POCOP)Co(R) (R = hydrocarbyl, O ^t Bu, NPh) compounds..... | 181 |
| Scheme 6-6. Synthesis of (POCOP)Co(CF ₃) (613). | 183 |
| Scheme 6-7. Attempts at synthesis of (POCOP)Co(H) (614). | 184 |
| Scheme 6-8. Synthesis of (POCOP)Co(Cl) ₂ (618) and (POCOP)Co(Cl ₂)(PMe ₃) (619). ORTEP drawing (50% probability ellipsoids) of 618. ⁸⁴ Select atom labeling. Hydrogen atoms are omitted for clarity. Selected bond distances (Å) and angles (deg) for 618 follow: Co1-Cl1, 2.285(2); Co1- | |

| | |
|--|-----|
| Cl2, 2.238(2); Co1-C1, 1.934(4), C1-Co1-C1, 110.3(1); C1-Co1-Cl2, 144.4(1); P1-Co1-P2, 159.10(3). | 187 |
| Scheme 6-9. Oxidation of (POCOP)Co(R) (R = hydrocarbyl) complexes. | 188 |
| Scheme 6-10. Synthesis of (POCOP)Co(CF ₃)(Cl) (622) and (POCOP)Co(CF ₃)(OTf) (623). | 190 |

LIST OF TABLES

| | Page |
|--|------|
| Table 1-1. Calculated activation parameters and thermodynamics parameters for C-C RE from (PCP ^{tBu})Rh(R)(R'). | 20 |
| Table 2-1. Summary of catalytic C–C coupling reactions. | 32 |
| Table 3-1. Catalytic C-N Coupling with 205. | 68 |
| Table 3-2. Rates of C-N reductive elimination for 304 from 75 °C - 105 °C and corresponding Eyring plot parameters. | 88 |
| Table 4-1. Effect of aryl halide concentration. | 108 |
| Table 4-2. Catalyst test reactions. | 133 |
| Table 4-3. Solvent optimization. | 134 |
| Table 4-4. Base optimization. | 134 |
| Table 4-5. Coupling reactions with alkyl-thiols. | 136 |
| Table 4-6. Coupling reactions with aryl-thiols. | 137 |
| Table 4-7. Optimized TON for synthesis of (<i>p</i> -FC ₆ H ₄)S(C ₆ H ₁₁). | 138 |
| Table 4-8. Optimized TON for synthesis (<i>p</i> -CF ₃ C ₆ H ₄)S(<i>p</i> -MeC ₆ H ₄). | 139 |

CHAPTER I

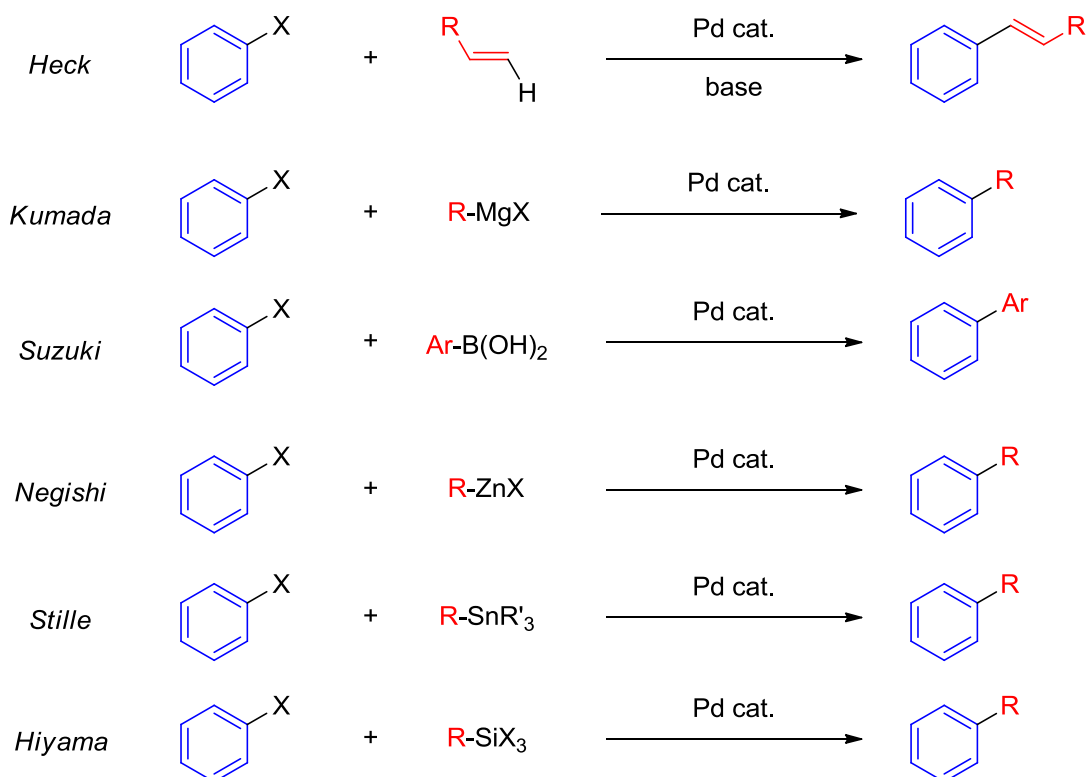
INTRODUCTION AND LITERATURE REVIEW

1.1 Introduction

Transition metal catalyzed cross-coupling reactions of aryl halides are some of the most valuable synthetic strategies available to chemists with uses spanning pharmaceuticals, agrochemicals, and new materials.^{1,2} From the initial optimization of C-C coupling reactions (Heck, Negishi, Suzuki, etc.), to the expansion including C-N (Buchwald-Hartwig), C-S, and C-O; these reactions have revolutionized the synthesis of organic molecules.³⁻⁵ The contribution of this chemistry to the scientific community has been so great that the work of Heck, Negishi, and Suzuki was acknowledged with the 2010 Nobel Prize in chemistry “for palladium-catalyzed cross-coupling in organic synthesis.”⁶ Many of these reactions are now used in the industrial production of a number of pharmaceuticals including Losartan,⁷ Singulair,⁸ and Diflunisal⁹ as well as other applications including the synthesis of liquid crystals⁵ and coatings¹⁰ for electronic materials. Even though there has been extensive development of cross-coupling reactions, there remain challenges including the direct functionalization of NH₃,¹¹ the formation of C-F bonds,¹² and coupling reactions with CF₃ and CHF₂ substrates.^{13,14}

Prior to transition metal catalyzed cross-coupling reactions, the functionalization of aryl halides was not straightforward.⁵ While nucleophilic functionalization of alkyl halides occurs through S_N2 and S_N1 type reactions, aryl halides do not generally react with nucleophiles through direct S_N2 or S_N1 reactions.¹⁵ For S_N2 type reactions, the

backside attack of the nucleophile is sterically blocked by the aryl ring, while for S_N1 type reactions the high energy and instability of aryl cations hinders halide elimination from aryl halides. Functionalization of aryl halides is possible through S_NAr reactions, however these processes are limited to electron deficient aryl halides substituted with electron withdrawing groups *ortho* or *para* to the halide.¹⁵ Success has also been achieved with $S_{RN}1$ reactions with aryl halides, but these reactions can suffer from decreased selectivity due to competing reactions involving the radical anion including electron transfer or fragmentation.¹⁶ The value of transition metal catalyzed cross-coupling reactions initially came from their ability to functionalize aryl halides with carbon centered anions to form new C-C bonds with a high degree of selectivity. The original use of lithium and Grignard reagents suffered from decreased functional group tolerance, but the utilization of less basic zinc (Negishi), boron (Suzuki), tin (Stille), and silicon (Hiyama) reagents in transition metal catalyzed cross-coupling reactions significantly improved the range of functional group tolerance (Scheme 1-1).¹⁷

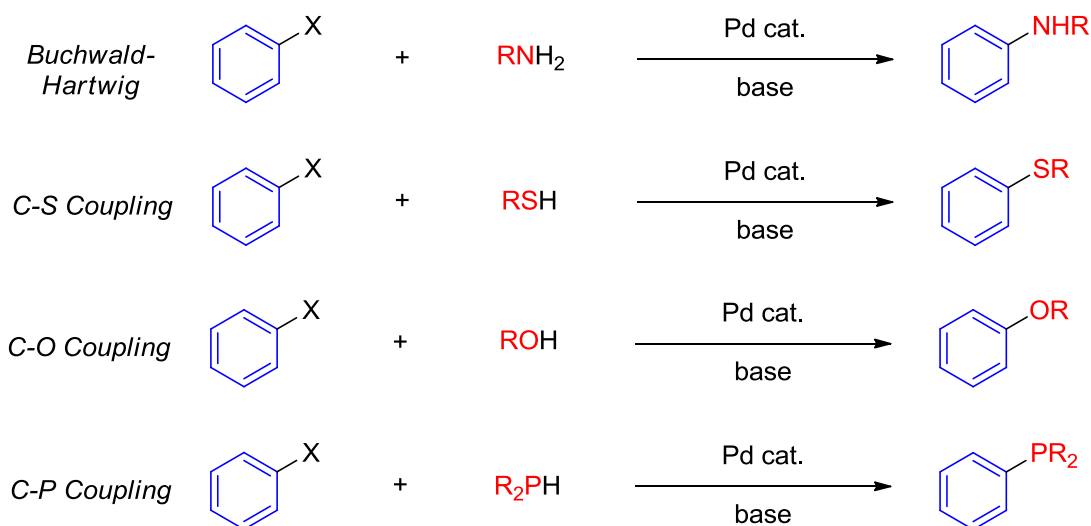


Scheme 1-1. Examples of Pd catalyzed C-C cross-coupling reactions.

Pd catalysts have undergone the greatest development and are the most utilized for cross-coupling reactions, but Ni catalysts have also been used for many of these transformations, including Suzuki, Negishi, and Kumada-Corriu coupling.^{18,19,20} The benefits of Pd include decreased sensitivity to oxygen as well as potential decreased toxicity relative to Ni.⁴ Also, the use of Pd catalysts typically results in a decreased quantity of undesired byproducts.⁵ Ni catalysts have the tendency to undergo single-electron radical chemistry, similar to other first-row transition metals, increasing the prevalence of byproduct formation. The high efficiency and specificity of Pd catalysts has made them industrially more relevant, especially in the synthesis of pharmaceuticals that have strict regulations pertaining to product purity.¹

Cu catalysts also have the ability to catalyze cross coupling reactions.^{21,22} Ullman²³ first described C-C and C-N coupling reactions with stoichiometric Cu in the early 1900s, followed shortly after by the use of catalytic Cu by Goldberg.²⁴ Many of the early reports of Cu catalyzed coupling reactions required temperatures in excess of 200 °C, however more recently the use of Cu catalysts supported by ancillary ligands has increased the scope and improved reaction conditions.²¹

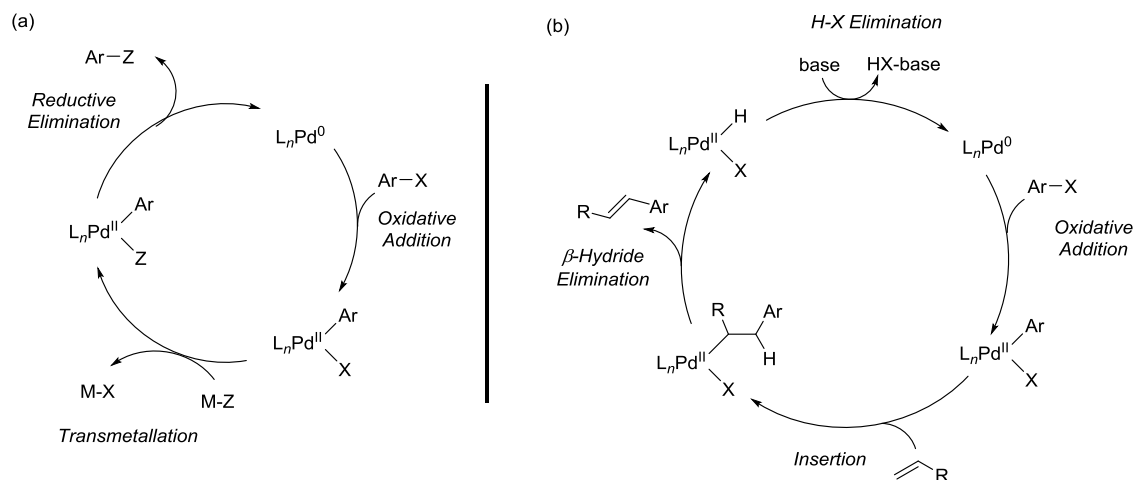
Over the last 20 years, some of the greatest developments in transition metal catalyzed cross-coupling reactions have been the application of transition metal catalysts for C-heteroatom bond-forming reactions (Scheme 1-2). Even though these reactions are less thermodynamically favorable compared to C-C coupling reactions, significant progress has been made in this area.⁵ Ni^{25,26} and Cu^{22,27,28} catalysts for C-heteroatom cross-coupling reactions have been described, but Pd catalysts are the most developed.^{29,30,31,32} The utility of Pd catalysts for C-N coupling reactions with aryl halides and amines has been the most explored. Since the initial reports from Buchwald³³ and Hartwig³⁴ on the arylation of primary amines with Pd catalysts with triarylphosphine ligands, extensive research on this process by Buchwald and Hartwig as well as the Stradiotto group³⁵ has resulted in improved reaction conditions and greatly expanded the functional group tolerance. The development of Pd catalysts for other C-heteroatom coupling reactions including C-S, C-P, and C-O have also been successful.^{31,32,36,37}



Scheme 1-2. Examples of Pd catalyzed C-heteroatom cross-coupling reactions.

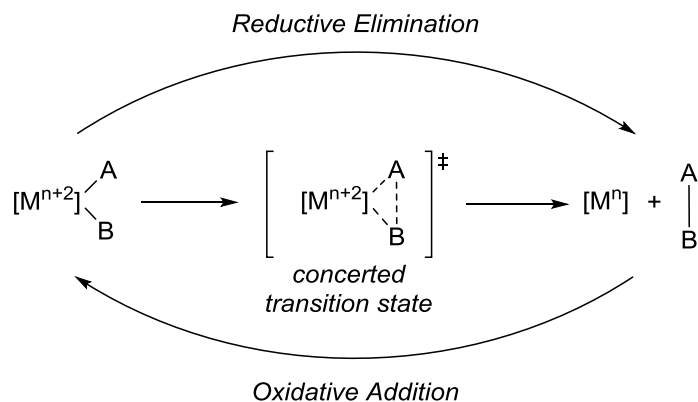
1.2 Mechanism of Pd Catalyzed Cross-Coupling Reactions

The majority of Pd catalyzed C-C and C-heteroatom cross-coupling reactions follow a similar three step catalytic cycle (Scheme 1-3, a).⁴ Aryl halide oxidative addition (OA) to Pd(0) forms a Pd(II) aryl/halido complex. This is followed by transmetalation of the Pd(II) aryl/halido complex with the nucleophilic carbon or heteroatom source. Reductive elimination (RE) from the Pd(II) complex forms the coupled organic product and regenerates the Pd(0) species. The mechanism for Heck type coupling reactions (Scheme 1-3, b) also involves aryl halide OA to Pd(0), however this is followed by insertion of the olefin into the Pd-Ar bond.⁴ The functionalized olefin product is then formed by β -hydride elimination (BHE) from the Pd(II) alkyl/halido. Base assisted release of HX from the resulting Pd(II) hydrido/halido complex regenerates Pd(0) and closes the cycle.



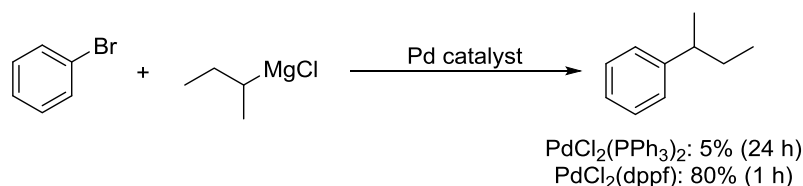
Scheme 1-3. General cycles for Pd catalyzed cross-coupling. (a) Catalytic cycle for Pd catalyzed C-C and C-heteroatom coupling. (b) Catalytic cycle for Pd catalyzed Heck coupling.

The ability of Pd to catalyze cross-coupling reactions is due to its tendency to undergo two-electron changes in oxidation states, which is imperative for the OA and RE elimination steps of the catalytic cycle. OA involves the cleavage of a bond of an organic or main group reagent that results in the formation of two new metal-ligand bonds (Scheme 1-4).³⁸ During this process, the metal is formally oxidized resulting in an increase of the metal oxidation state by two. RE is the reverse of OA, resulting in the breaking of two metal-ligand bonds and the formation of a new bond in the released substrate.³⁹ The oxidation state of the metal center decreases by two following RE. In the case of Pd catalyzed coupling reactions with aryl halides, both OA and RE occur in a concerted fashion. Concerted OA and RE are defined by a three-centered transition state, in which the bonds are being broken and formed simultaneously (Scheme 1-4).^{39,40}



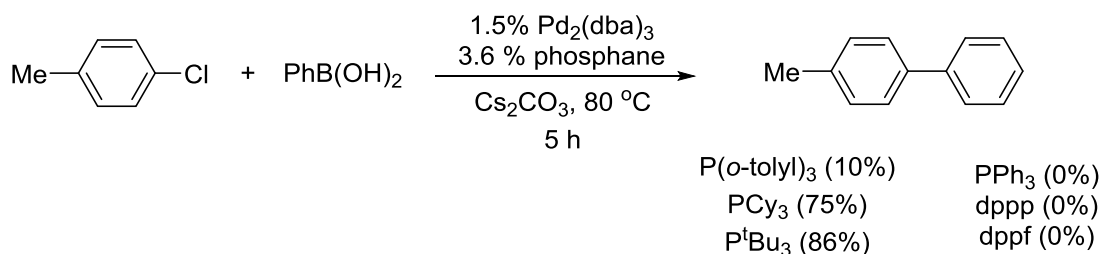
Scheme 1-4. General reaction scheme for oxidative addition (OA) and reductive elimination (RE).

The design and implementation of new ligands has been instrumental to the development of Pd catalyzed cross-coupling reactions.¹⁷ Simple phosphine ligands such as PPh₃ were originally used for cross-coupling reactions, but it was observed that the ligand properties can drastically affect the performance of the catalyst. The steric effect of ligands was first observed in the increased activity of Pd catalysts with bidentate ligands such as bis(diphenylphosphino)ferrocene (dppf) compared to PPh₃ (Scheme 1-5) for Kumada coupling.⁴¹ Concerted RE requires a *cis* coordination of the eliminating ligands that is enforced by bidentate ligands.³⁹ In addition, bidentate ligands with a larger bite angle favor RE, because the complex is preorganized to be closer in geometry to the resulting two-coordinate Pd(0) complex.⁴²



Scheme 1-5. Comparison of monodentate and bidentate phosphine ligands for Pd catalyzed cross-coupling.

Ligand loss commonly precedes OA from two-coordinate Pd(0) complexes in order to achieve the reactive monocoordinate intermediate, because OA is faster to coordinatively unsaturated transition metal complexes.³⁸ The use of sterically encumbered electron-donating phosphines allowed for the utilization of aryl chlorides in addition to aryl bromides and iodides. The use of aryl chlorides is desirable due to their low cost and wide availability.⁴³ However, their use in early examples of cross-coupling reactions was hindered, because of the difficulty of aryl chloride OA.⁴⁴ In the late 1990s Fu reported on the successful functionalization of aryl chlorides with Pd catalysts supported by bulky P^tBu_3 ligands (Scheme 1-6).^{42a,45} The success of Pd/ P^tBu_3 system with aryl chlorides was attributed to the more easily accessed monocoordinate Pd(P^tBu_3) due to the large steric bulk of the P^tBu_3 ligand.⁴⁶



Scheme 1-6. Pd catalyzed Suzuki coupling with aryl chlorides.

RE from d^8 transition metal complexes is typically fastest from three-coordinate complexes.^{39,47,48} RE elimination from four-coordinate Pd(II) is not rare, particularly with *cis*-bidentate ligands such as BINAP or DPPF.³⁹ However, Pd catalysts substituted with monodentate ligands will often undergo ligand dissociation from four-coordinate Pd(II) complexes prior to RE in order to achieve the more reactive three-coordinate species. For this reason, sterically demanding ligands that can more easily access three-coordinate Pd(II) complexes by dissociation generally facilitate more facile RE. In 2003, Hartwig described the RE of diarylethers from arylpalladium aryloxy complexes with monophosphines.⁴⁹ Thermolysis of Pd complexes with PPh_3 or $P(o\text{-tolyl})_3$ ligands resulted in no formation of the diarylether, but successful C-O RE was achieved when hindered alkylmonophosphine ligands such as ferrocenyl-di-*tert*-butylphosphine (PFC^tBu_2) were used.

The electronics of the ancillary ligands also play a key role in the development of successful cross-coupling catalysts. The aryl halide OA step is typically encouraged by a more electron rich metal center, due to the increased partial positive charge formed at the metal center following OA.^{38,49} Alternatively, the product forming RE step is favored by electron poor metal centers, because the resulting metal complex has more electron density at the metal center.^{39,50} For this reason, there is a fine balance that must be achieved electronically in addition to the steric properties of a successful catalyst. The most successful ligands for Pd catalyzed cross-coupling today include the phosphinobiphenyl ligands introduced by Buchwald,⁵¹ the dialkylferrocene phosphine based ligands developed by Hartwig,^{30,52} Stradiotto's P,N-phenylene ligands,³⁵ and N-

heterocyclic carbenes (NHC) utilized by Nolan (Figure 1-1).⁵³ Each of these ligand designs possesses a good balance of steric and electronic properties, resulting in some of the most active Pd catalysts to date. The sterically demanding nature of these ligands encourages OA and RE by facilitating easier access to monocoordinate Pd(0) and three-coordinate Pd(II) intermediates.⁵⁴ In addition, the electronics of these ligands are easily modified and tuned by functionalizing the ligands with various substituents.

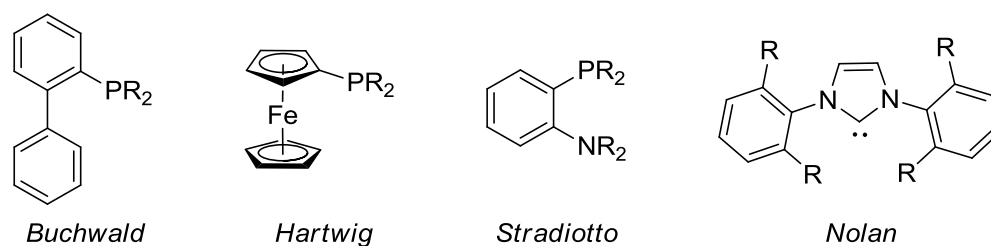
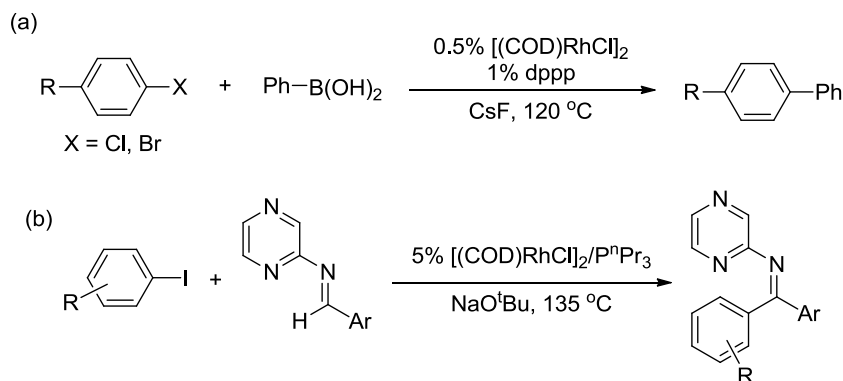


Figure 1-1. Successful ligand scaffolds for Pd catalyzed cross-coupling reactions.

1.3 Rhodium Catalyzed Cross-Coupling Reactions

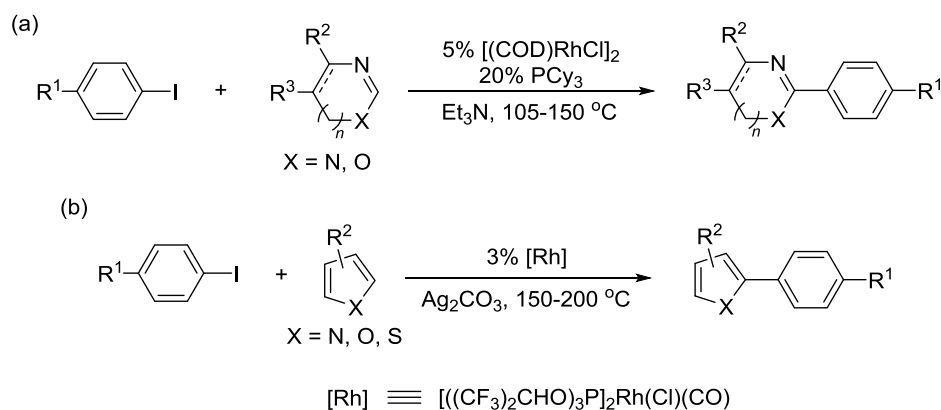
While Pd, Ni, and Cu are the most common transition metals for cross-coupling reactions, several examples of Rh catalyzed cross-coupling reactions have been reported in the literature.⁵⁵ In 2005, Miura reported the Suzuki type coupling of aryl chlorides and bromides with PhB(OH)₂ using catalytic amounts of [(COD)RhCl]₂ and 1,4-bis(diphenylphosphino)propane (dppp) ligand in the presence of CsF (Scheme 1-7, a).⁵⁶ The reaction resulted in high yields (88-98%) of the coupled products after 2 h at 120 °C, but the scope was not extensive. Hartwig has described the Rh catalyzed Heck type coupling of aryl halides with *N*-pyrazyl aldimines with decent yields (Scheme 1-7, b).⁵⁷ The reactions worked well with aryl iodides, but the system was not successful with aryl

bromides. Hartwig proposes a mechanism similar to that of the previously described Heck reactions, in which the aldimine inserts into the Rh-Ar bond, followed by product forming BHE.



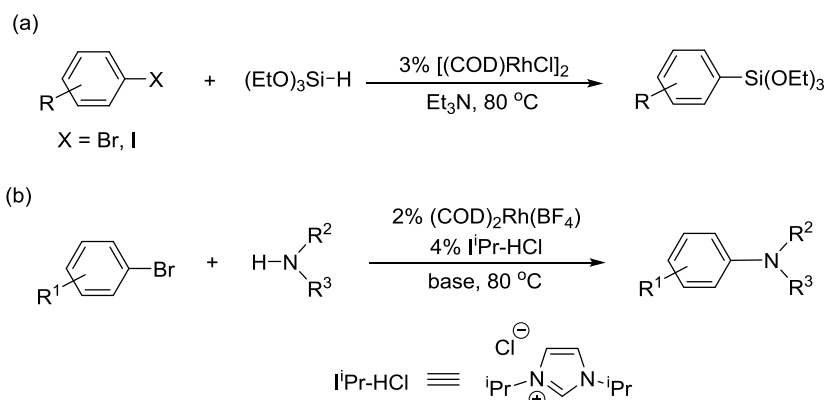
Scheme 1-7. Rh catalyzed C-C cross-coupling reactions. (a) Rh catalyzed Suzuki type coupling reaction. (b) Rh catalyzed Heck type coupling reaction.

Many of the reports of Rh catalyzed C-C cross-coupling with aryl halides involve the direct functionalization of C-H bonds. Bergman⁵⁸ (Scheme 1-8, a) and Itami⁵⁹ (Scheme 1-8, b) have both reported on the arylation of heterocycles with aryl iodides using Rh catalysts and phosphine ligands. Both groups proposed a mechanism involving aryl iodide OA, electrophilic metallation of the heterocycle C-H bond, and product forming RE.



Scheme 1-8. Rh catalyzed C-C bond forming reactions involving the direct functionalization of C-H bonds.

Rh catalyzed C-heteroatom cross-coupling reactions have also been described. In 2002, Murata and coworkers described the Rh catalyzed silylation of aryl halides to form aryltriethoxysilanes (Scheme 1-9, a).⁶⁰ Their system utilized [(COD)RhCl]₂ as the catalyst in the absence of ancillary ligands and Et₃N as base. The reaction worked well for both aryl bromides and iodides giving yields between 76-88%, but was unsuccessful with aryl chlorides. In 2010, Chang reported the Buchwald-Hartwig type amination of aryl bromides using a Rh catalyst and NHC ligands (Scheme 1-9, b).⁶¹ The reaction was successful with primary and secondary amines giving high yields (up to 96%) after 12 h at 80 °C.

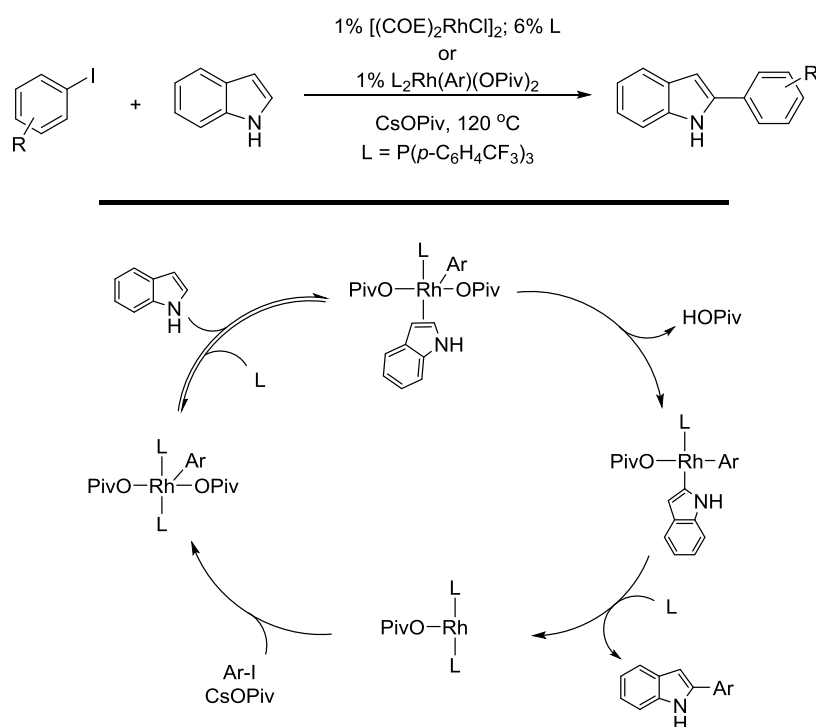


Scheme 1-9. Catalytic C-heteroatom cross-coupling with Rh.

1.4 Mechanism of Rh Catalyzed Cross-Coupling Reactions

Many of the reported examples of Rh catalyzed cross-coupling reactions propose a Rh(I)/Rh(III) mechanism similar to that of the previously described Pd(0)/Pd(II) mechanism, involving aryl halide OA and product forming RE.⁵⁶⁻⁶¹ However, there has been limited experimental work to directly support the proposed mechanisms. One of the best understood Rh catalytic systems was reported by Sames in 2005 involving the direct C-H arylation of indoles with aryl iodides (Scheme 1-10).^{55e} This system was successful for a range of substituted indoles with aryl iodides using 1% [(COE)₂RhCl]₂ in the presence of P(*p*-C₆H₄CF₃)₃ and CsOPiv. Inspection of the ³¹P NMR spectrum during catalysis showed the presence of a single phosphorus containing Rh species, identified as the Rh-aryl complex [P(*p*-C₆H₄CF₃)₃]₂Rh(Ar)(OPiv)₂. The complex is formed via phosphine coordination, aryl iodide OA, and anion exchange with CsOPiv. The use of this complex as catalyst provided rates and yields identical to those obtained with [(COE)₂RhCl]₂/P(*p*-C₆H₄CF₃)₃. Treatment of the complex with a stoichiometric amount of indole also resulted in the formation of the C-arylated product. These results are

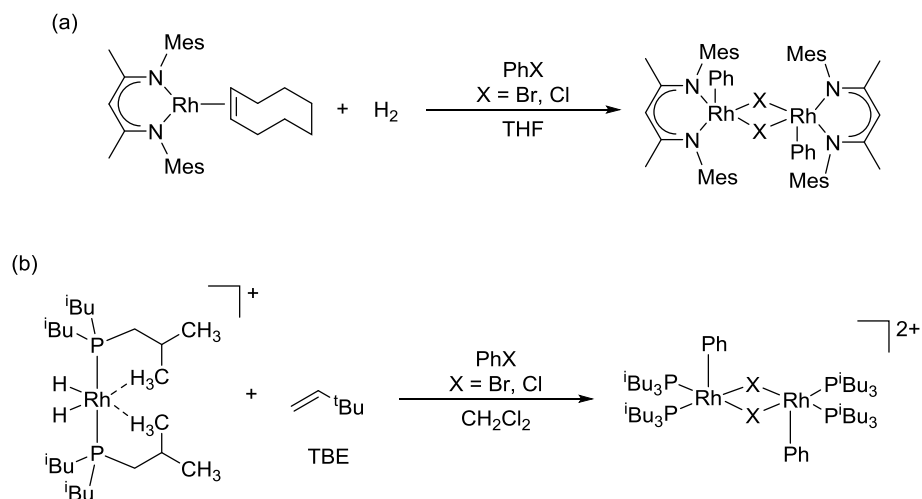
consistent with the proposed mechanism (Scheme 1-10) involving initial formation of $[P(p\text{-C}_6\text{H}_4\text{CF}_3)_3]_2\text{Rh}(\text{Ar})(\text{OPiv})_2$ from $[(\text{COE})_2\text{RhCl}]_2$ followed by displacement of phosphine with indole and subsequent C-H metalation. RE forms the the desired arylated indole and the Rh(I) complex $[P(p\text{-C}_6\text{H}_4\text{CF}_3)_3]_2\text{Rh}(\text{OPiv})$. The reactive three-coordinate Rh(I) complex undergoes rapid aryl iodide OA and halide-pivolate exchange to regenerate the Rh(III) $[P(p\text{-C}_6\text{H}_4\text{CF}_3)_3]_2\text{Rh}(\text{Ar})(\text{OPiv})_2$ and close the cycle.



Scheme 1-10. Rh catalyzed arylation of indoles with aryl iodides.

Direct observation of aryl halide OA to Rh(I) has been demonstrated in some instances.^{62,63,64,65} Similar to Pd, aryl halide OA is faster at low coordinate Rh(I) complexes. Budzelaar and coworkers have described addition of both aryl chlorides and

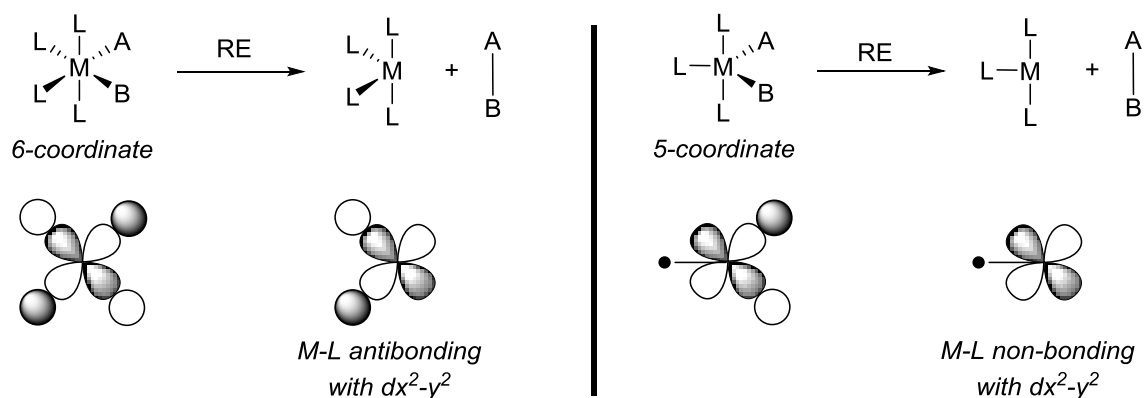
bromides to Rh(I).^{66,67} In one case, the *in situ* generation of a low-coordinate Rh(I) center supported by β -diimine ligand undergoes facile OA of PhCl and PhBr (Scheme 1-11, a).⁶⁷ Weller also described the OA of PhCl and PhBr to low-coordinate Rh(I) (Scheme 1-11, b).⁶⁸ In this instance, treatment of $[(P^iBu_3)_2Rh(H)_2]^+$ with *tert*-butylethylene (TBE) generated the solvent stabilized $[(P^iBu_3)_2Rh(solv)_2]^+$. Exposure of the solvent stabilized Rh(I) species to PhBr or PhCl resulted in quantitative conversion to the OA products. The isolated Rh(III) OA products reported by Budzelaar and Weller are both dimers with five-coordinate square pyramidal geometry about each Rh center.⁶⁹



Scheme 1-11. Examples of OA to Rh(I).

RE from Rh(III) involving aryl ligands has not been thoroughly examined.⁶⁵ RE from d^6 transition metals is kinetically more favorable from 5-coordinate complexes. Hartwig has explained this effect by examining the frontier orbitals of the metal complex before and after RE (Scheme 1-12).³⁹ The two additional d-electrons in the immediate

four-coordinate species that forms as a result of RE from six-coordinate complexes are strongly antibonding with the dx^2-y^2 orbital. Alternatively, the three-coordinate species that forms immediately after RE from five-coordinate d^6 complexes places those electrons in a molecular orbital that is nonbonding, which would be more favorable.



Scheme 1-12. Comparison of frontier orbital interactions for RE from six- and five-coordinate Rh. *Figure adapted from J. F. Hartwig, *Organotransition Metal Chemistry: From Bonding to Catalysis*; University Science Books: Sausalito, 2009; Ch. 8.

1.5 Utility of Pincer Ligands for Examination of OA and RE at Rh

The use of pincer supported Rh complexes has provided an excellent platform for the analysis of OA and RE at Rh.^{63,64,65} Pincer ligands are traditionally tridentate ligands composed of two neutral side arms stemming from a central anionic group that coordinate to the metal center in a meridional fashion (Figure 1-2).^{70,71} These ligands offer a multitude of structural possibilities by varying X, Y, Z, E, and R, which allows for precise steric and electronic tuning at the metal center. The rigid nature of pincer ligands also offers structural and thermal stability to their metal complexes.

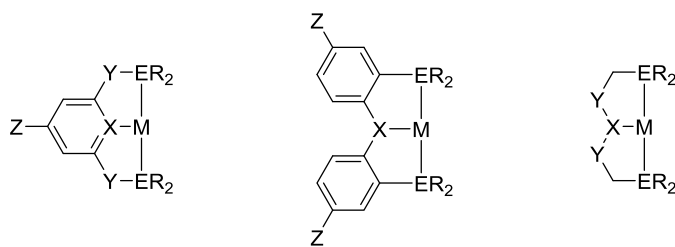
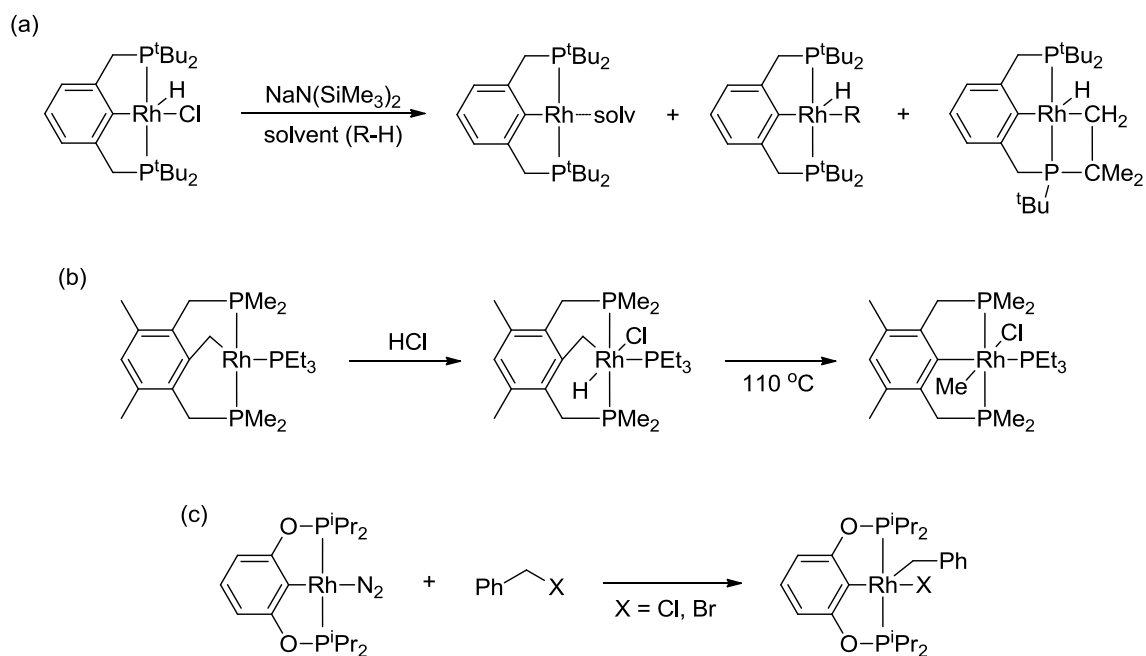


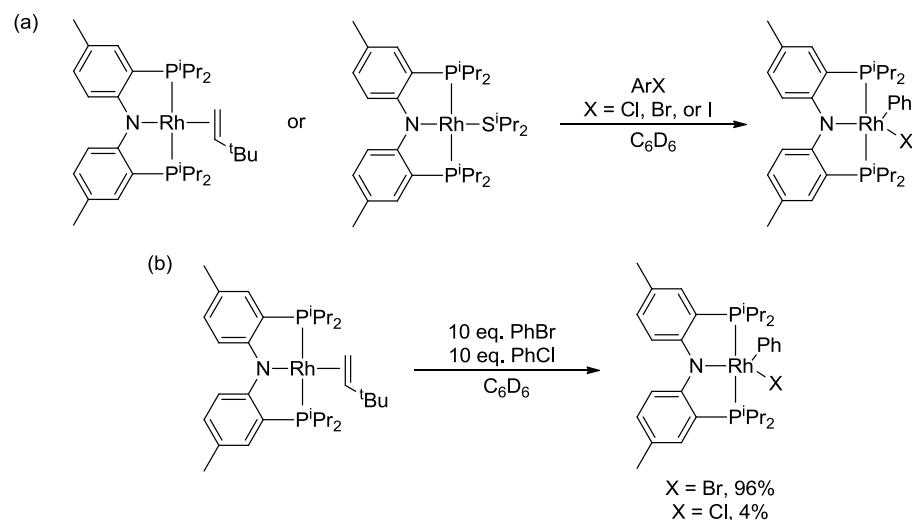
Figure 1-2. Common pincer ligand frameworks.

In 1983, Kaska described the activation of aromatic and aliphatic C-H bonds at $(PCP^{tBu})Rh$ (Scheme 1-13, a).⁷² Treatment of $(PCP^{tBu})Rh(H)(Cl)$ with $NaN(SiMe_3)_2$ formed the reactive solvent stabilized Rh(I) complex $(PCP^{tBu})Rh(solv)$, which was shown to activate the C-H bonds of the hydrocarbon solvent, including benzene, cyclohexane, and pentane. This was evidenced by the formation of Rh-H in the 1H NMR spectrum. C-H activation of the tBu groups of the side-arms was also observed. Milstein has reported both C-H and C-C OA at Rh(I) involving the aryl backbone of the PCP pincer framework (Scheme 1-13, b).⁷³ At lower temperatures, the C-H OA product was favored; however at elevated temperatures, the C-C OA product was formed irreversibly. Similar C-O activation was observed with pincer ligands containing an Ar-OMe group.⁷⁴ Milstein also reported the OA of benzyl chlorides and iodides to $(POCOP)Rh(N_2)$ to form the Rh(III) $(POCOP)Rh(CH_2Ph)(X)$ ($X = Cl, Br$) compounds (Scheme 1-13, c).⁷⁵



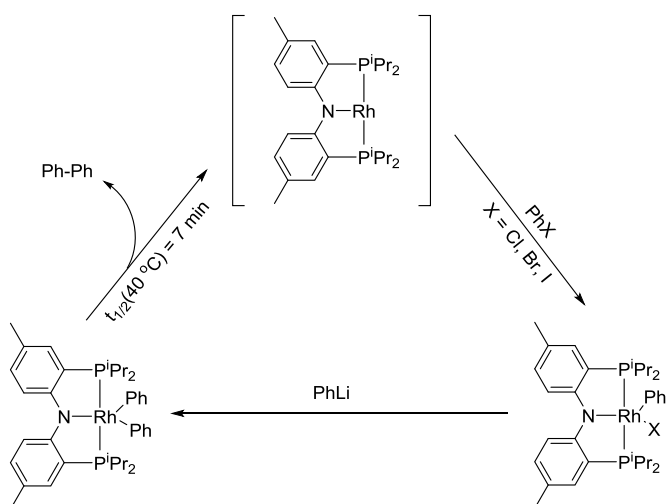
Scheme 1-13. Oxidative addition reactions involving (pincer)Rh.

Our group has previously described OA of aryl halides to Rh(I) complexes supported by PNP pincer ligands.^{63,64,65} Treatment of (PNP)Rh^I stabilized by weakly coordinating bulky dative ligands such as TBE or diisopropylsulfide (SⁱPr₂) with aryl halides resulted in quantitative formation of the five-coordinate (PNP)Rh(Ar)(X) complex (Scheme 1-14, a). The success of (PNP)Rh complexes to undergo aryl halide OA is attributed to ability to access the coordinately unsaturated three-coordinate (PNP)Rh^I fragment provided by dissociation of the weakly coordinating dative ligands.⁶⁴ Competition experiments between aryl bromides and aryl chlorides demonstrated the clear favorability of aryl bromide OA compared to aryl chlorides (Scheme 1-14, b), similar to what has been observed with Pd.⁶³



Scheme 1-14. Aryl halide OA to (PNP)Rh. (a) OA to (PNP)Rh^I stabilized by weakly coordinating bulky dative ligands. (b) OA competition experiment between PhBr and PhCl.

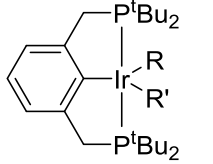
The (PNP)Rh system also provided access to the direct observation of C-C RE at Rh(III) (Scheme 1-15).⁶⁵ Transmetalation of (PNP)Rh(Ph)(Br) with PhLi or PhMgBr resulted in formation of (PNP)Rh(Ph)₂, which evolved biphenyl. Analysis of biphenyl elimination from (PNP)Rh(Ph)₂ in the presence of PhBr indicated clean first-order kinetics and $t_{1/2}$ of 7 min at 40 °C. Elimination of toluene from (PNP)Rh(Ph)(Me) was also monitored in the presence PhBr and showed $t_{1/2}$ of 17 min at 40 °C. The rate of both reactions was independent of the concentration of PhBr. These results are consistent with rate-limiting C-C RE to generate the coordinatively unsaturated (PNP)Rh^I fragment, which undergoes rapid PhBr OA.



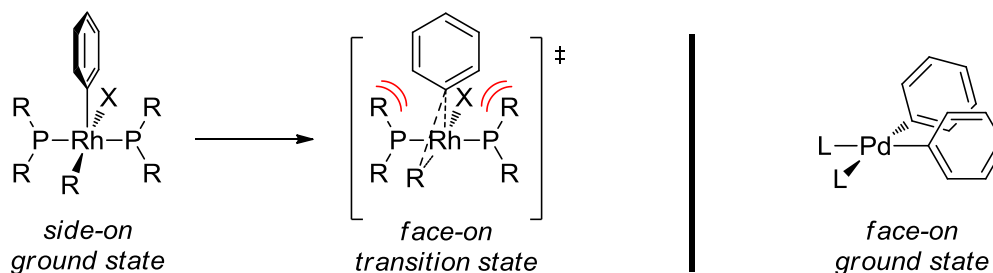
Scheme 1-15. C-C RE from (PNP)Rh(Ph)₂.

In 2008, Goldman and coworkers reported a thorough experimental and theoretical analysis on C-C RE from five-coordinate d⁶ Ir complexes supported by PCP pincer ligands.⁷⁶ Many of the observations described in this study may be applied to RE from similar pincer supported d⁶ Rh complexes. RE was more thermodynamically favorable as the bulk of the eliminating ligands increased (Table 1-1), similar to what has been observed with d⁸ Pd. This trend is linked to decreased congestion at the metal center following RE.

Table 1-1. Calculated activation parameters and thermodynamics parameters for C-C RE from (PCP^{tBu})Rh(R)(R').

|  (PCP ^{tBu})Rh(R)(R') | <i>R</i> | <i>R</i> ' | ΔG^\ddagger (kcal/mol) | ΔG (kcal/mol) |
|---|----------|------------|--------------------------------|-----------------------|
| | | Ph | Me | 27.1 |
| | Ph | Ph | 32.4 | -25.9 |
| | Ph | Vinyl | 20.7 | -23.1 |
| | Vinyl | Me | 17.7 | -15.7 |
| | Vinyl | CCPh | 18.1 | -0.5 |
| | CCPh | CCPh | 7.0 | -10.2 |

However, unlike RE from d^8 complexes, the rate of RE from d^6 compounds was hindered as the size of the participating groups increased (Table 1-1).⁷⁶ This is a result of the side-on orientation of vinyl or aryl groups in the ground state metal complex prior to RE (Scheme 1-16). For example, at the transition state for RE involving an aryl group, the aryl group needs to have a face-on orientation with the other eliminating ligand, which means the aryl must rotate from its orientation in the ground state structure. The barrier for this rotation is increased as the bulk of the rotating apical group is increased, resulting in a decrease in the rate of RE. This is consistent with the lower activation barrier for elimination of vinyl-Me compared to Ph-Me. For processes involving not involving aryl or vinyl ligands, such as Me or CCH, this is not an issue because the orientation of the eliminating Me or CCH does not change at the transition state. This was confirmed by the elimination of HCC-CCH having the lowest ΔG^\ddagger . Alternatively, the ground state structure of d^8 complexes has the eliminating ligands prearranged in the face-on orientation prior to RE (Scheme 1-16). This results in faster RE as the steric bulk of the ancillary ligands is increased, because no rotation is necessary at the transition state.



Scheme 1-16. Comparison of ground states structure between d^6 Rh and d^8 Pd complexes prior to RE.

CHAPTER II
CATALYSIS OF KUMADA-TAMAO-CORRIU COUPLING BY A (POCOP)RH
PINCER COMPLEX*

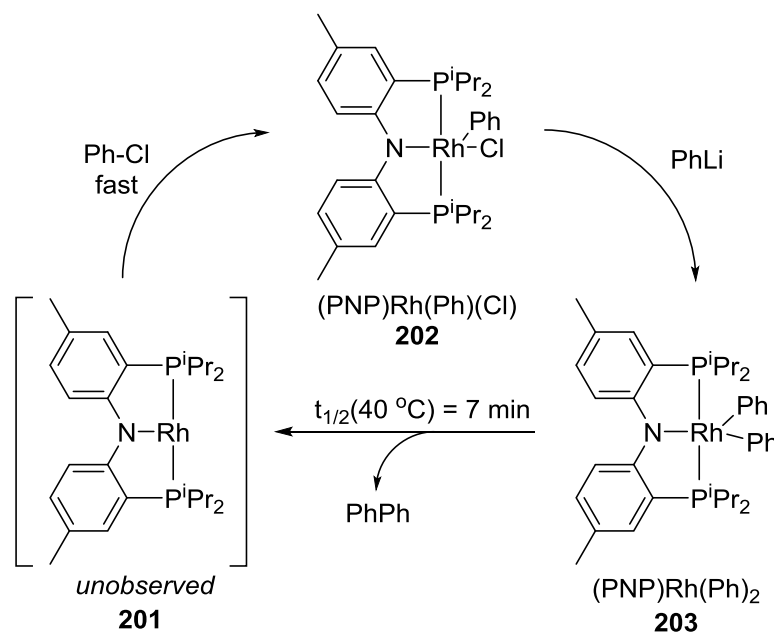
2.1 Introduction

Transition metal catalyzed coupling reactions have revolutionized the functionalization of aryl halides.^{3,77} With regards to C–C bond forming reactions, this chemistry has been extensively explored with group 10 catalysts, particularly Pd and Ni.^{78,79} The success of group 10 catalysts lies in their ability to easily undergo two-electron changes in oxidation state, which is essential for oxidative addition (OA) and reductive elimination (RE).⁴ The use of other transition metal catalysts in the literature is less prevalent;^{22,80} however, several examples of Rh catalyzed C–C bond forming reactions have been reported.^{55-56,58-59} While the mechanism for the transformation is still relatively unexplored,^{62,66-68} they are believed to utilize an analogous Rh^I/Rh^{III} catalytic cycle. We were hopeful that a pincer supported Rh system would allow for enhanced examination of the mechanistic cycle and also the potential for a recoverable catalyst attributed to the enhanced stability of pincer ligated metal complexes.

We have previously illustrated the ability of Rh(I) and Rh(III) centers supported by PNP pincer ligands to undergo OA and RE, respectively.^{63-65,81} In 2006, our group reported the facile OA of aryl halides, including chlorides, to an unsaturated (PNP)Rh^I

* “Catalysis of Kumada-Tamao-Corriu Coupling by a (POCOP)Rh Pincer Complex,” Timpa, S. D.; Fafard, C. M.; Herbert, D. E.; Ozerov, O. V. *Dalton Trans.*, **2011**, 40, 5426 – Reproduced by permission of The Royal Society of Chemistry.

fragment (**201**) to form (PNP)Rh(Ph)(Cl) (**202**) and C-C RE from (PNP)Rh(Ph)₂ (**203**) system (Scheme 2-1).⁶⁵ The low rate of C–C RE would hinder efficient catalysis with (PNP)Rh; however, this did show that pincer supported rhodium complexes can undergo each of the necessary steps to perform catalytic cross-coupling reactions (aryl halide OA, transmetalation, and RE). We wanted to examine the potential of alternative (pincer)Rh complexes for this chemistry and decided to investigate the donating bisphosphinite POCOP ligand (ν_{CO} of (POCOP)RhCO⁷⁵ is 1962 cm⁻¹ vs. 1945 cm⁻¹ for (PNP)RhCO⁸²). The less donating POCOP ligand was expected to favor a Rh center with a lower oxidation state, which should increase the favorability of C–C RE and formation of resulting (POCOP)Rh^I intermediate.



Scheme 2-1. C-C reductive elimination (RE) from (PNP)Rh center.

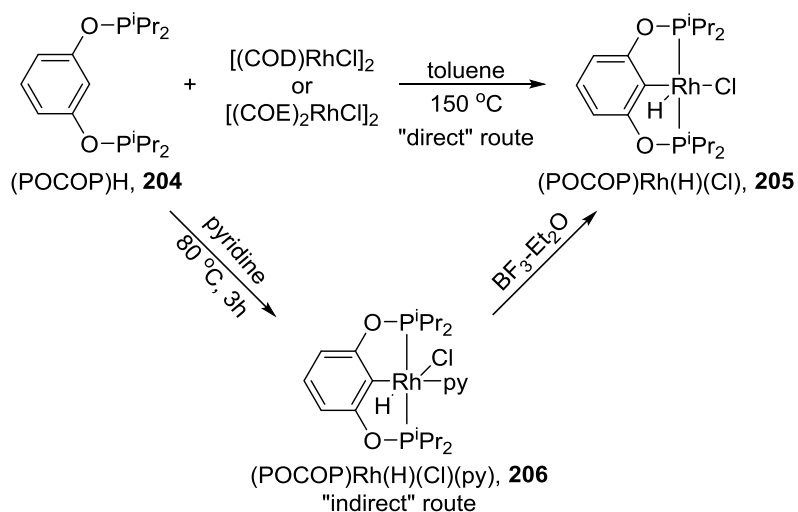
2.2 Results and Discussion

2.2.1 Synthesis of (POCOP)Rh(H)(Cl)

In 2008, Milstein and coworkers reported the synthesis of (POCOP)Rh(H)(Cl) (**205**) from (POCOP)H (**204**) and [(COE)₂RhCl]₂,⁸³ however, they were unable to achieve greater than 90% purity and provided no identification of the impurities. Our attempts to follow this synthesis resulted in formation of impure **205** with *ca.* 80% purity using [(COE)₂RhCl]₂ and *ca.* 50% purity using [(COD)RhCl]₂ (Scheme 2-2).

The reaction between **204** and [(COD)RhCl]₂ in non-coordinating solvents such as toluene or benzene resulted in a mixture of products, with a maximum purity of the desired product *ca.* 60%. However, the same reaction in pyridine formed a single product, determined to be the six-coordinate solvent adduct, (POCOP)Rh(H)(Cl)(py) (**206**) (Scheme 2-2). **206** was isolated as a single isomer in 78% yield. Similarly, the reaction in acetonitrile formed the analogous (POCOP)Rh(H)(Cl)(NCMe) (**207**).

Isolation of pure **205** was achieved by pyridine ligand extraction from **206** with the Lewis acid BF₃-OEt₂ (Scheme 2-2). This route produced pure **205** in good yields (75%). X-ray quality crystals of **205** were grown from a 5:1 pentane:toluene mixture at RT (Figure 2-1). The solid-state structure obtained by X-ray diffractometry showed a geometry about rhodium intermediate between square pyramidal (apical hydride) and Y-shaped.⁶⁹



Scheme 2-2. Direct and indirect routes to the synthesis of $(\text{POCOP})\text{Rh}(\text{H})(\text{Cl})$ (**205**).

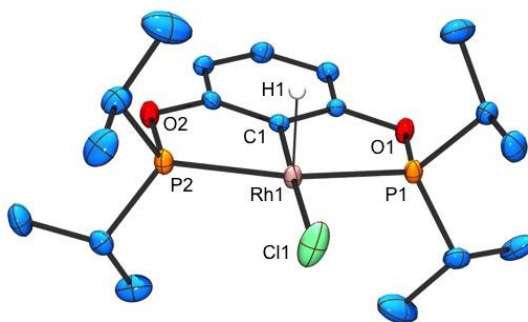
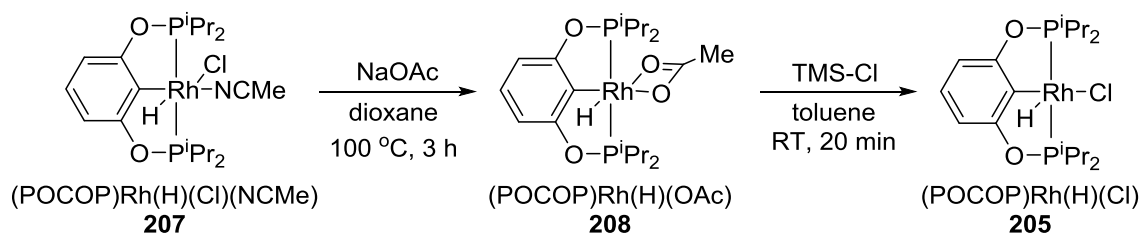


Figure 2-1. ORTEP drawing (50% thermal ellipsoids) of $(\text{POCOP})\text{Rh}(\text{H})(\text{Cl})$ (**205**).⁸⁴ Selected atom labeling. Hydrogen atoms are omitted for clarity except for Rh-H. Selected bond distances (\AA) and angles (deg): Rh1-P1, 2.2786(8); Rh1-C1, 2.3840(9); Rh1-Cl1, 1.987(2); Rh1-H1, 1.51(2); P1-Rh1-P2, 160.59(2); C1-Rh1-Cl1, 168.97(5); C1-Rh1-H1, 75.2(9).

Formation of **205** was also observed following treatment of $(\text{POCOP})\text{Rh}(\text{H})(\text{OAc})$ (**208**) with Me_3SiCl . The reaction of **204** with $[(\text{cod})\text{RhOAc}]_2$ in toluene gave a mixture of products, with **208** never constituting greater than 40% of the product mixture. However, the synthesis of *ca.* 85% purity **208** was achieved by the

reaction of **207** with NaOAc in dioxane at 100 °C (Scheme 2-3). Treatment of **208** (ca. 85% purity) with Me₃SiCl resulted in formation of **205** as the major product (89%) after 20 min at RT. The reaction also formed a minor product (11%), but the identity of this impurity was not determined.



Scheme 2-3. Synthesis of (POCOP)Rh(H)(Cl) (**205**) via (POCOP)Rh(H)(OAc) (**208**).

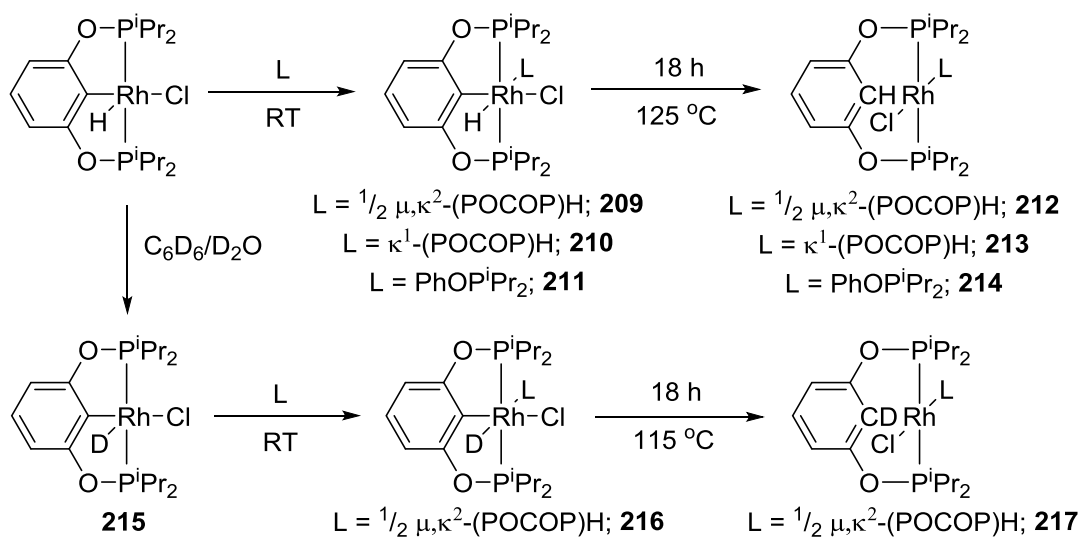
2.2.1.1 Determination of Reaction Impurities from Direct Synthesis

The ³¹P{¹H} NMR spectrum for the direct synthesis of **205** presented the major impurity as an AM₂Z spin system (Z = Rh), which was consistent with a Rh center with two equivalent *trans*-phosphines *cis* to a third unique phosphine. The pattern appears as a doublet of doublets and a doublet of triplets in 2:1 ratio with a $J_{PP} = 16$ Hz. The $J_{RhP} = 149$ and 161 Hz for the impurity are much greater than the $J_{RhP} = 122$ Hz for **205**. Similar to analogous (PNP)Rh complexes,⁶⁴ the J_{RhP} coupling for (POCOP)Rh complexes may be used as an indicator for the oxidation state of the rhodium center (higher J_{RhP} indicate Rh(I); lower J_{RhP} indicate Rh(III)). The higher J_{RhP} is indicative of a more electron rich Rh(I) center.

The impurity is likely the result of coordination of one of the phosphines of free **204** to a POCOP-ligated Rh. **204** could potentially coordinate in two fashions: a bridging

coordination mode forming a dimer, or κ^1 forming a monomer. Both complexes would display the characteristic AM_2Z system resonance pattern, but the κ^1 complex would also display an additional singlet corresponding to the unbound phosphine.

To test this assumption, pure **205** was treated with slightly more than 0.5 equivalents of **204** and the reaction was monitored by $^{31}\text{P}\{^1\text{H}\}$ NMR spectroscopy (Scheme 2-4). Upon mixing, the NMR signals corresponding to **205** disappeared and two new sets of signals appeared assigned to the bridging product $[(\text{POCOP})\text{Rh}(\text{H})(\text{Cl})]_2(\text{POCOP})\text{H}$ (**209**) (major) and the κ^1 bound product $(\text{POCOP})\text{Rh}(\text{H})(\text{Cl})(\text{POCOP})$ (**210**) (Figure 2-2, b). The presence of the κ^1 bound product **210** was supported by the presence of a resonance in the $^{31}\text{P}\{^1\text{H}\}$ NMR spectrum corresponding to an unbound phosphine. The major product displayed two resonances of an AM_2Z system in the $^{31}\text{P}\{^1\text{H}\}$ NMR spectrum, with $J_{\text{PP}} = 16$ Hz, but the presence of a hydride signal ($\delta -16.34$ ppm) in the ^1H NMR spectrum and the low $J_{\text{RhP}} = 112$ and 108 Hz indicated a straightforward Rh(III) hydride adduct, not a Rh(I) complex. When the reaction with **205** and **204** was heated at 125 °C, the resonances for Rh(III) products decreased and a set of new signals assigned to $[(\text{POCHOP})\text{Rh}(\text{Cl})]_2(\text{POCOP})\text{H}$ (**212**) identical to those of the impurity in the direct synthesis of **205** (Figure 2-2, c). An additional minor set of signals assigned to $(\text{POCHOP})\text{Rh}(\text{Cl})(\text{POCOP})$ (**213**) also appeared after thermolysis.



Scheme 2-4. Independent synthesis of compounds **209** – **217**.

To support the NMR assignment of **212** as the impurity, the analogous reaction of **205** and *ca.* 1 equiv PhOP^iPr_2 was examined (Scheme 2-4). This reaction gave similar $^3\text{P}\{^1\text{H}\}$ NMR spectra to both the RT and heated reaction with **204**, presumably forming $(\text{POCOP})\text{Rh}(\text{H})(\text{Cl})(\text{PhOP}^i\text{Pr}_2)$ (**211**) and $(\text{POCHOP})\text{Rh}(\text{Cl})(\text{PhOP}^i\text{Pr}_2)$ (**214**) (Figure 2-2, d & e). This allowed the confident assignment of **212** as the major impurity in the direct synthesis of **205**.

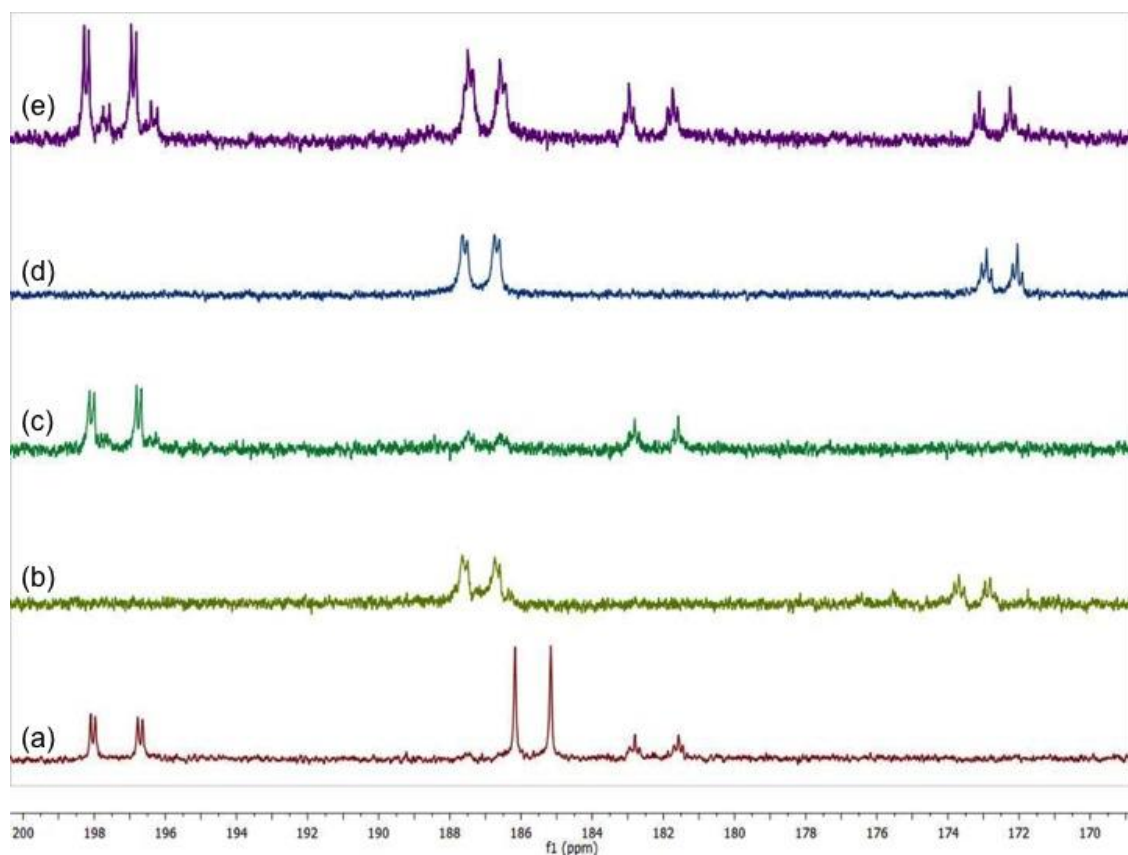


Figure 2-2. $^{31}\text{P}\{^1\text{H}\}$ NMR spectra of selected complexes collected in C_6D_6 . (a) Synthesis of $(\text{POCOP})\text{Rh}(\text{H})(\text{Cl})$ (**205**) by a direct route. Small resonance at 157.9 ppm not shown. (b) Reaction of **205** with 0.60 eq. of **204** at RT. The singlet resonance representing the uncoordinated phosphine at 151.8 ppm is not shown. (c) Reaction of **205** with 0.53 eq. of **204** after thermolysis at 125 °C. (d) Reaction of **205** with 1.0 eq. of PhOP^iPr_2 at RT. (e) Reaction of **205** with 1.0 eq. of PhOP^iPr_2 after thermolysis at 125 °C.

The formation of **212** from **209** via C-H reductive elimination was supported by deuterium exchange experiments (Scheme 2-4). $(\text{POCOP})\text{Rh}(\text{D})(\text{Cl})$ (**215**) was synthesized by thermolysis of **205** in C_6D_6 in the presence of D_2O and displays a single prominent ^2H resonance at -22.6 ppm in *protio*-dioxane (-25.4 ppm in *protio*-toluene). The resonance shifted to -16.1 ppm upon addition of **204** forming **216**, and to 7.9 ppm after thermolysis, indicating C-D RE and formation of **217** (Figure 2-3).

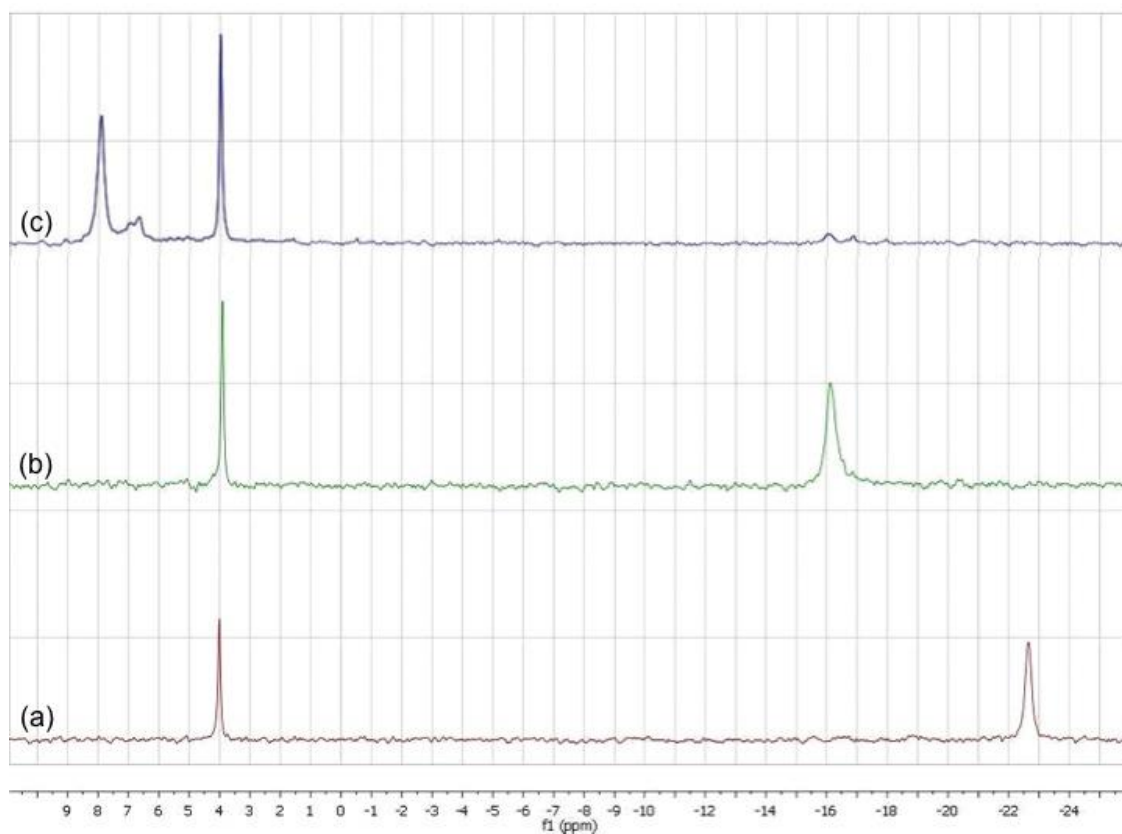
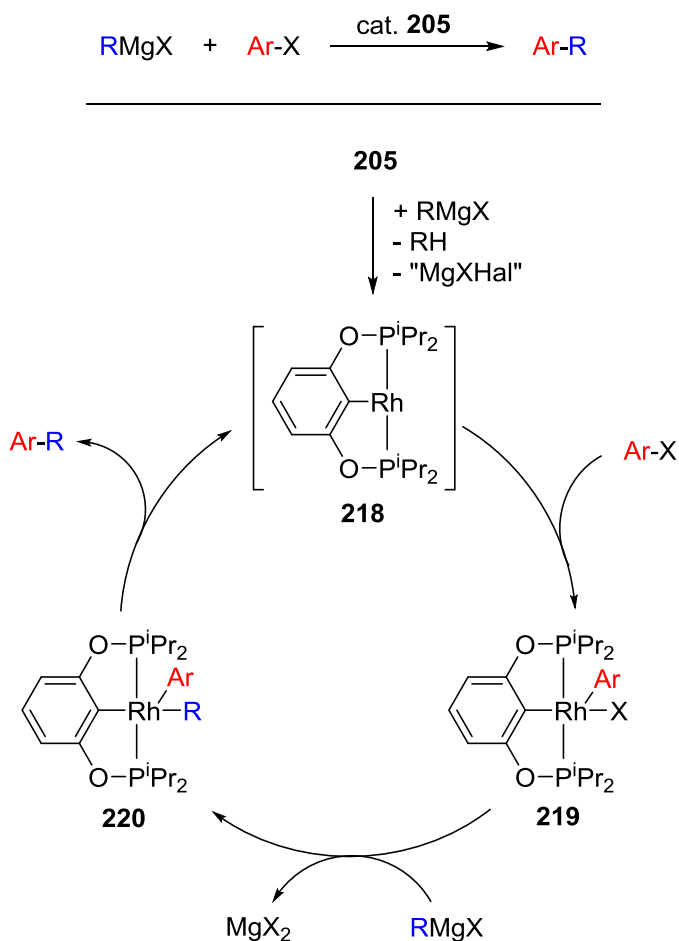


Figure 2-3. ^2H NMR spectra of deuterium exchange reactions. (collected in 1,4-dioxane) (a) Exchange of **205** with D_2O to give $(\text{POCOP})\text{Rh}(\text{D})(\text{Cl})$ (**215**). (b) 0.53 eq of **204** added to **215** to give **216**. (c) After overnight thermolysis of **215** at $115\text{ }^\circ\text{C}$ to give **216**.

2.2.2 Catalysis

We set out to test the $(\text{POCOP})\text{Rh}$ system for the catalytic coupling of Grignards with aryl halides (Scheme 2-5). We anticipated that **205** will provide access to the active three-coordinate species **218** via dehydrochlorination with the first equivalent of the Grignard and then follow the proposed catalytic cycle depicted in Scheme 2-5. This cycle is analogous to the $\text{Pd}(0)/\text{Pd}(\text{II})$ cycle:⁸⁵ aryl halide OA to form $(\text{POCOP})\text{Rh}(\text{Ar})(\text{X})$ (**219**), transmetallation with 1 equiv of Grignard to form

(POCOP)Rh(Ar)(R) (**220**), and RE to produce the C-C coupled product and regenerate **218**.



Scheme 2-5. Net reaction and proposed mechanism for Rh-catalyzed C–C coupling.

We employed **205** from the direct route in catalytic reactions despite impurities, because it was more simply obtained (Table 2-1). Catalytic reactions with impure **205** were carried out by Dr. Claudia Fafard during her doctoral work at Brandeis University. Catalytic coupling of PhMgBr with sterically unencumbered aryl iodides proceeded

rapidly with 1% catalyst loading with excellent yields and selectivity. The amount of undesired side products was 1% or less, on the order of the content of impurities in reagents. This reaction can also proceed selectively and to completion with 0.1% catalyst, albeit more slowly. The reaction with *o*-MeC₆H₄I proceeded sluggishly but could be brought to 88% yield of *o*-methylbiphenyl at 100 °C. However, in this case, 12% of homocoupling product was also observed. The reaction with *p*-MeC₆H₄Cl did not produce any coupling product and the reaction with *p*-FC₆H₄Br gave only a small yield of the desired *p*-fluorobiphenyl after 17 h at 100 °C.

Table 2-1. Summary of catalytic C–C coupling reactions.

| R ^a | Ar–X | Cat. (mol%) | T (°C) | Time | Products & Yields ^b |
|------------------------------------|--|----------------|--------|--------|--|
| Ph | <i>p</i> -FC ₆ H ₄ Br | 1 | 100 | 17 h | <i>p</i> -FC ₆ H ₄ Ph 20% |
| Ph | <i>p</i> -MeC ₆ H ₄ Cl | 1 | 100 | 20 h | NR |
| Ph | <i>p</i> -FC ₆ H ₄ I | 1 | 22 | 2 min | <i>p</i> -FC ₆ H ₄ Ph >99% (77%) |
| Ph | <i>p</i> -ClC ₆ H ₄ I | 1 | 22 | 5 min | <i>p</i> -ClC ₆ H ₄ Ph >99% (79%) |
| Ph | <i>p</i> -MeC ₆ H ₄ I | 1 | 22 | 3 min | <i>p</i> -MeC ₆ H ₄ Ph >99% (79%) |
| Ph | <i>p</i> -MeOC ₆ H ₄ I | 1 | 22 | 10 min | <i>p</i> -MeOC ₆ H ₄ Ph >99% (83%) |
| Ph | <i>o</i> -MeC ₆ H ₄ I | 1 | 100 | 20 h | <i>o</i> -MeC ₆ H ₄ Ph (82%) ^c ; Ph-Ph (11%) |
| Ph | <i>p</i> -FC ₆ H ₄ I | 0.1 | 90 | 20 h | <i>p</i> -FC ₆ H ₄ Ph >99% |
| Et | <i>p</i> -FC ₆ H ₄ I | 1 | 22 | 3 d | C ₆ H ₅ F; <i>p</i> -FC ₆ H ₄ Et; (<i>p</i> -FC ₆ H ₄) ₂ |
| Me ₃ SiCH ₂ | <i>p</i> -FC ₆ H ₄ I | 1 | 22 | 5 min | <i>p</i> -FC ₆ H ₄ CH ₂ SiMe ₃ >99% |
| PhMe ₂ CCH ₂ | <i>p</i> -FC ₆ H ₄ I | 1 | 22 | 18 h | <i>p</i> -FC ₆ H ₄ CH ₂ CMe ₂ Ph >97% (95%) |

^a RMgBr except the last two entries that are RMgCl. ^b Yields by NMR, isolated yields in parentheses. ^c Yield by GC-MS and NMR in a mixture.

We also tested alkyl Grignards. The reaction with EtMgBr with *p*-FC₆H₄I after 3 d at RT led to the formation of fluorobenzene and 4,4'-difluorobiphenyl in addition to the desired *p*-FC₆H₄Et. The presence of fluorobenzene is likely linked to the β-hydrogen elimination (BHE) from the intermediate Rh(III)-ethyl complex. When non-β-hydrogen containing Me₃SiCH₂MgCl and PhMe₂CCH₂MgCl were used, the desired alkyl-aryl coupling was readily and selectively accomplished at ambient temperature. The presence of homocoupling products does not necessarily indicate radical pathways. In some experiments with *p*-FC₆H₄I we detected formation of *p*-FC₆H₄MgX (¹⁹F NMR evidence, independently prepared from *p*-FC₆H₄I and ¹PrMgCl), ostensibly from Mg/I exchange, which may then engage in C-C coupling.

In order to ascertain the importance of the pincer ligand in catalysis, we have attempted to perform coupling of PhMgBr with *p*-FC₆H₄I using either [(COD)RhCl]₂ or a 1:2 mixture of [(COD)RhCl]₂ with Cy₃P as catalyst (1% mol Rh). Both reactions were much slower (only partial conversion after 1 h at 100 °C) and unselective. No C–C coupling took place between PhMgBr and *p*-FC₆H₄I in the absence of Rh. We think it is possible that the beneficial role of the pincer ligand is in facilitating access to the three-coordinate Rh(I) intermediate **218**, which is necessary for the OA step.

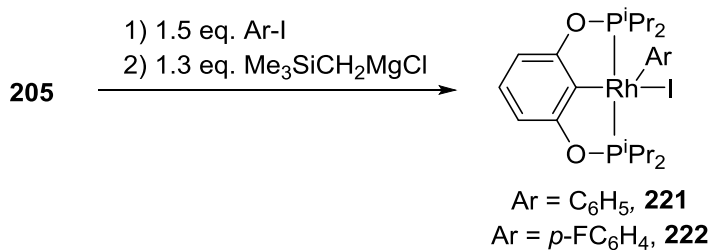
2.2.2.1 Role of Impurities in Catalysis

In order to evaluate the role of impurities in catalysis, we set up three experiments for the coupling of PhMgBr with *p*-FC₆H₄I using 0.5% mol Rh. The first experiment used pure **205**, and the other two used solutions of the same concentration of Rh prepared by thermolysis of **205** with (POCOP)H or with PhOPⁱPr₂ (containing

mixtures of **209-211** and **212-214**). The experiment with pure **205** displayed complete conversion 5 min after mixing, while the other two experiments registered only 3% and 9% conversion, respectively (by ^{19}F NMR spectroscopy). The solution with **204** reached 68% conversion in 24 h, and the solution with PhOP^iPr_2 reached 98% conversion in 2.5 h, displaying the same high selectivity as pure **205**. Thus, it appears that impurities such as **212-214** merely represent a version of the catalyst where presumably the extra phosphine donor blockades the coordination site needed for catalysis. Based on these results, the use of impure **205** should not be detrimental to catalysis besides the incremental loss of activity due to the lower content of the active catalyst.

2.2.3 Isolation of $(\text{POCOP})\text{Rh}(\text{Ar})(\text{X})$

We envisioned that if aryl iodide was used in excess, then the terminal Rh product of the catalytic reaction mixture would be a Rh(III) aryl iodide oxidative addition complex. Treatment of a mixture of 1.0 equiv of **205** and 1.5 equiv of an aryl iodide ($\text{C}_6\text{H}_5\text{I}$ or $p\text{-FC}_6\text{H}_4\text{I}$) with 1.3 equiv of $\text{Me}_3\text{SiCH}_2\text{MgCl}$ resulted in the isolation of $(\text{POCOP})\text{Rh}(\text{Ph})(\text{I})$ (**221**) or $(\text{POCOP})\text{Rh}(p\text{-C}_6\text{H}_4\text{F})(\text{I})$ (**222**) in *ca.* 85% yield after workup (Scheme 2-6). The solid-state structure of **221** was determined by X-ray diffraction methods (Figure 2-4). The structure exhibits a 5-coordinate Rh center with a slightly distorted square pyramidal geometry about Rh (apical Ph), with slight deviation of the iodide from the basal plane.⁶⁹



Scheme 2-6. Synthesis of (POCOP)Rh(Ar)(I).

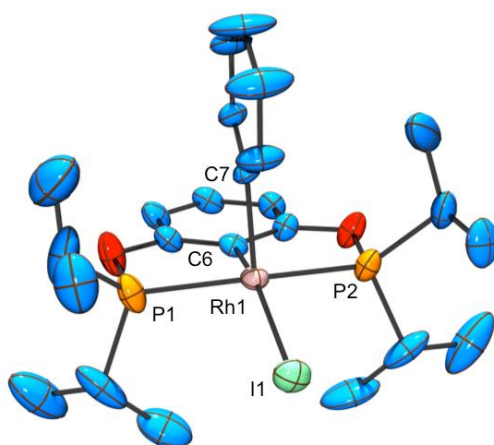


Figure 2-4. ORTEP drawing (50% thermal ellipsoids) of (POCOP)Rh(Ph)(I) (**221**).⁸⁴ Selected atom labeling. Hydrogen atoms are omitted for clarity. Selected bond distances (Å) and angles (deg): Rh1-P1, 2.341(3); Rh1-P2, 2.334(3); Rh1-C6, 2.037(9); Rh1-C7, 2.072(8); Rh1-I1, 2.792(2); P1-Rh1-P2, 159.33(10); C6-Rh1-I1, 159.8(2); C6-Rh1-C7, 87.1(4).

2.3 Conclusion

In summary, we have demonstrated that a (POCOP)Rh complex is a competent catalyst for the coupling of select aryl and alkyl Grignards with aryl iodides at RT. The pincer ligand is critical for the successful catalysis, which ostensibly operates *via* a Rh(I)/Rh(III) OA/RE cycle.

2.4 Experimental

2.4.1 General Considerations

Unless otherwise specified, all manipulations were performed under an argon atmosphere using standard Schlenk line or glove box techniques. Toluene, THF, pentane, and isooctane were dried and deoxygenated (by purging) using a solvent purification system and stored over molecular sieves in an Ar-filled glove box. C₆D₆ and hexanes were dried over and distilled from NaK/Ph₂CO/18-crown-6 and stored over molecular sieves in an Ar-filled glove box. Fluorobenzene was dried with and then distilled or vacuum transferred from CaH₂. (POCOP)H (**204**) and PhOPⁱPr₂ were synthesized according to published procedures.^{86,87} Synthesis of (POCOP)Rh(H)(Cl) (**205**) from **204** and [(COE)₂RhCl]₂ was accomplished according to the literature procedure.⁸³ All other chemicals were used as received from commercial vendors. NMR spectra were recorded on a Varian iNova 300 (¹H NMR, 299.951 MHz; ¹³C NMR, 75.426 MHz, ³¹P NMR, 121.422 MHz, ¹⁹F NMR, 282.211 MHz) spectrometer. ²H NMR spectra were recorded on a Varian iNova 400 (²H NMR, 61.333 MHz). Chemical shifts are reported in δ (ppm). For ¹H and ¹³C NMR spectra, the residual solvent peak was used as an internal reference. ³¹P NMR spectra were referenced externally using 85% H₃PO₄ at δ 0 ppm. ¹⁹F NMR spectra were referenced externally using 1.0 M CF₃CO₂H in CDCl₃ at -78.5 ppm. ²H NMR spectra were referenced externally using C₆D₆ at δ 7.15 ppm. Elemental analyses were performed by CALI Labs, Inc. (Parsippany, NJ).

2.4.2 Stoichiometric Reactions

Direct synthesis of (POCOP)Rh(H)(Cl) (205) by reaction of [(COD)RhCl]₂ with (POCOP)H (204) in toluene. In a J. Young tube, [(COD)RhCl]₂ (38.5 mg, 0.077 mmol) was combined with **204** (52.4 mg, 0.154) and dissolved in toluene. The reaction was heated in a 150 °C oil bath overnight producing a dark red-brown solution. The solution was passed through a pad of Celite and the volatiles were removed. Analysis by ³¹P{¹H} NMR indicates 47% of **205**, 45% of one impurity (assigned as **212**), and another impurity (8%). ³¹P{¹H} NMR (C₆D₆): δ 197.4 (dd, *J*_{Rh-P} = 161 Hz, *J*_{P-P} = 16 Hz, **212**), 185.7 (d, *J*_{Rh-P} = 122 Hz, **205**), 182.2 (dt, *J*_{Rh-P} = 149 Hz, *J*_{P-P} = 16 Hz, **212**), 157.9 (d, *J*_{Rh-P} = 105 Hz).

Synthesis of (POCOP)Rh(H)(Cl)(py) (206). In a Schlenk flask [(cod)RhCl]₂ (353 mg, 1.04 mmol) was combined with **204** (256 mg, 0.512 mmol) and dissolved in pyridine. The reaction was heated for 3 h at 80 °C producing a light yellow solution. The solution was passed through Celite and the volatiles were removed. A yellow-white solid was collected (453 mg, 78% yield) by recrystallization in a minimum of fluorobenzene layered with pentane and dried under vacuum. ³¹P{¹H} NMR (C₆D₆): δ 181.3 (d, *J*_{Rh-P} = 120 Hz); ¹H NMR (C₆D₆): δ 10.32 (bs, 1H, Py-*H*), 7.72 (bs, 1H, Py-*H*), 6.90 (t, 1H, Ar-*H*, 7.2 Hz), 6.82(s, 1H, Py-*H*), 6.75 (d, 2H, Ar-*H*, 7.5 Hz), 6.63 (bs, 1H, Py-*H*), 6.12 (bs, 1H, Py-*H*), 2.33 (m, 2H, CHMe₂), 1.91 (m, 2H, CHMe₂), 1.42 (q, 6H, CHMe₂, 7.5 Hz), 1.22 (q, 6H, CHMe₂, 7.5 Hz), 1.06 (q, 6H, CHMe₂, 7.4 Hz), 1.00 (q, 6H, CHMe₂, 7.5 Hz), -16.58 (dt, 1H, Rh-*H*, *J*_{Rh-H} = 24.6, *J*_{P-H} = 5.7 Hz); ¹³C (C₆D₆): δ 164.3 (t, 7.3 Hz, Ar), 152.6 (Py), 150.8 (Py), 136.5 (Py), 133.8 (dt, *J*_{P-C} = 31 Hz, *J*_{Rh-C} = 5.5 Hz, Ar),

125.4 (Ar), 124.1 (Ar), 123.9 (Py), 105.7 (t, 6.1 Hz, Py), 30.4 (dt, $J_{\text{Rh-C}} = 85$ Hz, $J_{\text{P-C}} = 11$ Hz), 17.9, 17.4 (t, 4.9 Hz), 16.7 (t, 2.4 Hz), 16.0.

Synthesis of (POCOP)Rh(H)(Cl)(NCMe) (207). **204** (675 mg, 1.98 mmol) and [(COD)RhCl]₂ (495 mg, 0.99 mmol) were combined in a Schlenk flask and dissolved in acetonitrile. The reaction was heated at 100 °C overnight, resulting in a color change to a yellow-white solution. The reaction was filtered through a pad of Celite and volatiles were removed by vacuum. The solid was recrystallized from acetonitrile at -35 °C to give **206** as a clean white solid (640 mg, 63%). ³¹P{¹H} NMR (C₆D₆): δ 183.4 (d, $J_{\text{Rh-P}} = 115$ Hz); ¹H NMR (C₆D₆): δ 6.80 (t, 9.0 Hz, 1H, P^OC^OP), 6.68 (d, 8.0 Hz, 2H, P^OC^OP), 3.01 (bs, 2H, CHMe₂), 2.31 (m, 2H, CHMe₂), 1.45 (q, 7.2 Hz, 6H, CHMe₂), 1.39 (q, 7.2 Hz, 6H, CHMe₂), 1.20 (q, 7.2 Hz, 6H, CHMe₂), 1.13 (q, 7.2 Hz, 6H, CHMe₂), 0.54 (s, 3H, NCMe), -18.19 (bs, Rh-H).

Synthesis of (POCOP)Rh(H)(Cl) (205) from 206. In a Schlenk flask **206** (200 mg, 360 μmol) was partially dissolved in a 5:1 mixture of pentane:toluene. BF₃-OEt₂ (60 μL, 478 μmol) was added to the flask resulting in a color change from light yellow to red. After stirring 3 h at RT, the solution was left without stirring for 3 h. The resultant mixture was passed through a pad of Celite and then through a thin pad of silica gel. The volatiles were removed. An orange-red solid was collected (101 mg, 59% yield) and dried under vacuum. An X-ray quality single crystal was obtained from the 5:1 pentane:toluene solution at RT. ³¹P{¹H} NMR (C₆D₆): δ 185.7 (d, $J_{\text{Rh-P}} = 122$ Hz); ¹H NMR (C₆D₆) 6.84 (t, 1H, Ar-H, 5.4 Hz), 6.68 (d, 2H, Ar-H, 6.3 Hz), 2.45 (m, 2H, CHMe₂), 2.11 (m, 2H, CHMe₂), 1.23 (q, 6H, CHMe₂, 5.4 Hz), 1.16 (q, 6H, CHMe₂, 5.1

Hz), 1.05 (m, 12H, CHMe₂), -25.32 (dt, 1H, Rh-H, $J_{\text{Rh-H}} = 43.5$, $J_{\text{P-H}} = 12.6$ Hz); ¹³C{¹H} NMR (C₆D₆): δ 166.7 (t, $J_{\text{P-C}} = 7.4$ Hz, Ar), 128.5 (s, Ar), 126.5 (s, Ar), 106.1 (t, $J_{\text{P-C}} = 5.4$ Hz, Ar), 29.7 (t, $J_{\text{P-C}} = 11.0$ Hz, PCH(CH₃)₂), 28.2 (t, $J_{\text{P-C}} = 12.8$ Hz, PCH(CH₃)₂), 17.2 (s, PCH(CH₃)₂), 17.1 (s, PCH(CH₃)₂), 16.7 (s, PCH(CH₃)₂), 16.2 (s, PCH(CH₃)₂). Elem. Anal. Calc. for C₁₈H₃₂ClO₂P₂Rh: C, 44.97; H, 6.71. Found: C, 44.90; H, 6.67%.

Reaction of (POCOP)Rh(H)(Cl) (5) with pyridine to give 206. In a J. Young tube, **205** (15.2 mg, 0.031 mmol) was dissolved in pyridine. The reaction instantly became light yellow. The solution was passed through a pad of Celite and the volatiles removed leaving a yellow-white solid. ³¹P{¹H} and ¹H NMR were identical to the sample of **206** obtained from its synthesis by the reaction of **204** with [(COD)RhCl]₂ in pyridine.

Synthesis of (POCOP)Rh(H)(OAc) (208). **207** (200 mg, 0.385 mmol) and NaOAc (300 mg, 3.65 mmol) were combined in a Schlenk flask and dissolved in dioxane. The reaction was heated at 100 °C for 3 h. Analysis of the ³¹P{¹H} NMR spectrum shows complete conversion of the starting material to one major product (80%) with several minor side products. The reaction was filtered through Celite and the volatiles were removed by vacuum. The solid was recrystallized from pentane at -35 °C to give **208** as a yellow solid (85% purity). ³¹P{¹H} NMR (C₆D₆): δ 183.8 (d, $J_{\text{RhP}} = 124$ Hz); ¹H NMR (C₆D₆): δ 6.81 (t, 7.2 Hz, 1H, P^OC^OP), 6.66 (d, 8.4 Hz, 2H, P^OC^OP), 2.36 (m, 2H, CHMe₂), 2.09 (m, 2H, CHMe₂), 1.92 (s, 3H, OAc), 1.25 (m, 12H, CHMe₂), 1.11 (m, 12H, CHMe₂), -21.34 (dt, $J_{\text{RhH}} = 28$ Hz, $J_{\text{PH}} = 12$ Hz, Rh-H).

Synthesis of (POCOP)Rh(H)(Cl) (205) from 208. **208** (50 mg, 0.025 mmol, 85% purity) was added to a J. Young tube and dissolved in C₆D₆. CH₃Si-Cl (16 μL, 0.13 mmol) was added to the sample resulting in an immediate color change to red. Analysis of the reaction by ³¹P NMR and ¹H NMR spectroscopy after 20 min at RT shows **205** as the major product (89%) and the appearance of Me₃SiOAc.

Reaction of (POCOP)Rh(H)(Cl) (205) with (POCOP)H (204): observation of compounds 209, 210, 212. In a J. Young tube, **205** (21.2 mg, 0.044 mmol) was combined with **204** (9.1 μL, 0.027 mmol) and dissolved in C₆D₆. An instant color change to a light yellow-orange occurred. Analysis by ³¹P{¹H} NMR spectroscopy indicated conversion to two new products in a 9:1 ratio. The major product is assigned as **209**, minor as **210**. ³¹P{¹H} NMR (C₆D₆) Major (**209**): δ 187.1 (dd, *J*_{Rh-P} = 112 Hz, *J*_{P-P} = 20 Hz), 173.2 (dt, *J*_{Rh-P} = 108 Hz, *J*_{P-P} = 20 Hz). ¹H NMR (C₆D₆): δ -16.34 (m, 1 H, Rh-H). ³¹P{¹H} NMR (C₆D₆) Minor (**210**): δ 175.8 (dt, *J*_{Rh-P} = 105 Hz, *J*_{P-P} = 16 Hz), 170.8 (dt, *J*_{Rh-P} = 105 Hz, *J*_{P-P} = 16 Hz). ³¹P{¹H} NMR data also showed the presence of uncoordinated phosphine at 151.8 ppm, probably belonging to **210**. The solution was heated in a 125 °C oil bath overnight resulting in the color darkening slightly and 75% conversion to a new product. The new major product is assigned as **212**. **213** could not be reliably identified in the mixture. ³¹P{¹H} NMR (C₆D₆): δ 197.4 (dd, *J*_{Rh-P} = 161 Hz, *J*_{P-P} = 16 Hz), 182.2 (dt, *J*_{Rh-P} = 149 Hz, *J*_{P-P} = 16 Hz). Additional heating (140 °C, 2 d) did not result in additional conversion to **212**.

Reaction of 205 with PhOPⁱPr₂: observation of compounds 211 and 214. In a J. Young tube, **205** (24.1 mg, 0.050 mmol) was combined with PhOPⁱPr₂ (11.0 μL, 0.050

mmol) and dissolved in C_6D_6 . An instant color change to a light yellow solution occurred. $^{31}P\{^1H\}$ NMR analysis indicated conversion to a single product, assigned as **211**. $^{31}P\{^1H\}$ NMR (C_6D_6): δ 187.1 (dd, $J_{Rh-P} = 108$ Hz, $J_{P-P} = 16$ Hz), 172.5 (dt, $J_{Rh-P} = 105$ Hz, $J_{P-P} = 16$ Hz); 1H NMR (C_6D_6): δ 6.91 (m, 8 H, Ar-*H*), 3.90 (m, 2H, *CHMe*₂) 2.28 (m, 2H, *CHMe*₂), 2.02 (m, 2H, *CHMe*₂), 1.30 (m, 36 H, *CHMe*₂), -16.32 (m, 1H, Rh-*H*). The sample was heated in a 125 °C oil bath overnight resulting in approximately 50% conversion to a new product with some unreacted **211** remaining, as indicated by $^{31}P\{^1H\}$ NMR. The new product is assigned as **214**. $^{31}P\{^1H\}$ NMR (C_6D_6) for **214**: δ 197.5 (dd, $J_{Rh-P} = 161$ Hz, $J_{P-P} = 16$ Hz), 182.3 (dt, $J_{Rh-P} = 149$ Hz, $J_{P-P} = 16$ Hz). Another unidentified product gave rise to an additional dd at 197.0 ppm; however, the presumed other resonance for this compound could not be identified (likely contained underneath the dt of **211** at 172.5 ppm). Further heating (140 °C, 3 d) did not result in additional conversion to **214**.

Deuterium exchange reactions involving 215, 216, and 217. In a J. Young tube **205** (22.6 mg, 0.0472 mmol) was dissolved in C_6D_6 and heated in a 120 °C oil bath overnight. 2H NMR spectroscopy indicated no exchange. A small amount (ca. 1 mL) of fluorobenzene saturated with D_2O was added to the sample and heated overnight in a 120 °C oil bath. The volatiles were removed in vacuo and the sample was redissolved in toluene. The 2H NMR spectrum displayed a sharp singlet at -25.4 ppm indicating formation of (POCOP)Rh(D)(Cl) (**215**). The volatiles were removed from this solution in vacuo and the residue redissolved in 1,4-dioxane, shifting the 2H NMR signal to -22.6 ppm. (POCOP)H (**204**) (8.5 μ L, 0.025 mmol) was added to the sample. 2H NMR

spectrum after the addition displayed a singlet at -16.1 ppm indicating the formation of **216**. The sample was heated in a 115 °C oil bath overnight. The ^2H NMR spectrum displayed a new signal at 7.9 ppm (assigned to **217**) in the aromatic region as the major resonance.

Synthesis of (POCOP)Rh(C₆H₅)(I) (221). In a J. Young tube **205** (28.8 mg, 0.603 mmol), *p*-FC₆H₅I (10.1. μL, 0.903 mmol), and (CH₃)₃SiCH₂MgCl (80 μL, 0.080 μL) were combined and dissolved in C₆D₆. This resulted in an instant color change from orange to dark purple. The volatiles were removed in vacuo and the residue was recrystallized by dissolving in toluene and layering with pentane at -35 °C, giving a purple solid (33.1 mg, 84.7% yield). X-ray quality crystals were also obtained from toluene/pentane solution. $^{31}\text{P}\{^1\text{H}\}$ (C₆D₆): δ 176.8 (d, $J_{\text{Rh-P}} = 120$ Hz); ^1H NMR (C₆D₆): 8.03 (bs, 1H, Ph-*H*), 6.94 (t, 1H, Ar-*H*, 7.6 Hz), 6.77 (d, 2H, Ar-*H*, 7.8 Hz), 6.59 (bs, 1H, Ph-*H*), 6.53 (t, 1H, Ph-*H*, 6.9 Hz), 6.30 (bs, 1H, Ph-*H*), 5.99 (bs, 1H, Ph-*H*), 2.81 (m, 2H, CHMe₂), 2.10 (m, 2H, CHMe₂), 1.13 (m, 12H, CHMe₂), 1.01 (q, 6H, CHMe₂, 6.7 Hz), 0.75 (q, 6H, CHMe₂, 7.2 Hz); ^{13}C (C₆D₆): δ 164.6 (t, 6.1 Hz, Ar), 146.1 (dt, $J_{\text{Rh-C}} = 36$ Hz, $J_{\text{P-C}} = 9.1$ Hz, Ph), 141.6 (dt, $J_{\text{Rh-C}} = 35$ Hz, $J_{\text{P-C}} = 4.8$ Hz, Ar), 136.2 (Ph), 128.6 (Ar), 127.1 (Ar), 124.3 (Ph), 107.2 (t, 6.1 Hz, Ph), 31.8 (t, 11 Hz), 28.5 (t, 13 Hz), 18.1, 17.0, 16.6, 16.2. Elem. Anal. Calc. for C₂₄H₃₆IO₂P₂Rh: C, 44.46; H, 5.60. Found: C, 44.28; H, 5.45%.

Synthesis of (POCOP)Rh(C₆H₄F-*p*)(I) (222). In a J. Young tube **5** (28.9 mg, 0.060 mmol) was combined with *p*-FC₆H₄I (11.2 μL, 0.0971 mmol) and dissolved in C₆D₆. (CH₃)₃SiCH₂MgCl (81 μL, 0.081 mmol) was added to the sample resulting in an

instant color change from orange to dark purple. Analysis by ^{19}F NMR shows the presence of unreacted $\text{FC}_6\text{H}_4\text{I}$ (-115.5 ppm), $\text{FC}_6\text{H}_4\text{CH}_2\text{Si}(\text{CH}_3)_3$ (-120.9 ppm), and a signal at -121.8 ppm. The volatiles were removed in vacuo and the residue was redissolved in C_6D_6 , resulting in only the signal at -121.8 ppm remaining in the ^{19}F NMR. The volatiles were again removed in vacuo and the residue was recrystallized by dissolving in toluene and layering with pentane at $-35\text{ }^\circ\text{C}$, giving a purple solid (35 mg, 87% yield). $^{31}\text{P}\{^1\text{H}\}$ (C_6D_6): δ 176.4 (d, $J_{\text{Rh-P}} = 119\text{ Hz}$); ^1H NMR (C_6D_6): 7.91 (bs, 1H, Ph-H), 6.94 (t, 1H, Ar-H, 8.4 Hz), 6.75 (d, 2H, Ar-H, 8.4 Hz), 6.37 (bs, 1H, Ph-H), 6.05 (bs, 1H, Ph-H), 5.82 (bs, 1H, Ph-H), 2.28 (m, 2H, CHMe_2), 2.05 (m, 2H, CHMe_2), 1.11 (m, 12H, CHMe_2), 0.98 (q, 6H, CHMe_2 , 6.9 Hz), 0.71 (q, 6H, CHMe_2 , 7.8 Hz); ^{19}F NMR (C_6D_6): -121.8 (s, Ph-F). ^{13}C (C_6D_6): δ 164.6 (t, 6.1 Hz, Ar), 162.6 (Ph), 159.3 (Ar), 141.5 (dt, $J_{\text{Rh-C}} = 35\text{ Hz}$, $J_{\text{P-C}} = 6.0\text{ Hz}$, Ph), 136.6 (dt, $J_{\text{Rh-C}} = 37\text{ Hz}$, $J_{\text{P-C}} = 7.5\text{ Hz}$, Ar), 127.3 (Ph), 113.9 (Ph), 107.0 (t, 6.1 Hz, Ph), 31.8 (t, 11 Hz), 28.5 (t, 15 Hz), 18.0, 17.0, 16.5, 16.2.

2.4.3 Catalytic Reactions

Catalytic coupling reaction of $p\text{-FC}_6\text{H}_4\text{Br}$ and PhMgBr with impure **205 as catalyst.** **205** (5.7 mg, 0.012 mmol) was dissolved in $p\text{-FC}_6\text{H}_4\text{Br}$ (400 μL , 1.20 mmol) followed by addition of PhMgBr (135 μL , 1.23 mmol). The solution was heated at $100\text{ }^\circ\text{C}$ for 18 h. Analysis of the solution by ^{19}F NMR spectroscopy revealed $p\text{-FC}_6\text{H}_4\text{Br}$ (80%) and $p\text{-fluorobiphenyl}$ (20%).

Catalytic coupling reaction of $p\text{-FC}_6\text{H}_4\text{I}$ and PhMgBr with impure **205 as catalyst.** **205** (5.8 mg, 0.012 mmol) was dissolved in $p\text{-FC}_6\text{H}_4\text{I}$ (138.4 μL , 1.2 mmol)

followed by addition of PhMgBr (400 μ L, 1.2 mmol). The solution began to boil, a precipitate was formed and the solution became brown in color. Once the solution had stopped bubbling, analysis by ^{19}F NMR spectroscopy of the solution displayed only one resonance at -118.9 ppm. The solution was passed through a pad of silica gel and volatiles removed under vacuum. *p*-Fluorobiphenyl (159 mg, 77 %) was isolated as a very light pink solid. ^1H NMR (CD_3) $_2\text{CO}$: δ 7.68 (m, 2H, Ar-*H*), 7.62 (d, 2H, *J* = 8 Hz, Ar-*H*), 7.45 (t, 2H, *J* = 7 Hz, Ar-*H*), 7.36 (t, 1H, *J* = 7 Hz, Ar-*H*), 7.22 (t, 2H, *J* = 8 Hz, Ar-*H*). ^{19}F NMR (CD_3) $_2\text{CO}$: δ -116.6.

Catalytic coupling reaction of *p*-MeC₆H₄Cl and PhMgBr with impure **205 as catalyst.** **205** (5.8 mg, 0.012 mmol) was dissolved in *p*-MeC₆H₄Cl (142.0 μ L, 1.2 mmol) followed by addition of PhMgBr (400 μ L, 1.2 mmol). No immediate change observed. A ^1H NMR spectrum was taken (unlocked) and only starting material was observed. The solution was heated at 100 $^\circ\text{C}$ for 20 h. No new products observed by NMR.

Catalytic coupling reaction of *p*-MeC₆H₅I and PhMgBr with impure **205 as catalyst.** In a screw capped vial with a stir bar, *p*-MeC₆H₄I (262 mg, 1.2 mmol), PhMgBr (3.0 M in Et₂O, 400 μ L, 1.2 mmol) and **205** (5.8 mg, 0.012 mmol) were combined and dissolved in toluene (2 mL). Immediately the solution became dark in red then changed to brown and began to boil. A precipitate was observed. Once the solution appeared to stop boiling, in *ca.* 2-3 min the vial was brought out of the box, the solution passed through a plug of silica gel and extracted with pentane. A white fluffy solid was collected, *p*-methylbiphenyl (159 mg, 79% yield). ^1H NMR (CD_3) $_2\text{CO}$: δ 7.62 (d, 2H, *J*

= 8 Hz Ar-*H*), 7.53 (d, 2H, *J* = 7 Hz, Ar-*H*), 7.43 (t, 2H, *J* = 8 Hz, Ar-*H*), 7.32 (t, 1H, *J* = 7 Hz, Ar-*H*), 7.26 (d, 2H, *J* = 7 Hz, Ar-*H*), 2.36 (s, 3H, Ar-*Me*). GC-MS (EI) *m/z*: 168.

Catalytic coupling reaction of *p*-MeOC₆H₄I and PhMgBr with impure **205 as catalyst.** In a screw capped vial with stir bar *p*-MeOC₆H₄I (281 mg, 1.2 mmol), PhMgBr (3.0 M in Et₂O, 400 μL, 1.2 mmol) and **205** (5.8 mg, 0.012 mmol) were combined. Immediately the solution became dark in color. The vial began to warm and bubbles were observed for ca. 10 min. The vial was brought out of the box, the solution passed through a plug of silica gel and extracted with pentane. A very light pink fluffy solid was collected, *p*-methoxybiphenyl (182 mg, 83%). ¹H NMR (CD₃)₂CO: δ 7.60 (m, 4H, Ar-*H*), 7.42 (t, 2H, *J* = 7 Hz, Ar-*H*), 7.30 (t, 1H, *J* = 7 Hz, Ar-*H*), 7.01 (d, 2H, *J* = 8 Hz, Ar-*H*), 3.83 (s, 3H, *OMe*).

Catalytic coupling reaction of *p*-ClC₆H₄I and PhMgBr with impure **205 as catalyst.** In a screw capped vial with a stir bar, *p*-ClC₆H₄I (286 mg, 1.2 mmol), PhMgBr (3.0 M in Et₂O, 400 μL, 1.2 mmol) and **205** (5.8 mg, 0.012 mmol) were combined. Immediately the solution began to heat up and became dark red in color. Reaction appeared complete after ca. 5 min. The vial was brought out of the box, the solution passed through a plug of silica gel and extracted with pentane. A very light pink fluffy solid was collected, *p*-chlorobiphenyl (178 mg, 79%). ¹H NMR (CD₃)₂CO: δ 7.66 (m, 4H, Ar-*H*), 7.47 (m, 4H, Ar-*H*), 7.38 (t, 1H, *J* = 8 Hz, Ar-*H*).

Catalytic coupling reaction of *o*-MeC₆H₄I and PhMgBr with impure **205 as catalyst.** In a screw capped vial with a stir bar, *o*-MeC₆H₄I (153 μL, 1.2 mmol), PhMgBr (3.0 M in Et₂O, 400 μL, 1.2 mmol) and **205** (5.8 mg, 0.012 mmol) were combined. The

solution was orange in color. The solution did not warm up. It was heated at 100 °C for 20 h. The solution had turned dark brown in color. The vial was brought out of the box, the solution passed through a plug of silica gel and extracted with pentane. A clear liquid was collected (186 μ L). ^1H NMR and GC-MS analysis showed that it was a mixture of 88% of the desired *o*-phenyltoluene product and 12% biphenyl. GC-MS: m/z 168 (*o*-phenyltoluene), 154 (biphenyl). In the ^1H NMR spectrum most of the aryl signals for both compounds are overlapped. To determine the percentages by ^1H NMR the integration ratios of the doublet at 7.65 ppm for biphenyl and the singlet at 2.24 ppm for *o*-phenyltoluene were used. Assuming density of 1.0 g/mL (density of 3-phenyltoluene, which is a liquid at RT is 1.02 g/mol, according to Aldrich), these results correspond to 82% yield of *o*-phenyltoluene and 11% yield of biphenyl.

Catalytic coupling reaction of *p*-FC₆H₄I and PhMgBr with impure **205 at 0.1% catalyst loading.** In a J. Young tube *p*-FC₆H₄I (138.4 μ L, 1.2 mmol), PhMgBr (3.0 M in Et₂O, 400 μ L, 1.2 mmol) and **205** (0.040 M in C₆D₆, 30 μ L, 0.0012 mmol) were combined. A ^{19}F NMR spectrum was collected upon mixing. Observed *p*-FC₆H₄I (97%) and 4-fluorobiphenyl (3%). After heating the mixture at 90 °C for 1 h, ^{19}F NMR analysis revealed the presence of *p*-FC₆H₄I (78%), 4-fluorobiphenyl (21%) and a trace of another compound resonating at -118.5 ppm. This resonance is consistent with *p*-FC₆H₄MgX. A similar resonance observed when *p*-FC₆H₄I was treated with $^i\text{PrMgCl}$. The solution was heated for a total of 20 h at 90 °C, resulting in >99% of *p*-fluorobiphenyl and <1% *p*-FC₆H₄MgX. The solution solidified upon cooling. GC-MS $m/z = 172$.

Catalytic coupling reaction of *p*-FC₆H₄I and EtMgBr with impure 205 as catalyst. 205 (14.3 μL of a 0.042 M solution in C₆D₆, 6.0x10⁻⁴ mmol), *p*-FC₆H₄I (138.4 μL, 1.2 mmol) and EtMgBr (3.0 M in Et₂O, 400 μL, 1.2 mmol) were combined. The solution became yellow gray in color. The solution was heated at 95 °C for 1 h. The solution was passed through silica gel and analyzed by GC-MS. The analysis revealed the presence of fluorobenzene, *p*-fluoroethylbenzene, *p*-FC₆H₄I and 4,4'-fluorobiphenyl.

Catalytic coupling reaction of *p*-FC₆H₄I and Me₃SiCH₂MgCl with impure 205 as catalyst. 205 (5.8 mg, 0.012 mmol), *p*-FC₆H₄I (138 μL, 1.2 mmol) and Me₃SiCH₂MgCl (1 M in Et₂O; 1.2 mL, 1.2 mmol) were combined. The solution warmed to the touch. Analysis of the solution by ¹⁹F NMR spectroscopy revealed only one resonance at -121.0 ppm. The solution was passed through a pad of silica gel and the volatiles removed under vacuum. *p*-Fluorobenzyltrimethylsilane was isolated as a tan colored oily solid. ¹H NMR (C₆D₆): δ 7.05 (t, 2H, Ar-H), 6.92 (m, 2H, Ar-H), 2.05 (2H, CH₂), 0.15 (9H, SiMe₃); ¹⁹F NMR (C₆D₆): δ -120.3 ppm.

Catalytic coupling reaction of *p*-FC₆H₄I and PhMe₂CCH₂MgCl with impure 205 as catalyst. 205 (2.9 mg, 0.006 mmol), *p*-FC₆H₄I (69.2 μL, 0.6 mmol) and (*o*-methyl-*o*-phenylpropyl)MgCl (0.5 M in Et₂O; 1.2 mL, 0.6 mmol) were combined. The solution became red in color. Analysis of the solution by ¹⁹F spectroscopy showed > 80% *p*-FC₆H₄I and ca. 20% of a new product. The solution was left at room temp. for 18 h. The solution changed to yellow in color and a precipitate had formed. The solution was passed through a pad of silica gel and the volatiles removed under vacuum. *p*-fluoro-(*o*-methyl-*o*-phenylpropyl)benzene was isolated as a tan colored oil (130 mg,

95%). ^1H NMR (C_6D_6): δ 7.21-7.00 (5H, Ar-H), 6.65 (t, 2H, Ar-H), 6.48 (m, 2H, Ar-H), 2.58 (2H, CH_2), 1.20 (6H, CMe_2); ^{19}F NMR (C_6D_6): δ -117.4 ppm.

Control catalytic reaction using $[(\text{COD})\text{RhCl}]_2/\text{PCy}_3$. $[(\text{COD})\text{RhCl}]_2$ (3.0 mg, 0.012 mmol) was combined with PCy_3 (6.8 mg, 0.024 mmol) and C_6D_6 (~0.2 mL) in a J. Young tube. This was followed by addition of *p*- $\text{FC}_6\text{H}_4\text{I}$ (138 μL , 1.2 mmol) and PhMgBr (3.0 M in Et_2O , 400 μL , 1.2 mmol). The solution became orange in color. ^{19}F NMR analysis showed only *p*- $\text{FC}_6\text{H}_4\text{I}$ present. The solution was placed in a 100 $^\circ\text{C}$ oil bath for 1 h. ^{19}F NMR analysis showed the presence of ~25% *p*- $\text{FC}_6\text{H}_4\text{I}$, 25% *p*- $\text{FC}_6\text{H}_4\text{MgX}$ and 50% *p*-fluorobiphenyl and 4,4'-fluorobiphenyl (signals overlap). The solution was heated an additional 17 h. ^{19}F NMR spectroscopy indicated that no more *p*- $\text{FC}_6\text{H}_4\text{I}$ was left. The solution was passed through a pad of silica gel. GC-MS analysis of the solution revealed the presence of *p*-fluorobiphenyl, 4,4'-fluorobiphenyl and biphenyl.

Control catalytic reaction using $[(\text{COD})\text{RhCl}]_2$. $[(\text{COD})\text{RhCl}]_2$ (3.0 mg, 0.012 mmol) in a J. Young tube with *p*- $\text{FC}_6\text{H}_4\text{I}$ (138 μL , 1.2 mmol) and PhMgBr (3.0 M in Et_2O , 400 μL , 1.2 mmol). The solution became orange in color. ^{19}F NMR analysis showed only *p*- $\text{FC}_6\text{H}_4\text{I}$ present. The solution was placed in a 100 $^\circ\text{C}$ oil bath for 1 h. ^{19}F NMR analysis showed the presence of ~36% *p*- $\text{FC}_6\text{H}_4\text{I}$, 40% *p*- $\text{FC}_6\text{H}_4\text{MgX}$ and 20% *p*-fluorobiphenyl and 4,4'-fluorobiphenyl (signals overlap).

Preparation of stock solutions containing 204/205, 209/212, and 211/214 for the catalytic testing of impurities. Catalytic reactions were performed using 0.040 M stock solutions of **205** (Solution A), thermolyzed mixture of **205** and **204** (containing primarily **209** and **212**, Solution B), and thermolyzed mixture of **205** and PhOP^iPr_2

(containing primarily **211** and **214**, Solution C). The 0.040 M stock solution of **205** (Solution A) was prepared by dissolving **205** (57 mg, 0.120 mmol) in C₆D₆ (3.0 mL). The other two stock solutions were prepared directly from the 0.040 M solution of **205**. Solution B was prepared by combining **204** (8.2 μL, 0.024 mmol) with the 0.040 M solution of **205** (1.0 mL, 0.040 mmol Rh) and heating overnight at 120 °C. Solution C was prepared by combining PhOPⁱPr₂ (4.0 μL, 0.043 mmol) with the 0.040 M solution of **205** (1.0 mL, 0.040 mmol Rh) and heating overnight at 120 °C.

Catalytic coupling reaction of *p*-FC₆H₄I and PhMgBr with Solution A, 0.5% catalyst loading. In a J. Young *p*-FC₆H₄I (138 μL, 1.20 mmol) and Solution A (0.040 M Rh in C₆D₆, 150 μL, 0.0060 mmol) were combined. PhCF₃ (50 μL) was added to the sample as an internal standard. ¹⁹F NMR analysis indicated a 57:43 ratio of PhCF₃ (-63.1 ppm) to *p*-FC₆H₄I (-115.5 ppm). Additional C₆D₆ (1.5 mL) was added to help contain the heat evolved during the reaction and prevent evaporation of PhCF₃ and then PhMgBr (2.5 M in Et₂O, 480 μL, 1.2 mmol) was added to the reaction. The solution became hot to touch with some bubbling and became dark orange-brown in color. Analysis of the solution by ¹⁹F NMR spectroscopy after 5 min indicated a 56:44 ratio of PhCF₃ to FC₆H₄-C₆H₅ (-116.9 ppm). Minor impurities do appear in the ¹⁹F NMR spectrum, one at -116.5 ppm (0.5 %) and one at -117.4 ppm (0.5 %).

Catalytic coupling reaction of *p*-FC₆H₄I and PhMgBr with Solution B, 0.5% catalyst loading. In a J. Young tube, *p*-FC₆H₄I (138 μL, 1.20 mmol) and Solution B (0.040 M in C₆D₆, 150 μL, 0.0060 mmol Rh) were combined. PhCF₃ (50 μL) was added to the sample as an internal standard. ¹⁹F NMR analysis indicated a 57:43 ratio of PhCF₃

to *p*-FC₆H₄I. Additional C₆D₆ (1.5 mL) was added to help contain the heat evolved during the reaction and prevent evaporation of PhCF₃ and then PhMgBr (2.5 M in Et₂O, 480 μL, 1.2 mmol) was added to the reaction. The solution became warm to the touch and the color became slightly darker. Analysis by ¹⁹F NMR spectroscopy after 5 min indicated approximately 3% conversion to FC₆H₄-C₆H₅ and approximately 68% conversion after 24 h.

Catalytic coupling reaction of *p*-FC₆H₄I and PhMgBr with Solution C, 0.5% catalyst loading. In a J. Young *p*-FC₆H₄I (138 μL, 1.20 mmol) and Solution C (0.040 M in C₆D₆, 150 μL, 0.0060 mmol) were combined. PhCF₃ (50 μL) was added to the sample as an internal standard. ¹⁹F NMR analysis indicated a 53:47 ratio of PhCF₃ to *p*-FC₆H₄I, respectively. Additional C₆D₆ (1.5 mL) added to help contain the heat evolved during the reaction and prevent evaporation of PhCF₃ and then PhMgBr (2.5 M in Et₂O, 480 μL, 1.2 mmol) was added to the reaction. No heat evolution or color change accompanied the addition of the Grignard. Analysis of ¹⁹F NMR spectra after 5 min indicated approximately 9% conversion to FC₆H₄-C₆H₅ and approximately 98% conversion after 2.5 h.

2.4.4 X-ray Crystallography

X-Ray data collection, solution, and refinement for 205. A fragment of suitable size and quality (0.2 × 0.1 × 0.6 mm) was broken off of an orange, multi-faceted crystal selected from a representative sample of crystals of the same habit using an optical microscope, mounted onto a nylon loop and placed in a cold stream of nitrogen (110 K). Low-temperature X-ray data were obtained on a Bruker APEXII CCD based

diffractometer (Mo sealed X-ray tube, $K_{\alpha} = 0.71073 \text{ \AA}$). All diffractometer manipulations, including data collection, integration and scaling were carried out using the Bruker APEXII software.⁸⁸ An absorption correction was applied using SADABS.⁸⁸ The space group was determined on the basis of systematic absences and intensity statistics and the structure was solved by direct methods and refined by full-matrix least squares on F^2 . The structure was solved in the triclinic P-1 space group using XS⁸⁹ (incorporated in SHELXTL). No obvious missed symmetry was reported by PLATON.⁹⁰ The absence of higher symmetry appears to derive from the bending of one of the chloride atoms out of the plane of the metal, phosphorus and *ipso* carbon. All non-hydrogen atoms were refined with anisotropic thermal parameters. Hydrogen atoms were placed in idealized positions and refined using riding model with the exception of the hydrogen bound to rhodium which was located from the difference map. The structure was refined (weighted least squares refinement on F^2) to convergence. Slight disorder of the peripheral isopropyl groups is responsible for the large $U_{eq(max)}/U_{eq(min)}$ ratios noted in the CheckCIF report.

X-Ray data collection, solution, and refinement for 221. A fragment of suitable size and quality (0.1 x 0.06 x 0.05 mm) was broken off of a red, multi-faceted crystal selected from a representative sample of crystals of the same habit using an optical microscope, mounted onto a nylon loop and placed in a cold stream of nitrogen (110 K). Low-temperature X-ray data were obtained on a Bruker APEXII CCD based diffractometer (Mo sealed X-ray tube, $K_{\alpha} = 0.71073 \text{ \AA}$). All diffractometer manipulations, including data collection, integration and scaling were carried out using

the Bruker APEXII software.⁸⁸ An absorption correction was applied using SADABS.⁸⁸ The space group was determined on the basis of systematic absences and intensity statistics and the structure was solved by direct methods and refined by full-matrix least squares on F^2 . The structure was solved in the monoclinic $p21/c$ space group using XS⁸⁹ (incorporated in X-Seed). This symmetry was reported by PLATON.⁹⁰ All non-hydrogen atoms were refined with anisotropic thermal parameters. Hydrogen atoms were placed in idealized positions and refined using riding model. The structure was refined (weighted least squares refinement on F^2) to convergence. Slight disorder exists among the isopropyl carbons, but this is to be expected for the terminal atoms. Modeling of this disorder did not improve the R or wR2 value.

CHAPTER III
THE FATE OF ARYL/AMIDO COMPLEXES OF RH(III) SUPPORTED BY A
POCOP Pincer Ligand: C-N Reductive Elimination and Beta-
Hydrogen Elimination

3.1 Introduction

The coupling of aryl halides with nitrogenous nucleophiles is most commonly catalyzed by Pd complexes in what is known as the Buchwald-Hartwig reaction.^{3-4,29-30,77b,91} The critical C-N bond-forming step in this process has been shown to take place via concerted C-N reductive elimination (RE).^{4,92} This process has been extended to other transition metal catalysts including Ni²⁵ and Cu,^{22,27b,93} however, examples of well-characterized C(aryl)-N RE outside of group 10 are scarce.⁹⁴

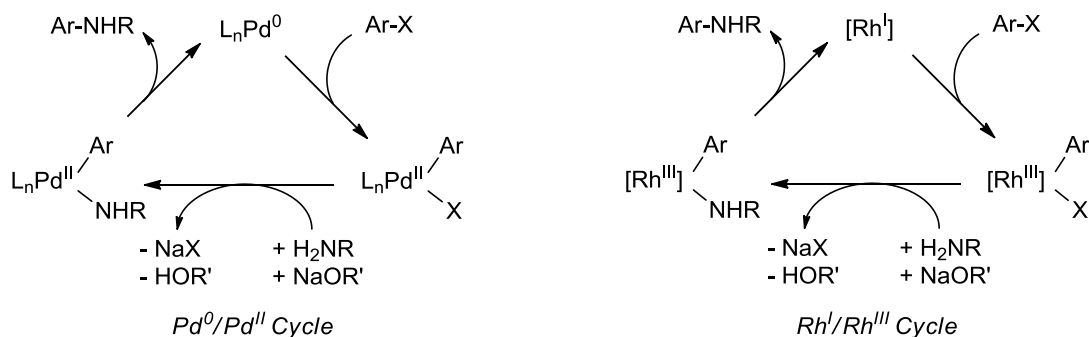
Extensive research by the Buchwald^{29a,95} and Hartwig⁹⁶ groups, as well as more recently by Stradiotto et al.,³⁵ has resulted in the development of phosphine/palladium catalysts for this process that have extended functional group tolerance and achieved high TON under mild reaction conditions. This improvement is due to the development of complex bulky phosphine ligands such as the ferrocene-based ligands used by Hartwig⁹⁶ and the phosphinobiaryl ligands used by Buchwald.^{28a,92} The large steric profile of these ligands encourages RE and also helps access low-coordinate Pd(0) intermediates that readily undergo aryl halide oxidative addition (OA). Pd catalyzed amination reactions follow a mechanism analogous to other Pd catalyzed aryl halide coupling reactions (Scheme 3-1): OA of an aryl halides to Pd(0), transmetallation at

Pd(II) to form an aryl amido complex, and product forming RE to regenerate Pd(0).^{4,29-30} The remarkable propensity of Pd to easily undergo the OA and RE steps shuttling between Pd(0) and Pd(II) oxidation states is critical to its prowess in coupling catalysis. The transmetallation step to form aryl/amido Pd(II) complexes can be achieved by anion exchange of aryl/halido Pd(II) complexes with amide salts, but is more commonly accomplished *via* amine deprotonation by aryl/OCMe₃ Pd(II) intermediates.^{92,97}

Our group has been particularly interested in the concerted OA and RE reactions of pincer-supported complexes of group 9 metals as new ways for making or breaking chemical bonds. We previously reported on the stoichiometric chemistry of aryl halide OA and C-C RE with (PNP)Rh;⁶³⁻⁶⁵ and later demonstrated that substitution of the diarylamido/bis(phosphine) PNP^{98,70,99} for the less electron rich aryl/bis(phosphinite) POCOP⁸⁶ pincer ligand allows for catalytic C-C coupling with (POCOP)Rh as described in Chapter II.¹⁰⁰ Non-pincer Rh complexes have been used for C-C coupling reactions with aryl halides over the last decade,^{55g,56-57,59-60,101} however, most of this work focused on the synthetic applications and less so on the fundamental knowledge about the requisite catalytic steps.¹⁰² Kim and Chang reported the amination of aryl bromides with N-heterocyclic carbene-ligated Rh catalysts, but the mechanism was not investigated beyond the influence of additives on the yields.⁶¹

We were eager to explore whether a catalytic cycle for aryl-nitrogen coupling can function analogously for Rh(I)/Rh(III) as it does for Pd(0)/Pd(II) (Scheme 3-1). Our previous work had already indicated that clean concerted OA of aryl halides was facile whenever a three-coordinate (pincer)Rh transient is generated.^{63-65,100} Herein, we take

advantage of the convenience that pincer ligands afford in studying elementary reactions at transition metal centers. We describe a combined experimental and computational investigation of aryl-nitrogen RE from Rh that proceeds via concerted mechanism in the (POCOP)Rh system. Although this system appears to be only a meager catalyst for catalytic aryl-nitrogen coupling, we do demonstrate catalytic turnover with aryl bromides and chlorides and observe each of the individual steps of the presumed “Pd-like” catalytic cycle.



Scheme 3-1. General Pd(0)/Pd(II) and Rh(I)/Rh(III) cycle for catalytic C-N coupling reactions.

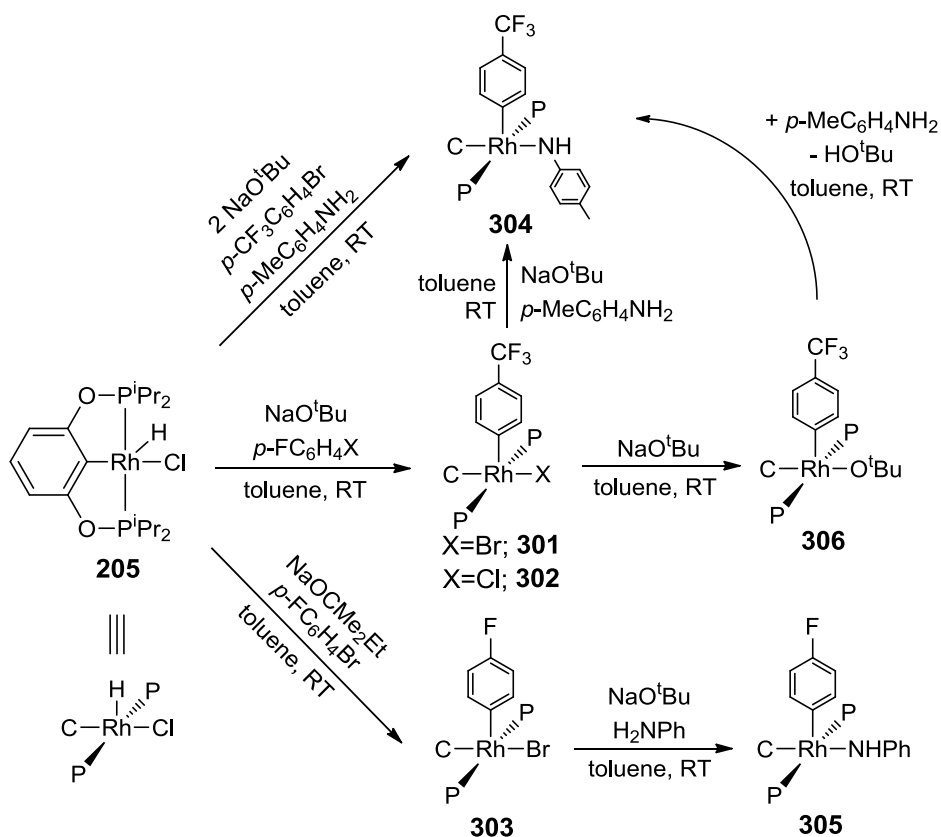
3.2 Results and Discussion

3.2.1 Synthesis of (POCOP)Rh(Ar)(anilido) Complexes

We were interested in characterizing the stoichiometric reactions that make up the proposed Rh(I)/Rh(III) catalytic cycle (Scheme 3-1). We decided to utilize the POCOP pincer framework here based on our previous success with enhanced C-C RE^{100,103} with the ostensibly less electron-rich (POCOP)Rh compared to (PNP)Rh ($\nu_{CO} = 1962 \text{ cm}^{-1}$ for (POCOP)RhCO;⁷⁵ $\nu_{CO} = 1945 \text{ cm}^{-1}$ for (PNP)RhCO¹⁰⁴), which was

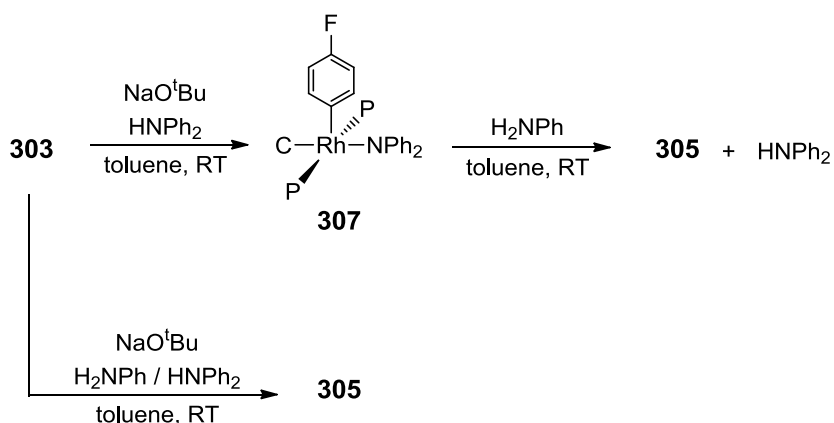
attributed to the less electron donating character of the POCOP ligand. We had already established aryl halide oxidative addition to (POCOP)Rh,¹⁰⁰ so the focus in this study was placed on the transmetallation step to form Rh(III) aryl/amido and the C-N RE step.

Complexes of the type (POCOP)Rh(Ar)(NHR) were prepared by a few related methods (Scheme 3-2). Treatment of (POCOP)Rh(H)(Cl) (**205**) with 1 equiv of sodium *t*-alkoxide bases in the presence of aryl halides results in immediate formation of the aryl halide OA product, (POCOP)Rh(Ar)(X) (**301** – **303**). This is believed to proceed by dehydrochlorination of **205** with sodium *t*-alkoxide to generate an unsaturated (POCOP)Rh fragment, which undergoes facile aryl halide OA. (POCOP)Rh(C₆H₄CF₃)(NH(C₆H₄Me)) (**304**) and (POCOP)Rh(C₆H₄F)(NHPh) (**305**) were both synthesized by treatment of the corresponding Rh aryl/halido complex with NaO^tBu and NH₂(*p*-C₆H₄Me) or NH₂Ph, respectively. When **302** was reacted with 1 equiv NaO^tBu in the absence of an aniline, formation of (POCOP)Rh(C₆H₄CF₃)(O^tBu) (**306**) was observed. Exposure of **306** to NH₂(C₆H₄Me) resulted in immediate conversion to **304**. **304** was also synthesized by the one-pot reaction of **205** with 2 equiv NaO^tBu and 1 equiv of both *p*-CF₃C₆H₄Br and *p*-MeC₆H₄NH₂.



Scheme 3-2. Synthetic pathways to (POCOP)Rh aryl/anylido complexes.

The Rh(III) aryl/diarylamido complex (POCOP)Rh(C₆H₄F)(NPh₂) (**307**) was prepared analogously from (POCOP)Rh(C₆H₄F)(Br) (**303**) (Scheme 3-3). The reaction of **303** with NaO^tBu and NPh₂ resulted in formation of **307**. Treatment of **307** with 1 equiv NH₂Ph resulted in immediate conversion to **305** with concomitant formation of NPh₂. Similar proton transfer reactions between aryl/diarylamido Pd(II) complexes and anilines have been reported.^{30c} A competition experiment between equimolar amounts of NH₂Ph and NPh₂ in the presence of **307** and NaO^tBu resulted in quantitative formation of **305**.



Scheme 3-3. Synthesis and reactivity of $(\text{POCOP})\text{Rh}(\text{C}_6\text{H}_4\text{F})(\text{NPh}_2)$ (**307**).

The solid-state structure of **305** was determined by X-ray analysis of a single crystal grown from a saturated pentane solution at $-35\text{ }^\circ\text{C}$ (Figure 3-1). The molecule adopts a five-coordinate environment about Rh that is intermediate between square planar and Y-shaped, analogous to **301** – **303**.^{100,69} The Rh-bound aryl ring is “sandwiched” between two of the isopropyl phosphine substituents, resulting in slowed rotation about the Rh-C bond. This is reflected in the ^1H NMR spectrum of **305**, as well as **301/302** and **303**, with the observation of separate resonances within each pair of *ortho*- and *meta*- protons of the aryl ring.⁶³⁻⁶⁵ The presence of two Rh-bound aryl carbon atoms in **301** – **306** is also supported by the presence of two doublets of triplets ($^1J_{\text{C-Rh}} = 25 - 37\text{ Hz}$, $^2J_{\text{C-P}} = 6 - 10\text{ Hz}$) in each of their $^{13}\text{C}\{^1\text{H}\}$ NMR spectra in the 135 – 150 ppm region.

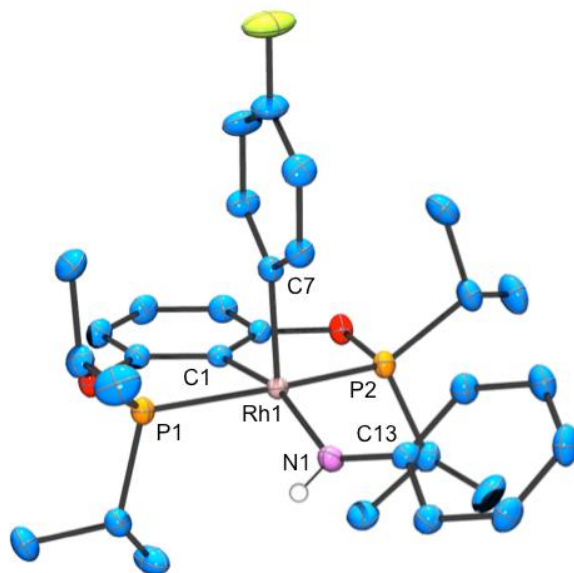
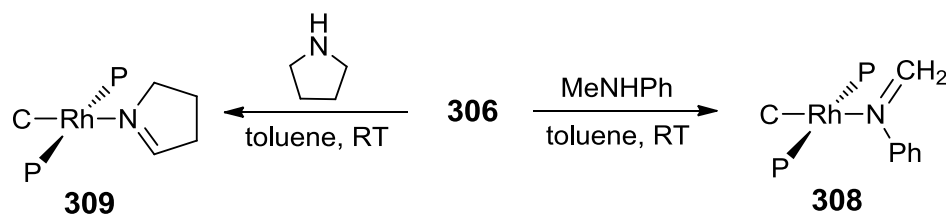


Figure 3-1. ORTEP drawing (50% probability ellipsoids) of (POCOP)Rh(*p*-C₆H₄F)(NHPh) (**305**).⁸⁴ Shown with selected atom labeling. Hydrogen atoms are omitted with the exception of the NH. Selected bond distances (Å) and angles (deg) for **305** follow: Rh1-P1, 2.3218(6); Rh1-P2, 2.2891(6); Rh1-C1, 2.019(2); Rh1-C7, 2.012(2); Rh1-N1, 2.076(2); P1-Rh1-P2, 157.79(2); C1-Rh1-N1, 162.38(7); Rh1-N1-C13, 135.3(1).

3.2.2 Reactivity of Alkyl Amines

We also wanted to examine the reactivity of alkyl amido complexes, however when **306** was reacted with N-methylaniline or pyrrolidine, the respective (POCOP)Rh(Ar)(NR₂) were not the observed products (a fellow graduate student Christopher Pell collaborated on the work with alkyl amines; Scheme 3-4). Instead, clean formation of Rh(I) imine complexes **308** and **309** occurred with concomitant release of HO^tBu and ArH, which were identified by ¹H and ¹⁹F NMR spectroscopy. The large ¹J_{P-Rh} values of 182 and 184 Hz for **308** and **309**, respectively, are consistent with

the Rh(I) assignment. **308** and **309** also both exhibited diagnostic imine signals by ^1H NMR and $^{13}\text{C}\{^1\text{H}\}$ NMR spectroscopy. **308** displays a singlet at 7.27 ppm for the imine CH and a triplet at 168.7 ppm for the imine C in the ^1H and $^{13}\text{C}\{^1\text{H}\}$ NMR spectrum, respectively. The ^1H NMR spectrum of **309** displayed two broad singlets at 6.43 ppm and 6.28 ppm for the two imine CH_2 protons and a singlet at 156.1 ppm for the imine carbon in the $^{13}\text{C}\{^1\text{H}\}$ NMR spectrum. The syntheses of imidazolyl-imine Rh(I) carbonyl compounds have also been recently described and these complexes displayed similar NMR chemical shifts for the imine proton.¹⁰⁵ X-ray quality crystals of **308** were grown by slow vapor diffusion of pentane into a saturated toluene solution at $-35\text{ }^\circ\text{C}$. The X-ray structure shows a slightly distorted square planar geometry, with a C–Rh–N angle of $176.13(8)^\circ$ (Figure 3-2). The imine N–C bond is $1.272(3)\text{ \AA}$, consistent with an N–C double bond.



Scheme 3-4. Formation of (POCOP)Rh(imine) complexes with alkyl substituted amines.

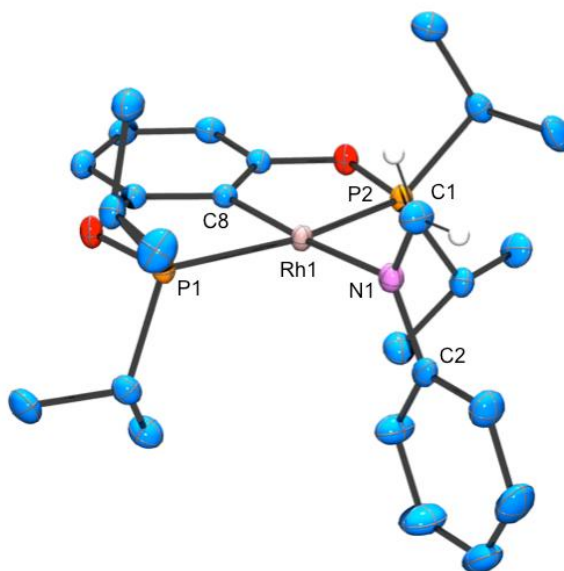


Figure 3-2. ORTEP drawings (50% probability ellipsoids) of (POCOP)Rh(NPh(CH₂)) (**308**).⁸⁴ Shown with selected atom labeling. Hydrogen atoms are omitted with the exception of the CH₂. Selected bond distances (Å) and angles (deg) for **308** follow: Rh1-P1, 2.245(1); Rh1-N1, 2.166(3); Rh1-C8, 1.993(3); N1-C1, 1.272(3); N1-C2, 1.440(3); P1-Rh1-P2, 158.40(2); C8-Rh1-N1, 176.13(9); C1-N1-C2, 119.9(2).

It is likely that the reactions with both *N*-methylaniline and pyrrolidine initially form their respective aryl-amido complexes, however from these species the pathway to form the imine complex is lower in energy than the pathway to form the C-N reductive elimination product (Calculations by Dr. Jia Zhou; Figure 3-3 and 3-4). Both **308** and **309** appear to have been formed via β -hydride elimination (BHE) from the initially formed (POCOP)Rh(Ar)(NR₂). Two BHE pathways were calculated for *N*-methylaniline in which the resulting hydride is either *trans* (**IM1**) or *cis* (**IM2**) to the aryl group (Figure 3-3). The *trans* pathway was meaningfully lower in energy than the *cis*; therefore, for pyrrolidine we only considered the *trans* pathway (**IM1'**). The barrier for BHE is under 20 kcal/mol for both *N*-methylaniline and pyrrolidine, consistent with this

transformation occurring at RT. This is followed by dissociation of the imine and the formation of a new distorted square pyramidal aryl-hydrido complex where the aryl and hydride are *cis*, **IM3** (N-methylaniline) and **IM2'** (pyrrolidine). Finally, C-H RE of trifluorotoluene and coordination of the imine to form **P1** and **P1'** (**308** and **309**). Interestingly, the barriers for both BHE and C-N RE were calculated to be lower for pyrrolidine than for N-methylaniline.

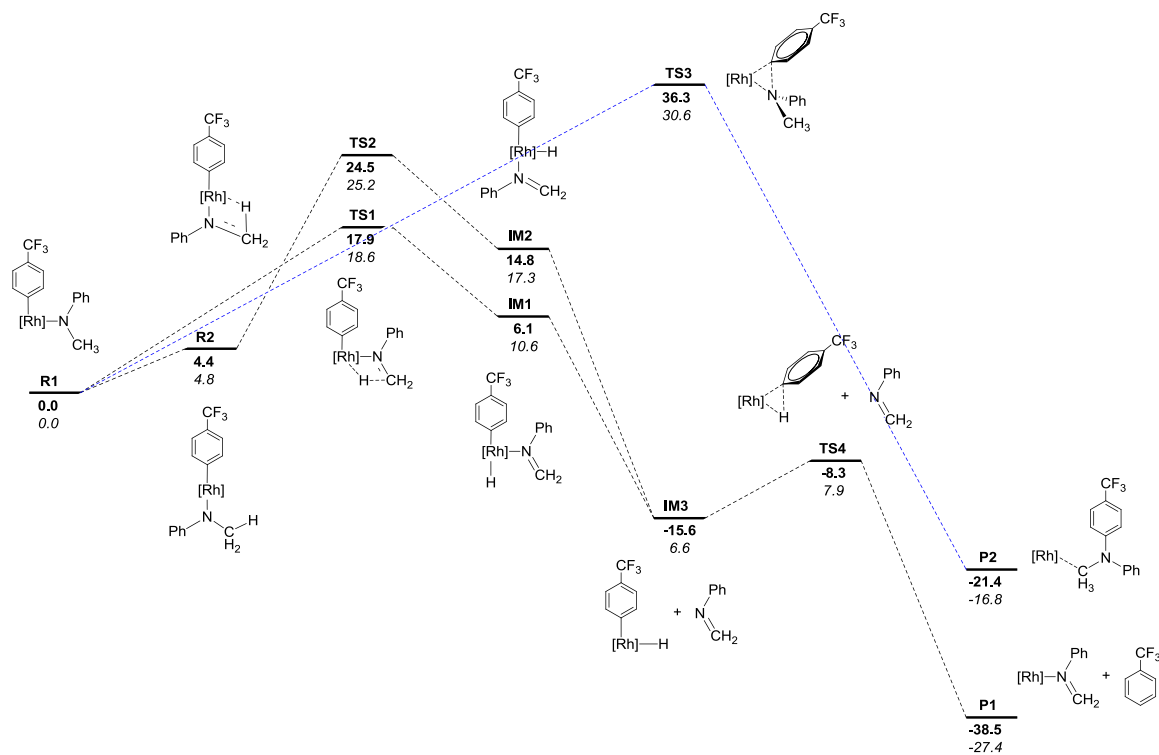


Figure 3-3. Calculated reaction coordinate diagram (Gibbs free energy, **B3LYP**, *MO6*) for the formation of **308**.

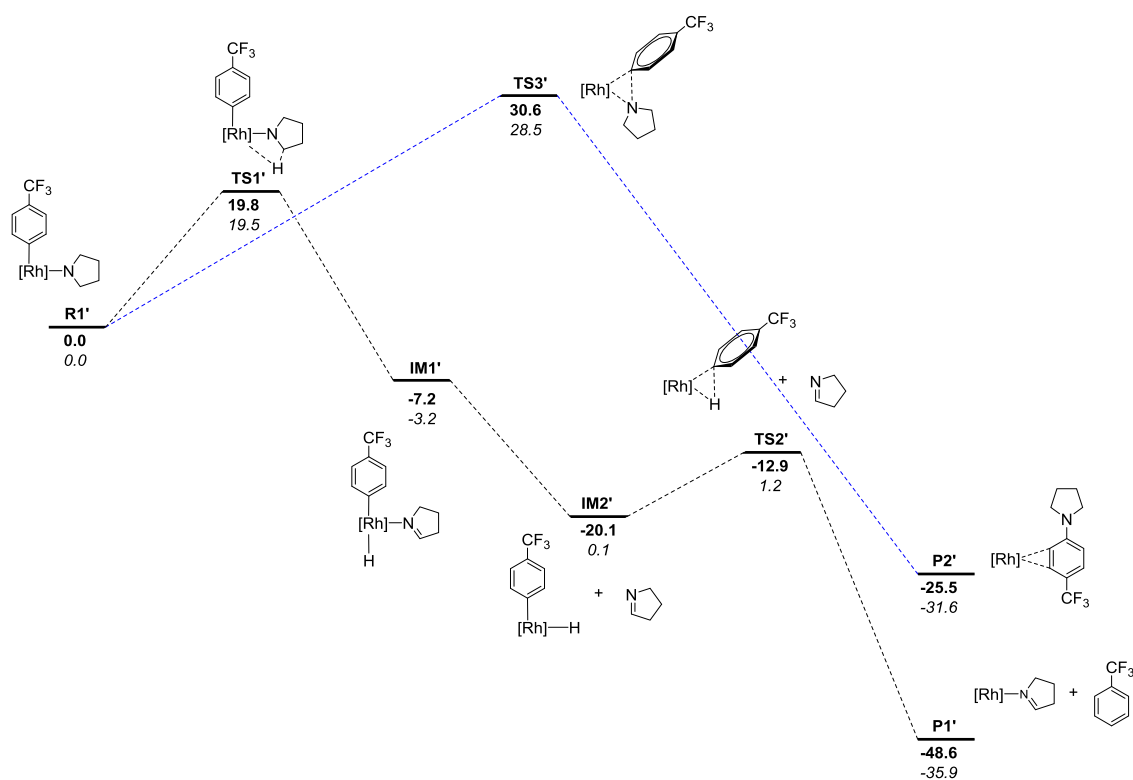
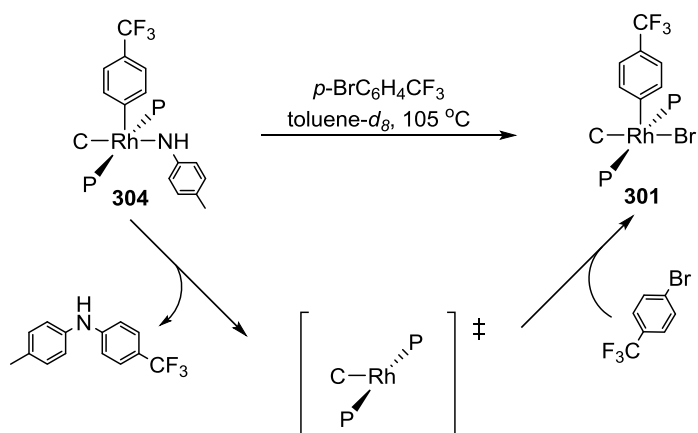


Figure 3-4. Calculated reaction coordinate diagram (Gibbs free energy, **B3LYP**, **MO6**) for the formation of **309**.

3.2.3 Concerted C-N Reductive Elimination

We decided to study C-N RE from **304** (Scheme 3-5), because we anticipated that the electron-withdrawing *p*-CF₃ group on the Rh-aryl and the electron-donating *p*-CH₃ group on the Rh-anilido should result in a slightly lower energy barrier for RE than their non-substituted analogues, a trend that has been observed and studied with C-N reductive elimination from Pd phosphine systems by Hartwig and coworkers.^{92,106} The CF₃ substituted aryl group also allowed for ease of analysis by ¹⁹F NMR spectroscopy.



Scheme 3-5. C-N reductive elimination from **304** in the presence of an aryl halide trap.

304 was thermolyzed at 105 °C in toluene- d_8 in the presence of p -CF₃C₆H₄Br in various concentrations. p -CF₃C₆H₄Br acted as a trap to capture the unsaturated (POCOP)Rh formed upon RE (Scheme 3-5). Each reaction was monitored for 2 – 3 half-lives of **304** and all displayed unambiguous first-order behavior, consistent with concerted first-order RE (Figure 3-5). However, analysis of the dependence of rate on the concentration of p -CF₃C₆H₄Br was not straightforward. The rate did increase with higher [p -CF₃C₆H₄Br], but the increase was only very modest – 40% rate increase for a 100-fold increase in [p -CF₃C₆H₄Br]. We surmised that this rate increase may be owing to the high [p -CF₃C₆H₄Br] effectively changing the medium of the reaction, rather than being indicative of the chemical involvement of p -CF₃C₆H₄Br in the rate-limiting step. To this end, we compared the rate of **304** decomposition in toluene *versus* o -C₆H₄F₂, but found the rate to be unaffected by the more polar solvent indicating the increased polarity of the solvent with increased p -CF₃C₆H₄Br is not the cause of the discrepancies in rate.

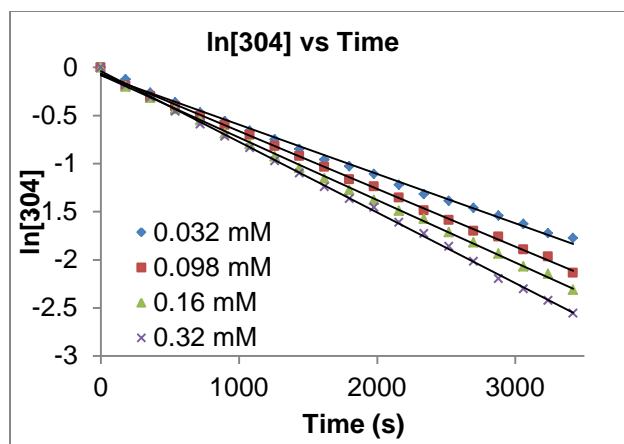


Figure 3-5. Plot of $\ln[304]$ vs. time for C-N RE from **304** in the presence of $p\text{-CF}_3\text{C}_6\text{H}_4\text{Br}$ in various concentrations.

Calculations for C-N RE from **304** indicate the process is characterized by $\Delta H^\ddagger = 24.7$ kcal/mol and $\Delta S^\ddagger = 7.5$ eu (calculations by Dr. Jia Zhou; Figure 3-6). The rate of RE from **304** in the 65 – 110 °C temperature range was analyzed to experimentally determine the activation parameters by Eyring analysis. While the process was unambiguously first order at each temperature, the Eyring plot of the data contained significant deviations from linearity (Figure 3-7). Additional experiments at 75 °C and 85 °C showed an irreproducibility of the rates obtained at the same temperature. The best fit of the Eyring datapoints produced the values of $\Delta H^\ddagger = 18.5(7)$ kcal/mol and $\Delta S^\ddagger = -25(2)$ eu. However, given the imperfect conformance to the linearity, these activation parameters may not be fully meaningful. Minor formation of benzotrifluoride was observed during this process, indicating the potential of side processes occurring in this temperature range, which could potentially affect these results and contribute to the differences between various runs at the same temperature. Overall, the peculiarities in the dependence of the apparent rates on the temperature and on the concentration of the

aryl halide trap remain unexplained. It is conceivable that two first-order processes might be responsible for the aggregate disappearance of **304** over time: first-order decay would be observed at each individual temperature, but relative contributions of each process would be different at different temperatures.

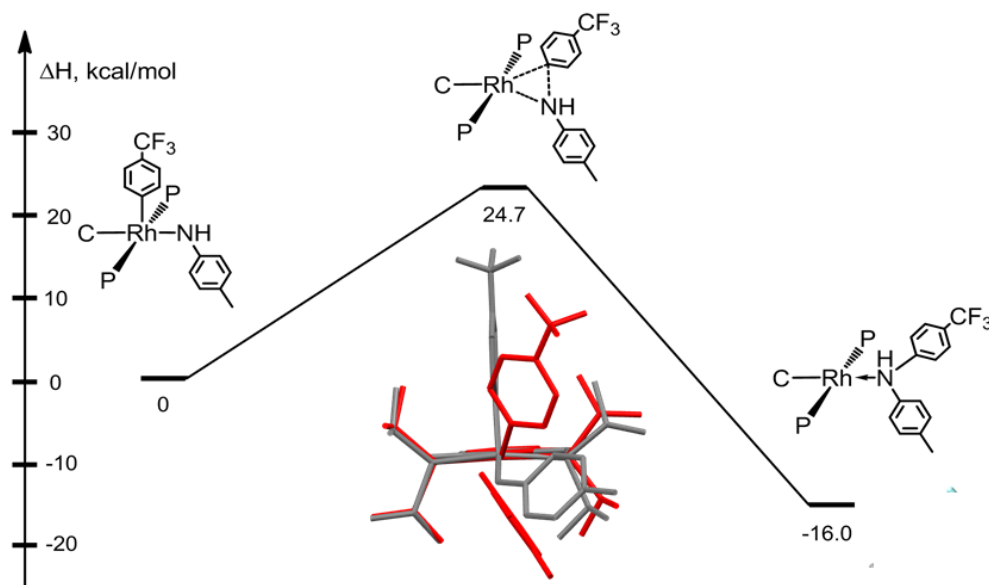


Figure 3-6. Calculated reaction barrier for C-N RE from **304** at 103 °C. All of the geometries were fully optimized in toluene solvent *via* the PCM¹⁰⁷ model at the M06¹⁰⁸ level of theory. Overlay of the calculated ground-state structure of **304** (gray) and the transition state (red) showing the aryl rotation that occurs prior to RE.

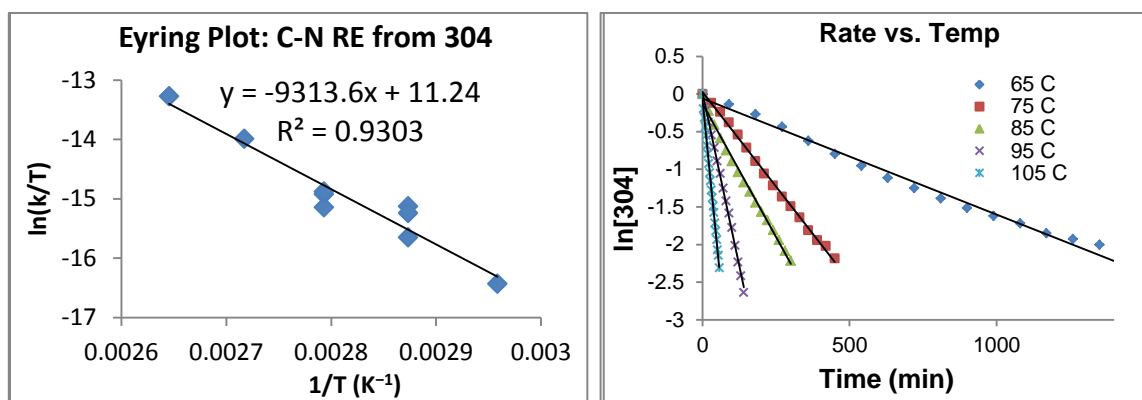


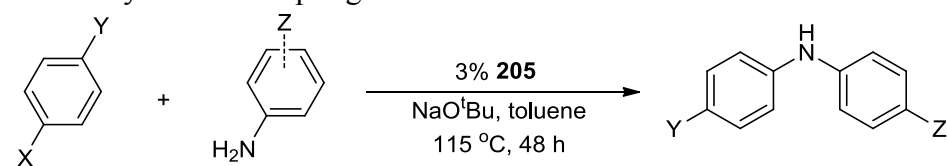
Figure 3-7. Left; Eyring plot for C-N RE from **304** in the 65 – 105 °C temperature range. Right; Plot of $\ln[304]$ vs. time for C-N reductive elimination from **304** in the 65 – 105 °C temperature range.

3.2.4 Catalytic C-N Coupling with (POCOP)Rh(H)(Cl)

Given that the individual reactions of the potential catalytic cycle have all been observed, we set out to test the catalytic proficiency of the (POCOP)Rh system. The results for catalytic coupling of aryl halides with anilines using (POCOP)Rh(H)(Cl) **205** as the pre-catalyst and sodium *tert*-pentoxide as base are collected in Table 3-1. While this is not a practical catalyst, it is worth noting that 10-15 turnovers were achieved with aryl bromides, and 6-10 turnovers with *p*-FC₆H₄Cl. It is interesting to note that reactions with the more electron poor *p*-CF₃C₆H₄Br, expected to lead to a faster reductive elimination step, produced no C-N coupled product with any of the amines examined. We also performed control reactions using catalytic amounts [(COD)RhCl]₂ or [(COD)RhCl]₂ in a 1:2 ratio with PCy₃ under the same conditions described in Table 1 for the coupling reaction of *p*-FC₆H₄Br with aniline. Neither reaction resulted in the formation of the C-N coupled product, indicating the necessity of the pincer-supported Rh center in forming C-N bonds.

The catalytic reactivity is limited by the sluggishness of C-N RE, which leaves room for competing, ostensibly catalyst-killing processes that take place in a catalytic reaction. The latter may be related to the observation of the hydrodehalogenation products, but we have no firm evidence for this notion. One reason for the slow C-N RE is that the Rh-bound aryl ring has to rotate to turn its “face” towards the anilido group in the TS (Figure 5). With the “sandwiching” isopropyl groups, that position for the aryl group is disfavored, as can be inferred from the ground state structure and the observed slow rotation about Rh-C on the NMR timescale. Goldman and Krogh-Jespersen studied a similar phenomenon in aryl-carbon elimination from (PCP)Ir complexes.⁷⁶ This is discussed in more detail in Chapter 1. It is possible that a judicious choice of smaller phosphorus substituents in the (POCOP)Rh system may lead to far more effective catalysts.

Table 3-1. Catalytic C-N Coupling with **205**.



| Entry | X | Y | Z | Ar ₂ NH | YC ₆ H ₅ | YC ₆ H ₄ X |
|-------|----|-----------------|--------------|--------------------|--------------------------------|----------------------------------|
| 1 | Br | F | H | 32% | 10% | 58% |
| 2 | Cl | F | H | 20% | 8% | 72% |
| 3 | Br | F | <i>p</i> -Me | 46% | 11% | 43% |
| 4 | Cl | F | <i>p</i> -Me | 27% | 8% | 65% |
| 5 | Br | F | <i>o</i> -Me | 33% | 10% | 57% |
| 6 | Cl | F | <i>o</i> -Me | 22% | 9% | 69% |
| 7 | Br | CF ₃ | H | - | - | 100% |
| 8 | Br | CF ₃ | <i>p</i> -Me | - | - | 100% |
| 9 | Br | CF ₃ | <i>o</i> -Me | - | - | 100% |

3.3 Conclusion

In summary, we have examined the potential utility of (POCOP)Rh complexes in catalysis of amination of aryl halides. The (POCOP)Rh system did catalyze the coupling of aryl bromides and chlorides with anilines, albeit sluggishly, and with significant amounts of hydrodehalogenation side products. We were able to isolate all the implied intermediates and examine the individual reactions of a catalytic cycle. It appears that slow C-N RE presents a major obstacle to successful catalysis. In reactions with alkyl-substituted amines, BHE from the N-alkyl group dominated, leading to stoichiometric formation of Rh(I) imine complexes and precluding C-N coupling. DFT studies demonstrated that the barrier for C-N coupling from a (POCOP)Rh(Ar)(NR₂) complex is substantially higher than the barrier for BHE from the R group.

3.4 Experimental

3.4.1 General Considerations

Unless otherwise specified, all manipulations were performed under an argon atmosphere using standard Schlenk line or glove box techniques. Toluene, THF, pentane, and isooctane were dried and deoxygenated (by purging) using a solvent purification system (Innovative Technology Pure Solv MD-5 Solvent Purification System) and stored over molecular sieves in an Ar-filled glove box. C₆D₆ and hexanes were dried over and distilled from NaK/Ph₂CO/18-crown-6 and stored over molecular sieves in an Ar-filled glove box. Fluorobenzene was dried with and then distilled or vacuum transferred from CaH₂. (POCOP)Rh(H)(Cl) (**205**)¹⁰⁰ was synthesized according to published procedures. All other chemicals were used as received from commercial

vendors. NMR spectra were recorded on a Varian NMRS 500 (^1H NMR, 499.686 MHz; ^{13}C NMR, 125.659 MHz, ^{31}P NMR, 202.298 MHz, ^{19}F NMR, 470.111 MHz) spectrometer. For ^1H and ^{13}C NMR spectra, the residual solvent peak was used as an internal reference. ^{31}P NMR spectra were referenced externally using 85% H_3PO_4 at δ 0 ppm. ^{19}F NMR spectra were referenced externally using 1.0 M $\text{CF}_3\text{CO}_2\text{H}$ in CDCl_3 at -78.5 ppm. Elemental analyses were performed by CALI Labs, Inc. (Parsippany, NJ).

3.4.2 Stoichiometric Reactions

Synthesis of (POCOP)Rh(*p*- $\text{C}_6\text{H}_4\text{CF}_3$)(Br) (301). 205 (206 mg, 0.429 mmol) was combined with NaO^tBu (42.2 mg, 0.439 mmol) and *p*- $\text{CF}_3\text{C}_6\text{H}_4\text{Br}$ (120 μL , 0.858 mmol) in a Schlenk flask and dissolved in toluene. The reaction was stirred at RT and immediately turned dark red. After stirring for 60 min at RT, the solution was passed through a pad of Celite and the volatiles were removed by vacuum. The compound was recrystallized by dissolving in toluene and layering with pentane at $-35\text{ }^\circ\text{C}$, yielding a red solid (226 mg, 79%). $^{31}\text{P}\{^1\text{H}\}$ NMR (C_6D_6): δ 173.5 (d, $J_{\text{Rh-P}} = 120$ Hz); ^1H NMR (C_6D_6 , Figure 3-8): δ 8.41 (bs, 1H, $\text{C}_6\text{H}_4\text{CF}_3$), 6.95 (t, 1H, POCOP, 9.0 Hz), 6.85 (bs, 1H, $\text{C}_6\text{H}_4\text{CF}_3$), 6.76 (d, 2H, POCOP, 9.0 Hz), 6.46 (bs, 1H, $\text{C}_6\text{H}_4\text{CF}_3$), 5.98 (bs, 1H, $\text{C}_6\text{H}_4\text{CF}_3$), 2.59 (m, 2H, CHMe_2), 1.95 (m, 2H, CHMe_2), 1.14 (q, 6H, CHMe_2 , 9.0 Hz), 1.01 (q, 6H, CHMe_2 , 9.0 Hz), 0.97 (q, 6H, CHMe_2 , 9.0 Hz), 0.67 (q, 6H, CHMe_2 , 9.0 Hz); ^{19}F NMR (C_6D_6): δ -62.6 (s, $\text{C}_6\text{H}_4\text{CF}_3$); $^{13}\text{C}\{^1\text{H}\}$ NMR (C_6D_6): δ 165.0 (t, $J_{\text{P-C}} = 10$ Hz, POCOP), 150.7 (dt, $J_{\text{Rh-C}} = 37$ Hz, $J_{\text{P-C}} = 10$ Hz, *p*- $\text{C}_6\text{H}_4\text{CF}_3$), 140.2 (dt, $J_{\text{Rh-C}} = 34$ Hz, $J_{\text{P-C}} = 6.0$ Hz, POCOP), 137.1 (bs, *p*- $\text{C}_6\text{H}_4\text{CF}_3$), 136.7 (bs, *p*- $\text{C}_6\text{H}_4\text{CF}_3$), 127.6 (s, POCOP), 126.4 (q, $J_{\text{F-C}} = 33$ Hz, CCF_3), 125.1 (q, $J_{\text{F-C}} = 271$ Hz, CF_3), 124.5 (bs, *p*-

$C_6H_4CF_3$), 123.1 (bs, p - $C_6H_4CF_3$), 107.5 (t, $J_{P-C} = 5.0$ Hz, POCOP), 31.1 (t, $J_{P-C} = 11$ Hz, $CHMe_2$), 28.4 (t, $J_{P-C} = 11$ Hz, $CHMe_2$), 18.0 (s, $CHMe_2$), 17.3 (s, $CHMe_2$), 16.1 (s, $CHMe_2$), 15.5 (s, $CHMe_2$). Elem. Anal. Calc. for $C_{25}H_{35}BrF_3O_2P_2Rh$: C, 44.86; H, 5.27. Found: C, 44.94; H, 5.17.

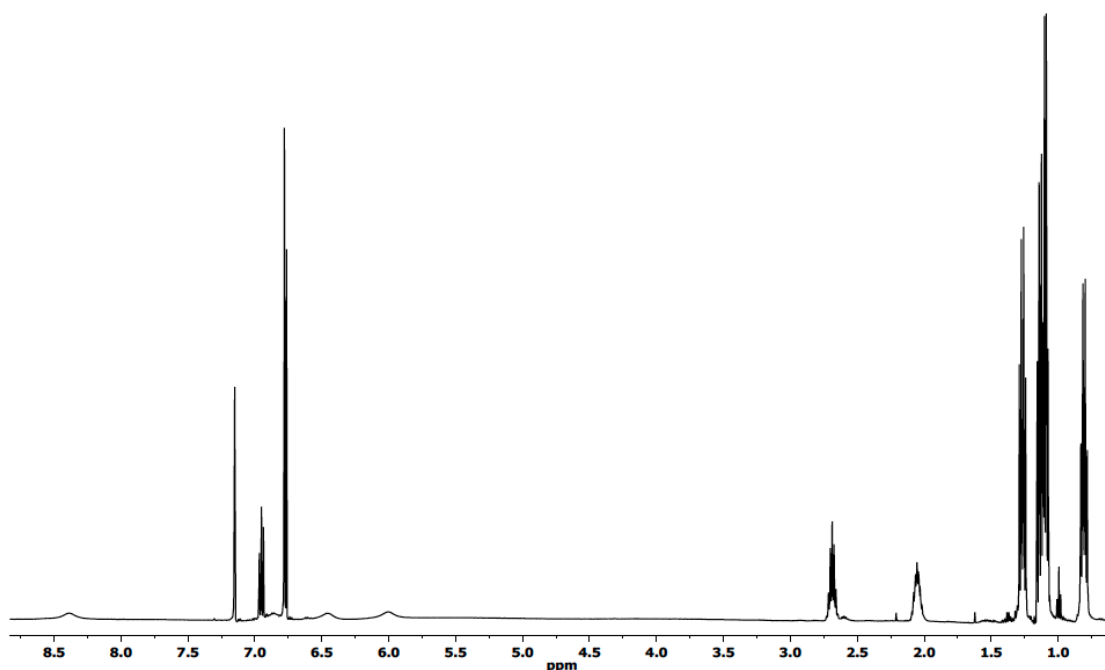


Figure 3-8. 1H NMR spectrum of $(POCOP)Rh(p-C_6H_4CF_3)(Br)$ (**301**) in C_6D_6 . Minor residual pentane present.

Synthesis of $(POCOP)Rh(p-C_6H_4CF_3)(Cl)$ (302**).** **205** (103 mg, 0.215 mmol) was added to a vial and dissolved in toluene. NaO^tBu (21 mg, 0.22 mmol) and p - $CF_3C_6H_4Cl$ (34 μL , 0.26 mmol) were added to the sample resulting in an immediate color change to red. After sitting for 60 min at RT, the reaction was passed through a pad

of Celite. The volatiles were removed under vacuum to give a clean red solid (116 mg, 86% yield). $^{31}\text{P}\{^1\text{H}\}$ NMR (C_6D_6): δ 171.8 (d, $J_{\text{Rh-P}} = 121$ Hz); ^1H NMR (C_6D_6 , Figure 3-9): δ 8.60 (bs, 1H, $p\text{-C}_6\text{H}_4\text{CF}_3$), 6.94 (t, 1H, POCOP, $J = 9.5$ Hz), 6.84 (bs, 1H, $p\text{-C}_6\text{H}_4\text{CF}_3$), 6.77 (d, 2H, POCOP, $J = 7.0$ Hz), 6.47 (bs, 1H, $p\text{-C}_6\text{H}_4\text{CF}_3$), 6.00 (bs, 1H, $p\text{-C}_6\text{H}_4\text{CF}_3$), 2.50 (m, 2H, CHMe_2), 1.91 (m, 2H, CHMe_2), 1.17 (q, 6H, CHMe_2 , $J = 7.5$ Hz), 0.96 (m, 12H, CHMe_2), 0.70 (q, 6H, CHMe_2 , $J = 7.5$ Hz); ^{19}F NMR (C_6D_6): δ -62.5 (s, CF_3); $^{13}\text{C}\{^1\text{H}\}$ NMR (C_6D_6): δ 165.3 (t, $J_{\text{P-C}} = 6.0$ Hz, POCOP), 150.4 (dt, $J_{\text{Rh-C}} = 39$ Hz, $J_{\text{P-C}} = 9.5$ Hz, $p\text{-C}_6\text{H}_4\text{CF}_3$), 139.6 (dt, $J_{\text{Rh-C}} = 34$ Hz, $J_{\text{P-C}} = 5.0$ Hz, POCOP), 136.9 (bs, 2 overlapping, $p\text{-C}_6\text{H}_4\text{CF}_3$), 127.6 (s), 126.3 (q, $J_{\text{F-C}} = 32$ Hz, CCF_3), 125.2 (q, $J_{\text{F-C}} = 271$ Hz, CF_3), 124.4 (bs, $p\text{-C}_6\text{H}_4\text{CF}_3$), 123.4 (bs, $p\text{-C}_6\text{H}_4\text{CF}_3$), 107.5 (t, $J_{\text{P-C}} = 5.9$ Hz, POCOP), 30.8 (t, $J_{\text{P-C}} = 10$ Hz, CHMe_2), 28.2 (t, $J_{\text{P-C}} = 11$ Hz, CHMe_2), 17.8 (t, $J_{\text{P-C}} = 2.3$ Hz, CHMe_2), 17.5 (s, CHMe_2), 15.9 (t, $J_{\text{P-C}} = 1.8$ Hz, CHMe_2), 15.3 (s, CHMe_2).

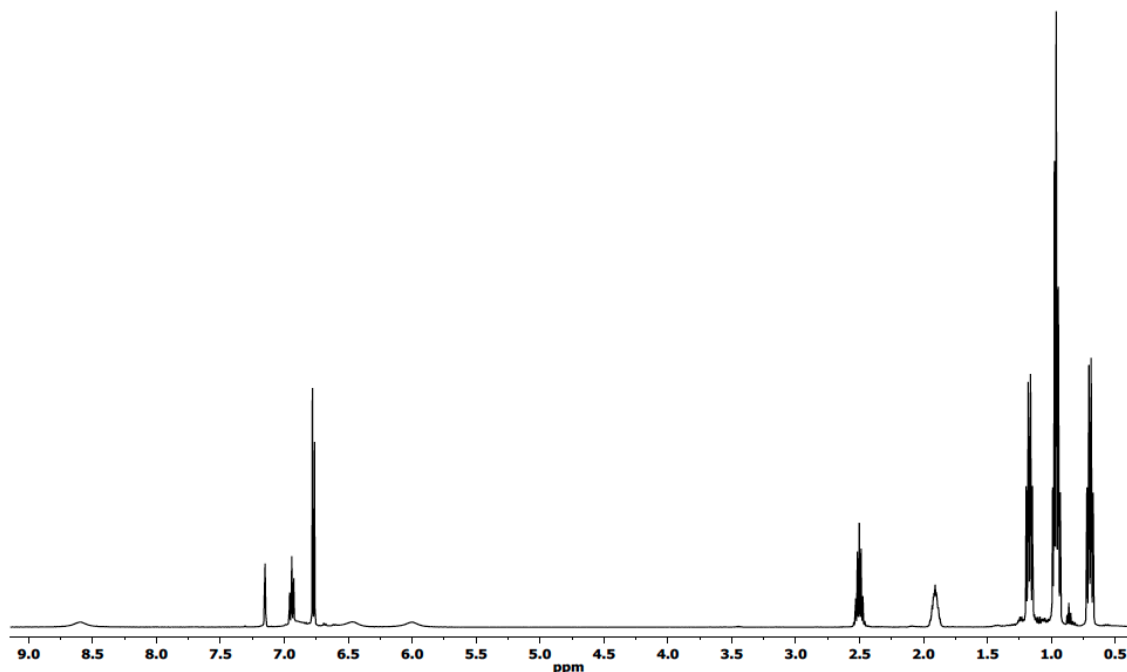


Figure 3-9. ^1H NMR spectrum of $(\text{POCOP})\text{Rh}(p\text{-C}_6\text{H}_4\text{CF}_3)(\text{Cl})$ (**302**) in C_6D_6 . Minor residual pentane present.

Synthesis of $(\text{POCOP})\text{Rh}(p\text{-C}_6\text{H}_4\text{F})(\text{Br})$ (303**).** **205** (231 mg, 0.483 mmol) was combined with NaO^tPent (106 mg, 0.967 mmol) and $p\text{-FC}_6\text{H}_4\text{Br}$ (106 μL , 0.967 mmol) in a Schlenk flask and dissolved in toluene. The reaction was stirred at RT and immediately turned red. After stirring for 60 min at RT, the solution was passed through a pad of Celite and the volatiles were removed by vacuum. The compound was recrystallized by dissolving in a minimum amount of toluene and layering with pentane at $-35\text{ }^\circ\text{C}$, yielding a red solid (216 mg, 72%). $^{31}\text{P}\{^1\text{H}\}$ NMR (C_6D_6): δ 173.2 (d, $J_{\text{Rh-P}} = 121$ Hz); ^1H NMR (C_6D_6 , Figure 3-10): δ 8.25 (bs, 1H, $p\text{-C}_6\text{H}_4\text{F}$), 6.93 (t, 1H, POCOP, 8.0 Hz), 6.76 (d, 2H, POCOP, 8.0 Hz), 6.43 (bs, 1H, $p\text{-C}_6\text{H}_4\text{F}$), 6.09 (bs, 1H, $p\text{-C}_6\text{H}_4\text{F}$),

5.83 (bs, 1H, *p*-C₆H₄F), 2.61 (m, 4H, CHMe₂), 2.00 (m, 4H, CHMe₂), 1.17 (q, 6H, CHMe, 8.0 Hz), 1.04 (q, 6H, CHMe, 8.0 Hz), 0.99 (q, 6H, CHMe, 8.0 Hz), 0.75 (q, 6H, CHMe, 8.0 Hz); ¹⁹F NMR (C₆D₆): δ -121.6 (s, *p*-C₆H₄F); ¹³C {¹H} NMR (C₆D₆): 165.1 (t, *J*_{P-C} = 6.4 Hz, POCOP), 160.9 (d, *J*_{F-C} = 243 Hz, CF), 140.2 (dt, *J*_{Rh-C} = 34 Hz, *J*_{P-C} = 7.1 Hz, POCOP), 137.1 (bs, *p*-C₆H₄F), 136.4 (dt, *J*_{Rh-C} = 37 Hz, *J*_{P-C} = 9.7 Hz, *p*-C₆H₄F), 136.3 (bs, *p*-C₆H₄F), 127.4 (s, POCOP), 114.3 (bs, *p*-C₆H₄F), 114.0 (bs, *p*-C₆H₄F), 107.4 (t, *J*_{P-C} = 6.0 Hz, POCOP), 31.1 (t, *J*_{P-C} = 11 Hz, CHMe₂), 28.3 (t, *J*_{P-C} = 12 Hz, CHMe₂), 18.0 (t, *J*_{P-C} = 2.3 Hz, CHMe₂), 17.3 (s, CHMe₂), 16.3 (s, CHMe₂), 15.6 (s, CHMe₂). Elem. Anal. Calc. for C₂₄H₃₅BrFO₂P₂Rh: C, 46.55; H, 5.70. Found: C, 46.72; H, 5.78.

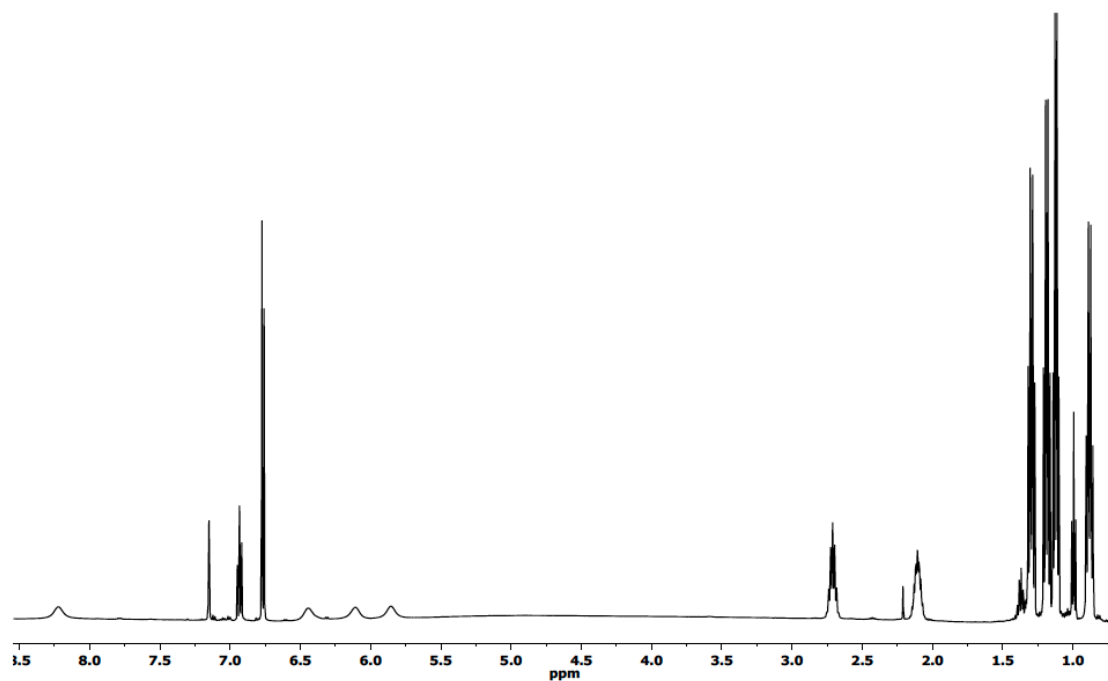


Figure 3-10. ¹H NMR spectrum of (POCOP)Rh(*p*-C₆H₄F)(Br) (**303**) in C₆D₆. Minor residual pentane and toluene present.

Synthesis of (POCOP)Rh(*p*-C₆H₄CF₃)(*p*-NH(C₆H₄Me)) (304). 205 (498 mg, 1.04 mmol) was combined with NaO^tBu (199 mg, 2.07 mmol), *p*-CF₃C₆H₄Br (218 μL, 1.56 mmol), and *p*-NH₂(C₆H₄Me) (114 mg, 1.06 mmol) in a Schlenk flask and dissolved in toluene. The reaction was stirred at RT and immediately turned a dark purple color. After stirring for 60 min at RT, the solution was passed through a pad of Celite and the volatiles were removed by vacuum. The compound was recrystallized by dissolving in a minimum amount of pentane at -35°C, yielding a purple solid (520 mg, 72%). ³¹P {¹H} NMR (C₆D₆): δ 172.6 (d, *J*_{Rh-P} = 125 Hz); ¹H NMR (C₆D₆, Figure 3-11): δ 8.13 (bs, 1H, C₆H₄CF₃), 7.08 (d, 2H, NH₂(C₆H₄Me), *J* = 8.0 Hz), 6.99 – 6.96 (overlapping t & d; t, 1H, POCOP, *J* = 7.0 Hz; d, 2H, NH(C₆H₄Me), *J* = 8.0 Hz), 6.90 (bs, 1H, C₆H₄CF₃), 6.84 (d, 2H, POCOP, *J* = 8.5 Hz), 6.60 (bs, 1H, C₆H₄CF₃), 6.13 (bs, 1H, C₆H₄CF₃), 5.76 (s, 1H, NH(C₆H₄Me)), 2.29 (s, 3H, NH(C₆H₄Me)), 2.12 (m, 4H, CHMe₂), 0.95 (q, 6H, CHMe₂, 7.0 Hz), 0.90 (q, 6H, CHMe₂, 7.0 Hz), 0.79 (q, 6H, CHMe₂, 7.0 Hz), 0.69 (q, 6H, CHMe₂, 7.0 Hz); ¹⁹F NMR (C₆D₆): δ -62.3 (s, C₆H₄CF₃); ¹³C {¹H} NMR (C₆D₆): 164.1 (t, *J*_{P-C} = 6.0 Hz, POCOP), 159.5 (s), 151.7 (dt, *J*_{Rh-C} = 34 hz, *J*_{P-C} = 9.8 Hz, *p*-C₆H₄CF₃), 142.5 (dt, *J*_{Rh-C} = 27 Hz, *J*_{P-C} = 6.0 Hz, POCOP), 137.5 (bs, 2 overlapping, *p*-C₆H₄CF₃), 130.0 (s), 126.1 (s), 125.8 (q, *J*_{F-C} = 33 Hz, CCF₃), 125.2 (q, *J*_{F-C} = 271 Hz, CF₃), 123.7 (bs, *p*-C₆H₄CF₃), 123.3 (bs, *p*-C₆H₄CF₃), 119.7 (s), 106.7 (t, *J*_{P-C} = 6.0 Hz, POCOP), 31.2 (t, *J*_{P-C} = 9.8 Hz, CHMe₂), 30.5 (t, *J*_{P-C} = 12 Hz, CHMe₂), 20.9 (s, *p*-NH(C₆H₄Me)), 18.1 (t, *J*_{P-C} = 2.8 Hz, CHMe₂), 17.9 (s, CHMe₂), 16.3 (s, 2 overlapping, CHMe₂). Elem. Anal. Calc. for C₃₂H₄₃F₃NO₂P₂Rh: C, 55.26; H, 6.23. Found: C, 55.19; H, 6.17.

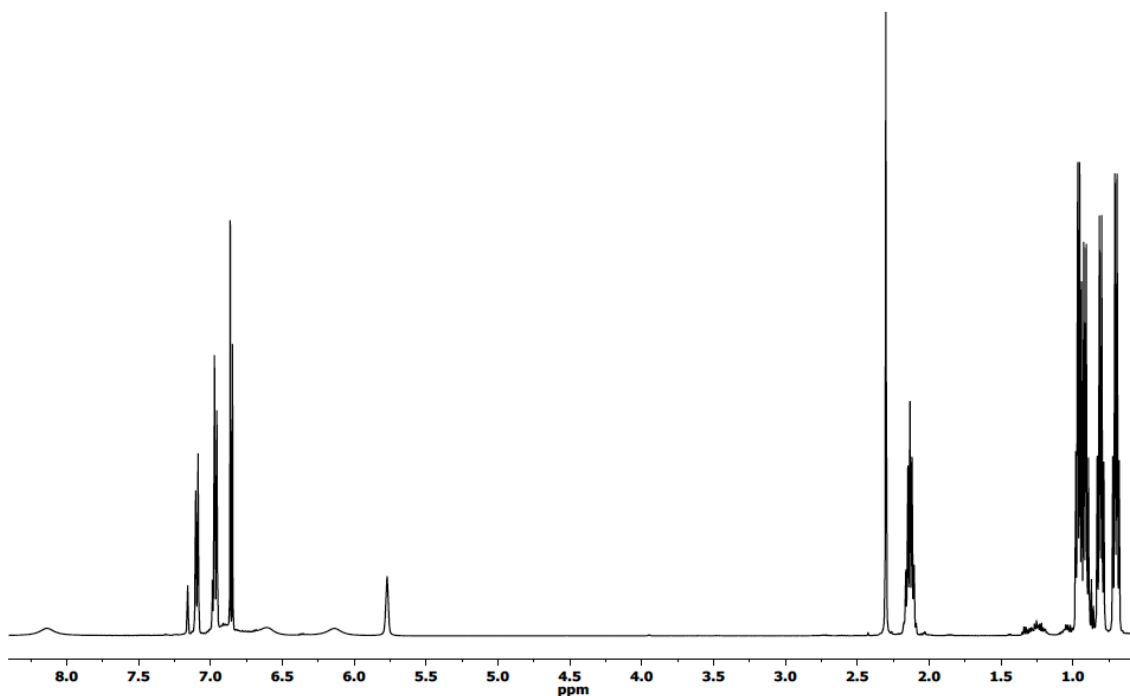


Figure 3-11. ^1H NMR spectrum of $(\text{POCOP})\text{Rh}(p\text{-C}_6\text{H}_4\text{CF}_3)(p\text{-NH}(\text{C}_6\text{H}_4\text{Me}))$ (**304**) in C_6D_6 . Minor residual pentane present.

Synthesis of $(\text{POCOP})\text{Rh}(p\text{-C}_6\text{H}_4\text{F})(\text{NHPh})$ (305**).** **303** (46.3 mg, 0.0747 mmol), NH_2Ph (6.8 μL , 0.747 mmol), and NaO^tBu (14 mg, 0.146 mmol) were combined in a Schlenk flask and dissolved in toluene. The reaction was stirred at RT resulting in an immediate color change from red to purple. After stirring for 60 min at RT the reaction was passed through a pad of Celite. The volatiles were removed under vacuum at 80 $^\circ\text{C}$ yielding a purple solid (34.5 mg, 73% yield). $^{31}\text{P}\{^1\text{H}\}$ NMR (C_6D_6): δ 172.1 (d, $J_{\text{Rh-P}} = 127$ Hz); ^1H NMR (C_6D_6 , Figure 3-12): 7.92 (bs, 1H, $p\text{-C}_6\text{H}_4\text{F}$), 7.28 (t, 2H, 6.5 Hz, $\text{NH}(\text{C}_6\text{H}_5)$), 7.02 (d, 2H, 7.5 Hz, $\text{NH}(\text{C}_6\text{H}_5)$), 6.95 (t, 1H, 7.5 Hz, POCOP), 6.84 (d, 2H,

8.0 Hz, POCOP), 6.82 (t, 1H, 6.0 Hz, NH(C₆H₅)), 6.47 (bs, 1H, *p*-C₆H₄F), 6.22 (bs, 1H, *p*-C₆H₄F), 5.95 (bs, 1H, *p*-C₆H₄F), 5.65 (s, 1H, NHPPh), 2.14 (m, 4H, CHMe₂), 0.96 (q, 6H, 6.5 Hz, CH(CH₃)₃), 0.90 (q, 6H, 6.5 Hz, CH(CH₃)₃), 0.86 (q, 6H, 6.5 Hz, CH(CH₃)₃), 0.76 (q, 6H, 6.5 Hz, CH(CH₃)₃). ¹⁹F NMR (C₆D₆): δ -122.6 (s, Ph-F); ¹³C{¹H} NMR (C₆D₆): 164.3 (t, *J*_{P-C} = 6.0 Hz, POCOP), 161.9 (s), 161.0 (d, *J*_{F-C} = 242 Hz, C-F), 142.5 (dt, *J*_{Rh-C} = 26 Hz, *J*_{P-C} = 6.0 Hz, POCOP), 137.4 (bs, *p*-C₆H₄F), 137.1 (bs, *p*-C₆H₄F), 136.2 (dt, *J*_{Rh-C} = 35 Hz, *J*_{P-C} = 10 Hz, *p*-C₆H₄F), 129.2 (s), 126.0 (s), 119.4 (s), 116.0 (s), 114.2 (bs, 2 overlapping, *p*-C₆H₄F), 106.6 (t, *J*_{P-C} = 6.0 Hz, POCOP), 31.2 (t, *J*_{P-C} = 10 Hz, CHMe₂), 30.2 (t, *J*_{P-C} = 10 Hz, CHMe₂), 18.1 (t, *J*_{P-C} = 3.0 Hz, CHMe₂), 18.0 (s, CHMe₂), 16.4 (s, 2 overlapping, CHMe₂). Elem. Anal. Calc. for C₃₀H₄₁FNO₂P₂Rh: C, 57.06; H, 6.54. Found: C, 57.03; H, 6.48.

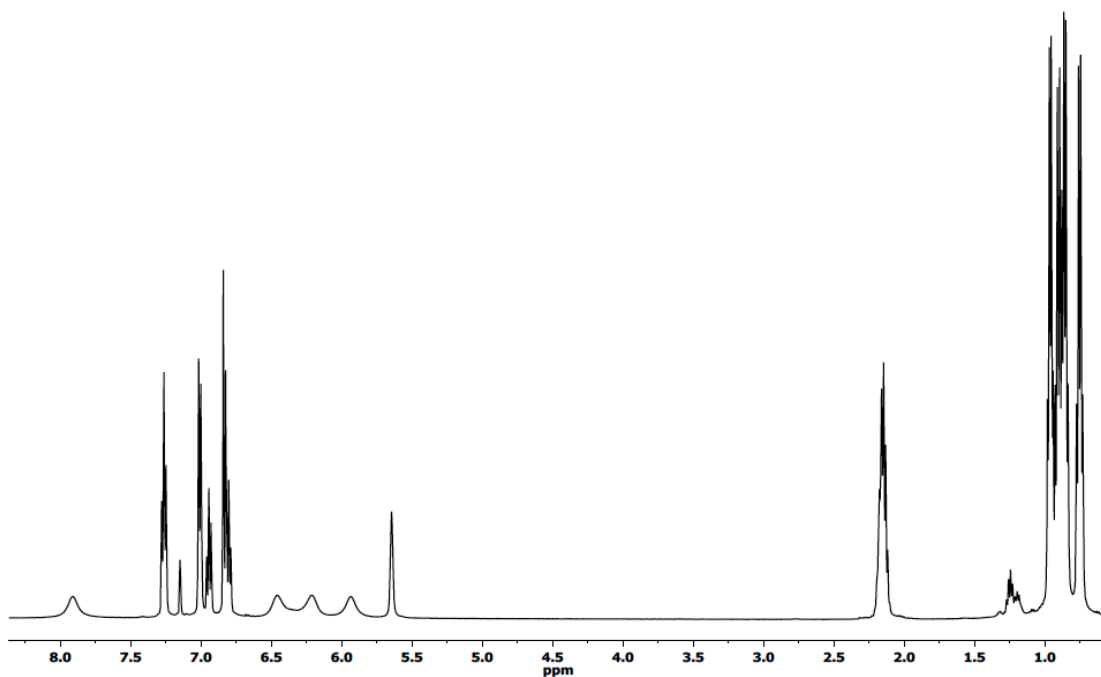


Figure 3-12. ^1H NMR spectrum of (POCOP)Rh(*p*-C₆H₄F)(NHPh) (**305**) in C₆D₆. Minor residual pentane present.

Reductive elimination of NH(*p*-C₆H₄CF₃)(*p*-C₆H₄Me) from **304.** **304** (11 mg, 0.016 mmol) was treated with *p*-CF₃C₆H₄Br (2.5 μL , 0.0165 mmol) in a J. Young tube and dissolved in toluene. C₆H₅F (5.0 μL , 0.053 mmol) was added to act as an internal standard. The sample was heated for 2 h in a 115 $^\circ\text{C}$ oil bath. Analysis of the reaction by ^{19}F NMR showed the complete disappearance of **304** and the presence of **301** (94%), NH(*p*-NH(C₆H₄Me))(*p*-C₆H₄CF₃) (90%), CF₃C₆H₅ (5%). The baseline showed the presence of several minor impurities, none of which individually amounted to more than 1% of the reaction mixture.

Synthesis of 304 from 302. **302** (20 mg, 0.032 mmol) was combined with NaO^tBu (5.0 mg, 0.052 mmol) and *p*-NH₂(C₆H₄Me) in a vial and dissolved in toluene. The reaction immediately turned from red to dark purple. The reaction was stirred at RT for 90 min and then passed over a pad of Celite. The volatiles were removed by vacuum leaving a purple solid. The ¹H and ³¹P{¹H} NMR spectra were consistent with formation of **304**.

Synthesis of (POCOP)Rh(*p*-C₆H₄CF₃)(O(CH₃)₃) (306). **302** (425 mg, 0.683 mmol) and NaO^tBu (131 mg, 1.37 mmol) were combined in a Schlenk flask and dissolved in toluene. The reaction was stirred at RT resulting in a slight color change from red to red-orange. After stirring for 3 h at RT the reaction was passed through a pad of Celite and stripped to remove volatiles giving a dark red-orange solid. The solid was recrystallized from pentane at -35° C (341 mg, 75% yield). ³¹P{¹H} NMR (C₆D₆): δ 166.6 (d, *J*_{Rh-P} = 127 Hz); ¹H NMR (C₆D₆, Figure 3-13): δ 8.45 (bs, 2H, *p*-C₆H₄CF₃), 6.94 (t, 1H, POCOP, *J* = 8.0 Hz), 6.80 (d, 2H, POCOP, *J* = 7.0 Hz), 6.02 (bs, 2H, *p*-C₆H₄CF₃), 2.40 (m, 2H, CHMe₂), 2.00 (m, 2H, CHMe₂), 1.52 (s, 9H, O(CH₃)₃), 1.16 (q, 6H, CHMe₂, *J* = 8.5 Hz), 1.05 (q, 6H, CHMe₂, *J* = 8.5 Hz), 0.93 (q, 6H, CHMe₂, *J* = 8.5 Hz), 0.54 (q, 6H, CHMe₂, *J* = 8.5 Hz); ¹⁹F NMR (C₆D₆): δ -62.3 (s, CF₃); ¹³C{¹H} NMR (C₆D₆): δ 165.2 (t, 5.9 Hz, POCOP), 149.3 (dt, *J*_{Rh-C} = 35 Hz, *J*_{P-C} = 10 Hz, *p*-C₆H₄CF₃), 137.4 (dt, *J*_{Rh-C} = 29 Hz, *J*_{P-C} = 6.0 Hz, POCOP), 137.1 (bs, 2 overlapping, *p*-C₆H₄CF₃), 126.0 (s, POCOP), 125.8 (q, *J*_{F-C} = 32 Hz, CCF₃), 125.5 (q, *J*_{F-C} = 271 Hz, CF₃), 106.8 (t, *J*_{P-C} = 6.0 Hz, POCOP), 70.0 (s, OC(CH₃)₃) 35.1 (s, OC(CH₃)₃), 30.9 (t, *J*_{P-C} = 9.7 Hz, CHMe₂), 29.1 (t, *J*_{P-C} = 12 Hz, CHMe₂), 19.1 (t, *J*_{P-C} = 2.3 Hz, CHMe₂), 16.8 (s,

CHMe₂), 16.4 (t, $J_{P-C} = 2.8$ Hz, CHMe₂), 16.2 (s, CHMe₂). Elem. Anal. Calc. for C₂₉H₄₄F₃O₃P₂Rh: C, 52.57; H, 6.69. Found: C, 52.48, H, 6.75.

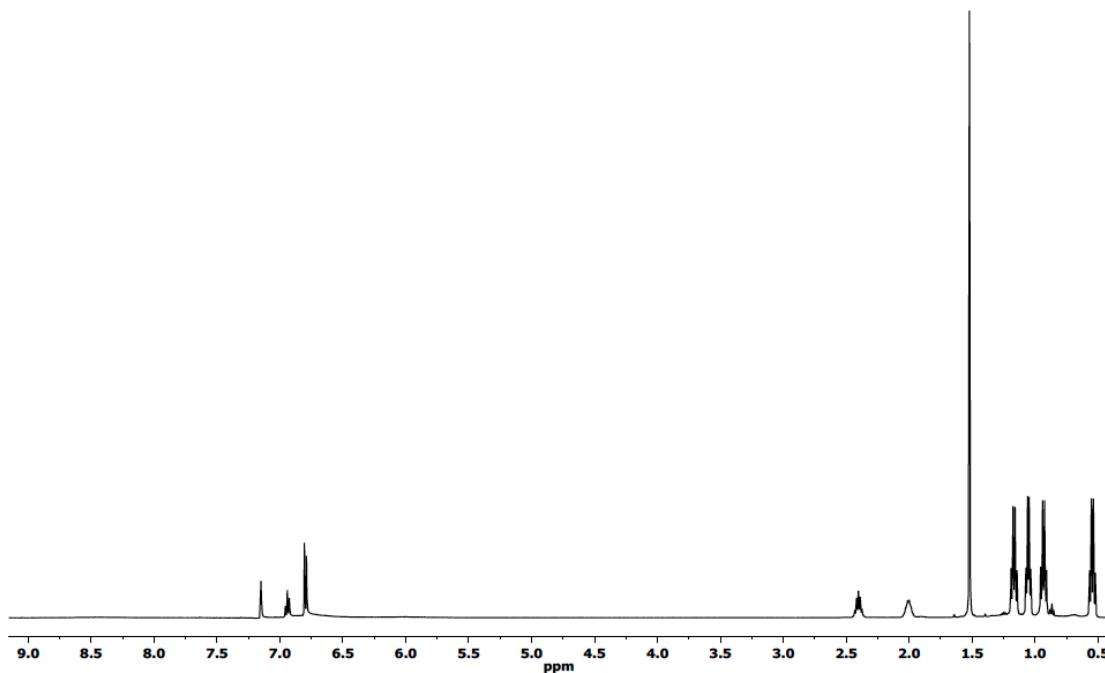


Figure 3-13. ¹H NMR spectrum of (POCOP)Rh(*p*-C₆H₄CF₃)(O(CH₃)₃) (**306**) in C₆D₆. Resonances corresponding to *p*-C₆H₄CF₃ protons are broad in the baseline.

Synthesis of 304 from 306. **306** (23 mg, 0.035 mmol) was added to a J. Young tube and dissolved in toluene. The red-orange solution was treated with *p*-NH₂(C₆H₄Me) (4 mg, 0.037 mmol) and the color immediately changed to dark purple. After 60 min at RT, the reaction was passed through a pad of Celite and the volatiles were removed leaving a purple solid. The ¹H and ³¹P{¹H} NMR spectrum were consistent with formation of **304**.

Synthesis of (POCOP)Rh(*p*-C₆H₄F)(NPh₂) (307). **303** (76 mg, 0.12 mmol) was combined with NaO^tBu (18 mg, 0.18 mmol) in a Schlenk flask and dissolved in toluene. NH₂Ph (20 mg, 0.12 mmol) was added to the solution, resulting in an immediate color change to purple. The reaction was stirred for 6 h at RT. The volatiles were removed by vacuum. The product was extracted with pentane and passed through a pad of Celite. The volatiles were removed to give a purple solid. The solid was dissolved in a minimum of pentane and left to recrystallize at -35 °C. Recrystallization yielded a purple crystalline solid (65 mg, 77%). ¹H NMR (C₆D₆, Figure 3-14): δ 7.75 (t, 6.0 Hz, 1H), 7.17 (t, 8.0 Hz, 3H), 6.93 (t, 9.5 Hz, 2H), 6.86 (m, 5H), 6.75 (d, 6.0 Hz, 2H), 6.67 (t, 6.0 Hz, 2H), 6.49 (t, 6.5 Hz, 1H), 6.30 (t, 6.0 Hz, 1H), 2.62 (m, 2H, CHMe₂), 1.90 (m, 2H, CHMe₂), 0.93 (q, 6.0 Hz, 6H, CHMe₂), 0.88 (q, 6.0 Hz, 6H, CHMe₂), 0.66 (q, 6.0 Hz, 6H, CHMe₂), 0.61 (q, 6.0 Hz, 6H, CHMe₂); ³¹P{¹H} NMR (C₆D₆): δ 169.5 (d, 115 Hz); ¹⁹F NMR (C₆D₆): δ 122.1 (s); ¹³C{¹H} NMR (C₆D₆): δ 162.4 (t, 6.4 Hz, *J*_{P-C} = 6.4 Hz, POCOP), 161.5 (d, *J*_{F-C} = 235 Hz, C-F), 139.4 (dt, *J*_{Rh-C} = 27 Hz, *J*_{P-C} = 10 Hz, POCOP), 138.9 (d, *J* = 22 Hz), 132.2 (s), 131.8 (s), 131.6 (bs), 126.3 (s, POCOP), 117.8 (s), 115.3 (d, *J* = 18 Hz), 113.5 (*J* = 19 Hz), 107.8 (s, P^OC^OP), 30.4 (t, *J*_{P-C} = 11 Hz, CHMe₂), 28.9 (t, *J*_{P-C} = 12 Hz, CHMe₂), 17.0 (bs, CHMe₂), 16.7 (bs, 2 overlapping, CHMe₂), 16.6 (bs, CHMe₂). Elem. Anal. Calc. for C₃₆H₄₅FNO₂P₂Rh: C, 61.11; H, 6.41. Found: C, 60.97; H, 6.29.

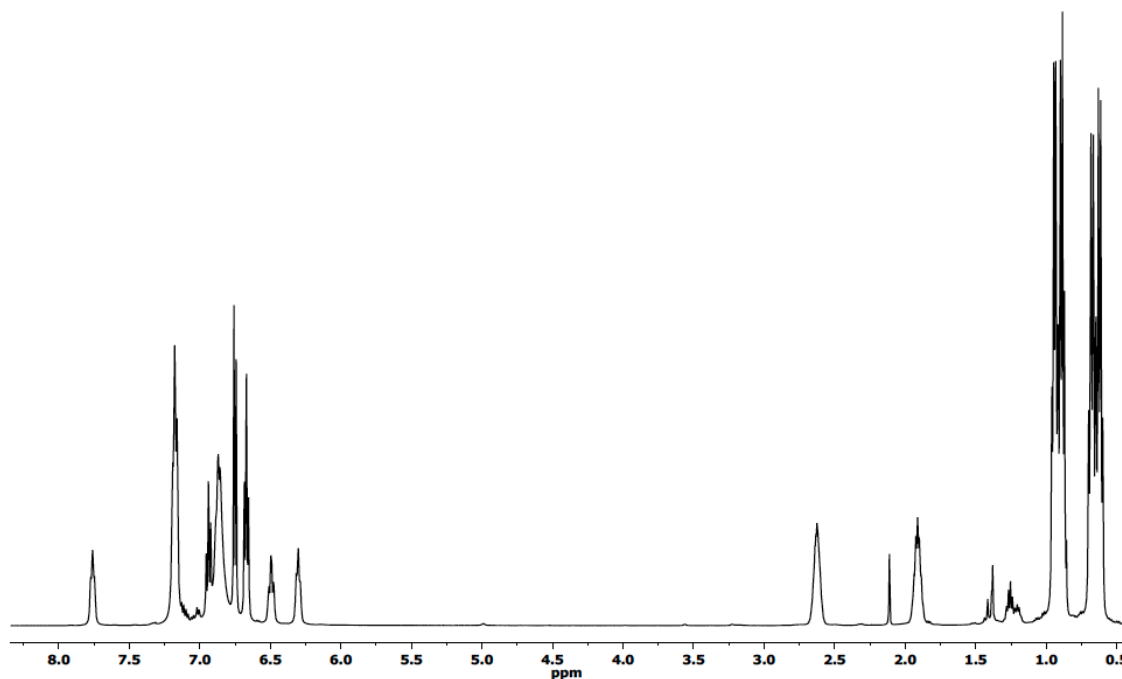


Figure 3-14. ^1H NMR spectrum of (POCOP)Rh(*p*-C₆H₄F)(NPh₂) (**307**) in C₆D₆. Minor residual pentane and toluene present. Also, minor residual NaO^tBu (1.34 ppm) present.

Thermolysis of 307. **307** (16 mg, 0.023 mmol) was treated with *p*-FC₆H₄Br (5.0 μL , 0.046 mmol) in a J. Young tube and dissolved in toluene. C₆H₅CF₃ (2 μL , 0.016 mmol) was added to act as an internal standard. The sample was heated overnight in a 115 °C oil bath. Analysis of the reaction by $^{31}\text{P}\{^1\text{H}\}$ NMR shows the complete conversion of **307** to **303** after 2 d at 110 °C. Analysis by ^{19}F NMR spectroscopy after 2 d at 110 °C also showed complete conversion to **303**. The ^{19}F NMR spectrum also showed the formation of C₆H₅F (70%) and NPh₂(C₆H₄F) (30%). Analysis of the ^1H NMR spectrum showed the presence of NHPh₂ (70%). The baseline showed the

presence of several minor impurities, none of which individually amounted to more than 2% of the reaction mixture.

Amine competition experiment with 303. **303** (26 mg, 0.042 mmol) was combined with NaO^tBu (6 mg, 0.062 mmol) in a J. Young tube and dissolved in C₆D₆. NH₂Ph (8.0 μL, 0.084 mmol) and NPh₂ (11 mg, 0.084 mmol) were added to the sample, resulting in an immediate color change from red to purple. After 30 min at RT, the reaction showed complete conversion to **305** by ³¹P{¹H} and ¹⁹F NMR spectroscopy.

Reaction of 307 with aniline. **307** (21 mg, 0.030 mmol) was added to a J. Young tube and dissolved in C₆D₆. NH₂Ph (3.0 μL, 0.036 mmol) was added to the sample. The color immediately became a lighter purple. After 60 min at RT, the reaction shows complete conversion to **305** by ³¹P{¹H} and ¹⁹F NMR spectroscopy.

Synthesis of (POCOP)Rh(N(Ph)CH₂) (308). **301** (62 mg, 0.092 mmol) was combined with NaO^tBu (9 mg, 0.094 mmol) and *N*-methylaniline (10 μL, 0.093 mmol) in a J. Young tube and dissolved in C₆D₆. The reaction underwent a slight color change from red to red-orange. The solution was stirred for 60 min at RT. The reaction was then passed through a pad of Celite. The volatiles were removed by vacuum to yield an orange solid. The solid was recrystallized by dissolving in a minimum of toluene, layering with pentane, and leaving the resultant solution in a -35 °C freezer (32 mg, 63% yield). X-ray quality crystals were grown by vapor diffusion of pentane into a saturated solution of the compound in toluene at -35 °C. ³¹P{¹H} NMR (C₆D₆): δ 183.6 (d, *J*_{Rh-P} = 175 Hz); ¹H NMR (C₆D₆, Figure 3-15): δ 7.38 (d, 8.0 Hz, 2H, Ph), 7.00 (t, 7.5 Hz, 2H, Ph), 6.95 (t, 7.5 Hz, 1H, POCOP), 6.88 (t, 7.5 Hz, 1H, Ph), 6.85 (d, 7.5 Hz, 2H,

POCOP), 6.43 (bs, 1H, CH_2), 6.28 (bs, 1H, CH_2), 1.93 (m, 4H, CHMe_2), 1.23 (q, 8.0 Hz, 12H, CHMe_2), 1.02 (q, 8.0 Hz, 12H, CHMe_2); $^{13}\text{C}\{^1\text{H}\}$ NMR (C_6D_6): δ 168.2 (t, $J_{\text{C-P}} = 9.3$ Hz, POCOP), 156.1 (s, CH_2), 140.4 (dt, $J_{\text{C-Rh}} = 23$ Hz, $J_{\text{C-P}} = 11$ Hz, POCOP), 128.7 (s), 126.1 (s), 125.4 (s), 122.0 (s), 104.1 (t, $J_{\text{C-P}} = 6.9$ Hz, POCOP), 30.0 (t, $J_{\text{C-P}} = 10$ Hz, CHMe_2), 17.9 (t, $J_{\text{C-P}} = 4.1$ Hz, CHMe_2), 17.5 (s, CHMe_2). Elem. Anal. Calc. for $\text{C}_{25}\text{H}_{38}\text{NO}_2\text{P}_2\text{Rh}$: C, 54.65; H, 6.97. Found: C, 54.61, H, 6.98.

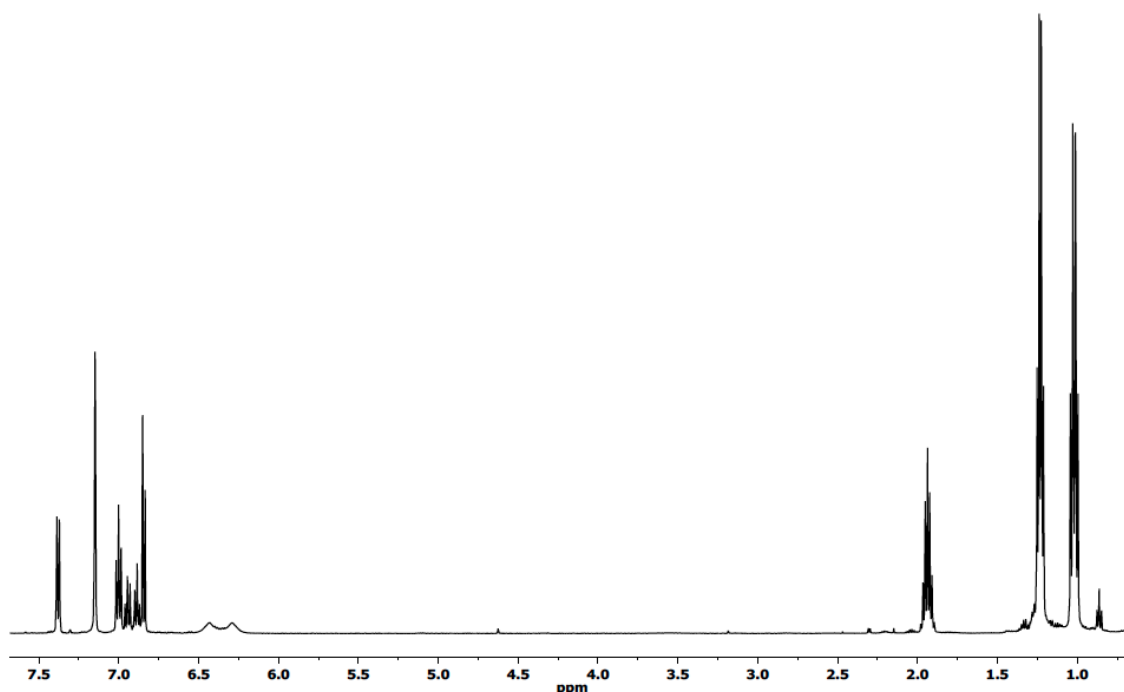


Figure 3-15. ^1H NMR spectrum of $(\text{POCOP})\text{Rh}(\text{N}(\text{Ph})\text{CH}_2)$ (**308**) in C_6D_6 . Minor residual pentane present.

Synthesis of $(\text{POCOP})\text{Rh}(\text{C}_4\text{H}_7\text{N})$ (309**).** **301** (54 mg, 0.081 mmol) was combined with NaO^tBu (8 mg, 0.083 mmol) and pyrrolidine (7 μL , 0.086 mmol) in a J.

Young tube and dissolved in C_6D_6 . The reaction underwent an immediate color change from red to yellow-orange. The solution was stirred for 60 min at RT. The reaction was then passed through a pad of Celite and stripped to remove the volatiles yielding a yellow solid. The solid was recrystallized by dissolving in a minimum of toluene, layering with pentane, and leaving the resultant solution in a $-35\text{ }^\circ\text{C}$ freezer (26 mg, 49% yield). $^{31}\text{P}\{^1\text{H}\}$ NMR (C_6D_6): δ 181.5 (d, $J_{\text{Rh-P}} = 182$ Hz); ^1H NMR (C_6D_6 , Figure 3-16): δ 7.27 (s, 1H, C_4H_7N), 6.96 (t, 1H, POCOP, $J = 9$ Hz), 6.89 (d, 2H, POCOP, $J = 7$ Hz), 3.62 (t, 2H, C_4H_7N , $J = 5.5$ Hz), 2.02 (m, 4H, $CHMe_2$), 1.67 (t, 2H, C_4H_7N , $J = 7$ Hz), 1.32 (q, 12H, $CHMe_2$, $J = 6$ Hz), 1.21 (t, 2H, C_4H_7N , $J = 7.5$ Hz), 1.09 (q, 12H, $CHMe_2$, $J = 6$ Hz); $^{13}\text{C}\{^1\text{H}\}$ NMR (C_6D_6): δ 168.7 (t, $J_{\text{P-C}} = 3.0$ Hz, N=C), 167.9 (t, $J_{\text{P-C}} = 9.7$ Hz, POCOP), 141.6 (dt, $J_{\text{Rh-C}} = 34$ Hz, $J_{\text{P-C}} = 11$ Hz, POCOP), 122.9 (s, POCOP), 103.8 (t, $J_{\text{P-C}} = 6.5$ Hz, POCOP), 65.6 (s, C_4H_7N), 35.7 (s, C_4H_7N), 30.5 (t, $J_{\text{P-C}} = 7.8$ Hz, $CHMe_2$), 20.9 (s, C_4H_7N), 18.5 (t, $J_{\text{P-C}} = 5.1$ Hz, $CHMe_2$), 17.9 (s, $CHMe_2$). Elem. Anal. Calc. for $C_{22}H_{38}O_2P_2Rh$: C, 51.47; H, 7.46. Found: C, 51.42, H, 7.43.

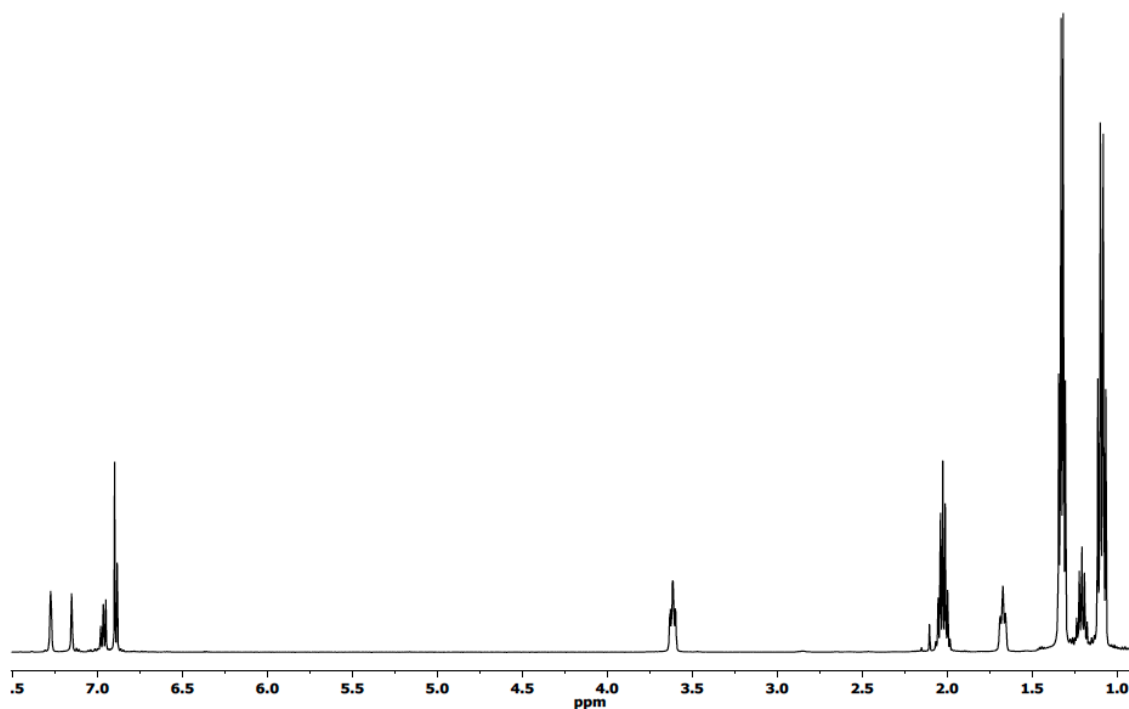


Figure 3-16. ^1H NMR spectrum of (POCOP)Rh(C₄H₇N) (**309**) in C₆D₆.

3.4.3 Kinetic Studies

Kinetic study of the C-N reductive elimination of NH(*p*-C₆H₄CF₃)(*p*-C₆H₄Me) from **304.** **304** (11 mg, 0.016 mmol) was treated with *p*-CF₃C₆H₄Br (four different experiments for four different concentrations of *p*-CF₃C₆H₄Br: 2.3 μL , 0.016 mmol, 0.032 mM; 6.8 μL , 0.049 mmol, 0.098 mM; 11 μL , 0.081 mmol, 0.16 mM; 23 μL , 0.16 mmol, 0.32 mM) in toluene in a J. Young NMR tube. C₆H₅F (5.0 μL , 0.053 mmol) was added to each sample to act as an internal standard. The sample was inserted into the NMR probe, which was preheated to 105 $^{\circ}\text{C}$. The disappearance of **304** was monitored by ^{19}F NMR at regular intervals for at least three half-lives.

Over the course of the reaction **304** (-62.3 ppm) was converted to **301** (-62.6 ppm) and free NH(*p*-C₆H₄Me)(*p*-C₆H₄CF₃) (-61.7 ppm). Minor additional signals (-61.0 ppm and -62.4 ppm) were also observed during the kinetic studies; however, these signals disappeared for the reactions that were monitored to completion resulting in the final spectrum exclusively displaying signals for **301**, free NH(*p*-C₆H₄Me)(*p*-C₆H₄CF₃), and the remaining excess *p*-BrC₆H₄CF₃.

Rate constants:

$$5.1(2) \times 10^{-4} \text{ for } 0.032 \text{ mM}$$

$$6.0(1) \times 10^{-4} \text{ for } 0.098 \text{ mM}$$

$$6.5(1) \times 10^{-4} \text{ for } 0.16 \text{ mM}$$

$$7.3(1) \times 10^{-4} \text{ for } 0.63 \text{ mM}$$

$$\text{Average } t_{1/2} \approx 19 \text{ min}$$

A note on the error calculation: the errors in the values of the rate constants were taken to be twice the standard deviation (σ) calculated using the LINEST function in the statistical analysis in MS excel.

A note on the temperature measurement: the temperature inside the NMR probe was determined to be 105.2 °C via a chemical shift thermometer (neat ethylene glycol). An uncertainty of 1 °C for this type of temperature measurement was assumed.

Determination of activation parameters for RE from 304 via Eyring plot.

304 (11 mg, 0.016 mmol) was treated with *p*-CF₃C₆H₄Br (6.8 μL, 0.049 mmol, 0.098

mM) in toluene in a J. Young NMR tube. C₆H₅F (5.0 μL, 0.053) was added to each sample to act as an internal standard. The sample was inserted into the NMR probe, which was preheated (five different experiments at five different temperatures: 105 °C, 95 °C, 85 °C, 75 °C, and 65 °C). The reactions were monitored for a minimum of three half-lives. Over the course of the reaction **304** was converted to **301**. The rates of C-N reductive elimination from **304** at the different temperatures were determined by analysis of the disappearance of **304** by ¹⁹F NMR spectroscopy (Table 3-2). An Eyring plot was used to obtain the enthalpy and entropy of activation, ΔH[‡] = 18.5(7) kcal/mol and ΔS[‡] = -25(2) eu, respectively.

Table 3-2. Rates of C-N reductive elimination for **304** from 65 °C – 105 °C and corresponding Eyring plot parameters.

| <i>T</i> (°C) | <i>T</i> (K) | <i>Rate</i> (s ⁻¹) | <i>ln</i> (<i>k</i> / <i>T</i>) | <i>1/T</i> (K ⁻¹) |
|---------------|--------------|--------------------------------|-----------------------------------|-------------------------------|
| 105 | 378 | 6.50 × 10 ⁻⁴ | -13.3 | 2.64 × 10 ⁻³ |
| 95 | 368 | 3.08 × 10 ⁻⁴ | -14.0 | 2.71 × 10 ⁻³ |
| 85 | 358 | 1.23 × 10 ⁻⁴ | -14.9 | 2.79 × 10 ⁻³ |
| 85 | 358 | 1.18 × 10 ⁻⁴ | -14.9 | 2.79 × 10 ⁻³ |
| 85 | 358 | 9.45 × 10 ⁻⁵ | -15.1 | 2.79 × 10 ⁻³ |
| 75 | 348 | 9.37 × 10 ⁻⁵ | -15.1 | 2.87 × 10 ⁻³ |
| 75 | 348 | 8.36 × 10 ⁻⁵ | -15.2 | 2.87 × 10 ⁻³ |
| 75 | 348 | 5.53 × 10 ⁻⁵ | -15.7 | 2.87 × 10 ⁻³ |
| 65 | 338 | 2.47 × 10 ⁻⁵ | -16.4 | 2.96 × 10 ⁻³ |

A note on the error calculation for the Eyring plot: the temperature inside the NMR probe was determined via a chemical shift thermometer (neat ethylene glycol). Assume an uncertainty of 1 °C for this type of temperature measurements. Errors in ΔH[‡] and ΔS[‡] were determined using the error propagation formulas presented by Girolami et

al.¹⁰⁹ It is worth noting that in the reaction at 65 °C, the graph was slightly non-linear (Figure 3-7). For reactions at this temperature, the incremental changes are smaller, which makes the relative importance of the error of measurement greater.

3.4.4 Catalytic Reactions

Catalytic coupling reaction of *p*-FC₆H₄Br and NH₂Ph with 205 as catalyst. 205 (3.3 mg, 0.0068 mmol) was combined with *p*-FC₆H₄Br (25 μL, 0.23 mmol), NaO^tPent (38 mg, 0.34 mmol), NH₂Ph (25 μL, 0.27 mmol), and partially dissolved in toluene. C₆H₅CF₃ (5.0 μL, 0.041 mmol) was added to the reaction to act as an internal standard. The reaction mixture immediately turned dark purple. The reaction was heated at 115 °C for 48 h. Analysis of the reaction by ¹⁹F NMR spectroscopy revealed NH(*p*-C₆H₄F)(Ph) (32%), C₆H₅F (10%), and *p*-FC₆H₄Br (58%).

Catalytic coupling reaction of *p*-FC₆H₄Br and *p*-NH₂(C₆H₄Me) with 205 as catalyst. 205 (3.3 mg, 0.0068 mmol) was combined with *p*-FC₆H₄Br (25 μL, 0.23 mmol), NaO^tPent (38 mg, 0.34 mmol), *p*-NH₂(C₆H₄Me) (29 mg, 0.27 mmol), and partially dissolved in toluene. C₆H₅CF₃ (5.0 μL, 0.041 mmol) was added to the reaction to act as an internal standard. The reaction mixture immediately turned dark purple. The reaction was heated at 115 °C for 48 h. Analysis of the reaction by ¹⁹F NMR spectroscopy revealed NH(*p*-C₆H₄F)(*p*-C₆H₄Me) (46%), C₆H₅F (11%), and *p*-FC₆H₄Br (43%).

Catalytic coupling reaction of *p*-FC₆H₄Br and *o*-NH₂(C₆H₄Me) with 205 as catalyst. 205 (3.3 mg, 0.0068 mmol) was combined with *p*-FC₆H₄Br (25 μL, 0.23 mmol), NaO^tPent (38 mg, 0.34 mmol), *o*-NH₂(C₆H₄Me) (29 μL, 0.27 mmol), and

partially dissolved in toluene. $C_6H_5CF_3$ (5.0 μ L, 0.041 mmol) was added to the reaction to act as an internal standard. The reaction mixture immediately turned dark purple. The reaction was heated at 115 °C for 48 h. Analysis of the reaction by ^{19}F NMR spectroscopy revealed $NH(p-C_6H_4F)(o-C_6H_5Me)$ (33%), C_6H_5F (10%), and $p-FC_6H_4Br$ (57%).

Catalytic coupling reaction of $p-FC_6H_4Cl$ and NH_2Ph with **205 as catalyst.**

205 (3.4 mg, 0.0071 mmol) was combined with $p-FC_6H_4Cl$ (25 μ L, 0.23 mmol), NaO^tPent (38 mg, 0.35 mmol), NH_2Ph (26 μ L, 0.28 mmol), and partially dissolved in toluene. $C_6H_5CF_3$ (5.0 μ L, 0.041 mmol) was added to the reaction to act as an internal standard. The reaction mixture immediately turned dark purple. The reaction was heated at 115 °C for 48 h. Analysis of the reaction by ^{19}F NMR spectroscopy revealed $NH(p-C_6H_4F)(Ph)$ (20%), C_6H_5F (8%), and $p-FC_6H_4Cl$ (72%).

Catalytic coupling reaction of $p-FC_6H_4Cl$ and $p-NH_2(C_6H_4Me)$ with **205 as catalyst.** **205** (3.4 mg, 0.0071 mmol) was combined with $p-FC_6H_4Cl$ (25 μ L, 0.23 mmol), NaO^tPent (38 mg, 0.35 mmol), $p-NH_2(C_6H_4Me)$ (30 mg, 0.28 mmol), and partially dissolved in toluene. $C_6H_5CF_3$ (5.0 μ L, 0.041 mmol) was added to the reaction to act as an internal standard. The reaction mixture immediately turned dark purple. The reaction was heated at 115 °C for 48 h. Analysis of the reaction by ^{19}F NMR spectroscopy revealed $NH(p-C_6H_4F)(p-C_6H_4Me)$ (27%), C_6H_5F (8%), and $p-FC_6H_4Cl$ (65%).

Catalytic coupling reaction of $p-FC_6H_4Cl$ and $o-NH_2(C_6H_4Me)$ with **205 as catalyst.** **205** (3.4 mg, 0.0071 mmol) was combined with $p-FC_6H_4Cl$ (25 μ L, 0.23

mmol), NaO^tPent (38 mg, 0.35 mmol), *o*-NH₂(C₆H₄Me) (30 μL, 0.28 mmol), and partially dissolved in toluene. C₆H₅CF₃ (5.0 μL, 0.041 mmol) was added to the reaction to act as an internal standard. The reaction mixture immediately turned dark purple. The reaction was heated at 115 °C for 48 h. Analysis of the reaction by ¹⁹F NMR spectroscopy revealed NH(*p*-C₆H₄F)(*o*-C₆H₄Me) (22%), C₆H₅F (9%), and *p*-FC₆H₄Cl (69%).

Catalytic coupling reaction of *p*-CF₃C₆H₄Br and NH₂Ph with 205 as catalyst.

205 (2.7 mg, 0.0054 mmol) was combined with *p*-CF₃C₆H₄Br (25 μL, 0.18 mmol), NaO^tPent (30 mg, 0.27 mmol), NH₂Ph (20 μL, 0.22 mmol), and partially dissolved in toluene. C₆H₅F (10 μL, 0.11 mmol) was added to the reaction to act as an internal standard. The reaction mixture immediately turned dark purple. The reaction was heated at 115 °C for 48 h. Analysis of the reaction by ¹⁹F NMR spectroscopy revealed no conversion from *p*-CF₃C₆H₄Br.

Catalytic coupling reaction of *p*-CF₃C₆H₄Br and *p*-NH₂(C₆H₄Me) with 205 as catalyst. **205** (2.7 mg, 0.0054 mmol) was combined with *p*-CF₃C₆H₄Br (25 μL, 0.18 mmol), NaO^tPent (30 mg, 0.27 mmol), *p*-NH₂(C₆H₄Me) (23 mg, 0.22 mmol), and partially dissolved in toluene. C₆H₅F (10 μL, 0.11 mmol) was added to the reaction to act as an internal standard. The reaction mixture immediately turned dark purple. The reaction was heated at 115 °C for 48 h. Analysis of the reaction by ¹⁹F NMR spectroscopy revealed no conversion from *p*-CF₃C₆H₄Br.

Catalytic coupling reaction of *p*-CF₃C₆H₄Br and *o*-NH₂(C₆H₄Me) with 205 as catalyst. 205 (2.7 mg, 0.0054 mmol) was combined with *p*-CF₃C₆H₄Br (25 μL, 0.18 mmol), NaO^tPent (30 mg, 0.27 mmol), *o*-NH₂(C₆H₄Me) (23 μL, 0.22 mmol), and partially dissolved in toluene. C₆H₅F (10 μL, 0.11 mmol) was added to the reaction to act as an internal standard. The reaction mixture immediately turned dark purple. The reaction was heated at 115 °C for 48 h. Analysis of the reaction by ¹⁹F NMR spectroscopy revealed no conversion from *p*-CF₃C₆H₄Br.

Control catalytic reaction using [(cod)RhCl]₂. [(cod)RhCl]₂ (1.7 mg, 0.0068 mmol Rh) was combined with *p*-FC₆H₄Br (25 μL, 0.23 mmol), NaO^tPent (38 mg, 0.34 mmol), NH₂Ph (25 μL, 0.27 mmol), and partially dissolved in toluene. C₆H₅CF₃ (5.0 μL, 0.041 mmol) was added to the reaction to act as an internal standard. The reaction was heated at 115 °C for 48 h. Analysis of the reaction by ¹⁹F NMR spectroscopy revealed no discernible formation of new products and no change in the concentration of *p*-FC₆H₄Br.

Control catalytic reaction using [(cod)RhCl]₂/PCy₃. [(cod)RhCl]₂ (1.7 mg, 0.0068 mmol Rh) was combined with PCy₃ (4.0 mg, 0.014 mmol), *p*-FC₆H₄Br (25 μL, 0.23 mmol), NaO^tPent (38 mg, 0.34 mmol), NH₂Ph (25 μL, 0.27 mmol), and partially dissolved in toluene. C₆H₅CF₃ (5.0 μL, 0.041 mmol) was added to the reaction to act as an internal standard. The reaction was heated at 115 °C for 48 h. Analysis of the reaction by ¹⁹F NMR spectroscopy revealed no discernible formation of new products and no change in the concentration of *p*-FC₆H₄Br.

3.4.5 X-ray Crystallography

X-Ray data collection, solution, and refinement for 305. A single purple crystal of suitable size and quality ($0.05 \times 0.06 \times 0.12$ mm) was selected from a representative sample of crystals of the same habit using an optical microscope, mounted onto a nylon loop and placed in a cold stream of nitrogen (110 K). Low-temperature X-ray data were obtained on a Bruker APEXII CCD based diffractometer (Mo sealed X-ray tube, $K_{\alpha} = 0.71073$ Å). All diffractometer manipulations, including data collection, integration and scaling were carried out using the Bruker APEXII software.⁸⁸ An absorption correction was applied using SADABS.⁸⁸ The space group was determined on the basis of systematic absences and intensity statistics and the structure was solved by direct methods and refined by full-matrix least squares on F^2 . The structure was solved in the orthorhombic *Pbca* space group using XS⁸⁹ (incorporated in X-Seed). This symmetry was confirmed by PLATON.⁹⁰ All non-hydrogen atoms were refined with anisotropic thermal parameters. Hydrogen atoms were placed in idealized positions and refined using riding model. The structure was refined (weighted least squares refinement on F^2) to convergence.

X-Ray data collection, solution, and refinement for 308. A single orange crystal of suitable size and quality ($0.6 \times 0.9 \times 0.05$ mm) was selected from a representative sample of crystals of the same habit using an optical microscope, mounted onto a nylon loop and placed in a cold stream of nitrogen (110 K). Low-temperature X-ray data were obtained on a Bruker APEXII CCD based diffractometer (Mo sealed X-ray tube, $K_{\alpha} = 0.71073$ Å). All diffractometer manipulations, including data collection, integration and scaling were carried out using the Bruker APEXII software.⁸⁸ An

absorption correction was applied using SADABS.⁸⁸ The space group was determined on the basis of systematic absences and intensity statistics and the structure was solved by direct methods and refined by full-matrix least squares on F^2 . The structure was solved in the monoclinic $P 2_1/m$ space group using XS⁸⁹ (incorporated in X-Seed). Half of the structure was symmetry generated across the central mirror plane. This symmetry was confirmed by PLATON.⁹⁰ All non-hydrogen atoms were refined with anisotropic thermal parameters. Hydrogen atoms were placed in idealized positions and refined using riding model. The structure was refined (weighted least squares refinement on F^2) to convergence.

CHAPTER IV

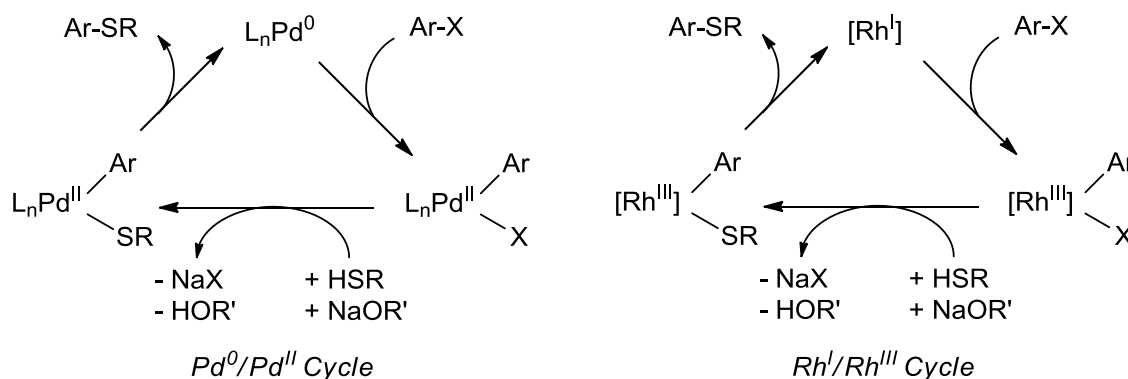
A WELL DEFINED (POCOP)RH CATALYST FOR THE COUPLING OF ARYL HALIDES WITH THIOLS

4.1 Introduction

The prevalence of aryl sulfides in biologically and pharmaceutically active compounds has sparked an increased interest towards improving methodologies to form these groups.¹¹⁰ Aryl-sulfur bonds can be formed by the direct reaction of thiolates with aryl halides under harsh conditions ($>200\text{ }^{\circ}\text{C}$).^{93,111} Early development of transition metal catalysts for C-S coupling was hindered due to catalyst poisoning by HSR of SR_2 , which was primarily seen with Pt catalysts.¹¹² Beginning with the Cu-catalyzed Ullman reaction,²⁸ the utilization of transition metals to catalyze this transformation has resulted in improved selectivity and more reasonable reaction conditions. Over the last decade, additional transition metals including Pd^{31,113}, Ni²⁶, and Co¹¹⁴ have also been used to catalyze the coupling of aryl halides with thiols to form aryl sulfides. While Ni and Cu catalysts have shown high turnover ($>95\%$) under reasonable conditions (RT – $80\text{ }^{\circ}\text{C}$), their success is limited to aryl bromides and iodides.

Pd catalysts have been developed to function with aryl chlorides with low catalyst loadings (0.005%) and up to 18,000 TON.³² However these reactions typically require higher reaction temperatures ($90 - 110\text{ }^{\circ}\text{C}$). In addition, the most successful Pd catalysts typically depend on evolved phosphine ligands that are costly or require multistep syntheses.^{30c,32} The mechanism for Pd catalyzed C-S cross-coupling reactions

was extensively examined by Hartwig and coworkers in 2009.¹¹⁵ The ability of Pd to effectively perform these transformations, as well as other carbon-heteroatom coupling reactions, is due to its capacity to undergo two-electron oxidative addition (OA) and reductive elimination (RE) events between Pd(0) and Pd(II) oxidation states. The mechanism of Pd catalyzed C-S cross-coupling involves three general steps (Scheme 1): OA, transmetalation, and RE.⁴ Aryl halide OA to Pd⁰ forms an aryl/halide Pd(II) complex. This species undergoes transmetalation with a thiolate salt to produce an aryl/thiolate Pd(II) complex, which then undergoes concerted RE to form the coupled product and regenerate the Pd(0) complex.¹¹⁵



Scheme 4-1. General Pd(0)/Pd(II) and Rh(I)/Rh(III) cycle for catalytic C-S coupling reactions.

We were hopeful to create a well-defined pincer supported Rh catalyst that could offer reactivity on par with that of Pd. Previous reports of aryl-sulfur coupling with Rh involved the thiolation of electron deficient aryl fluorides¹¹⁶ or the use of R₂S₂ reagents with alkyl thiols in the presence of a reducing agent.¹¹⁷ However, we were interested in

examining the potential of a Rh(I)/Rh(III) cycle (Scheme 1) analogous to the Pd(0)/Pd(II) cycle for coupling aryl halides with thiols. As previously described in Chapter I and II, our work has indicated that concerted OA of aryl halides is facile whenever a three-coordinate (pincer)Rh transient is generated.^{63,65,100} In addition, the stability of pincer supported Rh(I) and Rh(III) complexes allows for close examination of elementary reactions at transition metal centers.

Herein, we describe the ability of the (POCOP)Rh pincer system to catalyze the coupling of aryl chlorides and bromides with aryl and alkyl thiols with good yields under reasonable reaction conditions. Several analogues of each of the intermediates of the Rh(I)/Rh(III) cycle have been isolated and characterized, allowing for direct observation of each step of the proposed catalytic cycle. We also present a detailed examination of concerted C-S RE with the (POCOP)Rh system and analyze the implications these results have on the kinetics and mechanism of catalysis.

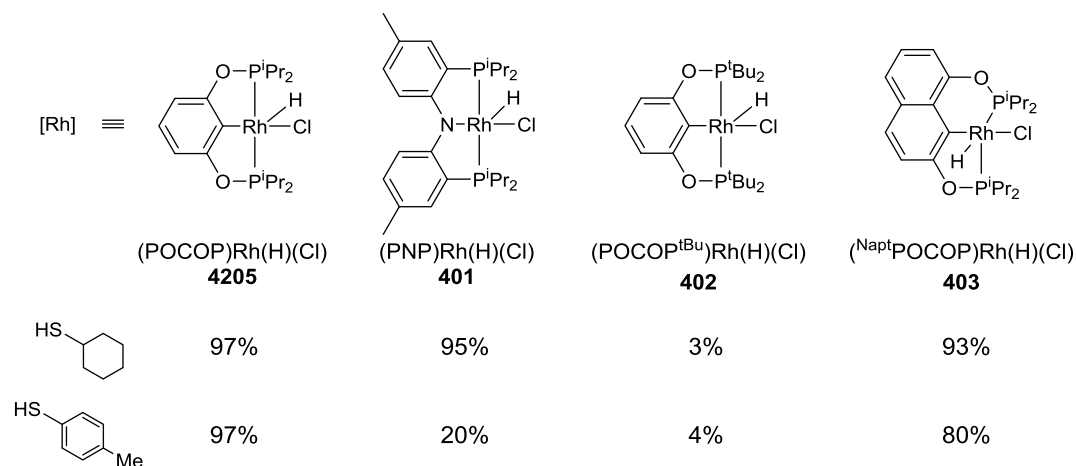
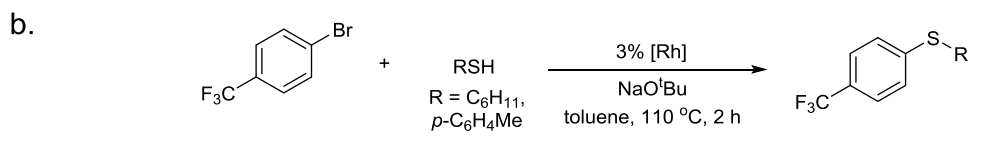
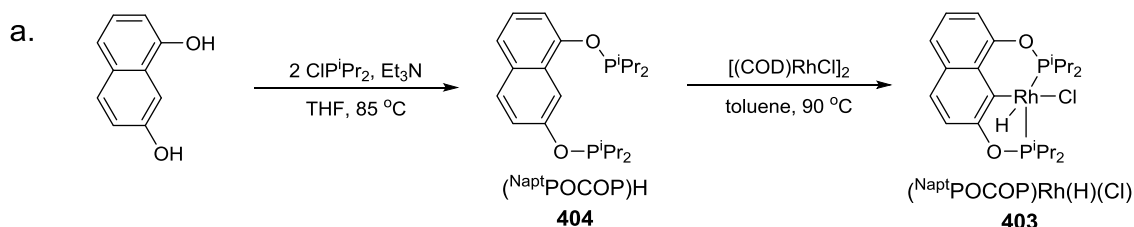
4.2 Results and Discussion

4.2.1 Catalytic C-S Coupling

4.2.1.1 Catalyst Screening

We set out to evaluate (POCOP)Rh(H)(Cl) **205**, (PNP)Rh(H)(Cl) **401**, (POCOP^{tBu})Rh(H)(Cl) **402**, and (^{Napt}POCOP)Rh(H)(Cl) **403** as a representative group of pre-catalysts. The synthesis of **205**, **401**, and **402** and their respective ligands has been described elsewhere.^{97,83,118} The naphthalenediol-based pincer ligand (^{Napt}POCOP)H **404** was synthesized by phosphinylation of 1,7-dihydroxynaphthalene. Thermolysis of **404**

with $[(\text{COD})\text{RhCl}]_2$ produced **403** in good yield (Scheme 4-2, a). The synthesis of **403** and **404** was accomplished by fellow graduate student Christopher Pell.



Scheme 4-2. (Pincer)Rh catalyst screening for C-S coupling. a. Synthesis of $(\text{Napt}^i\text{Pr}_2\text{POCOP})\text{H}$ **404** and $(\text{Napt}^i\text{Pr}_2\text{POCOP})\text{Rh}(\text{H})(\text{Cl})$ **403**; b. Catalyst screening for the coupling of $p\text{-CF}_3\text{C}_6\text{H}_4\text{Br}$ with cyclohexanethiol and $\text{HS}(p\text{-C}_6\text{H}_4\text{Me})$.

Complexes **205** and **401-403** are similar in that the Rh center in each is supported by a monoanionic pincer ligand with opposing phosphine/phosphinite arms. Complex **401** provides for a different central donor atom: amido in **401** vs aryl in others. Complex **402** possesses much greater steric bulk in the P^tBu_2 “arms”. Complex **403** presents a

five- and a six-membered ring fused about Rh, resulting in a different P-Rh-P pincer bite angle. Using Fryzuk's notation for pincer ligands,¹¹⁹ **403** can be described as a {[5,6]-PCP} ligand in contrast to {[5,5]-PCP} for **205** and **402** and {[5,5]-PNP} for **401**.

Each compound **205**, **401-403** was tested as a catalyst under the same conditions (3% loading, 2 h, 110 °C) for the coupling of *p*-MeC₆H₄SH or *c*-C₆H₁₁SH with *p*-BrC₆H₄CF₃ using sodium *tert*-butoxide as a base (Scheme 4-2, b). Dehydrochlorination of (pincer)Rh(H)(Cl) with NaO^tBu is expected to provide access to the catalytically relevant three-coordinate (pincer)Rh intermediate.^{63,65,100} The use of the CF₃-substituted aryl halide allowed for the reactions to be conveniently monitored by ¹⁹F NMR spectroscopy.

The reactions using the bulkiest complex **3** produced only a near-stoichiometric amount of the expected C-S coupling products, but the use of complexes that contained smaller PⁱPr₂ side arms (**205**, **401**, and **403**) clearly led to catalytic diorganosulfide production. **205** displayed the greatest activity yielding 97% of the C-S coupled products with both thiol substrates. The diarylamido-based **401** worked well with *c*-C₆H₁₁SH producing 95% of the coupled product, but gave only 20% conversion for the reaction with *p*-MeC₆H₄SH. The naphthalenediol-based **403** worked almost as well as **205** for both coupling test reactions. We selected **205** for more in-depth studies.

4.2.1.2 Scope of C-S Coupling

The results of a survey of the catalytic activity of **205** in the coupling of aryl chlorides and bromides with alkyl or aryl thiols are shown in Figure 4-1. Several general observations can be made that dovetail related trends in Pd catalysis.^{30,106} Aryl bromides were more reactive than aryl chlorides across the board. More electron-poor aryl halides also reacted faster. This can be exemplified by the ca. 50% yield of **a/b** starting from *p*-ClC₆H₄F vs >90% yield of **c/d** starting from *p*-ClC₆H₄CF₃ after the same period of time. Primary and secondary (*c*-C₆H₁₁SH) alkyl thiols reacted faster than aromatic thiols (e.g., **k/o** vs **a/b**), as they do with Pd catalysts.^{30c,32} Reactions to form **i** – **n** with aryl bromides were all complete after 3 h at 110 °C, with yields of 96% or greater. The analogous reactions with aryl chlorides were slower to reach completion, 20 h – 48 h, but product yields were still high (88% – 98%). The formation of **r** with the more electron rich *p*-chlorotoluene was also successful, yielding 93% after 36 h. However, the use of *p*-MeOC₆H₄Cl gave only 50% of **q** after 36 h.

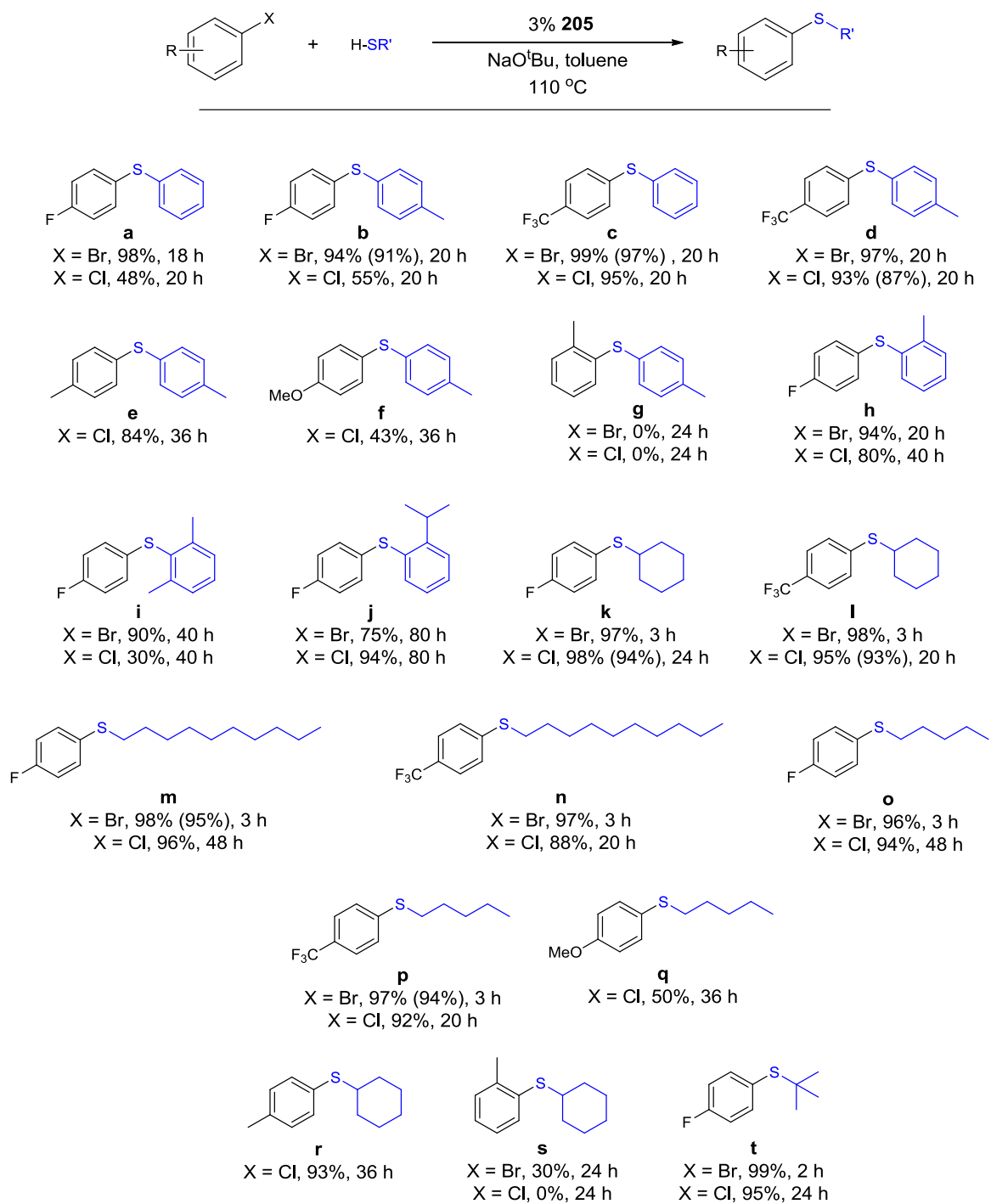


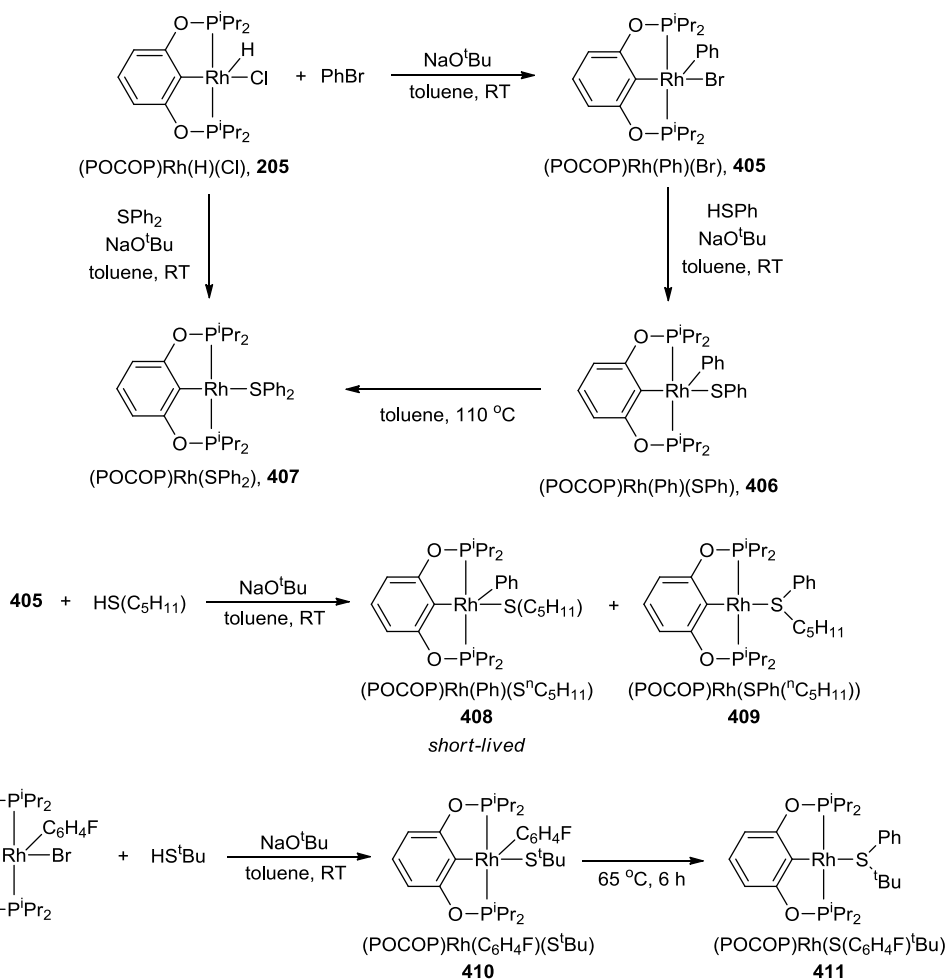
Figure 4-1. Scope of C-S coupling with (POCOP)Rh(H)(Cl) **205**.

c-C₆H₁₁SH gave a modest 30% yield of the coupling product when paired with *o*-MeC₆H₄Br and none with *o*-MeC₆H₄Cl. The attempted coupling of *o*-MeC₆H₄Cl or *o*-MeC₆H₄Br was entirely unsuccessful with an unencumbered aryl thiol (*p*-MeC₆H₄SH, **g**). However, *ortho*-substituted diarylsulfide products were synthesized in moderate to good yields via the coupling of *ortho*-substituted aryl thiols with *p*-ClC₆H₄F or *p*-BrC₆H₄F (**h-j**). As the steric bulk was increased from **h** to **i** and **j**, the reaction times required for high conversion also increased to 40 h and 80 h, respectively. Increased steric bulk of the reagents appears to be inhibitive of the catalysis, but it affects the thiol to a different degree than the aryl halide coupling partner. Many of the reactions also produced a minor quantity ($\leq 5\%$) of the corresponding Ar-H. Its origins remain unclear but we have been able to establish that traces of moisture are not responsible. We tested this by examining formation of PhF in the synthesis of **d** and **l** with ArBr using reagents either simply degassed or rigorously dried by distillation from CaH₂. However, all reactions produced an equal amount of *ca.* 3% PhF. The formation of Ar-H is not detrimental to product isolation when aryl halides of relatively low molecular weight are used.

In order to examine the longevity of the catalyst, we conducted a series of coupling reactions with decreased catalyst loadings using *p*-MeC₆H₄SH and *p*-CF₃C₆H₄X (X = Br or Cl) as substrates in one set of experiments, and *c*-C₆H₁₁SH and *p*-FC₆H₄X (X = Br or Cl) in another. We were able to observe conversion with as little as 0.01% catalyst with aryl bromide, and 0.1% with aryl chloride, with maximal observed TON of 2500 for ArBr and 350 for ArCl.

4.2.2 Synthesis of Intermediates

We previously described the synthesis of various (POCOP)Rh(Ar)(X) (X = Cl, Br, I) analogues.¹⁰⁰ (POCOP)Rh(Ph)(Br) (**405**) was formed by treatment of **205** with NaO^tBu in the presence of PhBr (Scheme 4-3). The reaction occurred upon mixing at RT as indicated by a distinct color change from orange to red.



Scheme 4-3. Synthesis of complexes **405–411**.

Treatment of **405** with an additional equivalent of NaO^tBu in the presence of HSPh resulted in immediate formation of (POCOP)Rh(Ph)(SPh) (**406**) (Scheme 4-3). Inspection of the ¹H and ³¹P{¹H} NMR spectra of a C₆D₆ solution of **406** after 1 wk at ambient temperature indicated approximately 3% conversion to (POCOP)Rh(SPh₂) (**407**). **407** was synthesized directly from **205** by treatment with NaO^tBu in the presence of SPh₂ at ambient temperature (Scheme 4-3). Independent thermolysis of **406** or **407** at 65 °C produced an equilibrium mixture of **407**:**406** in a 48:1 ratio.

The alkyl thiolate analogues, (POCOP)Rh(Ph)(SⁿC₅H₁₁) (**408**) and (POCOP)Rh(C₆H₄F)(S^tBu) (**410**), were synthesized using the same method as **406** (Scheme 4-3). **408** could only be observed in solution in a mixture and underwent full conversion to the reductive coupling product (POCOP)Rh(SPh(ⁿC₅H₁₁)) (**409**) after 1 h at RT, while **410** produced no observable quantity of its reductive coupling product (POCOP)Rh(S(C₆H₄F)^tBu) (**411**) after 24 h at RT. However, thermolysis of **410** (9 h at 65 °C) resulted in quantitative conversion to **411**.

Molecular structures of **406** and **407** in the solid state were determined by single-crystal X-ray diffractometry (Figure 4-2). X-ray quality crystals of **406** were obtained from a saturated pentane solution at -35 °C. The solid-state structure presented a distorted square pyramidal coordination environment about the *d*⁶ Rh(III) metal center.⁶⁹ The geometry about Rh is quite similar to the structure of (POCOP)Rh(Ph)(I) we reported previously and described in Chapter II.¹⁰⁰ The phenyl group in **406** minimizes the steric clash with the ⁱPr substituents on the phosphorus atoms by adopting a conformation where the plane of the phenyl ring is approximately perpendicular to the P-

Rh-P vector. X-ray quality crystals of **407** were grown from a saturated toluene solution layered with pentane at $-35\text{ }^{\circ}\text{C}$. **407** adopts a distorted square planar geometry about Rh, as would be expected for a four-coordinate Rh(I) complex.

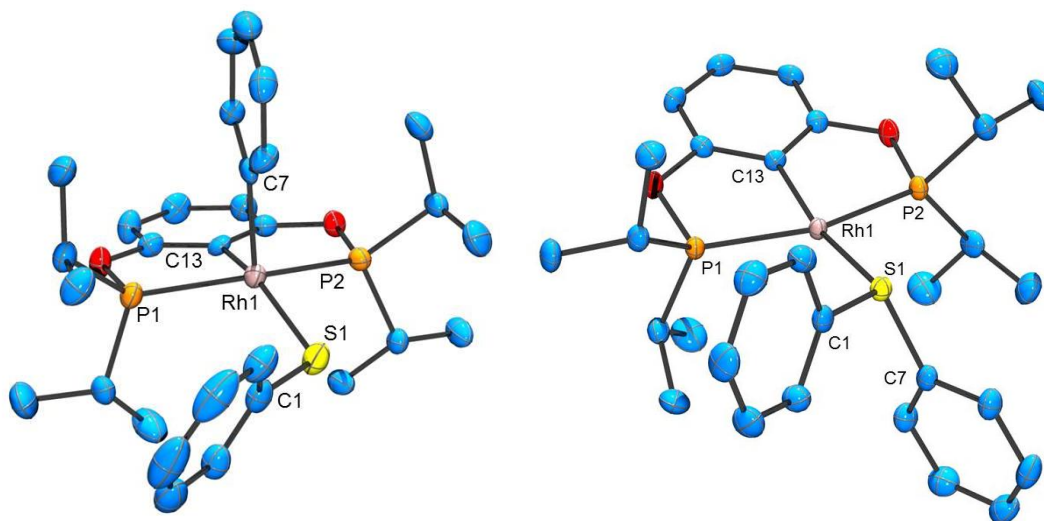
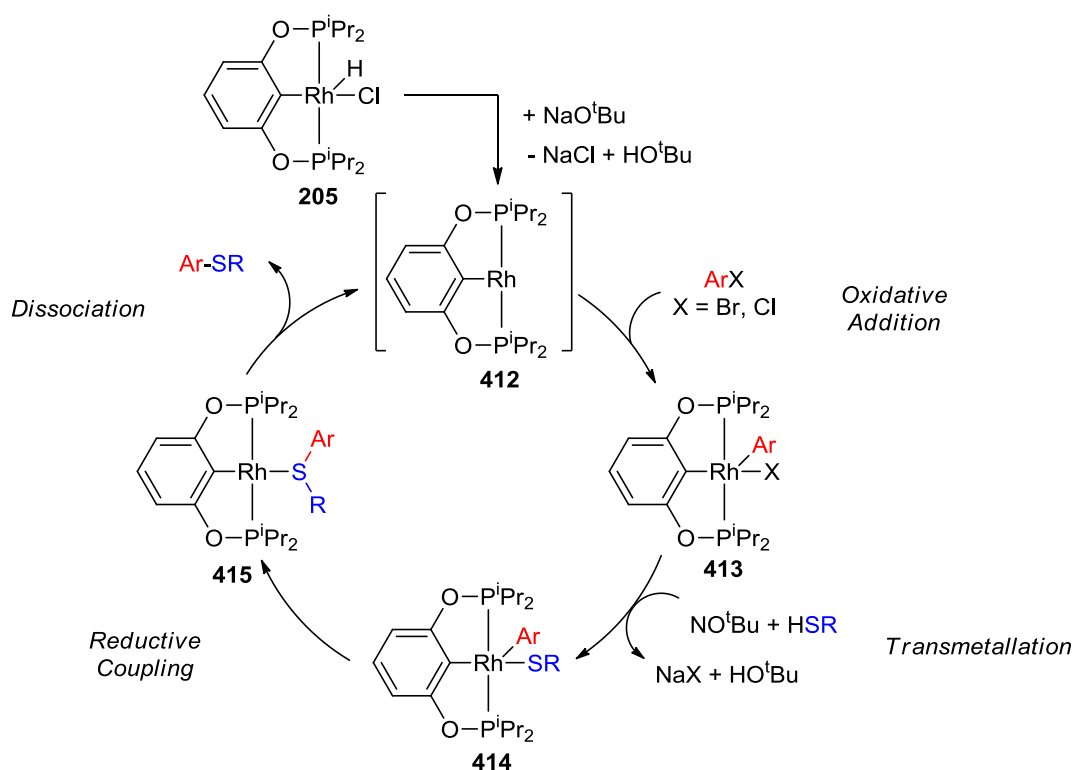


Figure 4-2. ORTEP drawings (50% probability ellipsoids) of (POCOP)Rh(Ph)(SPh) (**406**) (left) and (POCOP)Rh(SPh₂) (**407**) (right).⁸⁴ Selected atom labeling. Hydrogen atoms are omitted for clarity. Selected bond distances (Å) and angles (deg) for **406** follow: Rh1-S1, 2.366(1); S1-C1, 1.774(5); Rh1-C7, 2.3852(8), Rh1-S1-C1, 114.7(2); C13-Rh1-S1, 154.6(1); C13-Rh-C7, 87.7(1); C7-Rh1-S1, 116.2(1). Selected bond distances (Å) and angles (deg) for **407** follow: Rh1-S1, 2.3266(6); S1-C1, 1.786(2); S1-C7, 1.797(2); Rh1-S1-C1, 116.93(8); Rh1-S1-C7, 118.00(7); C13-Rh1-S1, 166.90(6); C1-S1-C7, 99.8(1).

4.2.3 Mechanism

The proposed mechanism for catalytic C-S coupling with **205** is shown in Scheme 4-4. NaO^tBu serves to dehydrochlorinate **205** and produce the unobserved, unsaturated (POCOP)Rh^I (**412**) fragment. We have previously demonstrated the importance of three-coordinate (pincer)Rh^I fragments in concerted OA reactions.^{63,65,100}

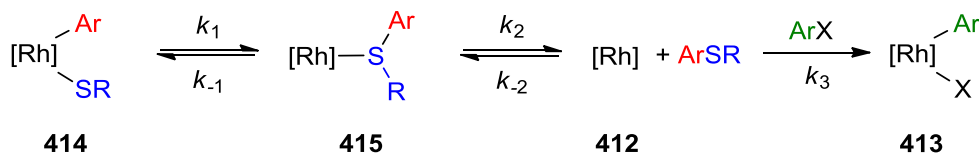
OA of an aryl halide to **412** would then produce (POCOP)Rh(Ar)(X) (**413**). This species would then undergo transmetalation with NaSR to produce (POCOP)Rh(Ar)(SR) (**414**). The aryl/thiolato complex **414** can undergo reductive coupling to form the thioether adduct (POCOP)Rh(ArSR) (**415**), followed by thioether dissociation to re-form the unsaturated (POCOP)Rh^I fragment.



Scheme 4-4. Proposed catalytic cycle for the coupling of aryl halides with thiols using **205** as the catalyst.

Isolation of compounds **405-407** allowed for closer study of each of the elementary reactions making up the proposed catalytic cycle. We were especially interested in elucidating parameters affecting the overall rate of catalysis. The

transmetallation step can be confidently dismissed from this consideration given that it is rapid and irreversible even at RT. Thus, we focused on the remaining three steps with potential to be rate-limiting: reductive coupling (**414**→**415**), product dissociation (**415**→**412**) and OA (**412**→**413**). Scheme 4-5 illustrates these three steps and highlights the rate constants relevant to the following discussion. The OA step is clearly irreversible in all cases, and we need only concern ourselves with the forward reaction (k_3). On the other hand, the reductive coupling step (k_1/k_{-1}) and the product dissociation step (k_2/k_{-2}) deserved closer attention.



Scheme 4-5. Rate constants for reductive coupling, thioether dissociation, and OA.

As was mentioned above, the equilibrium between **406** and **407** or **408** and **409** strongly favors the C-S coupled Rh(I) product. This means that the $k_1 \gg k_{-1}$ and that the oxidative cleavage reaction (corresponding to k_{-1}) is not relevant to considerations of the rate-limiting step. Interestingly, we previously described an equilibrium observed for the (PNP)Rh analogues of **406** and **407** with a 1:1 ratio of (PNP)Rh(Ph)(SPh) and (PNP)Rh(SPh₂).⁶⁴ The increased preference for the Rh^I isomer may be attributed to the less electron rich nature of the (POCOP)Rh system vs (PNP)Rh;^{75,104} which likely contributes to the enhanced catalytic performance with **205** compared to **401**.

Next, we explored the influence of the aryl halide substrate (Br vs Cl) on the reaction rates. In general, the use of ArBr led to faster catalysis than the use of analogous ArCl. In a specific comparison, we examined the apparent rate of the coupling of *p*-FC₆H₄X (X = Br, Cl) with *c*-C₆H₁₁SH using either 1.1 or 10 equiv of *p*-FC₆H₄X (Table 4-1). The apparent rate of catalysis was faster with *p*-FC₆H₄Br than with *p*-FC₆H₄Cl. It was the same with 1.1 equiv and 10 equiv of *p*-FC₆H₄Br, while the analogous reactions with FC₆H₄Cl exhibited enhanced conversion with 10 equiv FC₆H₄Cl. The reaction with 10 equiv ArCl also produced an increased concentration of C₆H₅F. In a related pair of experiments, we examined the thermolysis of **406** in the presence of PhBr or PhCl. In either reaction, 40% consumption of **406** was observed after 4 h at 65 °C. But, whereas **405** was the only product detected in the reaction with PhBr in 40% yield, the reaction with PhCl at the same point in time produced 30% **407** and 10% (POCOP)Rh(Ph)(Cl) (**416**). Additional thermolysis at 100 °C resulted in complete conversion to the respective (POCOP)Rh(Ph)(X) products in both reactions.

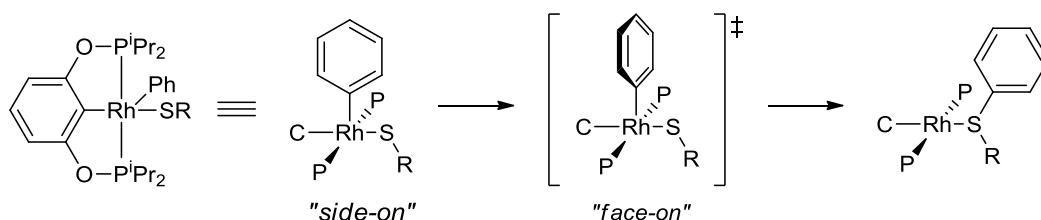
Table 4-1. Effect of aryl halide concentration.

| <i>X</i> | <i>Equiv Ar-X</i> | <i>Yield (1 h)</i> | <i>Yield (3 h)</i> |
|----------|-------------------|--------------------|--------------------|
| Br | 1.1 | 80% | 97% |
| Br | 10 | 81% | 97% |
| Cl | 1.1 | 17% | 40% |
| Cl | 10 | 50% | 90% |

These results indicate several things about the kinetics and mechanism for the coupling of simple aryl halides with thiophenol. The rate of reductive coupling is independent of the identity of ArX, which is consistent with concerted, monomolecular C-S reductive coupling. The reductive coupling (k_1) is the rate-limiting step in catalysis involving ArBr. Dissociation of ArSAr' is much faster ($k_2 \gg k_1$) and k_{-1} is of no concern given that $k_1 \gg k_{-1}$. Both the non-observation of **407** and the lack of apparent dependence on [ArBr] in catalysis suggest that once generated, the (POCOP)Rh intermediate is always trapped by ArBr to irreversibly form the OA product (POCOP)Rh(Ar)(Br) and the reverse trapping of (POCOP)Rh by the diarylsulfide product is not competitive ($k_3[\text{ArBr}] \gg k_2[\text{ArSAr}']$ in the relevant concentration ranges). In contrast, the the trapping of (POCOP)Rh with the diarylsulfides product is competitive with ArCl: $k_3[\text{ArCl}]$ is comparable to $k_2[\text{ArSAr}']$ and so the rate of catalysis is sensitive to [PhCl].

Changes in the steric bulk of the substrates have the potential to affect various steps along the along the catalytic cycle. Bulkier aryl halides or organothiols would result in sterically more imposing diarylsulfide products, which may accelerate catalysis by virtue of increasing k_2 and decreasing k_{-2} (Scheme 4-5). On the other hand, increased steric bulk can adversely affect k_1 and k_3 . As described in Chapter I section 1.5, Goldman, Krogh-Jespersen et al. previously showed that for Ar-X reductive elimination from five-coordinate (PCP)Ir(Ar)(X), the aryl group must be oriented “face-on” towards X in the transition state.⁷⁶ However, the steric influence of the phosphines in the ground state of (PCP)Ir(Ar)(X) favors the “side-on” orientation of the aryl group with respect to X, and the necessary rotation of the aryl can be a considerable component of the

activation barrier. This situation can be contrasted with the typical $(R_3P)_nPd(Ar)(X)$ ($n = 1, 2$) intermediates, where the steric bulk of the phosphines favors “face-on” orientation of the aryl with respect to X in the ground state. The $(POCOP)Rh(Ar)(X)$ system is sterically and electronically analogous to Goldman’s $(PCP)Ir(Ar)(X)$ system. From this vantage point, it is easy to understand why *ortho*-substituted aryl halides (Scheme 4-6) are poor substrates in our Rh chemistry: the rotation of the aryl group in $(POCOP)Rh(Ar)(SR)$ is greatly inhibited by the *ortho* substituent. The restricted rotation of even non-*ortho*-substituted aryls is also likely the greatest contributor to the poor performance of **401** as a catalyst (Scheme 4-2). *Ortho*-substitution also has the potential to inhibit OA of the aryl halide to $(POCOP)Rh$ since it presumably proceeds *via* a transition state with similar spatial requirements. However, reaction of **407** with 5 equiv *o*-MeC₆H₄Br resulted in >99% conversion to the two rotamers of $(POCOP)Rh(o\text{-}C_6H_4Me)(Br)$ (**417**) after 20 h at 65 °C, indicating that OA of an *ortho*-substituted aryl halide is not as much of an obstacle.



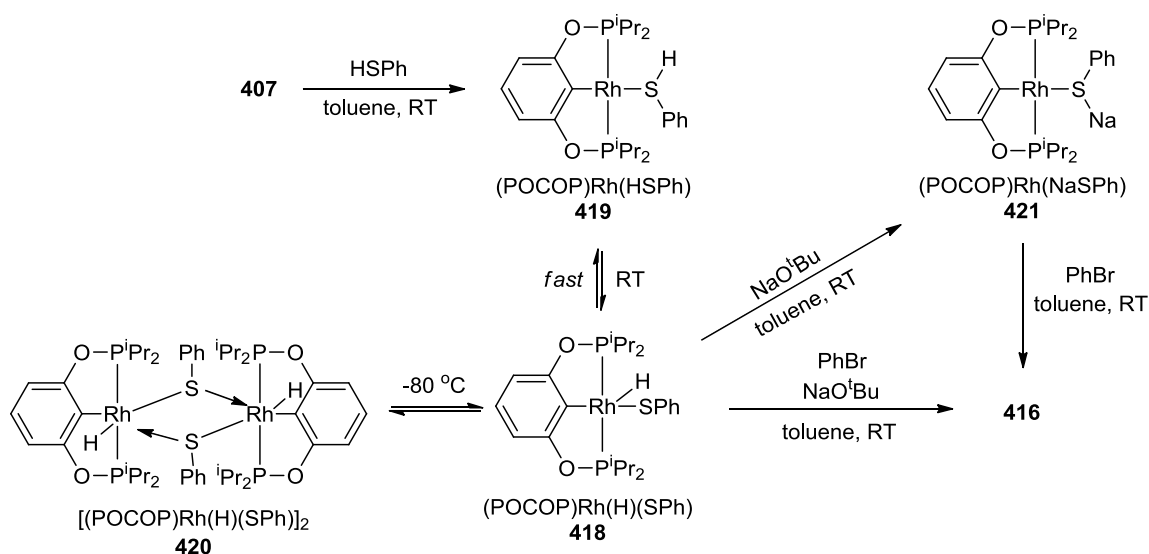
Scheme 4-6. For C(aryl)-S reductive coupling to occur, the aryl group must rotate to be face-on with the thiolate substituent. Increased steric bulk raises the barrier for this rotation.

However, steric bulk would only impact the rate of catalysis if the RLS is accelerated or decelerated. The observed effect of sterics of the thiolate group on the rate of catalysis and RE is less straight forward. It is clear from the relative stability of **410** vs that of **408** that increased steric bulk on the thiolate ligand ultimately increases the barrier for reductive coupling. However, the catalytic reaction to form **k** from the secondary alkyl thiol *c*-C₆H₁₁SH and *p*-FC₆H₄Cl was faster (98%, 24 h) than the reaction to form **o** from the primary alkyl thiol *n*-C₅H₁₁SH and *p*-FC₆H₄Cl (94%, 48 h). Examination of the catalytic coupling reactions with *ortho*-substituted aryl thiols (Figure 4-1, **h–j**) shows an eventual decrease in the rate of catalysis as the steric bulk of the substituent is increased from **h** to **i** and **j**. Compared to **h**, the reaction time increased by a factor of two for the formation of **i** and increased by a factor of four for **j**, consistent with an increased barrier for reductive coupling with bulky thiolate groups. Interestingly, the rate of formation of **h** is similar or even greater to that of the *para* substituted **b** and non substituted **a**. *Ortho*-substitution in the aryl thiol does not appear to have as dramatic of an inhibiting effect as *ortho*-substitution in the aryl halide, likely because it is farther removed from the Rh center and has less impact on the ease of achieving the orientation necessary for the C-S bond-forming transition state. All of these results indicate that there is a delicate balance between the sterics of the thiolate group and its effect on the rate of catalysis.

4.2.4 Additional Reactivity

Hartwig and coworkers previously identified $L_nPd(H)(SR)$ as the catalyst resting state for C-S coupling reactions catalyzed by $L_nPd(Ar)(X)$.¹¹⁵ We were interested to see if the (POCOP)Rh system would react with thiols in a similar fashion, as well as the potential for a hydrido/thiolato complex of this nature to impede catalysis. Treatment of **8** with HSPh resulted in formation of (POCOP)Rh(H)(SPh) (**418**) upon mixing (Scheme 4-7). The 1H NMR spectrum of **418** displayed a hydride resonance at -23.00 ppm and slightly broadened POCOP signals. The spectrum displayed 1 methine resonance and 2 signals for the methyl protons of the isopropyl groups, which is the pattern for a C_{2v} symmetric complex. However, **418** should be C_s symmetric (by analogy with **205**, for example) and should display 2 distinct methine resonances and 4 different resonances for the methyl protons. The apparent C_{2v} symmetry could be the result of fast reversible S-H reductive coupling on the metal, which would create a rapid exchange between two degenerate forms of **418** and the unobserved C_{2v} -symmetric thiol adduct (POCOP)Rh(HSPh) (**419**). **418** was examined by NMR spectroscopy in the 20 °C - -80 °C range. As a solution of **418** in d_8 -toluene was cooled to -60 °C, 2 distinct methine resonances and 4 distinct methyl resonances were visible in the 1H NMR spectrum, consistent with the expected C_s -symmetric structure for **418**. As the solution reached -80 °C, a new set of resonances appeared, corresponding to an additional C_s -symmetric compound. The new resonances included a new hydride resonance at -16.9 ppm, consistent with a hydride that is not *trans* to an open coordination site. These data led us to tentatively assign the new complex as [(POCOP)Rh(H)(SPh)]₂ (**420**), the dimer of

418. A rapid equilibrium between **418** and **420** would not explain the C_{2v} symmetry observed for **418** at RT. Moreover, the observed hydride chemical shift at -23.00 ppm at RT is consistent with a hydride *trans* to an empty site and is similar to the chemical shift of the hydride in **418** observed at -80 °C. Thus the dimeric **420** is not present in solutions of **418** at RT in a significant amount.



Scheme 4-7. Formation of $(\text{POCOP})\text{Rh}(\text{H})(\text{SPh})$ (**418**) and $(\text{POCOP})\text{Rh}(\text{NaSPh})$ (**421**).

Treatment of **418** with 1 equiv NaO^tBu resulted in an immediate color change to yellow-brown (Scheme 4-7). Analysis of the reaction by ^1H NMR showed conversion to a new compound accompanied by disappearance of the hydride resonance and the appearance of HO^tBu . The identity of the new compound was determined to be $(\text{POCOP})\text{Rh}(\text{NaSPh})$ (**421**) by X-ray crystallography (Figure 4-3), and is consistent with the formal deprotonation of the coordinated thiol by NaO^tBu . The extended solid-state

structure of **418** shows a chain structure where sodium has close interactions in one (POCOP)Rh(SPh) unit with sulfur (Na–S, 2.751(2) Å), and in another with the rhodium center (Na---Rh, 2.8958(13) Å) and the Rh-bound carbon (Na---C, 2.881(3) Å).¹²⁰

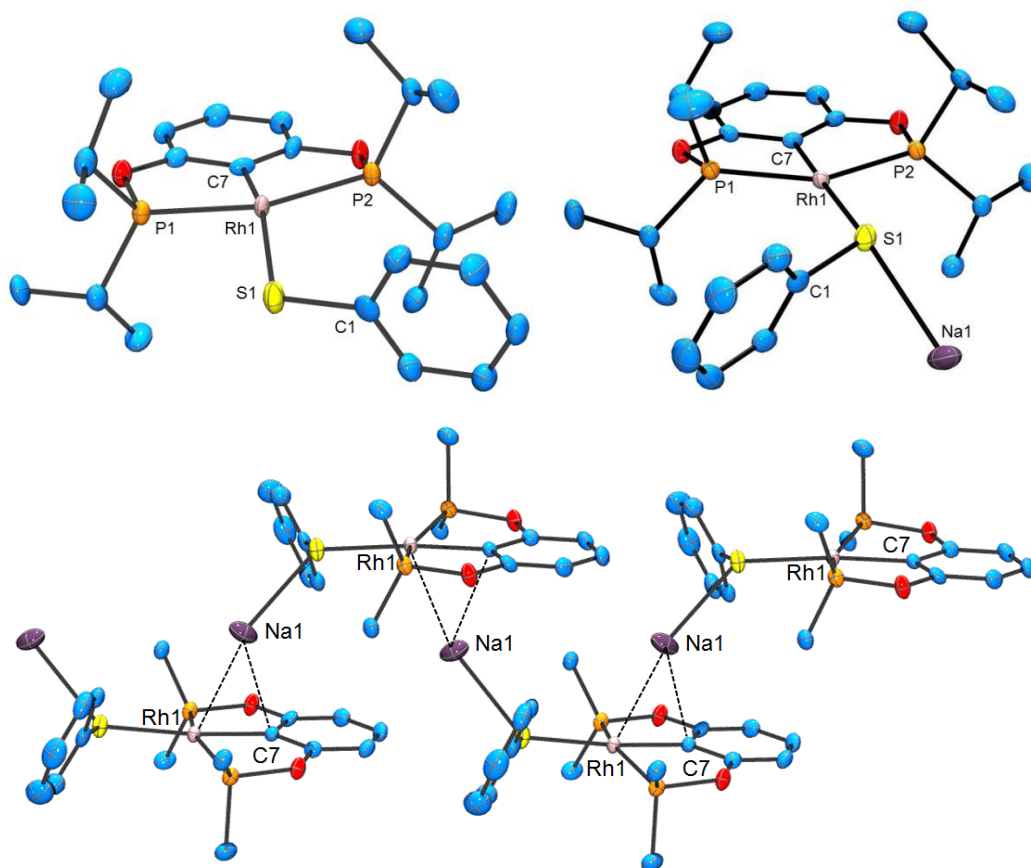


Figure 4-3. ORTEP drawings (50% probability ellipsoids) of (POCOP)Rh(H)(Ph)(SPh) (**418**) and (POCOP)Rh(NaSPH) (**421**).⁸⁴ Selected atom labeling. Hydrogen atoms are omitted for clarity. Selected bond distances (Å) and angles (deg) for **418** follow: Rh1–S1, 2.323(3); S1–C1, 1.78(1); Rh1–S1–C1, 113.8(8), C7–Rh1–S1, 157.7(3). Selected bond distances (Å) and angles (deg) for **421** follow: Rh1–S1, 2.3852(8); S1–C1, 1.790(3); S1–Na1, 2.751(2); Rh1–S1–C1, 112.60(8); Rh1–S1–Na1, 132.70(4); Na1–S1–C1, 87.59(8); C7–Rh1–S1, 174.45(7)(3). The extended crystal packing of **421** (bottom) showing selected atom labelling. Hydrogen atoms and isopropyl methyl groups are omitted for clarity. The extended crystal packing structure of **421** shows sodium interactions with sulfur (Na–S, 2.751(2) Å), neighboring rhodium centers (Na---Rh, 2.8958(13) Å), and the chelating aryl-carbon of the pincer framework (Na---C, 2.881(3) Å).

418 and **421** both convert to the product forming **406** under the conditions of catalysis (Scheme 4-7). **418** converts to **406** when treated with PhBr and NaO^tBu after 1 h at RT. Exposure of **421** to PhBr results in immediate formation of **406** at RT. These reactions illustrate that neither **418** nor **421** should form in an appreciable concentration under the conditions of catalysis.

4.3 Conclusion

In summary, we have presented a well-defined (POCOP)Rh system for the catalytic coupling of aryl bromides and chlorides with aryl and alkyl thiols. The synthesis of the catalytically active naphthalenediol-based **403** was also described. Our preliminary mechanistic studies showed the increased favorability towards aryl-sulfur reductive elimination with (POCOP)Rh relative to the analogous (PNP)Rh system. They also exposed the apparent dependence of the rate of catalysis on aryl chloride, but not aryl bromide concentration. The analysis of steric effects in the aryl halide and in the thiol component reveals a rather complex picture, where the influence of the sterics depends on the nature of the rate-limiting step for various substrate couples. Reactions of PhSH and PhSNa with the catalytically active species were examined and deemed not to be detrimental under catalytic conditions. These results support the proposed Rh(I)/Rh(III) mechanism for aryl halide thiol cross-coupling reactions with Rh.

4.4 Experimental

4.4.1 General Considerations

Unless otherwise specified, all manipulations were performed under an argon atmosphere using standard Schlenk line or glove box techniques. Toluene, THF, pentane, and isooctane were dried and deoxygenated (by purging) using a solvent purification system and stored over molecular sieves in an Ar-filled glove box. C₆D₆ and hexanes were dried over and distilled from NaK/Ph₂CO/18-crown-6 and stored over molecular sieves in an Ar-filled glove box. Fluorobenzene was dried with and then distilled or vacuum transferred from CaH₂. (POCOP)Rh(H)(Cl) **205**,¹⁰⁰ (PNP)Rh(H)(Cl) **401**,¹¹⁸ and (POCOP^{iBu})Rh(H)(Cl)⁷⁵ **402** were synthesized according to published procedures. All other chemicals were used as received from commercial vendors. NMR spectra were recorded on a Varian NMRS 500 (¹H NMR, 499.686 MHz; ¹³C NMR, 125.659 MHz, ³¹P NMR, 202.298 MHz, ¹⁹F NMR, 470.111 MHz) spectrometer. For ¹H and ¹³C NMR spectra, the residual solvent peak was used as an internal reference. ³¹P NMR spectra were referenced externally using 85% H₃PO₄ at δ 0 ppm. ¹⁹F NMR spectra were referenced externally using 1.0 M CF₃CO₂H in CDCl₃ at -78.5 ppm. Elemental analyses were performed by CALI Labs, Inc. (Parsippany, NJ).

4.4.2 Isolated Compounds and Stoichiometric Reactions

Synthesis of (^{Napt}POCOP)H (404). In a Teflon screw-top flask, 1,7-dihydroxynaphthalene (479 mg, 2.99 mmol) was dissolved in THF and ClPⁱPr₂ (956 mg, 6.26 mmol) was added slowly while stirring. The solution turned from dark to light brown with the dropwise addition of NEt₃ (1.37 mL, 9.82 mmol). The reaction mixture

was heated at 85 °C for 1.5 h. The mixture was then passed through Celite, and the volatiles were removed under vacuum to produce a thick brown oil that was determined to be >95% pure by ^1H NMR spectroscopy (926 mg, 79%). The purity of the ligand was suitable for further ligation reactions. $^{31}\text{P}\{^1\text{H}\}$ NMR (C_6D_6): δ 148.1 (s), 146.9 (s); ^1H NMR (C_6D_6): δ 8.41 (t, 1H, Ar-H, $J = 2.5$ Hz), 7.56 (t, 1H, Ar-H, $J = 2.5$ Hz), 7.53 (d, 1H, Ar-H, $J = 9.5$ Hz), 7.37 (m, 1H, Ar-H), 7.29 (d, 1H, Ar-H, $J = 8$ Hz), 7.15 (m, 1H, Ar-H), 1.83 (m, 4H, P-CHMe₂), 1.20 (m, 12H, CH(CH₃)₂), 1.01 (m, 12H, CH(CH₃)₂); $^{13}\text{C}\{^1\text{H}\}$ NMR (C_6D_6): δ 157.6 (d, Ar-OP, $J_{\text{C-P}} = 8$ Hz), 154.9 (d, Ar-OP, $J_{\text{C-P}} = 9$ Hz), 131.4 (Ar), 129.8 (Ar), 124.2 (Ar), 121.3 (Ar), 121.1 (d, Ar, $J_{\text{C-P}} = 6$ Hz), 111.8 (Ar), 111.7 (Ar), 108.4 (d, Ar, $J_{\text{C-P}} = 16$ Hz), 28.7 (d, 2 CHMe₂, $J = 19$ Hz), 18.0 (d, $J = 15$ Hz), 17.8 (d, $J = 15$ Hz), 17.3 (d, $J = 5$ Hz), 17.24 (d, $J = 5$ Hz).

Synthesis of (^{Nap}POCOP)Rh(H)(Cl) (403). In a Teflon screw-top flask, **404** (209 mg, 0.533 mmol) and [Rh(cod)Cl]₂ (131 mg, 1.066 mmol) were dissolved in toluene and stirred overnight at 90 °C. The reaction mixture was passed through Celite, and the volatiles were removed under vacuum. The resulting red solid was dissolved in a minimum amount of toluene and layered with pentane. A red solid precipitated out of solution (215 mg, 76%). $^{31}\text{P}\{^1\text{H}\}$ (C_6D_6): δ 183.7 (dd, $J_{\text{P-P}} = 424$ Hz, $J_{\text{P-Rh}} = 111$ Hz), 164.4 (dd, $J_{\text{P-P}} = 418$ Hz, $J_{\text{P-Rh}} = 121$ Hz); ^1H NMR (C_6D_6): δ 7.38 (t, 2H, Ar-H, $J = 8.5$ Hz), 7.20 (d, 1H, Ar-H, $J = 9$ Hz), 7.11 (d, 1H, Ar-H, $J = 7.5$ Hz), 7.05 (t, 1H, Ar-H, $J = 8$ Hz), 2.75 (m, 1H, PCHMe₂), 2.64 (m, 1H, PCHMe₂), 2.46 (m, 1H, PCHMe₂), 2.21 (m, 1H, PCHMe₂), 1.35 (dd, 3H, PCH(CH₃)₂, $J = 17.5$ Hz, $J = 7.5$ Hz), 1.18 (m, 21H, PCH(CH₃)₂), -24.10 (apparent dt, 1H, Rh-H, $J_{\text{H-Rh}} = 45$ Hz, $J_{\text{H-P}} = 15$ Hz); $^{13}\text{C}\{^1\text{H}\}$ NMR

(C₆D₆): δ 166.1 (m, Ar), 154.7 (Ar), 133.1 (s, Ar), 130.1 (d, $J = 9$ Hz), 128.4 (Ar), 125.4 (Ar), 123.4 (Ar), 123.1 (m, C-Rh) 115.5 (d, Ar, $J = 2.5$ Hz), 115.3 (d, $J = 13$ Hz), 29.8 (d, PCHMe₂, $J = 45$ Hz), 29.5 (d, PCHMe₂, buried underneath two doublets) 29.3 (d, PCHMe₂, $J = 48$ Hz), 28.17 (d, PCHMe₂, $J = 23$ Hz), 18.7, 18.67, 18.3 (s), 18.0 (s), 17.7 (s), 17.1 (s), 16.4 (s), 16.1 (s).

Synthesis of (POCOP)Rh(Ph)(Br) (405). In a Schlenk flask, **205** (72 mg, 0.15 mmol) was combined with NaO^tBu (17 mg, 0.18 mmol) and C₆H₅Br (19 μ L, 0.18 mmol) and dissolved in toluene. The color of the solution immediately changed to red. The reaction was stirred for 1 h at RT. The volatiles were removed and product was extracted with pentane and passed through a pad of Celite. The volatiles were removed under vacuum and the residual solid was recrystallized from a saturated toluene solution layered with pentane at -35 °C to give a red crystalline solid (70 mg, 78%). ³¹P{¹H} NMR (C₆D₆): δ 173.5 (d, $J_{\text{RhP}} = 121$ Hz); ¹H NMR (C₆D₆): δ 8.38 (bs, 1H, Ph), 6.94 (t, 6.5 Hz, 1H, POCOP), 6.78 (d, 6.0 Hz, 2H, POCOP), 6.62 (bs, 1H, Ph), 6.58 (t, 6.5 Hz, 1H, Ph), 6.34 (bs, 1H, Ph), 6.00 (bs, 1H, Ph), 2.65 (m, 2H, CHMe₂), 2.05 (m, 2H, CHMe₂), 1.20 (q, 9.0 Hz, 6H, CHMe₂), 1.07 (q, 9.0 Hz, 6H, CHMe₂), 1.02 (q, 9.0 Hz, 6H, CHMe₂), 0.79 (q, 9.0 Hz, 6H, CHMe₂); ¹³C{¹H} NMR (C₆D₆): δ 165.2 (t, $J_{\text{PC}} = 6.0$ Hz, POCOP), 145.8 (dt, $J_{\text{RhC}} = 36$ Hz, $J_{\text{PC}} = 9.2$ Hz), 140.6 (dt, $J_{\text{RhC}} = 34$ Hz, $J_{\text{PC}} = 4.7$ Hz), 136.3 (bs, Ph), 128.6 (bs, Ph), 127.1 (s), 124.2 (s), 107.3 (t, $J_{\text{PC}} = 6.0$ Hz, POCOP), 31.1 (t, $J_{\text{PC}} = 11$ Hz, CHMe₂), 28.3 (td, $J_{\text{PC}} = 13$ Hz, $J_{\text{RhC}} = 1.9$ Hz, CHMe₂), 18.1 (t, $J_{\text{PC}} = 2.3$ Hz, CHMe₂), 17.4 (s, CHMe₂), 16.3 (t, $J_{\text{PC}} = 1.8$ Hz, CHMe₂), 15.6 (t, $J_{\text{PC}} = 1.5$ Hz,

CHMe₂). Elem. Anal. Calc. for C₂₄H₃₆BrO₂P₂Rh: C, 47.94; H, 6.03. Found: C, 47.98; H, 6.15.

Synthesis of (POCOP)Rh(Ph)(Cl) (416). In a Schlenk flask, **205** (46.2 mg, 0.0967 mmol), NaO^tBu (10.4 mg, 0.108 mmol), and C₆H₅Cl (50.0 μL, 0.494 mmol) were combined and dissolved in toluene. The reaction underwent a gradual color change from light orange to dark red stirring at RT. After stirring for 60 m at RT, the reaction mixture was passed through a pad of Celite and the volatiles were removed under vacuum to yield a red solid (43.5 mg, 81% yield). ³¹P{¹H} NMR (C₆D₆): 171.9 (d, *J*_{Rh-P} = 123 Hz); ¹H NMR (C₆D₆): 8.55 (bs, 1H, Ph-*H*), 6.93 (t, 1H, 7.5 Hz, Ar-*H*), 6.78 (d, 2H, 8.0 Hz, Ar-*H*), 6.66 (bs, 1H, Ph-*H*), 6.61 (t, 1H, 7.0 Hz, Ph-*H*), 6.36 (bs, 1H, Ph-*H*), 6.02 (bs, 1H, Ph-*H*), 2.56 (m, 2H, CHMe₂), 2.02 (m, 2H, CHMe₂), 1.24 (q, 6H, 7.5 Hz, CH(CH₃)₃), 1.02 (m, 12 H, CH(CH₃)₃), 0.81 (q, 6H, 7.5 Hz, CH(CH₃)₃); ¹³C{¹H} NMR (C₆D₆): 165.4 (t, 5.6 Hz, Ar), 145.5 (dt, *J*_{Rh-C} = 37 Hz, *J*_{P-C} = 9.3 Hz, Ph), 139.9 (dt, *J*_{Rh-C} = 33 Hz, *J*_{P-C} = 9.1 Hz, Ar), 136.3 (s, Ph), 128.3 (s, Ar), 127.1 (s, Ph), 124.0 (s, Ar), 107.2 (t, 6.0 Hz, Ph), 30.7 (t, *J*_{P-C} = 10.2 Hz, CH(CH₃)₂), 28.1 (t, *J*_{P-C} = 12.1 Hz, CH(CH₃)₂), 17.9 (s, CHMe₂), 17.6 (s, CHMe₂), 16.1 (s, CHMe₂), 15.3 (s, CHMe₂).

Synthesis of (POCOP)Rh(Ph)(SPh) (406). **405** (104 mg, 0.173 mmol) was added to a Schlenk flask and dissolved in C₆D₆ to give a red solution. PhSH (18 μL, 0.18 mmol) and NaO^tBu (17 mg, 0.18 mmol) were added to the flask resulting in an immediate color change to dark purple. The reaction was stirred for 30 min at RT. The solution was then passed through a pad of Celite and the volatiles were removed under vacuum. The purple solid was then dissolved in a minimum amount of pentane and left

in a $-35\text{ }^{\circ}\text{C}$ freezer overnight. This yielded a purple crystalline solid (73 mg, 72%). $^{31}\text{P}\{^1\text{H}\}$ NMR (C_6D_6): δ 174.5 (d, $J_{\text{RhP}} = 122$ Hz); ^1H NMR (C_6D_6): δ 8.57 (bs, 1H, Rh-*Ph*), 7.88 (d, 7.5 Hz, 2H, S-*Ph*), 7.04 (t, 8.0 Hz, 2H, S-*Ph*), 6.93 (m, 2H), 6.82 (d, 7.5 Hz, 2H), 6.75 (bs, 1H, Rh-*Ph*), 6.68 (t, 6.0 Hz, 1H), 6.52 (bs, 1H, Rh-*Ph*), 6.11 (bs, 1H, Rh-*Ph*), 2.17 (m, 4H, CHMe_2), 1.17 (q, 8.0 Hz, 6H, CHMe_2), 1.01 (q, 8.0 Hz, 6H, CHMe_2), 0.93 (q, 8.0 Hz, 6H, CHMe_2), 0.70 (q, 8.0 Hz, 6H, CHMe_2); $^{13}\text{C}\{^1\text{H}\}$ NMR (C_6D_6): δ 163.8 (t, $J_{\text{PC}} = 6.5$ Hz, POCOP), 152.5 (t, $J_{\text{PC}} = 7.5$ Hz), 148.2 (dt, $J_{\text{RhC}} = 33$ Hz, $J_{\text{PC}} = 9.5$ Hz), 143.5 (dt, $J_{\text{RhC}} = 29$ Hz, $J_{\text{PC}} = 6.0$ Hz), 137.8 (bs), 133.6 (s), 127.7 (s), 127.5 (bs), 126.5 (s), 124.0 (s), 123.8 (s), 106.9 (t, $J_{\text{PC}} = 6.0$ Hz), 30.5 (t, $J_{\text{PC}} = 11$ Hz, CHMe_2), 29.0 (t, $J_{\text{PC}} = 13$ Hz, CHMe_2), 18.8 (s, CHMe_2), 16.9 (s, CHMe_2), 16.1 (s, CHMe_2), 15.9 (t, $J_{\text{PC}} = 2.0$ Hz, CHMe_2). Elem. Anal. Calc. for $\text{C}_{30}\text{H}_{41}\text{FO}_2\text{P}_2\text{RhS}$: C, 57.14; H, 6.55. Found: C, 57.13; H, 6.54.

Synthesis of (POCOP)Rh(SPh₂) (407). **205** (100 mg, 0.208 mmol) was added to a Schlenk flask and dissolved in C_6D_6 to give an orange solution. SPh₂ (38 μL , 0.23 mmol) and NaO^tBu (24 mg, 0.25 mmol) were added to the flask resulting in an immediate color change to yellow-orange. The reaction was stirred for 30 min at RT. The solution was then passed through a pad of Celite and the volatiles were removed under vacuum. The yellow-orange solid was dissolved in a minimum of toluene, layered with pentane, and left in a $-35\text{ }^{\circ}\text{C}$ freezer overnight. This yielded a crystalline yellow solid (85 mg, 64%). $^{31}\text{P}\{^1\text{H}\}$ NMR (C_6D_6): δ 188.6 (d, $J_{\text{Rh-P}} = 172$ Hz); ^1H NMR (C_6D_6): δ 7.58 (d, 4H, Ph, 7.5 Hz), 7.00 (t, 1H, POCOP, 8.0 Hz), 6.91 (m, 4H Ph & 2H POCOP), 6.85 (t, 2H, Ph, 7.5 Hz), 1.74 (m, 4H, CHMe_2), 1.25 (q, 12H, CHMe_2 , 7.5 Hz), 1.08 (q,

12H, CHMe₂, 7.5 Hz); ¹³C {¹H} NMR (C₆D₆): δ 167.7 (t, J_{PC} = 11 Hz, POCOP), 141.5 (dt, J_{RhC} = 34 Hz, J_{PC} = 10 Hz, POCOP), 140.3 (t, J_{PC} = 3.5 Hz, POCOP), 132.0 (s, Ph), 128.9 (s, Ph), 128.4 (s), 125.1 (s), 104.3 (t, J_{PC} = 7.0 Hz, POCOP), 30.3 (t, J_{PC} = 43 Hz, CHMe₂), 18.5 (t, J_{PC} = 18 Hz, CHMe₂), 17.5 (s, CHMe₂). Elem. Anal. Calc. for C₃₀H₄₁FO₂P₂RhS: C, 57.14; H, 6.55. Found: C, 57.17; H, 6.44.

Thermolysis of 406. **406** (11 mg, 0.017 mmol) was added to a J. Young tube and dissolved in C₆D₆. The sample was then heated in a 65 °C oil bath and monitored by ³¹P NMR spectroscopy. After 32 h at 65 °C, the ratio of **7** to **8** was 35:65. The reaction reached equilibrium after 80 h at 65 °C, with a **7:8** ratio of 5:95.

Thermolysis of 407. **407** (17 mg, 0.027 mmol) was added to a J. Young tube and dissolved in C₆D₆. The sample was then heated in a 65 °C oil bath and monitored by ³¹P NMR spectroscopy. After 32 h at 65 °C, the sample reached equilibrium with a **7:8** ratio of 5:95.

Thermolysis of 406 with C₆H₅Br. **406** (18 mg, 0.029 mmol) and C₆H₅Br (3.3 μL, 0.031 mmol) were combined in a J. Young tube and dissolved in C₆D₆. The sample was heated in a 65 °C oil bath and monitored by ³¹P NMR spectroscopy (Figure 4-4). After 8 h at 65 °C, the reaction reached a 60:40 ratio of **406:405**. The ratio shifted to 25:75 **406** to **405** after 20 h at 65 °C. The temperature of the oil bath was increased to 100 °C and after 5 h the reaction contained only **405**. **407** was never observed by ³¹P NMR spectroscopy.

Thermolysis of 406 with C₆H₅Cl. **406** (19 mg, 0.030 mmol) and C₆H₅Br (3.4 μL, 0.033 mmol) were combined in a J. Young tube and dissolved in C₆D₆. The sample

was heated in a 65 °C oil bath and monitored by ^{31}P NMR spectroscopy (Figure 4-5). After 8 h at 65 °C, the reaction had a **406:407:416** ratio of 60:30:10. The ratio shifted to 25:50:25 **406:407:416** after 20 h at 65°C. The temperature of the oil bath was increased to 100 °C and after 5 h, **406** was no longer observed and ratio of **407:416** was 20:80. After 5 additional hours at 100 °C, the sample only displayed the presence of **416** in the $^{31}\text{P}\{^1\text{H}\}$ NMR spectrum.

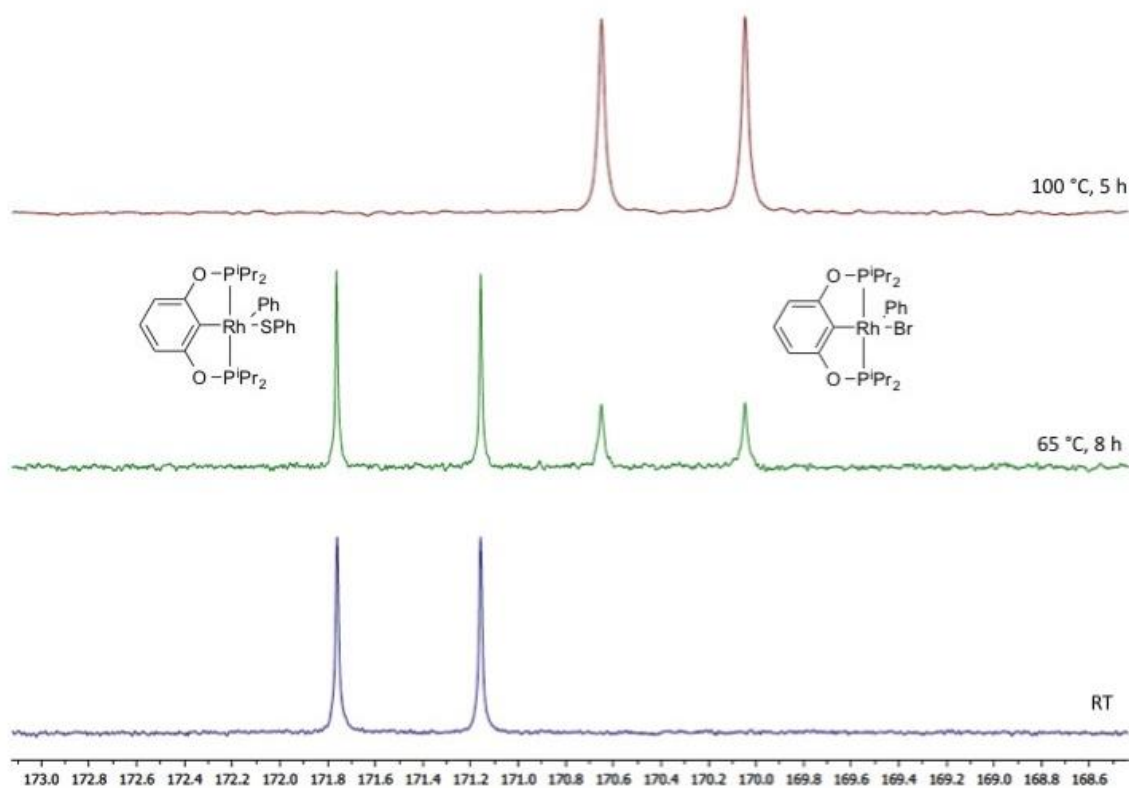


Figure 4-4. $^{31}\text{P}\{^1\text{H}\}$ NMR spectra for the thermolysis of **406** in the presence of $\text{C}_6\text{H}_5\text{Br}$ in C_6D_6 .

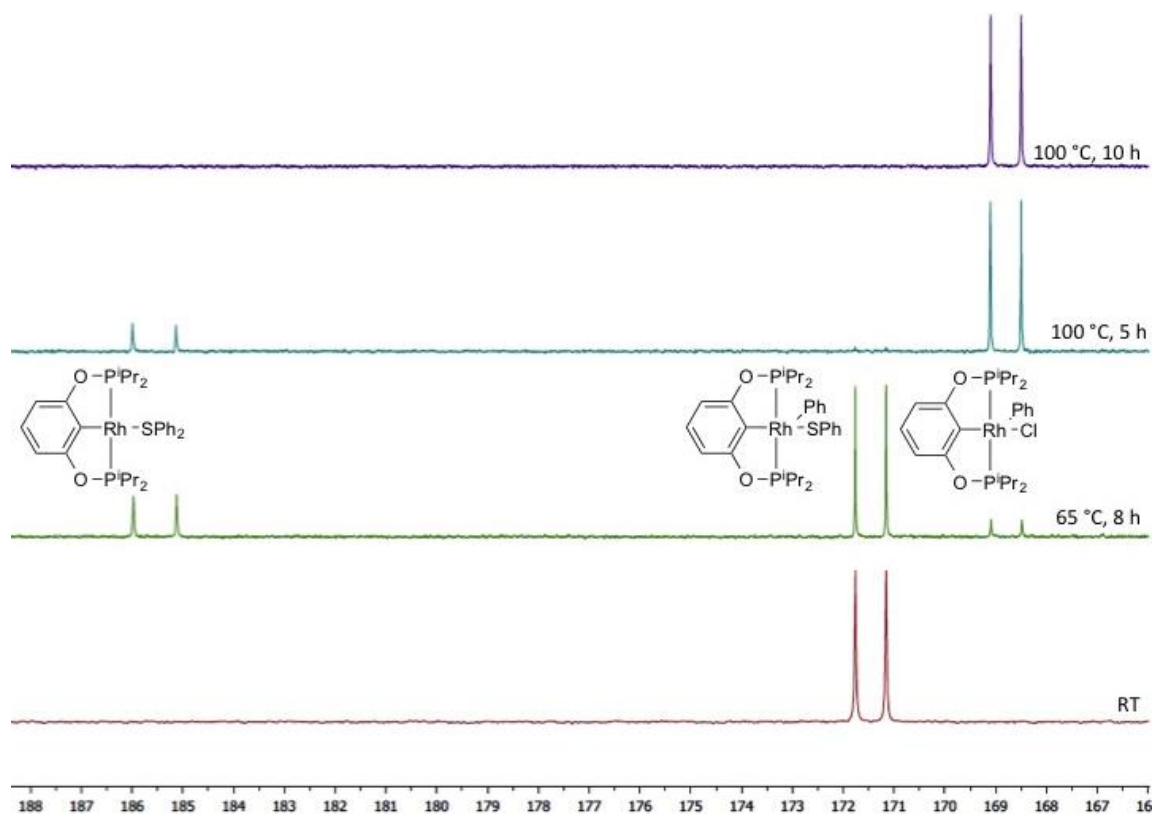


Figure 4-5. $^{31}\text{P}\{^1\text{H}\}$ NMR spectra for the thermolysis of **406** in the presence of $\text{C}_6\text{H}_5\text{Cl}$ in C_6D_6 .

Synthesis of (POCOP)Rh(Ph)($\text{S}^n\text{C}_5\text{H}_{11}$) (408**) and (POCOP)Rh(S(Ph) $^n\text{C}_5\text{H}_{11}$) (**409**).** **405** (110 mg, 0.18 mmol) was added to a Schlenk flask and dissolved in C_6D_6 . $n\text{-C}_5\text{H}_{11}\text{SH}$ (33 μL , 0.22 mmol) and NaO^tBu (21 mg, 0.22 mmol) were added to the flask and the reaction was stirred at RT. The solution underwent an immediate color change from red to purple. Analysis of the sample after 15 min at RT by ^{31}P NMR spectroscopy complete conversion of the starting material to two new products, one identified as (POCOP)Rh(Ph)($^n\text{C}_5\text{H}_{11}$) **408** (175.9, d, $J = 123$ Hz, 40%) and (POCOP)Rh(S(Ph) $^n\text{C}_5\text{H}_{11}$) **409** (189.4, d, $J = 173$ Hz, 60%). The reaction was left to stir overnight at RT, resulting in complete conversion to **409**. The solution was passed

through a pad a Celite and the volatiles were removed by vacuum. The residue was washed with cold pentane and dried to give a crystalline yellow solid (78 mg, 68%). $^{31}\text{P}\{^1\text{H}\}$ NMR (C_6D_6): δ 189.4 (d, 173 Hz); ^1H NMR (C_6D_6): δ 7.72 (d, 6.5 Hz, 2H, Ph), 6.98 (m, 3H), 6.91 (m, 3H), 2.89 (t, 6.5 Hz, 2H, Pent), 1.91 (m, 4H, CHMe_2), 1.45 (m, 2H, Pent), 1.27 (q, 6.5 Hz, 12H, CHMe_2), 1.17 (m, 16H, CHMe_2 & Pent), 0.78 (t, 6.5 Hz, 3H, Pent); $^{13}\text{C}\{^1\text{H}\}$ NMR (C_6D_6): δ 167.5 (t, 9.0 Hz, POCOP), 141.6 (dt, 33 Hz, 9.0 Hz, POCOP), 139.1 (s), 133.2 (s), 128.7 (s), 128.6 (s), 124.7 (s), 104.1 (t, 6.5 Hz, POCOP), 47.9 (s, Pent), 30.9 (s, Pent), 30.6 (t, 10 Hz, POCOP), 29.3 (s, Pent), 22.6 (s, Pent), 18.7 (s, POCOP), 17.6 (s, POCOP), 14.1 (s, Pent). Elem. Anal. Calc. for $\text{C}_{29}\text{H}_{47}\text{O}_2\text{P}_2\text{RhS}$: C, 55.77; H, 7.58. Found: C, 55.82; H, 7.47.

Synthesis of (POCOP)Rh($\text{C}_6\text{H}_4\text{F}$)(S^tBu) (410). (POCOP)Rh($\text{C}_6\text{H}_4\text{F}$)(Br) (130 mg, 0.21 mmol) was added to a Schlenk flask and dissolved in toluene. NaO^tBu (30 mg, 0.31 mmol) and HS^tBu (35 μL , 0.31 mmol) were added to the solution, resulting in an immediate color change from red to purple. The reaction was stirred for 60 min at RT. The volatiles were removed by vacuum. The residue was extracted with pentane and passed through a pad of Celite. The product was crystallized from a saturated toluene solution layered with pentane at -35 °C as a purple-red solid (111 mg, 84%). **410** was stable at RT in solution and the solid state indicated by no observable conversion after 24 h at RT. $^{31}\text{P}\{^1\text{H}\}$ NMR (C_6D_6): δ 174.5 (d, 121 Hz); ^1H NMR (C_6D_6): δ 8.28 (bs, $\text{C}_6\text{H}_4\text{F}$), 6.96 (t, 6.0 Hz, 1H, POCOP), 6.83 (d, 6.5 Hz, 2H, POCOP), 6.48 (bs, $\text{C}_6\text{H}_4\text{F}$), 6.19 (bs, $\text{C}_6\text{H}_4\text{F}$), 5.87 (bs, $\text{C}_6\text{H}_4\text{F}$), 2.65 (m, 2H, CHMe_2), 2.22 (m, 2H, CHMe_2), 1.79 (s, 9H, $\text{C}(\text{CH}_3)_3$), 1.15 (q, 6.0 Hz, 6H, CHMe_2), 1.08 (m, 12 H, CHMe_2), 0.74 (q, 6.0 Hz,

6H, CHMe₂); ¹⁹F NMR (C₆D₆): δ -122.5 (s); ¹³C{¹H} NMR (C₆D₆): δ 163.8 (t, J_{P-C} = 6.4 Hz, POCOP), 160.5 (d, J_{F-C} = 242 Hz, CF), 143.5 (dt, J_{Rh-C} = 29 Hz, J_{P-C} = 6.0 Hz), 140.3 (bs), 137.6 (bs), 137.7 (dt, J_{Rh-C} = 33 Hz, J_{P-C} = 10 Hz), 126.5 (s, POCOP), 113.9 (bs, 2 overlapping), 106.6 (t, J_{P-C} = 6.0 Hz, POCOP), 42.2 (t, J_{P-C} = 5.9 Hz, SC(CH₃)₃), 37.1 (s, SC(CH₃)₃), 31.9 (t, J_{P-C} = 11 Hz, CHMe₂), 29.8 (t, J_{P-C} = 13 Hz, CHMe₂), 19.9 (s, CHMe₂), 17.0 (t, J_{P-C} = 2.1 Hz, CHMe₂), 16.9 (s, CHMe₂), 16.7 (s, CHMe₂).

Synthesis of (POCOP)Rh(S(C₆H₄F)^tBu) (411) via thermolysis of (POCOP)Rh(C₆H₄F)(S^tBu). 410 (22 mg, 0.035 mmol) was added to a J. Young tube and dissolved in C₆D₆. The sample was heated at 65 °C for 6 h, resulting in 95% conversion to **411** (5% residual (POCOP)Rh(C₆H₄F)(S^tBu)) and a color change from purple to orange. Additional heating at 65 °C for 3 h resulted in quantitative conversion to **411**. ³¹P{¹H} NMR (C₆D₆): δ 186.6 (d, 174 Hz); ¹H NMR (C₆D₆): δ 7.65 (t, 6.5 Hz, 2H, C₆H₄F), 6.98 (t, 6.0 Hz, 1H, POCOP), 6.99 (d, 6.5 Hz, 2H, POCOP), 6.66 (t, 9.0 Hz, 2H, C₆H₄F), 2.12 (m, 2H, CHMe₂), 1.27 (q, 6.0 Hz, 12H, CHMe₂), 1.16 (q, 6.0 Hz, 12H, CHMe₂), 1.07 (s, 9H, C(CH₃)₃); ¹⁹F NMR (C₆D₆): δ -111.8 (s); ¹³C{¹H} NMR (C₆D₆): δ 167.5 (t, J_{P-C} = 9.2 Hz, POCOP), 163.8 (d, J_{F-C} = 250 Hz, CF), 138.7 (d, J_{F-C} = 7.8 Hz, C₆H₄F), 129.8 (d, J_{Rh-C} = 2.8 Hz, C₆H₄F), 124.8 (s, POCOP), 115.2 (d, J_{F-C} = 22 Hz, C₆H₄F), 104.0 (t, J_{P-C} = 6.9 Hz, POCOP), 46.9 (t, J_{P-C} = 4.6 Hz, SC(CH₃)₃), 31.1 (td, J_{P-C} = 10 Hz, J_{Rh-C} = 2.3 Hz, CHMe₂), 29.1 (s, SC(CH₃)₃), 18.7 (t, J_{P-C} = 3.8 Hz, CHMe₂), 17.7 (s, CHMe₂).

Synthesis of (POCOP)Rh(*o*-C₆H₄Me)(Br) (417). 205 (118 mg, 0.25 mmol) was added to a Schlenk flask and dissolved in toluene. NaO^tBu (26 mg, 0.27 mmol) and *o*-

MeC₆H₄Br (33 μ L, 0.27 mmol) were added to the Schlenk flask. The solution underwent an immediate color change dark red upon addition of the base and aryl halide. Analysis of the ³¹P{¹H} NMR spectrum after stirring for 30 min at RT showed complete conversion of the starting material to three new compounds: the two rotamers of **417** (major: 171.2 ppm, d, J_{RhP} = 122 Hz, 86%; minor: 172.4 ppm, d, J_{RhP} = 122 Hz, 9%) and unknown side product at 170.2 ppm (d, J_{RhP} = 123 Hz, 5%). The volatiles were removed by vacuum. The product was extracted with pentane and passed through a pad of Celite. The volatiles were removed to give a red solid (106 mg, 68%). Analysis of the red solid by ³¹P NMR spectroscopy shows the same three products; the two rotamers (89% and 8%) and the minor side product (3%). ³¹P{¹H} NMR: 171.7 (d, 122 Hz, major rotamer), 172.9 (d, 122 Hz, minor rotamer); ¹H NMR (major rotamer, C₆D₆): δ 6.87 (t, 7.0 Hz, 1H), 6.68 (m, 4H), 6.40 (t, 7.0 Hz, 1H), 6.03 (d, 9.0 Hz, 1H), 2.96 (m, 2H, CHMe₂), 2.88 (s, 3H, Me), 2.10 (m, 2H, CHMe₂), 1.32 (q, 9.0 Hz, 6H, CHMe₂), 1.12 (q, 9.0 Hz, 6H, CHMe₂), 0.94 (q, 9.0 Hz, 6H, CHMe₂), 0.60 (q, 9.0 Hz, 6H, CHMe₂); ¹³C{¹H} NMR (major rotamer, C₆D₆): δ 163.4 (t, J_{PC} = 6.5 Hz, POCOP), 142.1 (dt, J_{RhC} = 32 Hz, J_{PC} = 7.4 Hz), 137.6 (s), 137.4 (dt, J_{RhC} = 39 Hz, J_{PC} = 4.2 Hz), 134.9 (s), 131.0 (s), 126.5 (s), 126.3 (s), 124.3 (s), 107.5 (t, J_{PC} = 5.6 Hz, POCOP), 31.5 (t, J_{PC} = 12 Hz, CHMe₂), 28.7 (t, J_{PC} = 12 Hz, CHMe₂), 23.4 (s, Me), 18.1 (s, CHMe₂), 16.9 (s, CHMe₂), 16.2 (s, CHMe₂), 15.7 (s, CHMe₂).

Thermolysis of 407 with *o*-MeC₆H₄Br. **407** (11 mg, 0.17 mmol) and *o*-MeC₆H₄Br (10 μ L, 0.085 mmol) were added to a J. Young tube and dissolved in C₆D₆. The sample was heated in a 65 °C oil bath and monitored by ³¹P NMR spectroscopy

(Figure 4-6). The sample showed 38% conversion to the two rotamers of **417** after 1 h at 65 °C, 64% conversion to the two rotamers after 3 h at 65 °C, and >99% conversion after 20 h at 65 °C. The minor impurity (170.2 ppm, 123 Hz) that was observed in the synthesis of **417** from (POCOP)Rh(H)(Cl) was not observed.

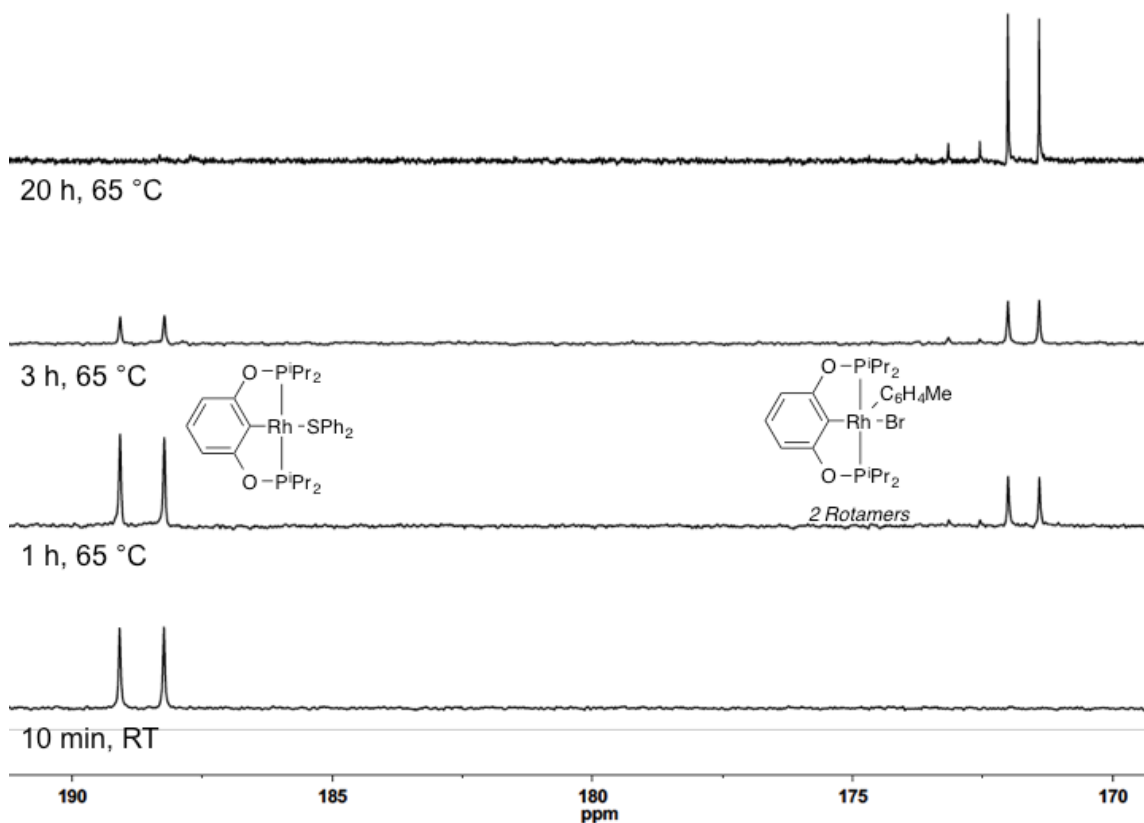


Figure 4-6. $^{31}\text{P}\{^1\text{H}\}$ NMR spectra in C_6D_6 for the thermolysis of **407** in the presence of *o*- $\text{MeC}_6\text{H}_4\text{Br}$.

Synthesis of (POCOP)Rh(H)(SPh) (418). **407** (209 mg, 0.33 mmol) was added to a J. Young tube and dissolved in C_6D_6 . PhSH (41 μL , 0.40 mmol) was added to the sample resulting in an immediate color change from orange to red. Analysis of the reaction after

30 min at RT by ^{31}P NMR spectroscopy indicated complete conversion to a new single product (191.4 ppm, d, 123 Hz). The volatiles were removed under vacuum. The red solid was washed with cold pentane to remove SPh_2 and dried under vacuum to give **418** as a clean red solid (130 mg, 71%). $^{31}\text{P}\{^1\text{H}\}$ NMR (C_6D_6): δ 191.4 (d, 123 Hz); ^1H NMR (C_6D_6): δ 7.70 (bs, 2H, Ph), 6.96 (m, 2H), 6.87 (m, 2H), 6.73 (d, $J = 6.0$ Hz, POCOP), 2.05 (m, 4H, CHMe_2), 1.10 (q, $J = 9.0$ Hz, 12H, CHMe_2), 1.04 (bm, 12H, CHMe_2), -23.00 (dt, $J_{\text{RhH}} = 35$ Hz, $J_{\text{PH}} = 13$ Hz, RhH); $^{13}\text{C}\{^1\text{H}\}$ NMR (C_6D_6): δ 165.3 (bs, POCOP), 153.3 (bs, Ph), 133.7 (s), 133.5 (bm, POCOP), 128.4 (s), 127.6 (s), 126.3 (s), 123.8 (s), 106.0 (t, $J_{\text{PC}} = 5.7$ Hz, POCOP), 29.3 (t, 13 Hz, CHMe_2), 17.5 (s, CHMe_2), 16.9 (s, CHMe_2). Anal. Calc. for $\text{C}_{24}\text{H}_{37}\text{O}_2\text{P}_2\text{RhS}$: C, 51.99; H, 6.73. Found: C, 51.86; H, 6.68.

Variable-Temperature NMR Spectroscopic Analysis of 418. **418** (17 mg, 0.031 mmol) was added to a J. Young tube and dissolved in d_8 -toluene. The sample was cooled from 20 °C to -80 °C and monitored by $^{31}\text{P}\{^1\text{H}\}$ NMR (Figure 4-7) and ^1H NMR (Figure 4-8 and 4-9). As the sample cooled, a new doublet emerged in the $^{31}\text{P}\{^1\text{H}\}$ NMR spectrum at 183.1 ppm ($J = 118$). By ^1H NMR, the methine resonance began to split in two at -40 °C and by -60 °C two new methines (Figure 4-9) appeared further downfield corresponding to the new doublet in the $^{31}\text{P}\{^1\text{H}\}$ NMR spectrum. At -80 °C, the presence of two distinct compounds was visible by ^1H NMR spectroscopy, 75% **418**. A hydride corresponding to the second compound was also present at -16.9 ppm in the ^1H NMR, indicating the hydride of the other compound is not *trans* to an empty site. Based

on these data, the identity of the compound was tentatively assigned to be the bridging thiolate dimer $[(\text{POCOP})\text{Rh}(\text{H})(\text{SPh})]_2$ (**420**).

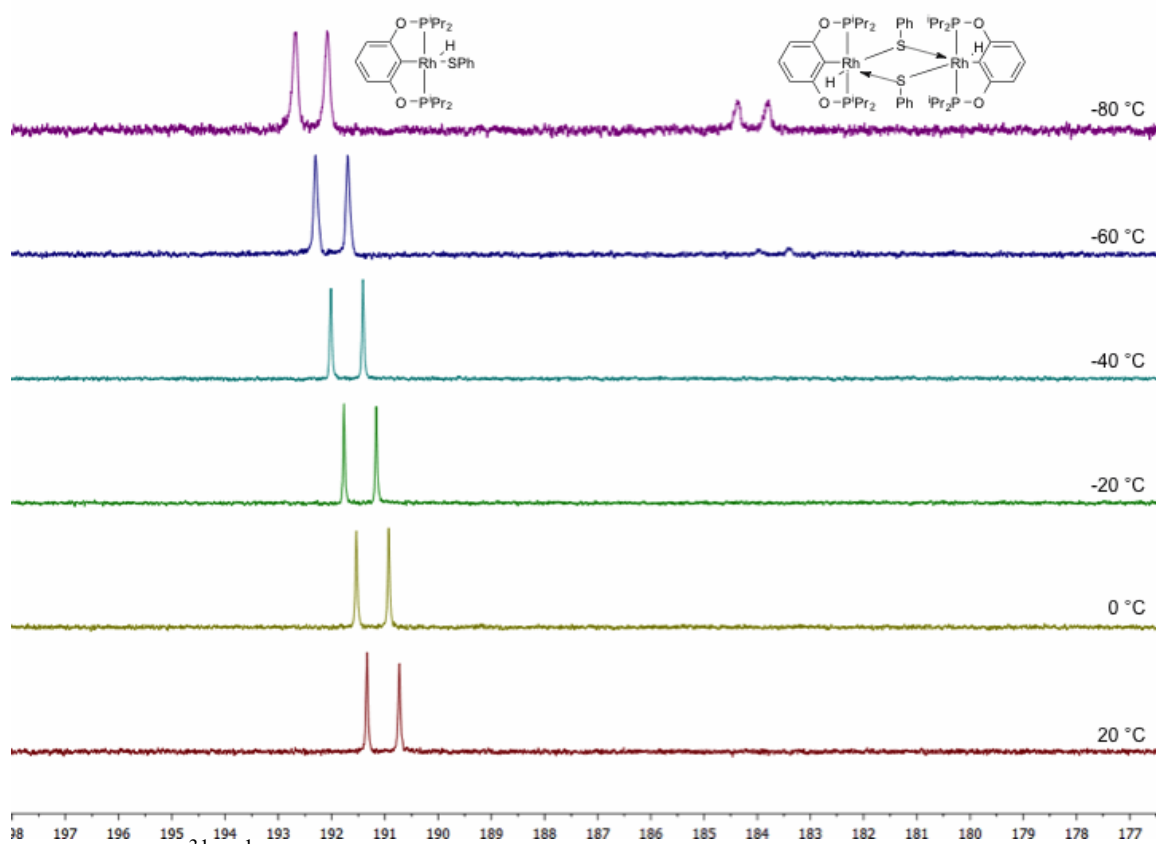


Figure 4-7. $^{31}\text{P}\{^1\text{H}\}$ NMR spectra for the thermolysis of **418** in d_8 -toluene. The presence of $[(\text{POCOP})\text{Rh}(\text{H})(\text{SPh})]_2$ (**420**) is indicated by the new doublet formed starting at -60 °C.

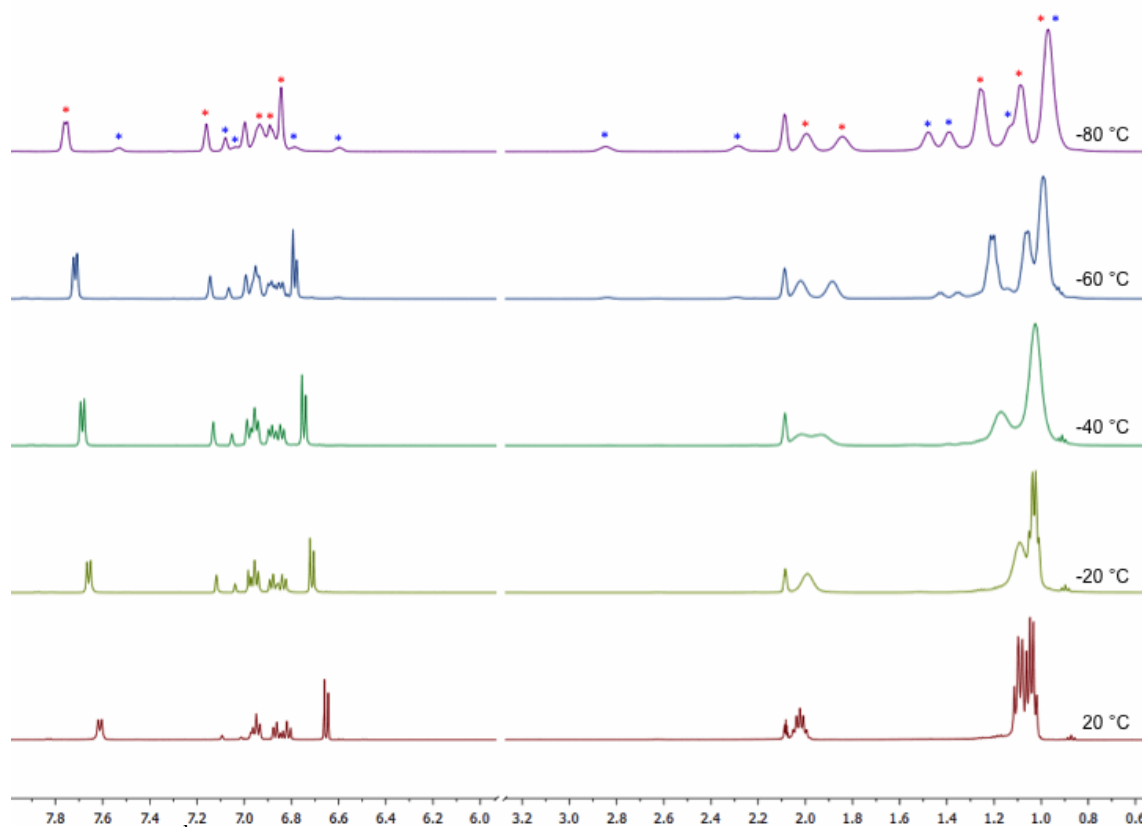


Figure 4-8. ^1H NMR spectra for the thermolysis of **418** in d_8 -toluene. The methine resonance for **418** begins to split at $-40\text{ }^\circ\text{C}$ and two new methine resonances occur for $[(\text{POCOP})\text{Rh}(\text{H})(\text{SPh})_2]$ (**420**) at $-60\text{ }^\circ\text{C}$. The resonances corresponding to **418** are marked with red (*) and the resonances corresponding to **420** are marked with blue (*) in the spectrum at $-80\text{ }^\circ\text{C}$.

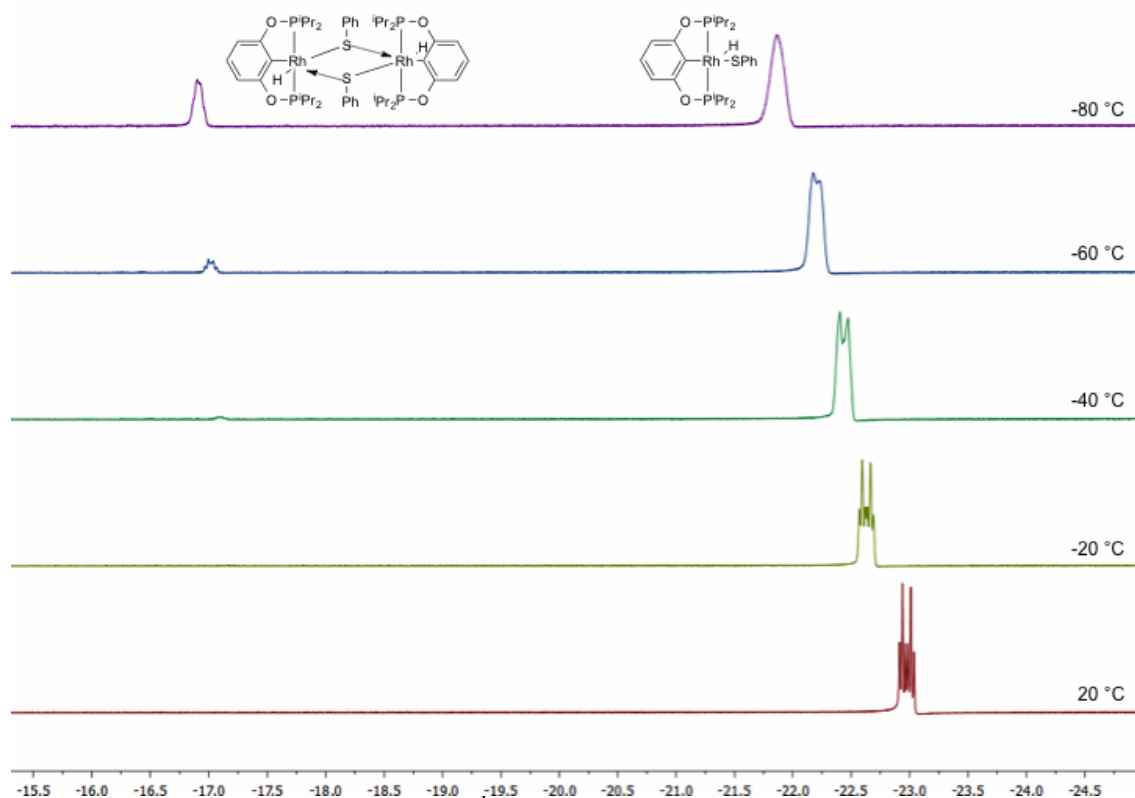


Figure 4-9. Hydride region of the ^1H NMR spectra for the thermolysis of **418** in d_8 -toluene. The hydride for $[(\text{POCOP})\text{Rh}(\text{H})(\text{SPh})]_2$ (**420**) occurs at -16.9 ppm beginning at -40 °C. The downfield hydride chemical shift indicates the hydride is not trans to an open coordination site.

Synthesis of $(\text{POCOP})\text{Rh}(\text{NaSPh})$ (421**).** **418** (106 mg, 0.020 mmol) was added to a Schlenk flask and dissolved in toluene. NaO^tBu (21 mg, 0.22 mmol) was added to the sample, resulting in an immediate color change to yellow-brown. The reaction was stirred for 1 h at RT. Analysis of the sample by ^{31}P NMR spectroscopy indicated complete conversion to a new Rh(I) complex (186.1 ppm, broad d, $J = 167$ Hz). The volatiles were removed by vacuum. The residual yellow solid was washed with pentane and dried under vacuum. Analysis of the isolated solid by ^1H NMR was not successful

due to poor solubility issues; however, X-ray quality crystals were obtained from a saturated toluene solution layered with pentane at RT. The structure was determined to be a polymer form of **421**. The composition of the product was also confirmed by elemental analysis. Anal. Calc. for $C_{24}H_{36}NaO_2P_2RhS$: C, 50.01; H, 6.30. Found: C, 49.78; H, 6.52.

Formation of 406 from 418. **418** (19 mg, 0.034 mmol) was added to a J. Young tube and dissolved in C_6D_6 . C_6H_5Br (4 μ L, 0.038 mmol) was added to the sample. No reaction occurred after 24 h at RT. NaO^tBu (4 mg, 0.041 mmol) was added to the sample, resulting in an immediate color change to yellow-green, indicative of formation of **421**. After 60 min at RT, the color of the sample changed to dark purple. Analysis of the sample by $^{31}P\{^1H\}$ NMR and 1H NMR spectroscopy showed complete conversion to **406**.

4.4.3 Catalytic Reactions

4.4.3.1 Examination of Various Catalysts

(pincer) $Rh(H)(Cl)$ (**205**, **401-403**, 0.0049 mmol) was combined with aryl-halide (0.18 mmol) and NaO^tBu (31 mg, 0.36 mmol) in a screw cap vial with a stir bar and dissolved in toluene (1.0 mL). The thiol reagent (0.16 mmol) was added to the sample along with C_6H_5F (10 μ L) to act as an internal standard. The reaction vial was closed and heated in a 110 $^{\circ}C$ oil bath. Reactions were monitored by ^{19}F NMR spectroscopy. Results included in Table 4-2.

The same test reactions were examined using [(cod)RhCl]₂ and a 1:2 Rh:PCy₃ ratio of [(cod)RhCl]₂ and PCy₃ (3% mol Rh) (Table 4-2). None of these reactions produced any observable amount of the coupled product by ¹⁹F NMR spectroscopy.

Table 4-2. Catalyst test reactions.

| Catalyst | Ar-X | R-SH | Yield (2h) | Yield (24 h) |
|---|---|--|------------|--------------|
| 205 | <i>p</i> -BrC ₆ H ₄ CF ₃ | <i>c</i> -C ₆ H ₁₁ SH | 97% | 96% |
| | <i>p</i> -BrC ₆ H ₄ CF ₃ | <i>p</i> -MeC ₆ H ₄ SH | 97% | 97% |
| 401 | <i>p</i> -BrC ₆ H ₄ CF ₃ | <i>c</i> -C ₆ H ₁₁ SH | 95% | 95% |
| | <i>p</i> -BrC ₆ H ₄ CF ₃ | <i>p</i> -MeC ₆ H ₄ SH | 20% | 20% |
| 402 | <i>p</i> -BrC ₆ H ₄ CF ₃ | <i>c</i> -C ₆ H ₁₁ SH | 3% | 3% |
| | <i>p</i> -BrC ₆ H ₄ CF ₃ | <i>p</i> -MeC ₆ H ₄ SH | 4% | 4% |
| 403 | <i>p</i> -BrC ₆ H ₄ CF ₃ | <i>c</i> -C ₆ H ₁₁ SH | 93% | 97% |
| | <i>p</i> -BrC ₆ H ₄ CF ₃ | <i>p</i> -MeC ₆ H ₄ SH | 80% | 95% |
| [(cod)RhCl] ₂ | <i>p</i> -BrC ₆ H ₄ CF ₃ | <i>c</i> -C ₆ H ₁₁ SH | - | - |
| | <i>p</i> -BrC ₆ H ₄ CF ₃ | <i>p</i> -MeC ₆ H ₄ SH | - | - |
| [(cod)RhCl] ₂ & PCy ₃ | <i>p</i> -BrC ₆ H ₄ CF ₃ | <i>c</i> -C ₆ H ₁₁ SH | - | - |
| | <i>p</i> -BrC ₆ H ₄ CF ₃ | <i>p</i> -MeC ₆ H ₄ SH | - | - |

4.4.3.2 Solvent Optimization

205 (121 μL of 0.04 M stock solution in toluene, 0.0049 mmol) was combined with *p*-ClC₆H₄F (16 μL, 0.18 mmol) and NaO^tBu (31 mg, 0.36 mmol) in a screw cap vial with a stir bar and dissolved in the solvent of choice (1.0 mL). *n*-C₅H₁₁SH (20 μL, 0.16 mmol) was added to the sample along with C₆H₅CF₃ (5 μL) to act as the internal

standard. The reaction vial was sealed and heated in a 110 °C oil bath for 24 h. Reactions were monitored by ^{19}F NMR spectroscopy. Results included in Table 4-3.

Table 4-3. Solvent optimization.

| Solvent | Yield |
|----------------|--------------|
| Toluene | 57% |
| THF | - |
| 1,4-dioxane | - |
| DMF | - |

4.4.3.3 Base Optimization

205 (121 μL of 0.04 M stock solution in toluene, 0.0049 mmol) was combined with *p*-ClC₆H₄F (16 μL , 0.18 mmol) and base (0.36 mmol) in a screw cap vial with a stir bar and dissolved in the solvent of choice (1.0 mL). *n*-C₅H₁₁SH (20 μL , 0.16 mmol) was added to the sample along with C₆H₅CF₃ (5 μL) to act as the internal standard. The reaction vial was sealed and heated in a 110 °C oil bath for 24 h. Reactions were monitored by ^{19}F NMR spectroscopy. Results included in Table 4-4.

Table 4-4. Base optimization.

| Base | Yield |
|---------------------------------|--------------|
| NaO ^t Bu | 57% |
| KOH | - |
| KH ₂ PO ₄ | - |
| NaO ^t Pent | 35% |
| NaHCO ₃ | - |

4.4.3.4 General Procedure for Catalytic C-S Coupling Reactions

205 (121 μL of 0.04 M stock solution in toluene, 0.0049 mmol) was combined with aryl-halide (0.18 mmol) and NaO^tBu (31 mg, 0.36 mmol) in a screw cap vial with a stir bar and dissolved in toluene (1.0 mL). The thiol reagent (0.16 mmol) was added to the sample along with the internal standard. For reactions with F-substituted aryl halides, benzotrifluoride ($\text{CF}_3\text{C}_6\text{H}_5$) was used as the internal standard. For reactions with CF_3 -substituted aryl-halides, fluorobenzene was used as the internal standard. Mesitylene was used as the internal standard for reactions containing no fluorine substituents. The reaction vial was sealed and heated in a 110 $^\circ\text{C}$ oil bath. Reactions were monitored by ^{19}F NMR or ^1H NMR spectroscopy. For product isolation, the sample was passed through a pad of Celite/silica gel and the volatiles were removed by vacuum. The results are included in Table 4-5 and Table 4-6.

Table 4-5. Coupling reactions with alkyl-thiols.

| Ar-X | R-SH | Time | Yield (Ar-SR) ^a | Yield (Ar-H) ^b |
|---|--|------|----------------------------|---------------------------|
| <i>p</i> -BrC ₆ H ₄ F | <i>n</i> -C ₅ H ₁₁ SH | 3 h | 96% | 4% |
| <i>p</i> -BrC ₆ H ₄ F | <i>n</i> -C ₁₀ H ₂₁ SH | 3 h | 98% (95%) | 2% |
| <i>p</i> -BrC ₆ H ₄ F | <i>c</i> -C ₆ H ₁₁ SH | 3 h | 97% | 3% |
| <i>p</i> -ClC ₆ H ₄ F | <i>n</i> -C ₅ H ₁₁ SH | 48 h | 94% | 2% |
| <i>p</i> -ClC ₆ H ₄ F | <i>n</i> -C ₁₀ H ₂₁ SH | 48 h | 96% | 3% |
| <i>p</i> -ClC ₆ H ₄ F | <i>c</i> -C ₆ H ₁₁ SH | 24 h | 98% (94%) | 2% |
| <i>p</i> -BrC ₆ H ₄ CF ₃ | <i>n</i> -C ₅ H ₁₁ SH | 3 h | 97% (94%) | 10% |
| <i>p</i> -BrC ₆ H ₄ CF ₃ | <i>n</i> -C ₁₀ H ₂₁ SH | 3 h | 97% | 3% |
| <i>p</i> -BrC ₆ H ₄ CF ₃ | <i>c</i> -C ₆ H ₁₁ SH | 3 h | 98% | 2% |
| <i>p</i> -ClC ₆ H ₄ CF ₃ | <i>n</i> -C ₅ H ₁₁ SH | 20 h | 92% | 3% |
| <i>p</i> -ClC ₆ H ₄ CF ₃ | <i>n</i> -C ₁₀ H ₂₁ SH | 20 h | 88% | 1% |
| <i>p</i> -ClC ₆ H ₄ CF ₃ | <i>c</i> -C ₆ H ₁₁ SH | 20 h | 95% (93%) | 1% |
| <i>p</i> -ClC ₆ H ₄ Me | <i>c</i> -C ₆ H ₁₁ SH | 36 h | 93% | 1% |
| <i>p</i> -ClC ₆ H ₄ OMe | <i>n</i> -C ₅ H ₁₁ SH | 36 h | 50% | - |
| <i>o</i> -BrC ₆ H ₄ Me | <i>c</i> -C ₆ H ₁₁ SH | 24 h | 30% | - |
| <i>o</i> -ClC ₆ H ₄ Me | <i>c</i> -C ₆ H ₁₁ SH | 24 h | - | - |
| <i>p</i> -BrC ₆ H ₄ F | (CH ₃) ₃ CSH | 2 h | 99% | - |
| <i>p</i> -ClC ₆ H ₄ F | (CH ₃) ₃ CSH | 24 h | 95% | - |

^a. Yields are measured *in situ* by ¹⁹F NMR spectroscopy with internal standard reference. Isolated yields are in parentheses. ^b. Ar-H yields are measured *in situ* by ¹⁹F NMR spectroscopy with an internal standard reference.

Table 4-6. Coupling reactions with aryl-thiols.

| Ar-X | R-SH | Time | Yield (Ar-SR) ^a | Yield (Ar-H) ^b |
|---|--|------|----------------------------|---------------------------|
| <i>p</i> -BrC ₆ H ₄ F | PhSH | 18 h | 98% | 5% |
| <i>p</i> -BrC ₆ H ₄ F | <i>p</i> -MeC ₆ H ₄ SH | 20 h | 94% (91%) | 4% |
| <i>p</i> -BrC ₆ H ₄ F | <i>o</i> -MeC ₆ H ₄ SH | 20 h | 94% | 3% |
| <i>p</i> -BrC ₆ H ₄ F | (2,5-MeC ₆ H ₃)SH | 40 h | 90% | 2% |
| <i>p</i> -BrC ₆ H ₄ F | (<i>o</i> -C ₆ H ₄ ⁱ Pr)SH | 80 h | 75% | 4% |
| <i>p</i> -ClC ₆ H ₄ F | PhSH | 20 h | 48% | 2% |
| <i>p</i> -ClC ₆ H ₄ F | <i>p</i> -MeC ₆ H ₄ SH | 20 h | 55% | 1% |
| <i>p</i> -ClC ₆ H ₄ F | <i>o</i> -MeC ₆ H ₄ SH | 40 h | 80% | 3% |
| <i>p</i> -ClC ₆ H ₄ F | (2,5-MeC ₆ H ₃)SH | 40 h | 30% | 2% |
| <i>p</i> -ClC ₆ H ₄ F | (<i>o</i> -C ₆ H ₄ ⁱ Pr)SH | 80 h | 94% | 1% |
| <i>p</i> -BrC ₆ H ₄ CF ₃ | PhSH | 20 h | 99% (97%) | 5% |
| <i>p</i> -BrC ₆ H ₄ CF ₃ | <i>p</i> -MeC ₆ H ₄ SH | 20 h | 97% | 3% |
| <i>p</i> -ClC ₆ H ₄ CF ₃ | PhSH | 20 h | 95% (87%) | 3% |
| <i>p</i> -ClC ₆ H ₄ CF ₃ | <i>p</i> -MeC ₆ H ₄ SH | 20 h | 93% | 4% |
| <i>p</i> -ClC ₆ H ₄ Me | <i>p</i> -MeC ₆ H ₄ SH | 36 h | 84% | - |
| <i>p</i> -ClC ₆ H ₄ OMe | <i>p</i> -MeC ₆ H ₄ SH | 36 h | 43% | 1% |
| <i>o</i> -BrC ₆ H ₄ Me | <i>p</i> -MeC ₆ H ₄ SH | 24 h | - | - |
| <i>o</i> -ClC ₆ H ₄ Me | <i>p</i> -MeC ₆ H ₄ SH | 24 h | - | - |

^a. Yields are measured *in situ* by ¹⁹F NMR spectroscopy with internal standard reference. Isolated yields are in parentheses. ^b. Ar-H yields are measured *in situ* by ¹⁹F NMR spectroscopy with an internal standard reference.

4.4.3.5 Maximizing the Turnover Number

Maximizing the turnover number for (*p*-FC₆H₄)S(C₆H₁₁). 205 (0.00008 – 0.0049 mmol, 0.04 M stock solution in toluene) was combined with an aryl halide (0.18 mmol) and NaO^tBu (31 mg, 0.36 mmol) in a screw cap vial with a stir bar and dissolved in toluene (1.0 mL). *c*-C₆H₁₁SH (20 μL, 0.16 mmol) was added to the sample along with C₆H₅CF₃ (5 μL) to act as an internal standard. The reaction vial was sealed and heated in a 110 °C oil bath. Reactions were monitored by ¹⁹F NMR spectroscopy. The reactions were heated until no additional conversion of the aryl halide occurred (Table 4-7).

Table 4-7. Optimized TON for synthesis of (*p*-FC₆H₄)S(C₆H₁₁).

| Aryl Halide | Catalyst Load | Reaction Time | Yield | TON |
|---|---------------|---------------|-------|------|
| <i>p</i> -BrC ₆ H ₄ F | 3% | 3 h | 97% | 32 |
| <i>p</i> -BrC ₆ H ₄ F | 1% | 24 h | 98% | 98 |
| <i>p</i> -BrC ₆ H ₄ F | 0.1% | 24 h | 93% | 930 |
| <i>p</i> -BrC ₆ H ₄ F | 0.05% | 24 h | 80% | 1600 |
| <i>p</i> -BrC ₆ H ₄ F | 0.01% | 36 h | 25% | 2500 |
| <i>p</i> -ClC ₆ H ₄ F | 3% | 24 h | 98% | 33 |
| <i>p</i> -ClC ₆ H ₄ F | 1% | 48 h | 94% | 94 |
| <i>p</i> -ClC ₆ H ₄ F | 0.1% | 48 h | 35% | 350 |

Maximizing the turnover number for (*p*-CF₃C₆H₄)S(*p*-MeC₆H₄). 205 (0.00008 – 0.0049 mmol, 0.04 M stock solution in toluene) was combined with arylhalide (0.18 mmol) and NaO^tBu (31 mg, 0.36 mmol) in a screw cap vial with a stir bar and dissolved in toluene (1.0 mL). *p*-MeC₆H₄SH (20 mg, 0.16 mmol) was added to the sample along with C₆H₅F (10 μL) to act as an internal standard. The reaction vial was sealed and heated in a 110 °C oil bath. Reactions were monitored by ¹⁹F NMR

spectroscopy. The reactions were heated until no additional conversion of the aryl halide occurred (Table 4-8).

Table 4-8. Optimized TON for synthesis (*p*-CF₃C₆H₄)S(*p*-MeC₆H₄).

| Aryl Halide | Catalyst Load | Reaction Time | Yield | TON |
|---|---------------|---------------|-------|-----|
| <i>p</i> -BrC ₆ H ₄ CF ₃ | 3% | 24 h | 98% | 33 |
| <i>p</i> -BrC ₆ H ₄ CF ₃ | 1% | 24 h | 99% | 99 |
| <i>p</i> -BrC ₆ H ₄ CF ₃ | 0.1% | 3 d | 94% | 940 |
| <i>p</i> -BrC ₆ H ₄ CF ₃ | 0.05% | 4 d | 17% | 340 |
| <i>p</i> -BrC ₆ H ₄ CF ₃ | 0.01% | 4 d | 3% | 300 |
| <i>p</i> -ClC ₆ H ₄ CF ₃ | 3% | 24 h | 92% | 31 |
| <i>p</i> -ClC ₆ H ₄ CF ₃ | 1% | 3 d | 80% | 80 |
| <i>p</i> -ClC ₆ H ₄ CF ₃ | 0.1% | 3 d | 20% | 200 |

4.4.3.6 Effect of Excess Aryl Halide on Catalysis

205 (121 μL of 0.04 M stock solution in toluene, 0.0049 mmol) was combined with aryl halide (0.18 – 1.6 mmol) and NaO^tBu (31 mg, 0.36 mmol) in a screw cap vial with a stir bar and dissolved in toluene (1.0 mL). *c*-C₆H₁₁SH (20 μL, 0.16 mmol) was added to the sample along with C₆H₅CF₃ (5 μL) to act as an internal standard. The reaction vial was sealed and heated in a 110 °C oil bath. Reactions were monitored by ¹⁹F NMR or ¹H NMR spectroscopy. These results are included in Table 4-1.

4.4.4 X-ray Crystallography

X-Ray data collection, solution, and refinement for 406. A single purple crystal of suitable size and quality (0.04 × 0.06 × 0.13 mm) was selected from a representative sample of crystals of the same habit using an optical microscope, mounted onto a nylon loop and placed in a cold stream of nitrogen (110 K). Low-temperature X-ray data were obtained on a Bruker APEXII CCD based diffractometer (Mo sealed X-ray

tube, $K_{\alpha} = 0.71073 \text{ \AA}$). All diffractometer manipulations, including data collection, integration and scaling were carried out using the Bruker APEXII software.⁸⁸ An absorption correction was applied using SADABS.⁸⁸ The space group was determined on the basis of systematic absences and intensity statistics and the structure was solved by direct methods and refined by full-matrix least squares on F^2 . The structure was solved in the monoclinic P 21/c space group using XS⁸⁹ (incorporated in X-Seed). This symmetry was confirmed by PLATON.⁹⁰ All non-hydrogen atoms were refined with anisotropic thermal parameters. Hydrogen atoms were placed in idealized positions and refined using riding model. The structure was refined (weighted least squares refinement on F^2) to convergence.

X-Ray data collection, solution, and refinement for 407. A single orange crystal of suitable size and quality ($0.11 \times 0.50 \times 0.55 \text{ mm}$) was selected from a representative sample of crystals of the same habit using an optical microscope, mounted onto a nylon loop and placed in a cold stream of nitrogen (110 K). Low-temperature X-ray data were obtained on a Bruker APEXII CCD based diffractometer (Mo sealed X-ray tube, $K_{\alpha} = 0.71073 \text{ \AA}$). All diffractometer manipulations, including data collection, integration and scaling were carried out using the Bruker APEXII software.⁸⁸ An absorption correction was applied using SADABS.⁸⁸ The space group was determined on the basis of systematic absences and intensity statistics and the structure was solved by direct methods and refined by full-matrix least squares on F^2 . The structure was solved in the monoclinic P 21/n space group using XS⁸⁹ (incorporated in X-Seed). This symmetry was confirmed by PLATON.⁹⁰ All non-hydrogen atoms were refined with

anisotropic thermal parameters. Hydrogen atoms were placed in idealized positions and refined using riding model. The structure was refined (weighted least squares refinement on F^2) to convergence.

X-Ray data collection, solution, and refinement for 418. A single orange crystal of suitable size and quality ($0.05 \times 0.10 \times 0.11$ mm) was selected from a representative sample of crystals of the same habit using an optical microscope, mounted onto a nylon loop and placed in a cold stream of nitrogen (110 K). Low-temperature X-ray data were obtained on a Bruker APEXII CCD based diffractometer (Mo sealed X-ray tube, $K_{\alpha} = 0.71073$ Å). All diffractometer manipulations, including data collection, integration and scaling were carried out using the Bruker APEXII software.⁸⁸ An absorption correction was applied using SADABS.⁸⁸ The space group was determined on the basis of systematic absences and intensity statistics and the structure was solved by direct methods and refined by full-matrix least squares on F^2 . The structure was solved in the triclinic P-1 space group using XS⁸⁹ (incorporated in X-Seed). This symmetry was confirmed by PLATON.⁹⁰ All non-hydrogen atoms were refined with anisotropic thermal parameters. Hydrogen atoms were placed in idealized positions and refined using riding model. The structure was refined (weighted least squares refinement on F^2) to convergence. Although the Rh-*H* ligand could not be confidently located in the crystal structure, its presence is indicated by ¹H NMR spectroscopic data.

X-Ray data collection, solution, and refinement for 421. A single yellow crystal of suitable size and quality ($0.05 \times 0.16 \times 0.18$ mm) was selected from a representative sample of crystals of the same habit using an optical microscope, mounted

onto a nylon loop and placed in a cold stream of nitrogen (110 K). Low-temperature X-ray data were obtained on a Bruker APEXII CCD based diffractometer (Mo sealed X-ray tube, $K_{\alpha} = 0.71073 \text{ \AA}$). All diffractometer manipulations, including data collection, integration and scaling were carried out using the Bruker APEXII software.⁸⁸ An absorption correction was applied using SADABS.⁸⁸ The space group was determined on the basis of systematic absences and intensity statistics and the structure was solved by direct methods and refined by full-matrix least squares on F^2 . The structure was solved in the monoclinic $P 2_1/n$ space group using XS⁸⁹ (incorporated in X-Seed). This symmetry was confirmed by PLATON.⁹⁰ All non-hydrogen atoms were refined with anisotropic thermal parameters. Hydrogen atoms were placed in idealized positions and refined using riding model. The structure was refined (weighted least squares refinement on F^2) to convergence.

CHAPTER V
TOWARDS CARBON-FLUORINE REDUCTIVE ELIMINATION WITH Pincer
RHODIUM: A THEORETICAL AND EXPERIMENTAL STUDY

5.1 Introduction

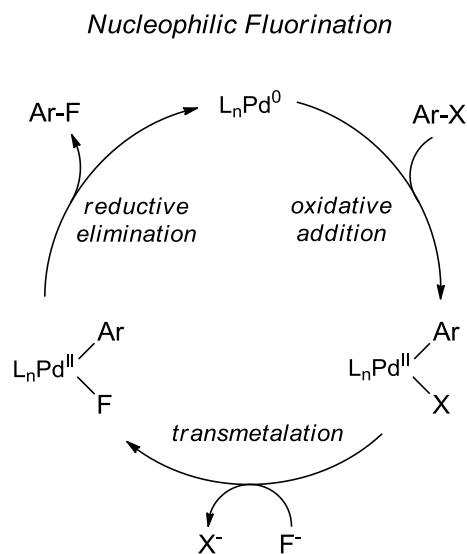
The C-F functional group is prevalent in a number of pharmaceuticals,¹²¹ agrochemicals,¹²² imaging agents,¹³ and new high performance materials.¹²³ However, while C-F bonds are common in many of these compounds, well-evolved methods for C-F bond formation are still uncommon. Many of the methods for forming C-F bonds, such as direct fluorination with F₂¹²⁴ and nucleophilic substitution with KF or CuF₂,¹²⁵ require harsh conditions and introduction of the functionality early in the synthesis, which reduces the scope of these processes.^{13b,126}

We are particularly interested in the formation of C(*sp*²)-F bonds, as well as other challenging C(*sp*²)-X (X = O) bond forming reactions, from aryl halides. Platinum group metals, particularly Pd, have shown tremendous utility in the formation of C(*sp*²)-X bonds, including C-N, C-S, and C-P.^{31,32,36,37} However, formation of C(*sp*²)-F bonds has remained a challenge due to the strength of M-F bonds as well as the poor nucleophilic character of the fluoro ligands.

In recent years, transition metals including Cu¹²⁷ and Pd¹²⁸ have all been used to form C(*sp*²)-F bonds with varying degrees of success. Thus far, the greatest amount of success has been achieved using Pd, which is able to form C(*sp*²)-F bonds through both an electrophilic^{129,130} and nucleophilic^{12b-d,131} pathway. The electrophilic pathway utilizes

electrophilic F reagents such as XeF_2 and proceeds *via* a Pd(II)/Pd(IV) cycle.¹³² Riiter et. al have described the successful late-stage formation of $\text{C}(sp^2)\text{-F}$ bonds, including ^{18}F -labeled small molecules, *via* the electrophilic route by using fluorine sources such as *N*-fluoropyridinium salts.^{13b}

Herin, we will focus on the nucleophilic approach to $\text{C}(sp^2)$ bond formation, which uses nucleophilic F sources such as CsF or AgF.¹³³ The nucleophilic pathway utilizes a Pd(0)/Pd(II) cycle analogous to Pd catalyzed C-N, C-S, and C-P coupling (Figure 5-1). The $\text{C}(sp^2)$ functional group is installed on Pd *via* oxidative addition (OA) of aryl halides to Pd(0). This is followed by transmetalation with a nucleophilic fluorine source to form Pd(II) aryl fluoride complex, which is then capable to undergo C-F reductive elimination (RE).¹³³



Scheme 5-1. Mechanism for nucleophilic C-F bond formation *via* Pd(0)/Pd(II) cycle.

Formation of $C(sp^2)$ -F bonds *via* the nucleophilic pathway has encountered many obstacles. Pioneering work by Grushin¹³⁴ and coworkers produced a series of PR_3 substituted $L_nPd(Ar)(F)$ ($L = PR_3$); however, none of these complexes underwent successful Ar-F reductive elimination. Theoretical analysis by Yandulov¹³⁵ identified two general issues with $L_nPd(Ar)(F)$: (1) access to the requisite three-coordinate $LPd(Ar)(F)$ and (2) the high barrier of C-F RE relative to other RE processes including C-C and P-F coupling.

More recently, Buchwald and coworkers have demonstrated the utility of their bulky phosphinobiaryl ligands, such as BrettPhos and RockPhos, with Pd to form Ar-F bonds both stoichiometrically and catalytically.^{12b,12d} The success of these ligands for challenging RE processes, including C-N and C-O coupling, is attributed to their large steric profile, which facilitates *pseudo* monocoordinate Pd(0) as well as *pseudo* three-coordinate Pd(II).^{12a,136} These ligands can also be electronically tuned by altering the phosphine substituents to achieve the desired electronic environment at the metal center. In this case, this ligand helps promote reductive elimination due to its large size, and also prevents formation of the fluorine-bridged dimer by forming *pseudo* three-coordinate compounds.

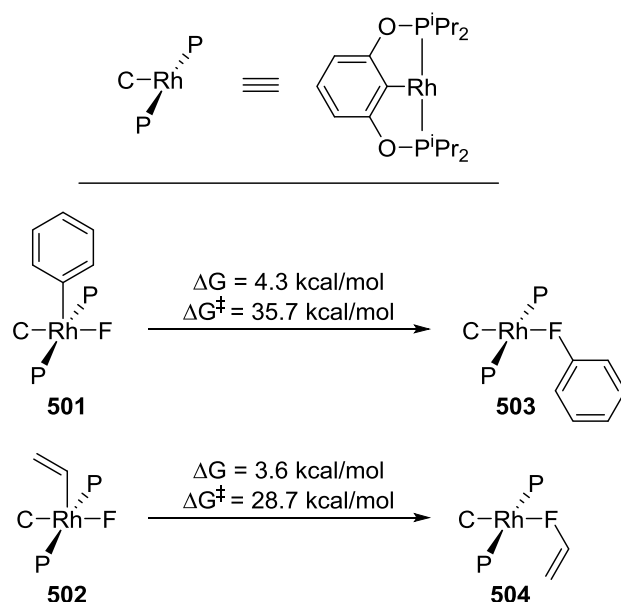
Based on our previous success with enhanced $C(sp^2)$ -X ($X = S, N$) RE with (POCOP)Rh, we thought it might be feasible to achieve $C(sp^2)$ -F RE with the same system. RE from d^6 Rh(III) is most faster from five-coordinate square-pyramidal complexes. Unlike isolation of three-coordinate Pd(II) complexes,¹³⁷ isolation of five-coordinate Rh(III) complexes is well-established.^{65,81,100,138} We were hopeful that

synthesis a (POCOP)Rh(R)(F) complex with the right C(sp²) group might provide the correct steric and electronic environment for C-F elimination.

5.2 Results and Discussion

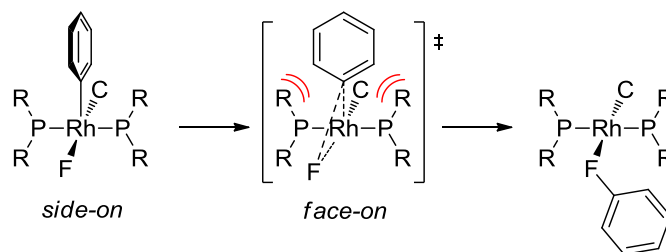
5.2.1 Theoretical Analysis

We selected (POCOP)Rh(Ph)(F) (**501**) and (POCOP)Rh(CHCH₂)(F) (**502**) for our theoretical analysis of the kinetic and thermodynamic accessibility of C-F reductive coupling as shown in Scheme 5-2 (Calculations done by Dr. Jia Zhou). The products were optimized as the F-bound adducts of fluorobenzene and fluoroethylene with (POCOP)Rh (**503** and **504**) in order to avoid steric and electronic differences between fluorobenzene and fluoroethylene binding via their π -systems. Binding of the π -system most likely occurs following the transition state, so it should only affect the thermodynamics and not the barrier for C-F reductive coupling. In a putative catalytic reaction, any C-F coupled product would most likely dissociate and be replaced by OA of the substrate organohalide (halide = Br, I, or OTf) to the unsaturated (POCOP)Rh^I center.⁶³⁻⁶⁴



Scheme 5-2. Calculated ΔG and ΔG^\ddagger for C-F RE from (POCOP)Rh(Ph)(F) (**501**) and (POCOP)Rh(CHCH₂)(F) (**502**).

The thermodynamics of the formation of **503** and **504** by C-F reductive coupling were calculated to be nearly the same (ΔG_{rxn} of 4.3 kcal/mol and 3.6 kcal/mol, respectively), suggestive of similar electronic factors in vinyl- and phenyl-fluoride bond formation. However, the reaction barrier was considerably lower for the vinyl-fluoride coupling ($\Delta G^\ddagger = 28.7$ kcal/mol) than for the phenyl-fluoride coupling ($\Delta G^\ddagger = 35.7$ kcal/mol). The disparity in reaction barriers for concerted reductive coupling reactions of phenyl vs vinyl in the (POCOP)Ir system was discussed in Chapter I section 1.5 and was attributed to the smaller steric profile of the vinyl group compared to phenyl.⁷⁶ The same trend holds true for C-F reductive coupling from (POCOP)Rh, in which the barrier for rotation at the transition state is smaller for vinyl than phenyl (Scheme 5-3).



Scheme 5-3. Transition state rotation for C-F RE from (POCOP)Rh(Ph)(F) (**501**).

We have also examined the potential for C-C reductive coupling involving the Rh-bound carbon of the POCOP ligand. Not surprisingly, calculations revealed the barrier for aryl-vinyl C-C coupling from **502/R1** is much lower than that for C-F coupling (Figure 5-1). However, the product formed *via* C-C reductive coupling (**P2**) is 8 kcal/mol less favorable than **P1** and is considerably unfavorable with respect to **R1**. C-C RE from (pincer)Rh(III) species is typically quite favorable, but in this case, the constraint of the chelate ligand makes for a product (**P2**) with a high degree of congestion and strain. Bearing this in mind, we decided to explore the experimental potential of C-F reductive coupling from **502**.

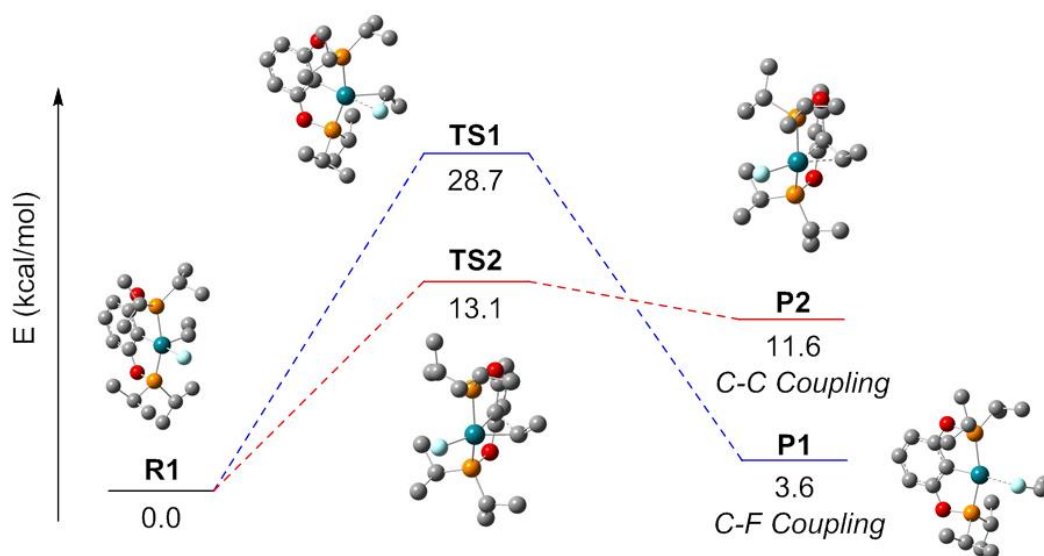


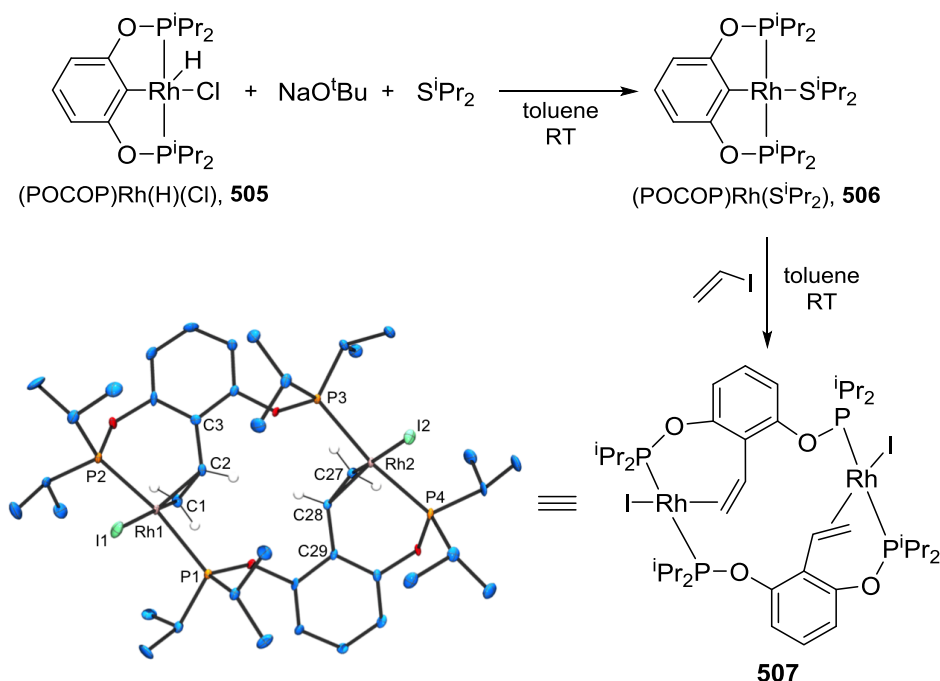
Figure 5-1. Potential energy surface of C(vinyl)-F RE and C(vinyl)-C(aryl) RE from (POCOP)Rh(CHCH₂)(F) (**502**).

5.2.2 Synthesis of Model Compounds

5.2.2.1 Attempted Synthesis of (POCOP)Rh(CHCH₂)(X) Compounds

We previously described OA of aryl halides to (PNP)Rh(SⁱPr₂)⁶³⁻⁶⁴ in Chapter I as well as aryl halide OA to (POCOP)Rh in Chapters II and III. We believed an analogous reaction between CH₂CHI and (POCOP)Rh(SⁱPr₂) could provide a synthetically useful precursor towards the synthesis of **502**. (POCOP)Rh(SⁱPr₂) (**505**) was synthesized by treating (POCOP)Rh(H)(Cl) (**205**) with SⁱPr₂ in the presence of NaO^tBu (Scheme 5-4). **505** was isolated in 84% yield and displayed a doublet at 185 ppm with $J_{\text{Rh-P}} = 174$ Hz by ³¹P NMR spectroscopy. The reaction of **505** with vinyl iodide resulted in a reaction upon mixing at RT. By analogy with (POCOP)Rh(Ar)(I), (POCOP)Rh(CHCH₂)(I) would be expected to display a doublet resonance in the ³¹P{¹H} NMR spectrum with $J_{\text{Rh-P}} \approx 120$ Hz; however, such a resonance was not in

evidence. The reaction instead resulted in a mixture of compounds with one dominant product (ca. 60%). This compound was isolated in a pure form in 52% yield from the reaction mixture as an orange crystalline solid and identified as **506** (Scheme 5-4) based on the solution NMR data and an X-ray structural study on a single crystal (Scheme 5-4). **506** displayed two sets of doublet of doublets by $^{31}\text{P}\{^1\text{H}\}$ NMR spectrum at 200.5 ppm ($J_{\text{RhP}} = 140$ Hz, $J_{\text{PP}} = 473$ Hz) and 163.7 ppm ($J_{\text{RhP}} = 128$ Hz, $J_{\text{PP}} = 473$ Hz). The solid-state structure showed a bimetallic complex containing two square-planar Rh(I) centers, ostensibly arising from **504** by way of C(aryl)-C(vinyl) reductive elimination to form **P2** and subsequent dimerization of the latter. The C-C bond lengths (1.420(6) Å and 1.412(6) Å) of the bound olefins are typical for an η^2 -olefin complex of Rh(I).¹³⁹

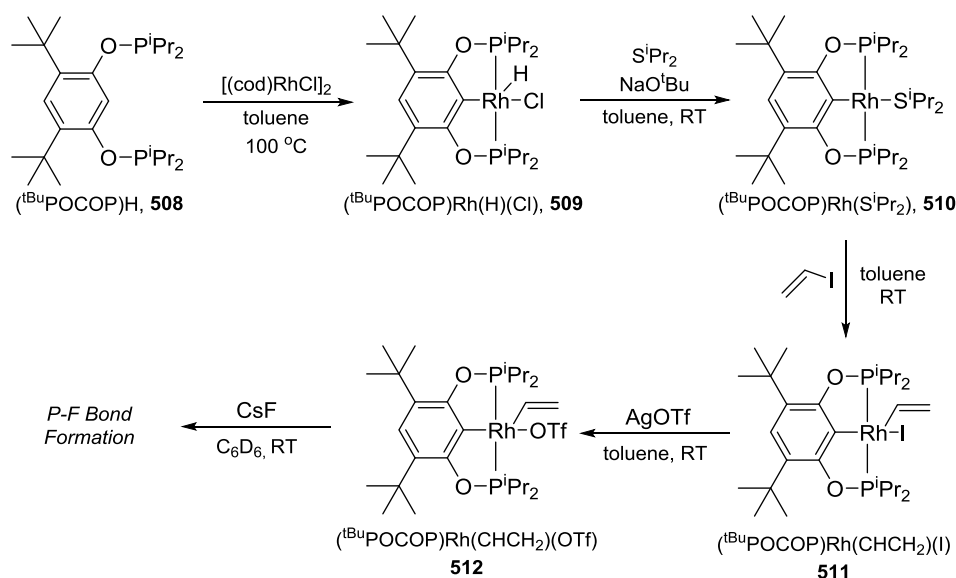


Scheme 5-4. Reactivity of vinyl iodide with $(\text{POCOP})\text{Rh}(\text{SiPr}_2)$ (**505**).

The key difference between the computationally evaluated **P2** and its dimer **506** is that the two phosphinite donors of the same POCOP ligand are bound to two different Rh atoms. This rearrangement relieves the strain inherent in **P2** and leads to geometrically “normal” Rh(I) product. From the X-ray structure, it is clear that in order for **506** to form, the phosphinites must be able to rotate about the C-O bond. We surmised that if this movement could be restricted, it should prevent formation of **506** and preclude formation of a stable Rh(I) product after C(aryl)-C(vinyl) RE.

5.2.2.2 Synthesis of (^tBuPOCOP)Rh Complexes.

We envisioned that the analogous *tert*-butyl substituted ^tBuPOCOP ligand would provide just such a restriction and investigated the synthesis of (^tBuPOCOP)Rh(CHCH₂)(I) (**510**, Scheme 5-5). Synthesis of (^tBuPOCOP)Rh(H)(Cl) (**508**) proved much more straightforward than that of the corresponding (POCOP)Rh(H)(Cl) (**205**).¹⁰⁰ **508** formed in nearly quantitative yield by the reaction of (^tBuPOCOP)H (**507**) with [(cod)RhCl]₂ after 2 h at 100 °C and displayed a characteristic hydride resonance appearing as a doublet of triplets ($J_{\text{RhH}} = 44$ Hz, $J_{\text{PH}} = 13$ Hz) at -25.19 ppm in the ¹H NMR spectrum. There was no indication of the POCOP-bridged side product that plagued the reaction of (POCOP)H with [(cod)RhCl]₂.¹⁰⁰ Notably, that side product must require the POCOP ligand to contort in a similar fashion observed in **506**.



Scheme 5-5. Reactivity of $(^t\text{BuPOCOP})\text{Rh}$ in the direction of a rhodium vinyl fluoride complex.

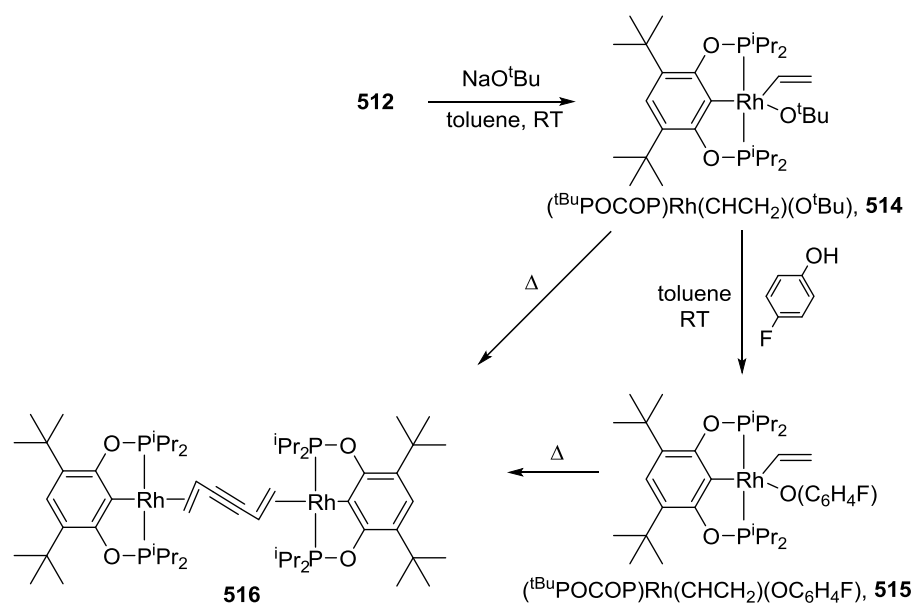
$(^t\text{BuPOCOP})\text{Rh}(\text{S}^i\text{Pr}_2)$ (**509**) was formed by reaction of **508** with NaO^tBu in the presence of S^iPr_2 . Treatment of **509** with vinyl iodide at RT resulted in an immediate color change to red and 95% conversion to $(^t\text{BuPOCOP})\text{Rh}(\text{CHCH}_2)(\text{I})$ (**510**) – a product analogous to **P2**. **510** was isolated as a red solid and displayed a doublet at 177.4 ppm with $J_{\text{RhP}} = 122$ Hz in the $^{31}\text{P}\{^1\text{H}\}$ NMR spectrum. The reaction consistently produced a side product *ca.* 5% at 204 ppm ($J_{\text{RhP}} = 155$ Hz) in the $^{31}\text{P}\{^1\text{H}\}$ NMR spectrum, which would be consistent with formation of Rh(I) olefin adduct. For example, the 1-hexene adduct of $(^t\text{BuPOCOP})\text{Rh}$ displays a doublet at 197.3 ppm with $J_{\text{RhP}} = 160$ Hz. We initially thought the impurity could be an equilibrium between the vinyl iodide olefin adduct and **510**. However, the reaction of $(^t\text{BuPOCOP})\text{Rh}(\text{CHCH}_2)(\text{OTf})$ (**511**), which is formed by treatment of **510** (*ca.* 95% purity) with AgOTf, with Me_3SiI resulted in clean conversion to **510** with no observation of the 5% impurity. The vinyl iodide was used as

received from the distributor with reported 95% purity, with no additional purification. Examination of the ^1H NMR spectrum vinyl iodide showed trace divinyl ether, which could be the olefin source for the 5% impurity.

Attempts to convert **511** to $(^t\text{BuPOCOP})\text{Rh}(\text{CHCH}_2)(\text{F})$ (**512**) were unsuccessful. Treatment of **512** with AgF in THF gave no reaction. The reaction of **512** with CsF in C_6D_6 after 24 h at RT resulted in complete conversion of **511** to a mixture of products. Analysis of the reaction mixture by ^{19}F NMR spectroscopy indicated P-F bond formation as evidenced by the presence of ^{19}F NMR resonances displaying very strong coupling to ^{31}P ($J_{\text{PF}} = 480 - 640$ Hz), but no signal attributable to a Rh-F bond. Former Ozerov group member Dr. Sylvain Gatard previously synthesized the unpublished $(\text{PNP})\text{Rh}(\text{Ph})(\text{F})$, which displayed $J_{\text{RhF}} = 136$ Hz. P-F bond formation has been observed previously with phosphine substituted Rh fluoride complexes, including the fluoride analogue of Wilkinson's catalyst.^{62e}

5.2.3 Attempted C-O Bond Formation

While this system was unsuccessful at forming C-F bonds, we thought it might be worthwhile to examine its potential for C-O bond formation. In this vein, we prepared two $(^t\text{BuPOCOP})\text{Rh}(\text{CHCH}_2)(\text{OR})$ ($\text{R} = ^t\text{Bu}, p\text{-C}_6\text{H}_4\text{F}$) complexes. $(^t\text{BuPOCOP})\text{Rh}(\text{CHCH}_2)(\text{O}^t\text{Bu})$ (**513**) was synthesized by reacting **511** with 1.2 equiv of NaO^tBu in toluene at RT and isolated in a 49% yield. $(^t\text{BuPOCOP})\text{Rh}(\text{CHCH}_2)(\text{OC}_6\text{H}_4\text{F})$ (**514**) was isolated in 68% yield from the reaction of **513** with 1 equiv $p\text{-FC}_6\text{H}_4\text{OH}$. **513** and **514** display doublets at 165.9 ppm ($J_{\text{RhP}} = 130$ Hz) and 169.2 ppm in by ^{31}P NMR spectroscopy, respectively.



Scheme 5-6. Reactivity of $(^t\text{BuPOCOP})\text{Rh}(\text{CHCH}_2)(\text{OR})$ complexes.

Independent thermolyses of **513** and **514** at 110 °C in toluene resulted in mixtures of products, however, both reactions formed the same major product as *ca.* 70% of the mixture. **513** also slowly decomposes to this mixture at RT. Neither reaction displayed resonances consistent with formation of the free or coordinated C-O RE product by ^1H NMR or ^{31}P NMR spectroscopy. The major product was isolated from the reaction mixtures and analyzed by ^1H NMR and ^{31}P NMR spectroscopy. Its ^1H NMR spectrum displayed no downfield vinylic proton resonances, indicating the absence of an η^1 -vinyl substituent. The spectrum also showed one aromatic resonance, corresponding to the C-H on the POCOP backbone, which indicated the $\text{OC}_6\text{H}_4\text{F}$ group was not present in the major product from the thermolysis of **514**. The product displayed an ABX pattern in the $^{31}\text{P}\{^1\text{H}\}$ NMR spectrum appearing as two doublets with $J_{\text{RhP}} = 158$ Hz at 197.6 ppm and 197.5 ppm. The side bands were not observed due to the close proximity of the

chemical shifts. The identity of the major product was determined to be the bridging divinylacetylene complex **515** by X-ray analysis of a single crystal grown from a saturated toluene solution at RT (Figure 5-2). The exact mechanism of how **515** forms is unclear.

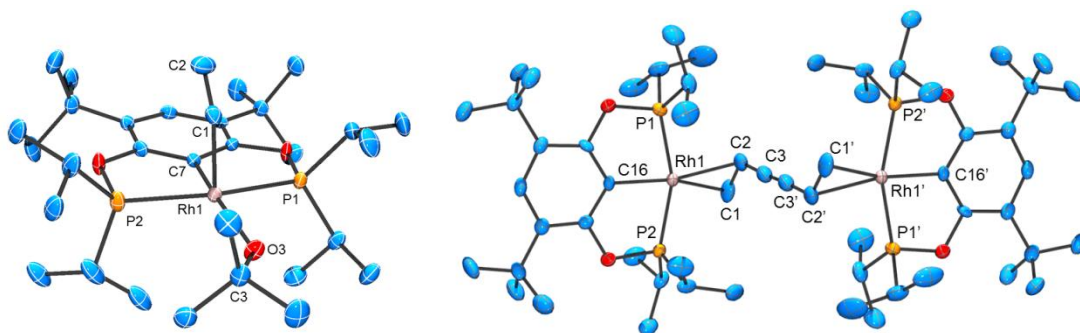


Figure 5-2. X-ray crystal structure of **513** and **515**.

5.3 Conclusion

The (POCOP)Rh and (^tBuPOCOP)Rh systems were unsuccessful for C-F bond formation. Both reactions suffered from dominating lower energy side processes, a problem that has plagued many metal systems. The (POCOP)Rh system underwent C-C RE with the aryl backbone of the pincer ligand, while the (^tBuPOCOP)Rh system underwent P-F bond formation. (^tBuPOCOP)Rh(CHCH₂)(OR) complexes were also examined for the ability to undergo C-O reductive elimination, but it was not observed.

5.4 Experimental

5.4.1 General Considerations

Unless otherwise specified, all manipulations were performed under an argon atmosphere using standard Schlenk line or glove box techniques. Toluene, THF, pentane, and isooctane were dried and deoxygenated (by purging) using a solvent purification system and stored over molecular sieves in an Ar-filled glove box. C₆D₆ and hexanes were dried over and distilled from NaK/Ph₂CO/18-crown-6 and stored over molecular sieves in an Ar-filled glove box. Fluorobenzene was dried with and then distilled or vacuum transferred from CaH₂. (POCOP)Rh(H)(Cl)¹⁰⁰ (**205**) was synthesized according to published procedures. All other chemicals were used as received from commercial vendors. NMR spectra were recorded on a Varian NMRS 500 (¹H NMR, 499.686 MHz; ¹³C NMR, 125.659 MHz, ³¹P NMR, 202.298 MHz, ¹⁹F NMR, 470.111 MHz) spectrometer. For ¹H and ¹³C NMR spectra, the residual solvent peak was used as an internal reference. ³¹P NMR spectra were referenced externally using 85% H₃PO₄ at δ 0 ppm. ¹⁹F NMR spectra were referenced externally using 1.0 M CF₃CO₂H in CDCl₃ at -78.5 ppm. Elemental analyses were performed by CALI Labs, Inc. (Parsippany, NJ).

5.4.2 Synthesis and Reactivity of Model Compounds

Synthesis of (POCOP)Rh(SⁱPr₂) (505). **205** (298 mg, 0.624 mmol), NaO^tBu (148 mg, 1.54 mmol), and SⁱPr₂ (82.4 μL, 0.624 mmol) were combined in a Schlenk flask and dissolved in toluene. The reaction underwent an immediate color change from light orange to a brown-yellow color stirring at RT. After stirring for 60 min at RT, the reaction was passed through a pad of Celite and the volatiles were removed by vacuum

to give a brown-yellow solid (294 mg, 84% yield). $^{31}\text{P}\{^1\text{H}\}$ NMR (C_6D_6): δ 184.8 (d, $J_{\text{Rh-P}} = 174$ Hz); ^1H NMR (C_6D_6): δ 6.99 (t, 1H, Ar-H, 7.5 Hz), 6.89 (d, 2H, Ar-H, 8.0 Hz), 2.70 (m, 2H, SCHMe₂), 2.20 (m, 4H, CHMe₂), 1.31 – 1.20 (m, 36H, CHMe₂); $^{13}\text{C}\{^1\text{H}\}$ NMR (C_6D_6): δ 167.7 (t, 8.4 Hz, Ar), 128.3 (s, Ar), 124.6 (s, Ar), 103.8 (t, 6.5 Hz, Ar), 40.8 (s, SCHMe₂), 30.5 (t, $J_{\text{P-C}} = 9.8$ Hz, CH(CH₃)₂), 30.4 (t, $J_{\text{P-C}} = 9.8$ Hz, CH(CH₃)₂), 24.0 (s, CHMe₂), 18.6 (t, $J_{\text{P-C}} = 4.1$ Hz, SCH(CH₃)₂), 17.5 (s, CHMe₂). Elem. Anal. Calc. for C₂₄H₄₅O₂P₂RhS: C, 51.24; H, 8.06. Found: C, 50.98; H, 7.97.

Reaction of 505 with CH₂CHI. **505** (110 mg, 0.20 mmol) was added to a J. Young tube and dissolved in C₆D₆. Vinyl iodide (15 μL , 0.21 mmol) was added to the solution, resulting in the immediate precipitation of a large amount of orange solid. Analysis of the solution after 24 h at RT by $^{31}\text{P}\{^1\text{H}\}$ NMR spectroscopy indicates no remaining (POCOP)Rh(SⁱPr₂) and several products. The major product (60%) appears as two sets of doublet of doublets (200.5 ppm, dd, $J_{\text{RhP}} = 140$ Hz, $J_{\text{PP}} = 473$ Hz; 163.7 ppm, dd, $J_{\text{RhP}} = 128$ Hz, $J_{\text{PP}} = 473$ Hz). There is no indication of the desired product, (POCOP)Rh(CHCH₂)(I) (**504**), by $^{31}\text{P}\{^1\text{H}\}$ NMR, which would be expected to display a doublet with a Rh-P coupling around 120 Hz. The sample was transferred to a Schlenk flask and the solvent was decanted off from the orange solid. The solid was washed with pentane and dried under vacuum. Analysis of the solid by $^{31}\text{P}\{^1\text{H}\}$ NMR identified the precipitate as the major product **506**. X-ray quality crystals of the solid were grown from a concentrated solution of the solid in toluene at RT. $^{31}\text{P}\{^1\text{H}\}$ NMR (CD_2Cl_2): δ 200.2 (dd, $J_{\text{RhP}} = 140$ Hz, $J_{\text{PP}} = 468$ Hz), 163.0 (dd, $J_{\text{RhP}} = 128$ Hz, $J_{\text{PP}} = 468$ Hz); ^1H NMR (CD_2Cl_2 , Figure 5-3): δ 6.99 (t, 7.5 Hz, 2H, POCOP), 6.77 (d, 9.0 Hz, 2H, POCOP), 6.63

(d, 9.0 Hz, 2H, POCOP), 5.41 (m, 2H, CHCH_2), 3.33 (m, 2H, CHCH_2), 3.22 (m, 2H, CHMe_2), 3.04 (m, 2H, CHMe_2), 2.85 (m, 2H, CHCH_2), 2.39 (m, 2H, CHMe_2), 1.68 (dd, 15 Hz, 7.5 Hz, 6H, CHMe_2), 1.59 (m, 12H, CHMe_2), 1.45 (m, 12H, CHMe_2), 1.18 (dd, 10 Hz, 7.0 Hz, 6H, CHMe_2), 1.08 (dd, 11 Hz, 7.5 Hz, 6H, CHMe_2), 1.00 (dd, 16 Hz, 7.0 Hz, CHMe_2). Elem. Anal. Calc. for $\text{C}_{40}\text{H}_{68}\text{I}_2\text{O}_4\text{P}_4\text{Rh}_2$: C, 40.15; H, 5.73. Found: C, 39.99; H, 5.59.

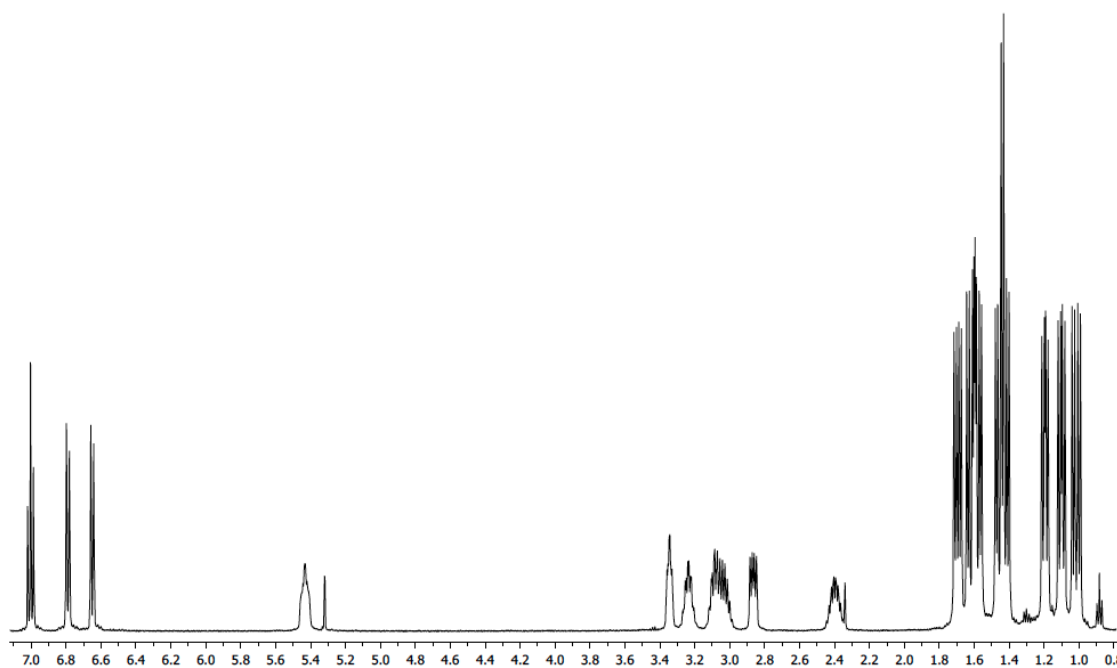


Figure 5-3. ^1H NMR spectrum of **506** in CD_2Cl_2 . Minor residual pentane and toluene present.

Synthesis of ($^t\text{BuPOCOP}$)H (507). 4,6-di-*tert*-butylresocinol (1.07 g, 4.8 mmol) was added to a reaction vial and dissolved in toluene. Et_3N (2.0 mL, 14.5 mmol) and

CIP^iPr_2 (1.51 mL, 10.1 mmol) were added to the solution and the reaction was heated at 110 °C for 24 h. The reaction was passed through a pad of Celite and the volatiles were removed by vacuum leaving an oily white solid. The solid was dissolved in a minimum of pentane and left at -35 °C. The product crashed out of solution as a crystalline white solid (1.0 g, 46%). $^{31}\text{P}\{^1\text{H}\}$ NMR (C_6D_6): δ 139.0 (s); ^1H NMR (C_6D_6 , Figure 5-4): 8.52 (t, 7.0 Hz, 1H, Ar-H), 7.46 (s, 1H, Ar-H), 1.83 (m, 4H, CHMe_2), 1.54 (s, 18H, ^tBu), 1.14 (dd, 7.5 Hz, 3.5 Hz, 12H, CHMe_2), 1.02 (dd, 7.5 Hz, 7.5 Hz, 12H, CHMe_2).

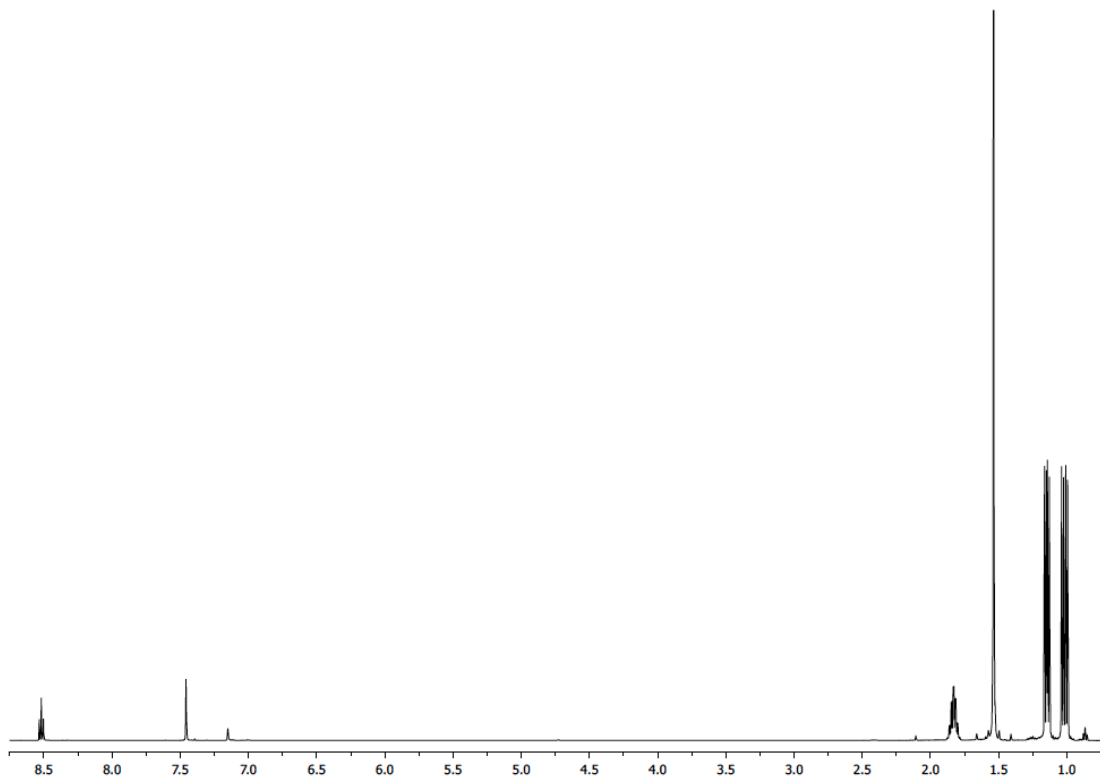


Figure 5-4. ^1H NMR spectrum of ($^t\text{BuPOCOP}$)H (**507**) in C_6D_6 .

Synthesis of (^tBuPOCOP)Rh(H)(Cl) (508). **507** (1.5 g, 3.3 mmol) was added to a reaction vial and dissolved in toluene. [(cod)RhCl]₂ (0.81 g, 1.6 mmol) was added to the solution and the reaction was stirred at 100 °C for 2 h. The solution was passed through a pad a Celite. The volatiles were removed by vacuum to give clean **508** as an orange solid (1.9 g, 95%). The product can be recrystallized from a saturated solution of toluene layered with pentane at -35 °C. ¹³P{¹H} NMR (C₆D₆): δ 184.4 (d, 122 Hz); ¹H NMR (C₆D₆, Figure 5-5): δ 7.22 (s, 1H, POCOP), 2.50 (m, 2H, CHMe₂), 2.10 (m, 2H, CHMe₂), 1.47 (s, 18H, ^tBu), 1.29 (q, 9.0 Hz, 6H, CHMe₂), 1.16 (q, 9.0 Hz, 6H, CHMe₂), 1.07 (m, 12H, CHMe₂), -25.19 (dt, J_{Rh-H} = 44 Hz, J_{P-H} = 13 Hz, 1H, Rh-H); ¹³C{¹H} NMR (C₆D₆): 162.3 (t, J_{PC} = 6.4 Hz), 130.5 (dt, J_{RhC} = 30 Hz, J_{PC} = 5.0 Hz), 127.6 (t, J_{PC} = 5.1 Hz), 122.0 (s), 34.7 (s, CMe₃), 30.4 (s, CMe₃), 30.0 (t, J_{PC} = 11 Hz, CHMe₂), 28.5 (td, J_{PC} = 14 Hz, J_{RhC} = 2.0 Hz, CHMe₂), 17.6 (s, CHMe₂), 17.4 (t, J_{PC} = 2.4 Hz, CHMe₂), 17.1 (t, J_{PC} = 4.4 Hz, CHMe₂), 16.8 (s, CHMe₂). Elem. Anal. Calc. for C₂₆H₄₈ClO₂P₂Rh: C, 52.66; H, 8.16. Found: C, 52.64; H, 8.20.

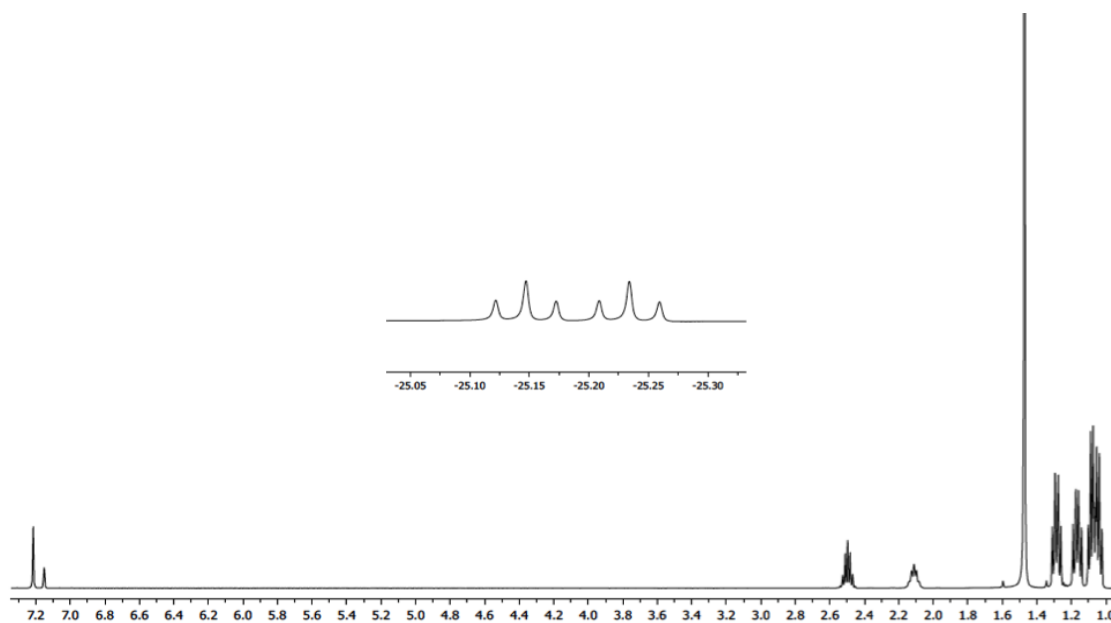


Figure 5-5. ^1H NMR spectrum of $(^t\text{BuPOCOP})\text{Rh}(\text{H})(\text{Cl})$ (**508**) in C_6D_6 .

Synthesis of $(^t\text{BuPOCOP})\text{Rh}(\text{S}^i\text{Pr}_2)$ (509**).** **508** (1.0 g, 1.7 mmol) was added to a Schlenk flask and dissolved in toluene. NaO^tBu (300 mg, 3.4 mmol) and S^iPr_2 (500 μL , 3.4 mmol) were added to the solution and the reaction was stirred for 1 h at RT. This resulted in an immediate color change to red-brown. The volatiles were removed by vacuum. The product was extracted with pentane and passed through a pad of Celite. The volatiles were removed by vacuum to give clean **509** as a brown-orange solid (1.1 g, 91%). $^{31}\text{P}\{^1\text{H}\}$ NMR (C_6D_6): δ 183.1 (d, 173 Hz); ^1H NMR (C_6D_6 , Figure 5-6): δ 7.24 (s, 1H, POCOP), 2.72 (m, 2H, CHMe_2), 2.20 (m, 2H, CHMe_2), 1.65 (s, 18H, ^tBu), 1.27 (m, 36H, CHMe_2 & S^iPr_2); $^{13}\text{C}\{^1\text{H}\}$ NMR (C_6D_6): δ 162.8 (t, $J_{\text{PC}} = 8.5$ Hz), 144.2 (dt, $J_{\text{RhC}} = 33$ Hz, $J_{\text{PC}} = 2.5$ Hz), 124.4 (t, $J_{\text{PC}} = 6.0$ Hz), 119.9 (s), 41.0 (t, $J_{\text{PC}} = 3.0$ Hz, SCHMe_2), 34.7 (s, CMe_3), 30.8 (s, CMe_3), 30.7 (td, $J_{\text{PC}} = 10$ Hz, $J_{\text{RhC}} = 3.0$ Hz, CHMe_2),

24.2 (s, SCHMe₂), 18.7 (t, J_{PC} = 3.5 Hz, CHMe₂), 17.8 (s, CHMe₂). Elem. Anal. Calc. for C₃₂H₆₁O₂P₂RhS: C, 56.96; H, 9.11. Found: C, 56.94; H, 9.08.

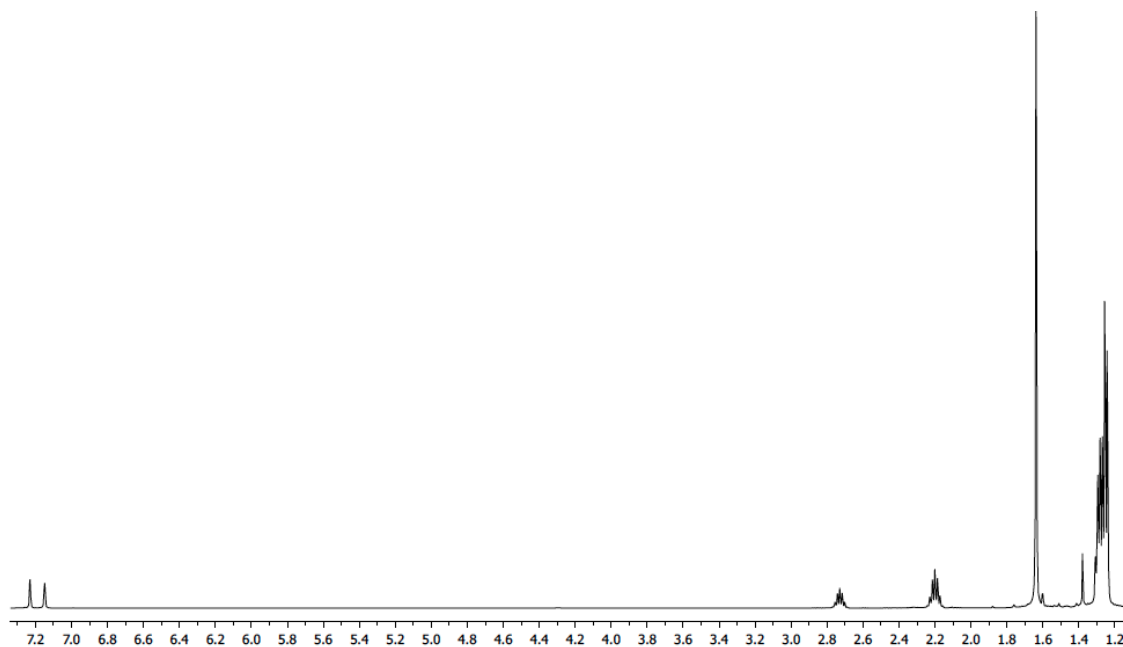


Figure 5-6. ¹H NMR spectrum of (^tBuPOCOP)Rh(SⁱPr₂) (**509**) in C₆D₆. Minor residual NaO^tBu present.

Synthesis of (^tBuPOCOP)Rh(CHCH₂)(I) (510**).** **509** (500 mg, 0.74 mmol) was added to a Schlenk flask and dissolved in toluene. Vinyl iodide (165 μL, 2.2 mmol) was added to the solution resulting in an immediate color change to red. The reaction was stirred for 20 min at RT. The solution was passed through a pad of Celite and the volatiles were removed by vacuum to give a red solid (489 mg, 93%). The red solid was 95% clean by ³¹P{¹H} NMR spectroscopy, with a minor impurity at 204 ppm (d, 155 Hz). The identity of the impurity is still unknown. ³¹P{¹H} NMR (C₆D₆): δ 177.4 (d, 122 Hz); ¹H NMR (C₆D₆, Figure 5-7): δ 7.30 (s, 1H, POCOP), 6.78 (d, 11 Hz, 1H, CHCH₂),

3.88 (s, 1H, CHCH₂), 3.79 (d, 14 Hz, 1H, CHCH₂), 2.65 (m, 4H, CHMe₂), 1.51 (s, 18H, ^tBu), 1.41 (q, 9.0 Hz, 6H, CHMe₂), 1.31 (q, 9.0 Hz, 6H, CHMe₂), 0.96 (q, 9.0 Hz, 6H, CHMe₂); ¹³C{¹H} NMR: δ 160.6 (t, J_{PC} = 5.9 Hz), 145.6 (d, J_{RhC} = 35 Hz, CHCH₂), 142.4 (dt, J_{RhC} = 34 Hz, J_{PC} = 10 Hz), 128.4 (s), 122.1 (d, J_{RhC} = 6.0 Hz, CHCH₂), 119.8 (t, J_{PC} = 4.4 Hz), 34.9 (s, CMe₃), 31.6 (t, J_{PC} = 11 Hz, CHMe₂), 30.4 (s, CMe₃), 28.6 (td, J_{PC} = 13 Hz, J_{RhC} = 2.0 Hz, CHMe₂), 18.3 (s, CHMe₂), 18.1 (s, CHMe₂), 17.8 (s, CHMe₂), 16.8 (s, CHMe₂).

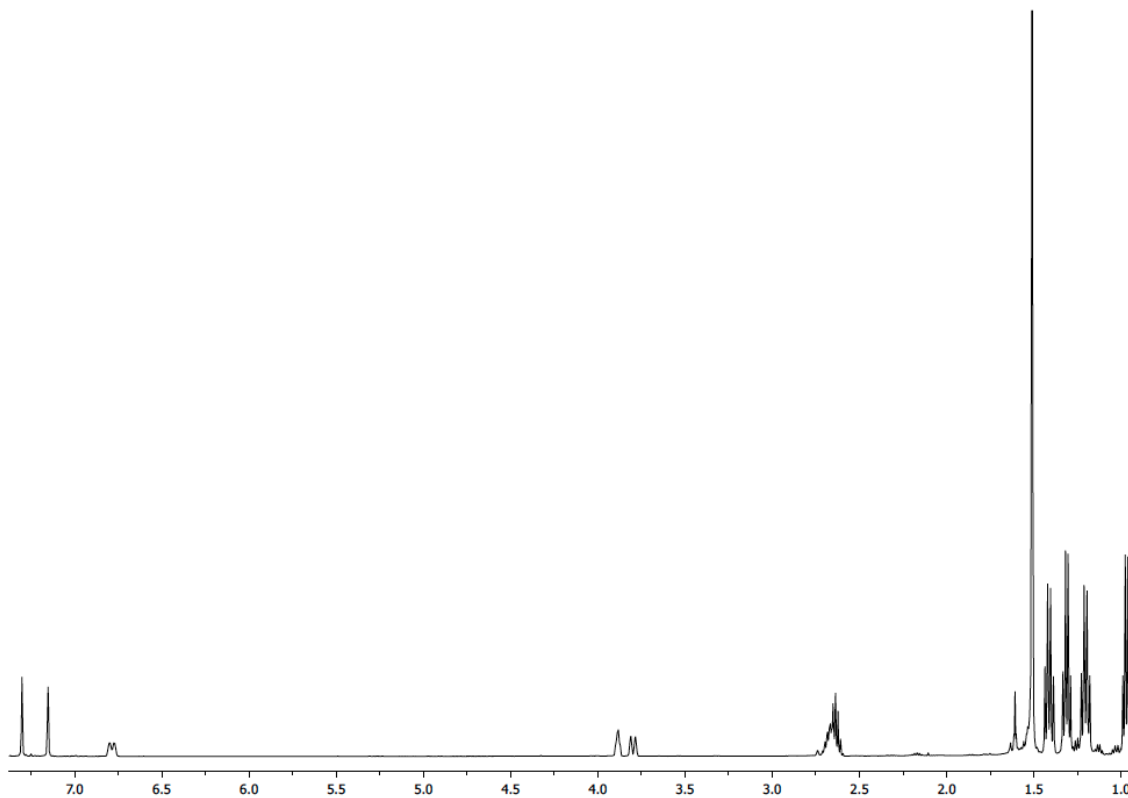


Figure 5-7. ¹H NMR spectrum of (^tBuPOCOP)Rh(CHCH₂)(I) (**510**) in C₆D₆.

Synthesis of (^tBuPOCOP)Rh(CHCH₂)(OTf) (511). **510** (101 mg, 0.15 mmol) was added a Schlenk flask and dissolved in toluene. AgOTf (46 mg, 0.18 mmol) was added to the sample resulting in immediate precipitation and a color change to brown. The sample was stirred at RT for 60 min. The volatiles were removed by vacuum. The product was extracted with pentane and passed through a pad of Celite. The volatiles were removed to give **511** as a brown-orange solid. ³¹P{¹H} NMR (C₆D₆): δ 173.0 (d, 126 Hz); ¹H NMR (C₆D₆, Figure 5-8): δ 7.25 (s, 1H, POCOP), 6.80 (d, 13 Hz, 1H, CHCH₂), 4.13 (m, 1H, CHCH₂), 3.94 (d, 13 Hz, 1H, CHCH₂), 2.66 (m, 2H, CHMe₂), 2.56 (m, 2H, CHMe₂), 1.43 (s, 18H, ^tBu), 1.21 (m, 12H, CHMe₂), 1.12 (q, 9.0 Hz, 6H, CHMe₂), 0.92 (q, 9.0 Hz, 6H, CHMe₂); ¹⁹F NMR (C₆D₆): δ -77.7 (s); ¹³C{¹H} NMR (C₆D₆): δ 162.0 (t, J_{PC} = 5.4 Hz), 140.2 (dt, J_{RhC} = 37 Hz, J_{PC} = 9.6 Hz, CHCH₂), 133.3 (dt, J_{RhC} = 40 Hz, J_{PC} = 5.1 Hz), 123.4 (s), 122.1 (s, CHCH₂), 118.1 (t, J_{PC} = 4.0 Hz), 34.8 (s, CMe₃), 30.9 (t, J_{PC} = 10 Hz, CHMe₂), 30.3 (s, CMe₃), 28.3 (td, J_{PC} = 13 Hz, J_{RhC} = 2.4 Hz, CHMe₂), 18.5 (t, J_{PC} = 3.0 Hz, CHMe₂), 18.1 (s, CHMe₂), 16.7 (t, J_{PC} = 2.2 Hz, CHMe₂), 16.1 (s, CHMe₂). Elem. Anal. Calc. for C₂₉H₅₀F₃O₅P₂RhS: C, 47.54; H, 6.88. Found: C, 47.60; H, 6.77.

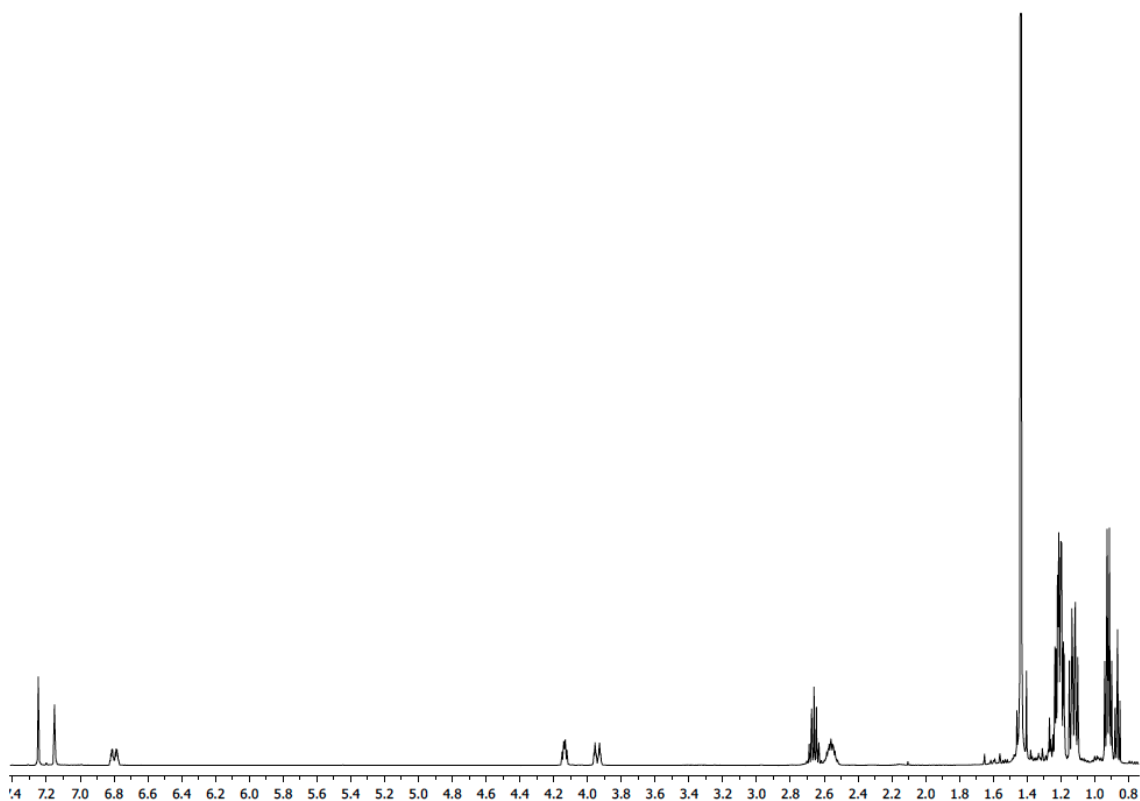


Figure 5-8. ^1H NMR spectrum of $(^t\text{BuPOCOP})\text{Rh}(\text{CHCH}_2)(\text{OTf})$ (**511**) in C_6D_6 . Minor residual pentane present.

Treatment of 511 with AgF. **511** (26 mg, 0.036 mmol) was added to a reaction vial and dissolved in THF. AgF (23 mg, 0.18 mmol) was added to the solution and the reaction was stirred overnight at RT. Analysis of the reaction by $^{31}\text{P}\{^1\text{H}\}$ NMR shows no reaction.

Treatment of 511 with CsF. **511** (33 mg, 0.045 mmol) was added to a Schlenk flask and dissolved in C_6D_6 . CsF (14 mg, 0.090 mmol) was added to the flask and the reaction was stirred at RT. After 24 h at RT, the reaction showed complete conversion to a mixture of new products by $^{31}\text{P}\{^1\text{H}\}$ NMR. Analysis of the ^{19}F NMR spectrum

indicates the presence P-F bond formation ($J = 639$ Hz and $J = 480$ Hz), but there are no signals indicating the formation of a Rh-F bond.

Synthesis of (^tBuPOCOP)Rh(CHCH₂)(O^tBu) (513). **511** (240 mg, 0.327 mmol) was combined with NaO^tBu (38 mg, 0.39 mmol) in a flask and dissolved in toluene. The reaction was stirred at RT for 60 min with no noticeable color change. The volatiles were removed by vacuum. The orange solid was extracted with pentane and passed through a pad of Celite. The volatiles were removed to yield an orange solid (154 mg, 72%). The solid was recrystallized from pentane at -35 °C to yield a crystalline orange solid (105 mg, 49%) and X-ray quality crystals. ³¹P{¹H} NMR (C₆D₆): 165.9 (d, $J_{\text{Rh-P}} = 130$ Hz); ¹H NMR (C₆D₆, Figure 5-9): 7.49 (m, 1H, CHCH₂), 7.22(s, 1H, POCOP), 4.54 (t, 5.5 Hz, 1H, CHCH₂), 3.93 (d, 14 Hz, 1H, CHCH₂), 2.58 (m, 2H, CHMe₂), 2.36 (m, 2H, CHMe₂), 1.57 (s, 27H, ^tBu and O^tBu), 1.32 (q, 8.0 Hz, 6H, CHMe₂), 1.25 (m, 12H, CHMe₂), 1.09 (q, 8.0 Hz, 6H, CHMe₂).

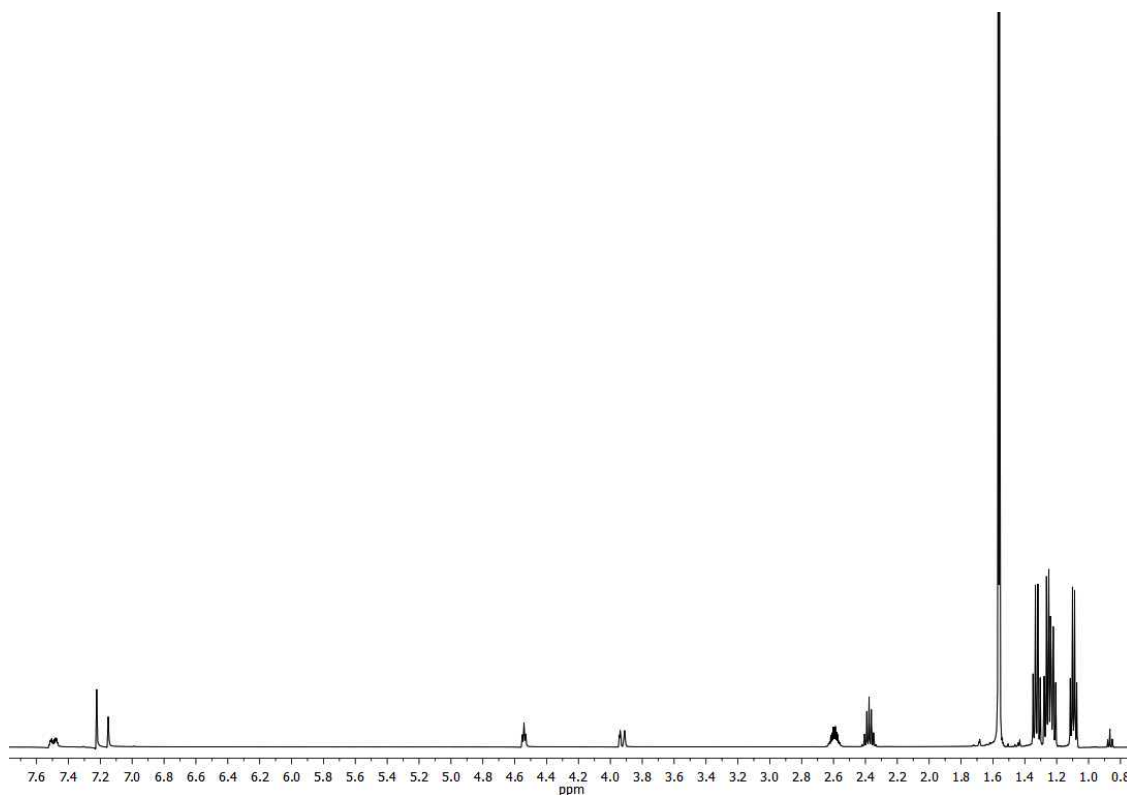


Figure 5-9. ^1H NMR spectrum of $(^t\text{BuPOCOP})\text{Rh}(\text{CHCH}_2)(\text{O}^t\text{Bu})$ (**513**) in C_6D_6 . Minor residual pentane present.

Thermolysis of 513. $(^t\text{BuPOCOP})\text{Rh}(\text{CHCH}_2)(\text{O}^t\text{Bu})$ (23 mg, 0.035 mmol) was added to a J. Young tube and dissolved in C_6D_6 . The sample was heated in a $110\text{ }^\circ\text{C}$ oil bath and monitored by $^{31}\text{P}\{^1\text{H}\}$ NMR and ^1H NMR spectroscopy. After 30 min at $110\text{ }^\circ\text{C}$, the reactions showed complete conversion from the starting material to three new compounds, with a major compound making up 70% of the reaction mixture. The ^1H NMR spectrum no longer displayed any downfield vinyl resonances, indicating there were no longer any η^1 vinyl complexes present in the mixture. Additional heating at $110\text{ }^\circ\text{C}$ for 24 h resulted in the presence of a new compound at 204.4 ppm (d, $J = 154.3\text{ Hz}$, 5%) in the $^{31}\text{P}\{^1\text{H}\}$ NMR spectrum, however the fraction of the major product was

unchanged (70%). The reaction was passed through a pad of Celite and the volatiles were removed by vacuum. The brown-orange solid was washed with pentane leaving a bright orange solid. Analysis of the solid by $^{31}\text{P}\{^1\text{H}\}$ NMR and ^1H NMR showed only the presence of the major product, identified as **515**. The $^{31}\text{P}\{^1\text{H}\}$ NMR spectrum displays the complex as two doublets with the same Rh-P coupling constant ($J = 157.7$ Hz). X-ray quality crystals of the solid were grown from a concentrated toluene solution at RT. The identity of the side products could not be determined.

Synthesis of (^tBuPOCOP)Rh(CHCH₂)(OC₆H₄F) (514). **513** (43 mg, 0.065 mmol) was added to a Schlenk flask and dissolved in toluene. HO(*p*-C₆H₄F) (7.4 mg, 0.065 mmol) was added to sample and the reaction was stirred for 30 min at RT. The reaction was passed through a pad of Celite and the volatiles were removed by vacuum to give a red solid. The solid was recrystallized from pentane at -35 °C to give a red crystalline product (31 mg, 68%). $^{31}\text{P}\{^1\text{H}\}$ NMR (C₆D₆): δ 169.2 (d, $J = 128.2$ Hz); ^1H NMR (C₆D₆, Figure 5-10): δ 7.29 (d, 13 Hz, 1H, CHCH₂), 7.24 (s, POCOP), 7.02 (t, 9.5 Hz, 2H, Ar), 6.71 (m, 2H, Ar), 4.45 (t, 6.0 Hz, 1H, CHCH₂), 4.02 (d, 13 Hz, 1H, CHCH₂), 2.48 (m, 2H, CHMe₂), 2.22 (m, 2H, CHMe₂), 1.51 (s, tBu), 1.14 (q, 7.5 Hz, 6H, CHMe₂), 1.07 (q, 7.5 Hz, 6H, CHMe₂), 1.03 (q, 7.5 Hz, 6H, CHMe₂), 0.99 (q, 7.5 Hz, 6H, CHMe₂); ^{19}F NMR (C₆D₆): δ -133.4 (s); $^{13}\text{C}\{^1\text{H}\}$ NMR (C₆D₆): δ 161.4 (t, $J_{\text{PC}} = 6.0$ Hz), 154.4 (d, $J_{\text{FC}} = 230$ Hz, CF), 140.2 (dt, $J_{\text{RhC}} = 36$ Hz, $J_{\text{PC}} = 11$ Hz), 138.9 (d, $J_{\text{RhC}} = 33$ Hz), 121.8 (s), 119.0 (s), 118.9 (s), 118.6 (t, $J_{\text{PC}} = 4.6$ Hz), 115.5 (s), 115.4 (s), 34.8 (s, CMe₃), 30.8 (t, $J_{\text{PC}} = 9.5$ Hz, CHMe₂), 30.4 (s, CMe₃) 28.4 (td, $J_{\text{PC}} = 15$ Hz, $J_{\text{RhC}} = 2.5$ Hz, CHMe₂), 18.6 (s, CHMe₂), 17.1 (t, $J_{\text{PC}} = 3.8$ Hz, CHMe₂), 16.7 (t, $J_{\text{PC}} = 2.0$ Hz,

CHMe₂), 16.2 (s). Elem. Anal. Calc. for C₃₄H₅₄FO₃P₂Rh: C, 58.79; H, 7.84. Found: C, 58.76; H, 7.79.

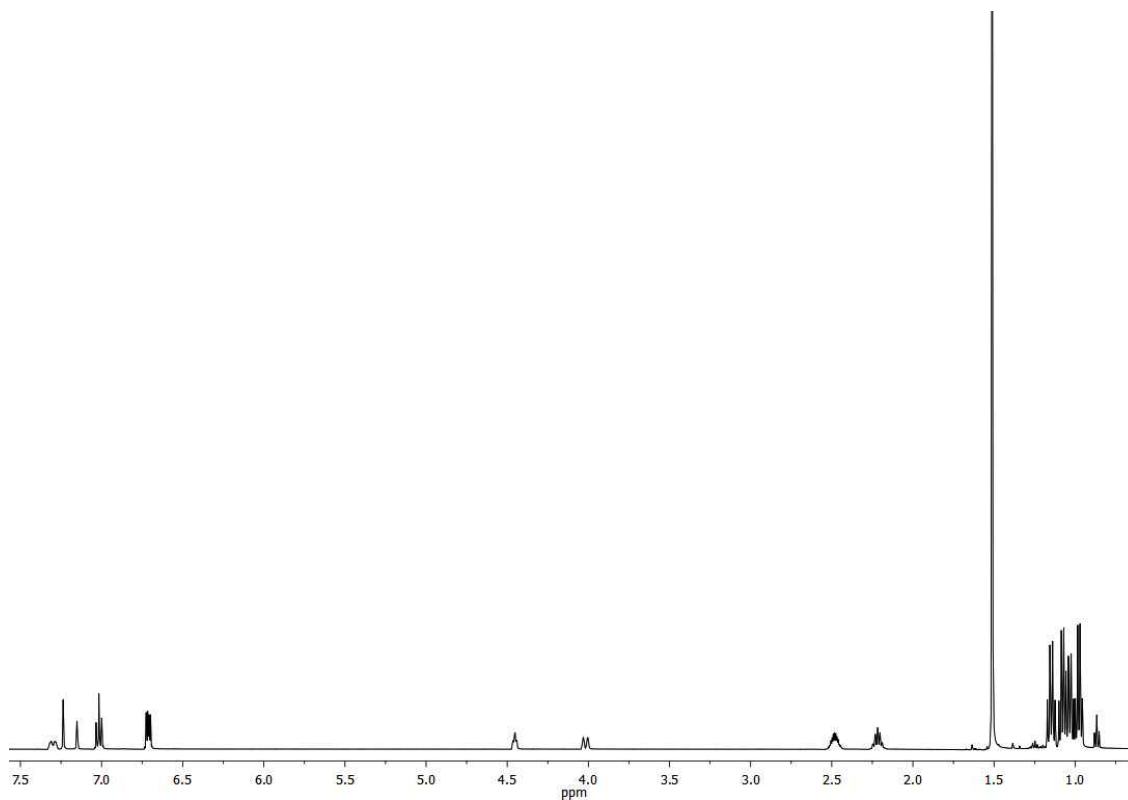


Figure 5-10. ¹H NMR spectrum of (^tBuPOCOP)Rh(CHCH₂)(*p*-OC₆H₄F) (**514**) in C₆D₆. Minor residual pentane present.

Thermolysis of 514. **514** (14 mg, 0.020 mmol) was added to a J. Young tube and dissolved in C₆D₆. The sample was heated in a 110 °C oil bath and monitored by ³¹P{¹H} NMR and ¹H NMR spectroscopy. Analysis of the ³¹P{¹H} NMR spectrum after 60 min indicates 30% conversion to two major products (197.5 ppm, d, J = 157.7 Hz, 17%; 183.9 ppm, d, J = 205.4 Hz, 15%). After 24 h at 110 °C, the reaction displayed complete conversion from the starting material and the presence of four products by

$^{31}\text{P}\{^1\text{H}\}$ NMR spectroscopy. The major product (197.5 ppm, d, $J = 157.7$ Hz, 70%) is the same major product from the thermolysis of $(^t\text{BuPOCOP})\text{Rh}(\text{CHCH}_2)(\text{O}^t\text{Bu})$, identified as **515**. The identity of the side products could not be determined.

5.4.3 X-ray Crystallography

X-Ray data collection, solution, and refinement for 506. (Solved by Dr. Nattamai Bhuvanesh.) A Leica MZ 7s microscope was used to identify a orange block with very well defined faces with dimensions (max, intermediate, and min) 0.10 mm x 0.09 mm x 0.02 mm from a representative sample of crystals of the same habit. The crystal mounted on a nylon loop was then placed in a cold nitrogen stream (Oxford) maintained at 110 K. A BRUKER GADDS X-ray (three-circle) diffractometer was employed for crystal screening, unit cell determination, and data collection. The goniometer was controlled using the FRAMBO software, v.4.1.05.¹⁴⁰ The sample was optically centered with the aid of a video camera such that no translations were observed as the crystal was rotated through all positions. The detector was set at 5.0 cm from the crystal sample. The X-ray radiation employed was generated from a Cu sealed X-ray tube ($K_{\alpha} = 1.5418$ Å with a potential of 40 kV and a current of 40 mA) fitted with a graphite monochromator in the parallel mode (175 mm collimator with 0.5 mm pinholes). 180 data frames were taken at widths of 0.5° . These reflections were used to determine the unit cell using Cell_Now.¹⁴¹ The unit cell was verified by examination of the $h k l$ overlays on several frames of data. No super-cell or erroneous reflections were observed. After careful examination of the unit cell, an extended data collection procedure (10 sets) was initiated using omega and phi scans. Integrated intensity

information for each reflection was obtained by reduction of the data frames with APEX2.¹⁴² The integration method employed a three dimensional profiling algorithm and all data were corrected for Lorentz and polarization factors, as well as for crystal decay effects. Finally the data was merged and scaled to produce a suitable data set. SADABS⁸⁸ was employed to correct the data for absorption effects. Systematic reflection conditions and statistical tests indicated the space group $P2_1/c$. A solution was obtained readily using SHELXTL (SHELXS).⁸⁹ Hydrogen atoms were placed in idealized positions and were refined using riding model. All non-hydrogen atoms were refined with anisotropic thermal parameters. The structure was refined (weighted least squares refinement on F^2) to convergence.⁸⁹ PLATON⁹⁰ was used to verify the absence of additional symmetry. However, it suggested presence of voids (86 \AA^3 , with $26 e^-$ /unit cell). We could not locate any solvent from the residual electron density probably due to partial occupancy and/or disorder. Also, our trials to SQUEEZE the solvent using PLATOON did not improve the reliability factors.

X-Ray data collection, solution, and refinement for (^tBuPOCOP)Rh(CHCH₂)(O^tBu) (513). A single red crystal of suitable size and quality ($0.60 \times 0.18 \times 0.05 \text{ mm}$) was selected from a representative sample of crystals of the same habit using an optical microscope, mounted onto a nylon loop and placed in a cold stream of nitrogen (110 K). Low-temperature X-ray data were obtained on a Bruker APEXII CCD based diffractometer (Mo sealed X-ray tube, $K_{\alpha} = 0.71073 \text{ \AA}$). All diffractometer manipulations, including data collection, integration and scaling were carried out using the Bruker APEXII software.⁸⁸ An absorption correction was applied

using SADABS.⁸⁸ The space group was determined on the basis of systematic absences and intensity statistics and the structure was solved by direct methods and refined by full-matrix least squares on F^2 . The structure was solved in the monoclinic $P 2_1/n$ space group using XS.⁸⁹ This symmetry was confirmed by PLATON.⁹⁰ All non-hydrogen atoms were refined with anisotropic thermal parameters. Hydrogen atoms were placed in idealized positions and refined using riding model. The structure was refined (weighted least squares refinement on F^2) to convergence. The disorder about the isopropyl groups on P2 was modeled. The P-C and C-C bond lengths of the isopropyl groups were restrained with SADI. The thermal parameters of the carbon atoms of the isopropyl groups were restrained using EADP.

X-Ray data collection, solution, and refinement for 515. A single orange crystal of suitable size and quality ($0.36 \times 0.20 \times 0.12$ mm) was selected from a representative sample of crystals of the same habit using an optical microscope, mounted onto a nylon loop and placed in a cold stream of nitrogen (110 K). Low-temperature X-ray data were obtained on a Bruker APEXII CCD based diffractometer (Mo sealed X-ray tube, $K_\alpha = 0.71073$ Å). All diffractometer manipulations, including data collection, integration and scaling were carried out using the Bruker APEXII software.⁸⁸ An absorption correction was applied using SADABS.⁸⁸ The space group was determined on the basis of systematic absences and intensity statistics and the structure was solved by direct methods and refined by full-matrix least squares on F^2 . The structure was solved in the monoclinic $P 2_1/n$ space group using XS⁸⁹ (incorporated in X-Seed). One half of the bridged dimer was symmetry generated. This symmetry was confirmed by

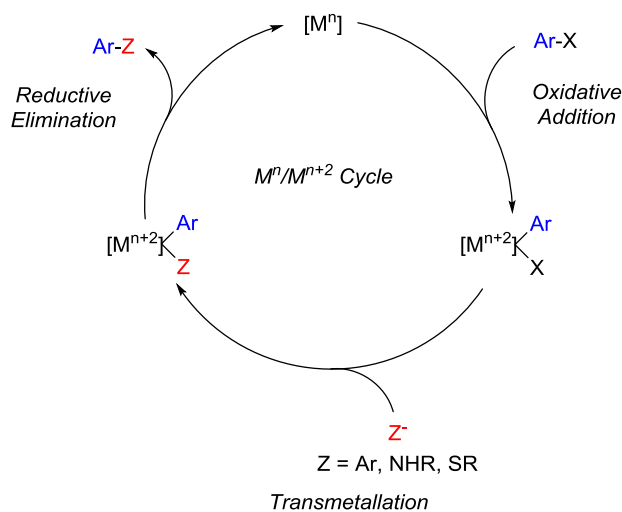
PLATON.⁹⁰ All non-hydrogen atoms were refined with anisotropic thermal parameters. Hydrogen atoms were placed in idealized positions and refined using riding model. The structure was refined (weighted least squares refinement on F^2) to convergence.

CHAPTER VI

SYNTHESIS AND REACTIVITY OF (POCOP)CO COMPLEXES

6.1 Introduction

The scope and applicability of transition metal catalyzed coupling reactions has continually increased. These reactions are typically catalyzed by second and third row platinum group metals.⁵ Palladium^{3,77,92,143} is the most commonly used metal for these transformations, but the group 9 metal Rh^{55a-f,56,58-59,100,144} has also had success in this arena. The use of the pincer ligated (POCOP)Rh system for C-C, C-N, and C-S coupling reactions was described in Chapter II, III, and IV, respectively. The success of second and third row transition metals is based in their ability to undergo two-electron reactivity, which is critical for the bond-breaking (oxidative addition) and bond-making (reductive elimination) steps in these processes (Scheme 6-1).

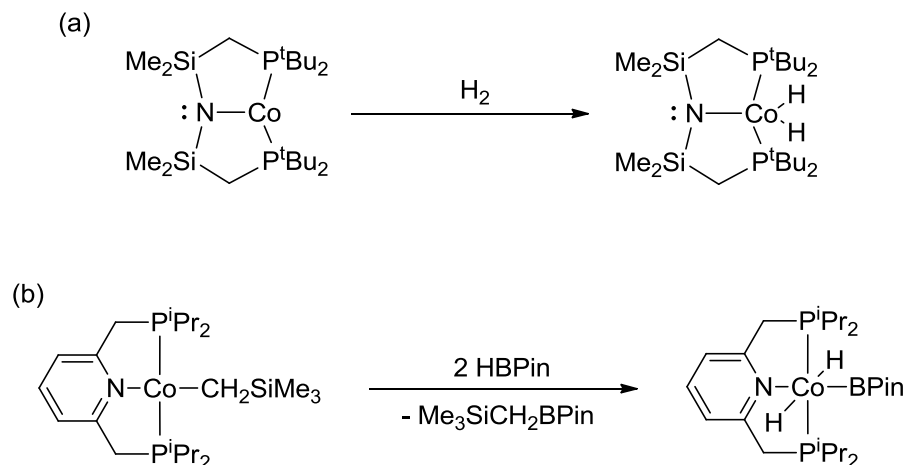


Scheme 6-1. General M^n/M^{n+2} for transition metal catalyzed coupling reactions between aryl halides with nucleophiles.

In recent years there has been an increased emphasis on moving towards more Earth abundant first row transition metals such as iron and cobalt due to their low cost and potential environmental advantages. However, the proclivity of first-row transition metals to undergo one-electron transformations has limited their success for coupling reactions with a M^n/M^{n+2} type cycle similar to Pd and Rh (Scheme 6-1). The Chirik group¹⁴⁵ and others¹⁴⁶ have managed to circumvent this issue with Fe and Co with the use of redox non-innocent ligands, such as bisiminopyridine ligands. These ligands allow for net two-electron processes to occur, by enabling cooperative metal ligand redox events.

Cobalt halides have previously been shown to catalyze coupling reactions including C-C and C-S coupling reactions, in which a Co^I/Co^{III} cycle is invoked with concerted reductive elimination (RE) as the product-forming step.^{114,147} However, mechanistic evidence or isolation of proposed intermediates has not been reported to support these claims. We were hopeful that the use of pincer ligands could help isolate potential Co(I) and Co(III) complexes that would allow for direct observation of the two-electron reactions composing an analogous synthetic cycle. In 2006, Caulton reported the isolation of the unsaturated three-coordinate $PN^{Si}P$ pincer supported Co(I) complex, which underwent concerted H_2 oxidative addition (OA) to form $(PN^{Si}P^{tBu})Co(H)_2$ (Scheme 6-2, a).¹⁴⁸ The Chirik group also reported H_2 as well as C-H OA to pyridine based $(PN^{py}P)Co^I$ complexes.¹⁴⁹ Chirik's $(PN^{py}P)Co$ system was also recently shown to catalyze C-H borylation of arenes, which they propose operates via a $Co(I)/Co(III)$ cycle.¹⁵⁰ Investigation of the proposed mechanism resulted in isolation of the 6-

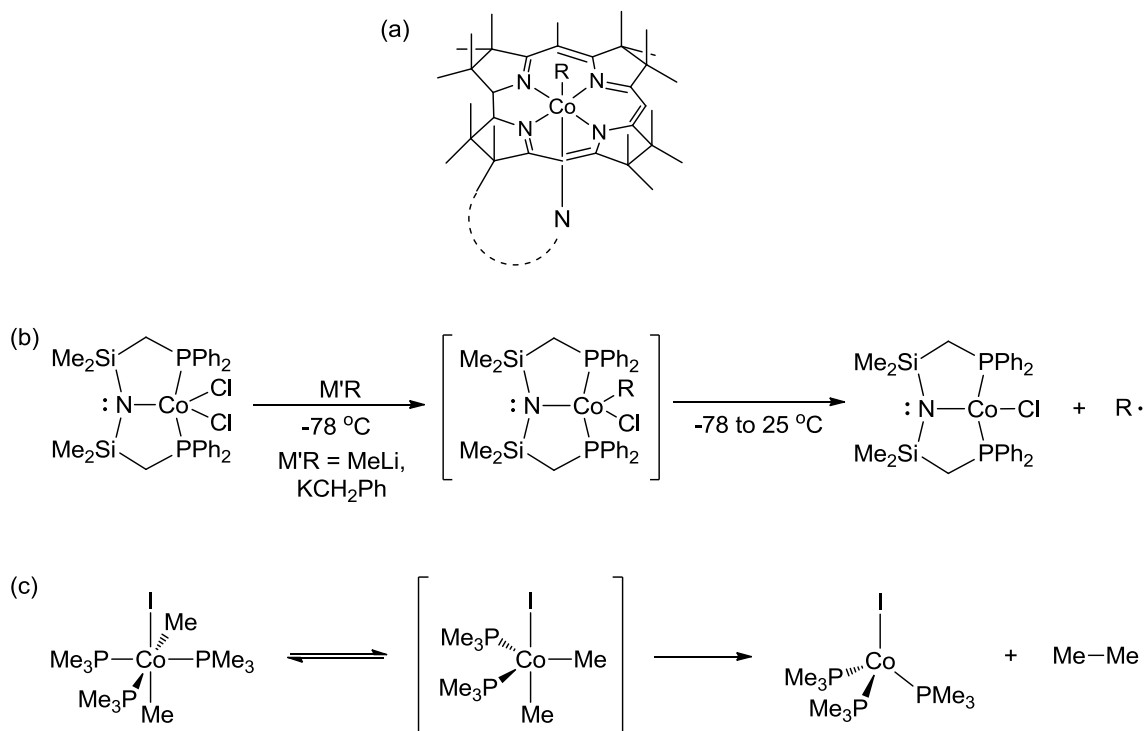
coordinate Co(III) (PN^{py}P)Co(H)₂(BPin) (Scheme 6-2, b). These results are promising towards the use of pincer ligands to help promote two-electron reactivity between Co(I) and Co(III) oxidation states.



Scheme 6-2. (a) Oxidative addition of H₂ to (PN^{Si}P^{tBu})Co. (b) Formation of (PN^{py}P)Co(H)₂(BPin).

We were particularly interested in studying the potential of pincer supported Co(III) complexes to undergo RE. Examples of RE from Co(III) are scarce due to the prevalence of these compounds to undergo single-electron transformations.¹⁵¹ Homolytic elimination of carbon radicals from Co(III) has been studied since the discovery that the vitamin B₁₂ active site (Scheme 6-3, a) contains a homolyzable Co(III)-carbon bond.^{152,153} Fryzuk reported elimination of methyl and benzyl radicals from a five-coordinate pincer supported Co^{III}(R)(X) complex supported by the phenyl analogue of the PN^{Si}P ligand used by Caulton (Scheme 6-3, b).¹⁵⁴ In 2011, Bernskoetter and coworkers reported ethane formation from thermolysis of (PMe₃)₃Co(CH₃)₂(I) (Scheme

6-3, c) *via* concerted RE.¹⁵⁵ Analogous to RE from other d^6 group 9 complexes,³⁹ the complex must first undergo phosphine dissociation to give the five-coordinate $(\text{PMe}_3)_2(\text{I})\text{Co}(\text{CH}_3)_2$ complex before RE can occur.



Scheme 6-3. (a) Active core of the vitamin B12. (b) Radical elimination from $(\text{PN}^{\text{Si}}\text{P}^{\text{Ph}})_2\text{Co}(\text{R})(\text{Cl})$. (c) Concerted C-C reductive elimination from $(\text{PMe}_3)_3\text{Co}(\text{I})(\text{Me})_2$.

We decided to utilize the bisphosphinite POCOP ligand based on our previous success with Rh, which demonstrated multiple catalytic and stoichiometric coupling reactions including C-C, C-N, and C-S coupling.¹⁰⁰ We also thought the strong field character of the aryl donor of POCOP would help stabilize low-spin 5-coordinate Co(III) complexes and decrease their potential to convert to more stable Co(II) complexes. The

use of strong field ligands to help stabilize low-spin complexes of first-row transition metals, including Co, has been successfully reported.^{146b,156} Lippard et. al previously described the synthesis of a series 5-coordinate Co(III) complexes using the macrocyclic tetradentate tropocoronand ligand (Figure 6-1).¹⁵⁷ Isolation of both 5-coordinate chloride and alkyl analogues revealed the chloride complexes to be paramagnetic at RT, while the alkyl substituted analogues were diamagnetic. This difference was attributed the strong Co-C σ -interaction with the strong-field alkyl ligands.

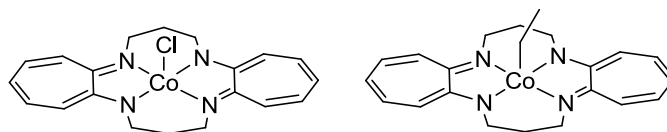


Figure 6-1. Examples of isolated five-coordinate Co(III) complexes.

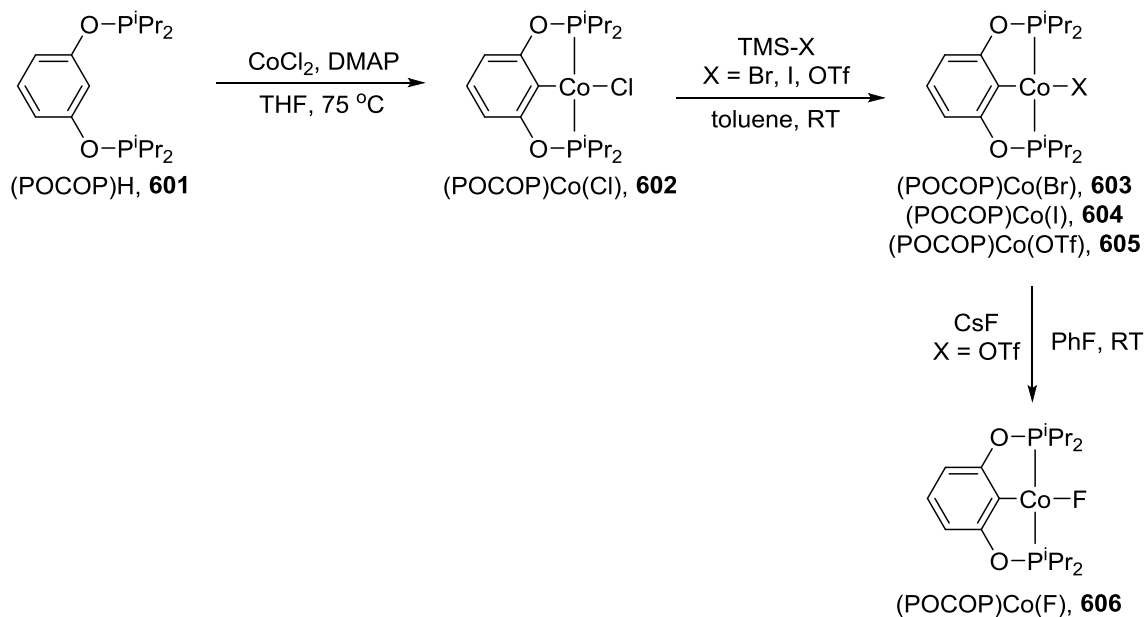
6.2 Results and Discussion

6.2.1 Synthesis of (POCOP)Co^{II} Complexes

6.2.1.1 Synthesis of (POCOP)Co(X) (X = halide) Compounds

A series of (POCOP)Co^{II} halide and pseudohalide complexes were synthesized as synthetic precursors (Scheme 6-4). The reaction of (POCOP)H (**601**) with anhydrous CoCl₂ in the presence of dimethylaminopyridine (DMAP) resulted in isolation of (POCOP)Co(Cl) (**602**) as a bright yellow solid in 35% yield (unoptimized yield). **602** was converted to the analogous (POCOP)Co(Br) (**603**), (POCOP)Co(I) (**604**), and (POCOP)Co(OTf) (**605**) by treatment with the corresponding Me₃SiX (X = Br, I, OTf) reagents. Each compound formed immediately at RT and displayed broad signals outside

the standard diamagnetic region of the ^1H NMR spectrum. $(\text{POCOP})\text{Co}(\text{F})$ (**606**) was synthesized by the reaction of **605** with CsF at RT.



Scheme 6-4. Synthesis of $(\text{POCOP})\text{Co}(\text{X})$ ($\text{X} = \text{Cl}, \text{Br}, \text{I}, \text{OTf}, \text{F}$) complexes.

602-605 were each identified using ^1H NMR spectroscopy based on interpretation of the peak integrations. In 2011, Hebden et. al reported the synthesis of the analogous square-planar *tert*-butyl substituted $(\text{POCOP}^{\text{tBu}})\text{Co}(\text{I})$ and described the use of ^1H NMR spectroscopy for analysis.¹⁵⁸ Analysis of $\text{Co}(\text{II})$ compounds by ^1H NMR spectroscopy is limited to low-spin $\text{Co}(\text{II})$ complexes. Isolation of high-spin tetrahedral $\text{Co}(\text{II})$ complexes of $(\text{PN}^{\text{Si}}\text{P}^{\text{Ph}})\text{Co}(\text{halide})$ by Fryzuk and coworkers did not give ^1H NMR spectra that could be interpreted for complete analysis; however, the corresponding low-spin square-planar $(\text{PN}^{\text{Si}}\text{P}^{\text{Ph}})\text{Co}(\text{alkyl})$ complexes produced ^1H NMR spectra in which all proton resonances could be assigned.¹⁵⁴ **602-605** displayed similar ^1H NMR spectra to

each other with five broad signals with integral ratios of 12:12:4:2:1, consistent with formation of paramagnetic Co(II) complexes (Figure 6-2). The peaks integrating to 12 and 4 correlate to the methyl and methine protons of the isopropyl groups, respectively; and the resonances integrating 2 and 1 correspond with the aromatic protons of the aryl backbone. The symmetry observed (1 methine with 2 methyl resonances) supports a square planar four-coordinate C_{2v} symmetric complex, consistent with what has been observed both spectroscopically and structurally with similar compounds.

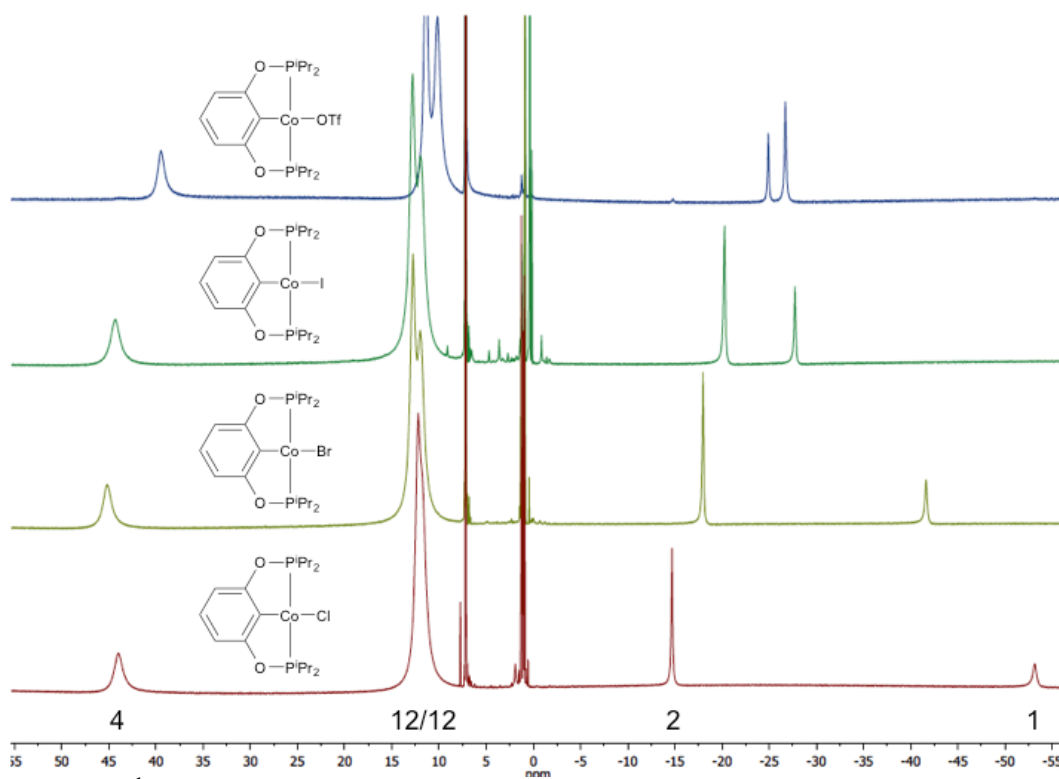
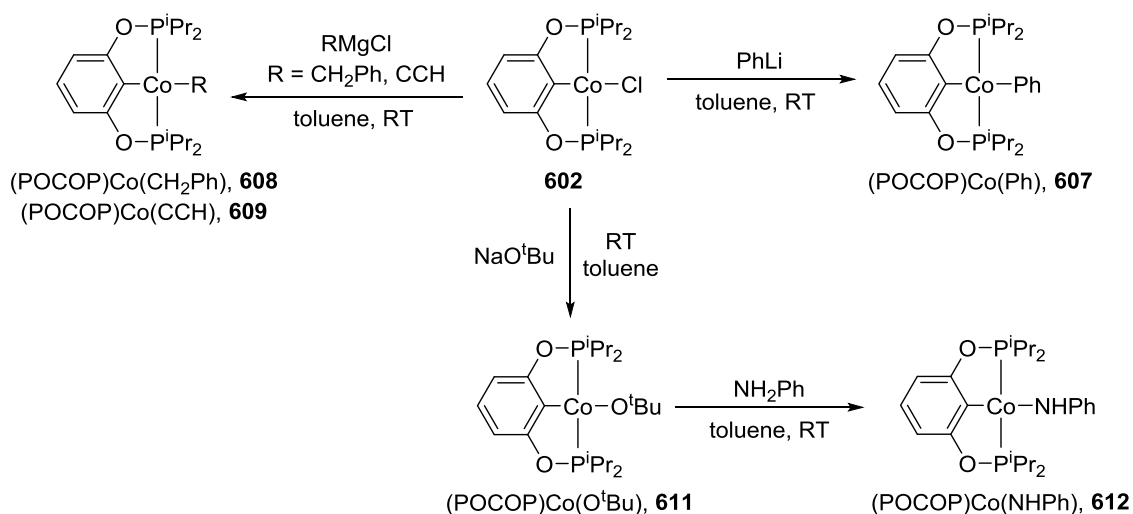


Figure 6-2. ^1H NMR spectrum of (POCOP)Co(Cl) (**602**), (POCOP)Co(Br) (**603**), (POCOP)Co(I) (**604**), and (POCOP)Co(OTf) (**605**). The values below the spectra correspond to the peak integration.

6.2.1.2 Synthesis of (POCOP)Co(R) Compounds

With (POCOP)Co(X) precursors in hand, we were able to synthesize a series of (POCOP)Co^{II} hydrocarbyl complexes by salt metathesis with lithium and Grignard reagents (Scheme 6-5). (POCOP)Co(Ph) (**607**) was isolated in 81% yield as a dark green solid by treatment of **602** with PhLi at RT. (POCOP)Co(CH₂Ph) (**608**) and (POCOP)Co(CCH) (**609**) were synthesized from the reaction between **602** and the corresponding Grignard reagent and were isolated 55% and 89% yield, respectively. **607–609** each displayed a paramagnetic ¹H NMR spectrum and had integral ratios consistent with formation of a C_{2v} symmetric (POCOP)Co^{II} complex, consistent with previously reported (PN^{Si}P^{Ph})Co^{II} alkyl complexes.



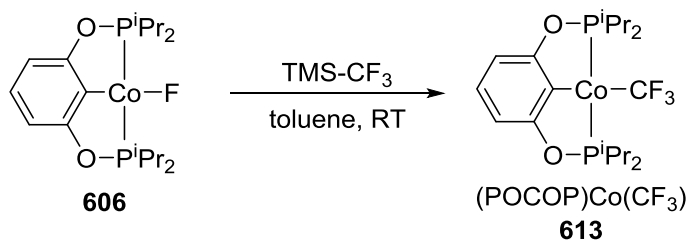
Scheme 6-5. Synthesis of (POCOP)Co(R) (R = hydrocarbyl, O^tBu, NHPh) compounds.

The reaction between **602** and vinyl Grignard was less straightforward. Treatment of **602** with 1.1 equiv (CH₂CH)MgCl (1.6 M in THF) resulted in

approximately 30% conversion from the starting material to a new paramagnetic product. When **602** was treated with 4 equiv of (CH₂CH)MgCl, the reaction showed complete disappearance of **602** in the ¹H NMR spectrum, and a complex array of singlets in the ³¹P{¹H} NMR spectrum. A single pentane-soluble diamagnetic product was isolated from the product mixture that displayed a broad singlet at 207.7 ppm in the ³¹P{¹H} NMR spectrum. Analysis of the ¹H NMR spectrum showed a product with a 1:2 ratio of ligand to vinylic protons, indicating two CHCH₂ groups per Co complex. Treatment of the solution with CO resulted in quantitative conversion to (POCOP)Co(CO) (**610**) and free 1,3-butadiene, which is indicative of the diamagnetic complex being a (POCOP)Co complex of 1,3-butadiene. The exact structure of the diamagnetic product is still under investigation and efforts are currently being made to isolate a single crystal of the complex for X-ray analysis.

The (POCOP)Co^{II} anilido complex (POCOP)Co(NHPh) (**612**) was synthesized by deprotonation of aniline with (POCOP)Co(O^tBu) (**611**) (Scheme 6-5). **611** was synthesized by the reaction of **602** with NaO^tBu at RT and isolated as an orange solid in 63% yield. **611** displayed broad resonances in the ¹H NMR spectrum with integral ratios consistent with the pincer framework as well as a diagnostic broad *tert*-butoxide signal integrating to 9 protons at -9.88 ppm. Treatment of **611** with NH₂Ph resulted in an immediate color change from orange to purple and formation of **612**. **612** was isolated as a purple solid in 59% yield and displayed an ¹H NMR spectrum with broad resonances with integral ratios characteristic of a paramagnetic (POCOP)Co^{II} complex containing the anilido functionality.

The trifluoromethyl complex (POCOP)Co(CF₃) (**613**) was isolated in 97% yield by treatment of **606** with Me₃SiCF₃ (Scheme 6-6). The ¹H NMR spectrum was less trivial to interpret than other (POCOP)Co^{II} complexes due to the large overlap of the broad signals; however, it was clear that the starting material had been fully consumed and only a single new paramagnetic product was present. Similar to the other prepared fluorine containing (POCOP)Co^{II} complexes (**605** and **606**), **613** displayed no signal in the ¹⁹F NMR spectrum.

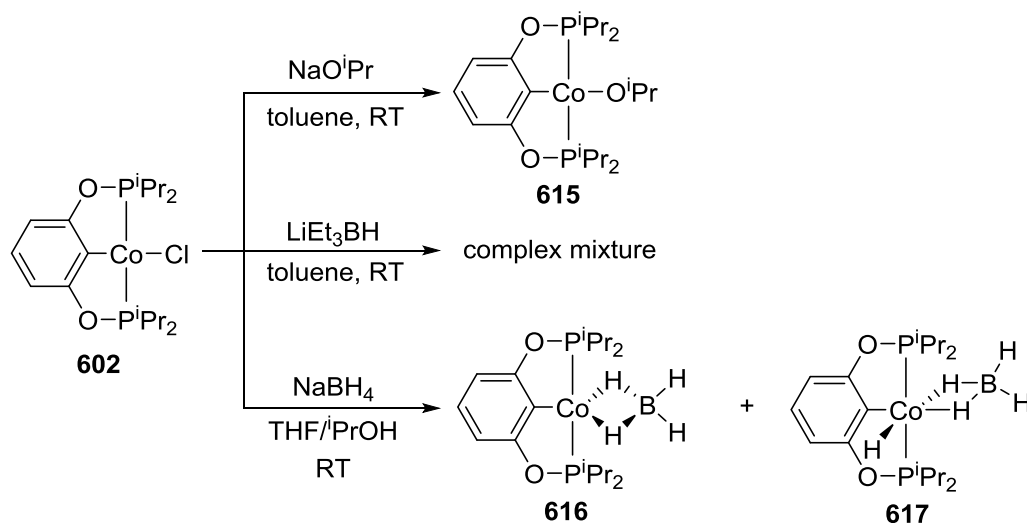


Scheme 6-6. Synthesis of (POCOP)Co(CF₃) (**613**).

6.2.1.3 Attempts towards (POCOP)Co(H)

Thus far our attempts at isolation of (POCOP)Co(H) (**614**) have not been successful (Scheme 6-7). We thought it might be possible to form **614** via β -hydrogen elimination (BHE) from a Co alkoxide complex. This is a common method for the synthesis of transition metal hydride complexes,^{39,139,159} but is not typical for pincer complexes due to the lack of an open coordination site required for BHE. Treatment of **602** with NaO^{*i*}Pr resulted in formation of (POCOP)Co(O^{*i*}Pr) (**615**), with no indication of **614** formation in the ¹H NMR spectrum. The byproducts of β -hydrogen abstraction were

also not observed in the ^1H NMR spectrum. The reaction between **602** and LiEt_3BH at RT gave a complex mixture of products.



Scheme 6-7. Attempts at synthesis of $(\text{POCOP})\text{Co}(\text{H})$ (**614**).

We also attempted to form **614** by the reaction between **602** with NaBH_4 . This reaction resulted in a product mixture composed of one diamagnetic and one paramagnetic product, assigned $(\text{POCOP})\text{Co}(\text{BH}_4)$ (**616**) and $(\text{POCOP})\text{Co}(\text{H})(\text{BH}_4)$ (**617**), respectively. The ^1H NMR spectrum showed three characteristic hydride signals for **617**, a sharp triplet at -22.8 ppm corresponding to the hydride and two broad singlets at -8.4 ppm and -11.8 ppm corresponding the protons of coordinated BH_4 . A similar hydride pattern was observed in the reported ^1H NMR spectrum of $(\text{POCOP})\text{Ir}(\text{H})(\text{BH}_4)$.¹⁶⁰ A single crystal obtained from the product mixture was identified as **616** by X-ray analysis (Figure 6-3). The solid state structure shows a Y-shaped geometry about cobalt with a $\kappa^2\text{-BH}_4$ bound to planar $(\text{POCOP})\text{Co}$. **616** would

be Co(II) and should give a paramagnetic ^1H NMR spectrum, consistent with what was observed in the ^1H NMR spectrum of the product mixture.

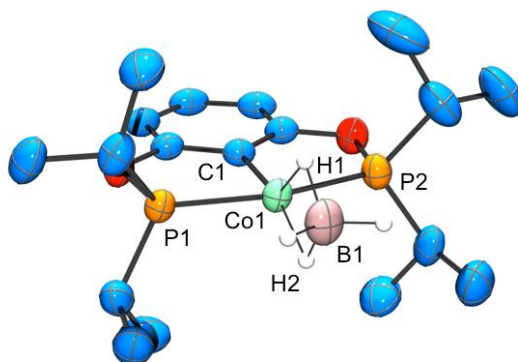
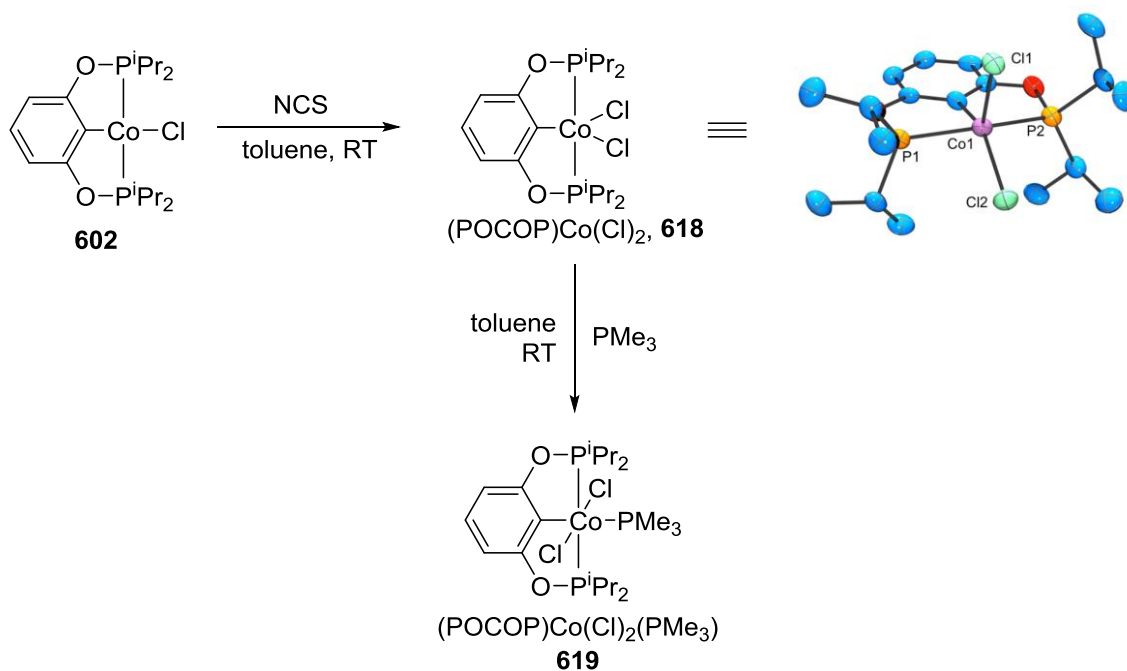


Figure 6-3. ORTEP drawing (50% probability ellipsoids) of (POCOP)Co(BH₄) (**616**).⁸⁴ Select atom labeling. Hydrogen atoms are omitted for clarity with the exception of B-H hydrogen atoms. Selected bond distances (Å) and angles (deg) for **616** follow: Co1-H1, 1.70(3); Co1-H2, 1.57(2); Co1-C1, 1.922(2), C1-Co1-H1, 133.9(9); C1-Co1-H2, 157.7(9); P1-Co1-P2, 162.30(3).

6.2.2 Synthesis of (POCOP)Co^{III} Compounds

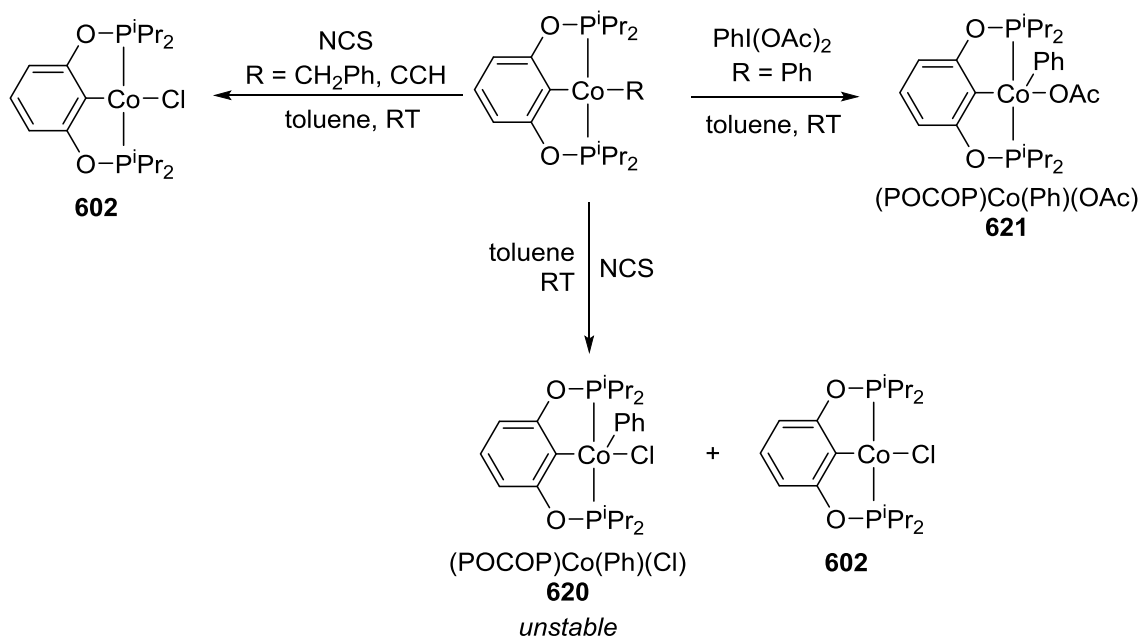
Oxidation of **602** with N-chlorosuccinimide (NCS) resulted in an immediate color change to dark brown and formation of new product exhibiting broad signals outside of the standard diamagnetic region in the ¹H NMR spectrum (Scheme 6-8). The identity of the product was determined to be (POCOP)Co(Cl)₂ (**618**) by X-ray study on a single crystal, which showed a geometry about Co that is intermediate between trigonal-bipyramidal and Y-shaped. This geometry is consistent with a paramagnetic d⁶ complex and is similar to other isolated 5-coordinate cobalt dihalides and trihalides.^{154,161} The monophosphine substituted (PPh₃)₂Rh(Ph)(X)₂ (X = Cl, Br, I) complexes each exhibit a nearly square pyramidal geometry in which the phenyl group occupies the apical position.^{62c,162} The magnetic moment of **618** was determined to be 2.44 and 2.46 μ_B by Evans method and the use of a magnetic susceptibility balance, respectively. This value is lower than what would be expected for a paramagnetic complex with 2 unpaired electrons. Similar (pincer)Co(X)₂ complexes give a magnetic susceptibility between 3.1-3.6 μ_B.¹⁵⁴ We are still investigating **618** to understand the unusually low magnetic moment. Treatment of **618** with 1 equiv of PMe₃ resulted in an immediate color change from brown to green and formation of diamagnetic (POCOP)Co(Cl)₂(PMe₃) (**619**). **619** displayed characteristic resonances in the ¹H NMR spectrum and broad singlets at 178.0 ppm and -16.7 ppm in the ³¹P NMR spectrum in a 2:1 ratio, respectively, consistent with an octahedral six-coordinate cobalt complex.



Scheme 6-8. Synthesis of (POCOP)Co(Cl)₂ (**618**) and (POCOP)Co(Cl)₂(PMe₃) (**619**). ORTEP drawing (50% probability ellipsoids) of **618**.⁸⁴ Select atom labeling. Hydrogen atoms are omitted for clarity. Selected bond distances (Å) and angles (deg) for **618** follow: Co1-Cl1, 2.285(2); Co1-Cl2, 2.238(2); Co1-C1, 1.934(4), C1-Co1-C1, 110.3(1); C1-Co1-Cl2, 144.4(1); P1-Co1-P2, 159.10(3).

Based on the success of NCS as an oxidant with **602** to form **618**, we decided to examine the potential of forming low-spin diamagnetic (POCOP)Co(R)(X) complexes. The reaction of (POCOP)Co(CH₂Ph) **608** and (POCOP)Co(CCH) **609** with 1 equiv of NCS resulted in conversion to **602**, with no discernible formation of any diamagnetic (POCOP)Co^{III} complexes (Scheme 6-9). However, treatment of **607** with NCS resulted in a mixture of **602** with a new diamagnetic product identified as (POCOP)Co(Ph)(Cl) (**620**). **620** displayed a singlet in the ³¹P{¹H} NMR spectrum at 176.7 ppm. The Ph protons of **620** displayed characteristic broad resonances in the ¹H NMR spectrum, with the exception of the *para*-H, indicative of the hindered Ph rotation by the isopropyl

groups of POCOP. The broad resonances are the result of slowed rotation of the phenyl group that is sandwiched between the isopropyl phosphine substituents, consistent with what has previously been observed with similar d^6 pincer ligated group 9 aryl complexes.^{63,81,100} This rotation would be expected to be even slower with Co compared to Rh and Ir as the decreased size of Co should facilitate greater congestion between the phenyl ring and the isopropyl substituents. Careful recrystallization did result in the isolation of a small amount of **620**, however the C_6D_6 solution of pure **620** converted back to a mixture **620** and **602** after only a few hours at RT.



Scheme 6-9. Oxidation of (POCOP)Co(R) (R = hydrocarbyl) complexes.

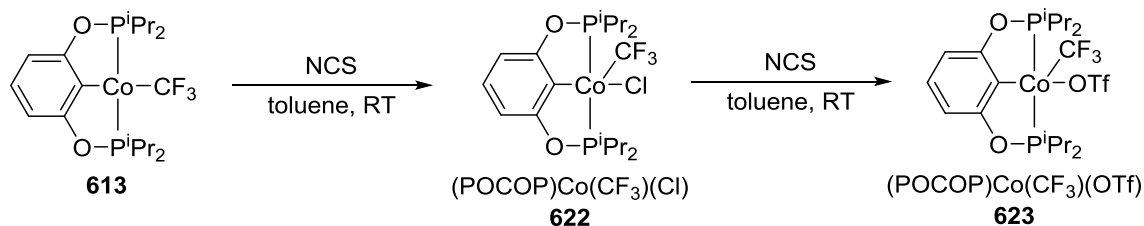
602 is formed by net elimination of phenyl radical from **620** to form the more stable (POCOP)Co^{II} complex. Biphenyl was observed in the ¹H NMR spectrum in

addition to **602**. Similar radical chemistry is also expected to be the cause of formation of **602** in the reactions between NCS with **608** and **609**. Fryzuk's 1998 study with the $(\text{PN}^{\text{Si}}\text{P}^{\text{Ph}})\text{Co}$ system illustrated various examples of one-electron reactivity.¹⁵⁴ Most similar to the reactivity observed here, Fryzuk noted that the reaction of $(\text{PN}^{\text{Si}}\text{P}^{\text{Ph}})\text{Co}(\text{X})_2$ with 1 equiv RLi or RMgX (R = alkyl) resulted in clean formation of $(\text{PN}^{\text{Si}}\text{P}^{\text{Ph}})\text{Co}(\text{X})$, which is believed to result from alkyl radical elimination from the unstable $(\text{PN}^{\text{Si}}\text{P}^{\text{Ph}})\text{Co}(\text{R})(\text{X})$ complex.

In an attempt to synthesize a more stable $(\text{POCOP})\text{Co}(\text{Ph})(\text{X})$ complex, we oxidized **607** with $\text{PhI}(\text{OAc})_2$ hoping to form $(\text{POCOP})\text{Rh}(\text{Ph})(\text{OAc})$ with the idea that the dative interaction of the acetate oxygen in the 6th coordination site would stabilize the Co^{III} complex in a fashion similar to reported six-coordinate $\text{Co}(\text{III})$ alkyl complexes. In fact, oxidation of **607** with $\text{PhI}(\text{OAc})_2$ did result in the formation of $(\text{POCOP})\text{Co}(\text{Ph})(\text{OAc})$ (**621**) after stirring overnight at RT. **621** was isolated as a red solid and displayed a singlet in the $^{31}\text{P}\{^1\text{H}\}$ NMR spectrum at 179.3 ppm and a ^1H NMR spectrum consistent with clean formation of a low-spin diamagnetic $(\text{POCOP})\text{Co}^{\text{III}}$ complex. Unlike **620**, the ^1H NMR spectrum of **621** displayed five sharp resonances for the phenyl group, indicating a phenyl group with even slower rotation. Inspection of the ^1H NMR spectrum indicated no formation of new products after several days at RT in solution or in the solid state. We attribute the stability of **621** to the 6-coordinate octahedral nature of cobalt facilitated by the κ^2 binding mode of the acetate group.

Oxidation of the trifluoromethyl complex **613** with NCS resulted in formation of the stable low-spin $\text{Co}(\text{III})$ complex $(\text{POCOP})\text{Co}(\text{CF}_3)(\text{Cl})$ (**622**) (Scheme 6-10). **622**

displayed a singlet in the $^{31}\text{P}\{^1\text{H}\}$ NMR spectrum at 181.1 ppm and a diagnostic triplet at 3.9 ppm ($J_{\text{P-F}} = 12$ Hz) in the ^{19}F NMR spectrum consistent with coordination of the CF_3 group to the pincer ligated Co center. Treatment of **622** with AgOTf in toluene resulted in immediate conversion to the triflate analogue (POCOP)Co(CF_3)(OTf) (**623**), which displayed a singlet at 184.2 ppm in the $^{31}\text{P}\{^1\text{H}\}$ NMR spectrum and a triplet at 2.5 ppm ($J_{\text{P-F}} = 13$ Hz) and a singlet at -77.8 ppm in the ^{19}F NMR spectrum. Analysis of the ^1H NMR spectrum of **622** and **623** after several days in in the solid state or in solution showed no formation of paramagnetic species. The increased stability of the trifluoromethyl complexes is attributed to the inertness and strength of late metal- CF_3 bonds.¹⁶³



Scheme 6-10. Synthesis of (POCOP)Co(CF_3)(Cl) (**622**) and (POCOP)Co(CF_3)(OTf) (**623**).

6.2.3 Towards (POCOP)Co(R)(R') Complexes

We then moved towards isolation of a stable (POCOP)Co(R)(R') species that would enable us to study the ability of (POCOP)Co^{III} complexes to undergo RE. Our study in this regard was not fruitful as no complexes of the type (POCOP)Co(R)(R') were isolated. Treatment of **621** with PhLi and (*p*-MeC₆H₄)Li resulted in formation of

paramagnetic products and no formation of diamagnetic Co(III) complexes. Treatment of **621** with Grignard reagents including PhMgBr and (CH₂CH)MgCl also resulted only in the formation of paramagnetic Co(II) products. **622** and **623** proved to be very stable against any reactivity with lithium or Grignard reagents. The only reactivity observed with **623** was anion exchange when reacted PhMgCl to form **622**.

6.3 Conclusion

In summary, we have synthesized a series of Co(II) and Co(III) complexes supported by the bisphosphinite POCOP pincer ligand. The complexes show reactivity similar to what has been reported in the literature, including the increased stability of six-coordinate Co(III) hydrocarbyl species against radical elimination. While several stable Co(III) complexes were synthesized, these complexes were unsuccessful as precursors to the synthesis of a (POCOP)Co(R)(R') species.

6.4 Experimental

6.4.1 General Considerations

Unless otherwise specified, all manipulations were performed under an argon atmosphere using standard Schlenk line or glove box techniques. Toluene, THF, pentane, and isooctane were dried and deoxygenated (by purging) using a solvent purification system and stored over molecular sieves in an Ar-filled glove box. C₆D₆ and hexanes were dried over and distilled from NaK/Ph₂CO/18-crown-6 and stored over molecular sieves in an Ar-filled glove box. Fluorobenzene was dried with and then

distilled or vacuum transferred from CaH_2 . $(\text{POCOP})\text{H}^{86}$ (**601**) was synthesized according to published procedures. All other chemicals were used as received from commercial vendors. NMR spectra were recorded on a Varian NMRS 500 (^1H NMR, 499.686 MHz; ^{13}C NMR, 125.659 MHz, ^{31}P NMR, 202.298 MHz, ^{19}F NMR, 470.111 MHz) spectrometer. For ^1H and ^{13}C NMR spectra, the residual solvent peak was used as an internal reference. ^{31}P NMR spectra were referenced externally using 85% H_3PO_4 at δ 0 ppm. ^{19}F NMR spectra were referenced externally using 1.0 M $\text{CF}_3\text{CO}_2\text{H}$ in CDCl_3 at -78.5 ppm. Elemental analyses were performed by CALI Labs, Inc. (Parsippany, NJ). Magnetic susceptibility collected using a JM Auto-Magnetic Susceptibility Balance.

6.4.2 Synthesis of $(\text{POCOP})\text{Co}$ Complexes

Synthesis of $(\text{POCOP})\text{Co}(\text{Cl})$ (602**).** $(\text{POCOP})\text{H}$ (**601**) (1.54 g, 4.52 mmol) was combined with CoCl_2 (586 mg, 4.51 mmol) and DMAP (552 mg, 4.52 mmol) in a Teflon capped flask and partially dissolved in dioxane. The flask was heated at 80 °C for 20 h producing a green solution. The solution was passed through a pad of Celite and volatiles were removed by vacuum. The product was extracted with pentane and dried under vacuum to give a bright yellow-green solid. The product was recrystallized from pentane at -35 °C to give yellow crystalline solid (689 mg, 35% yield). The compound displayed broad signals outside of the standard diamagnetic range in ^1H NMR spectrum, indicative of a paramagnetic complex. ^1H NMR (C_6D_6 , Figure 6-4): δ 43.72 (bs, 4H), 12.11 (bs, 24 H), -14.71 (bs, 2H), -53.02 (bs, 1H). Elem. Anal. Calc. for $\text{C}_{18}\text{H}_{31}\text{ClCoO}_2\text{P}_2$: C, 49.61; H, 7.17. Found: C, 49.54; H, 7.08. The magnetic moment for **601** was determined to be 2.18 μ_{B} by Evans Method.

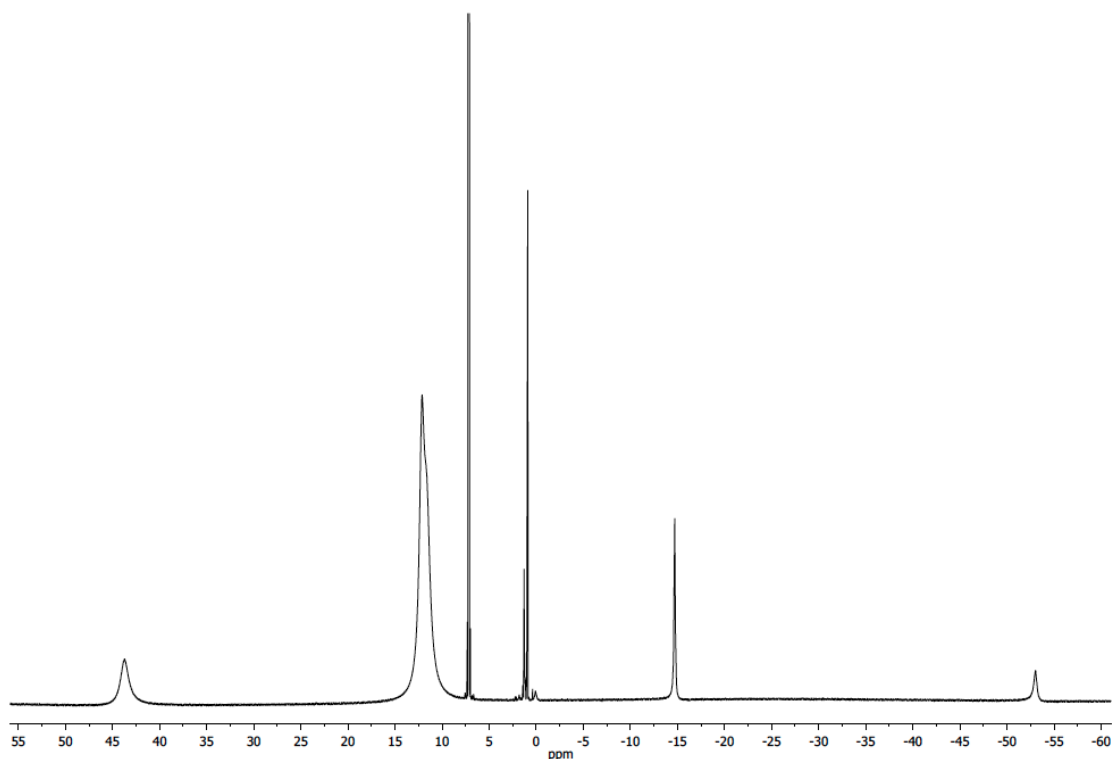


Figure 6-4. ^1H NMR spectrum of (POCOP)CoCl (**602**) in C_6D_6 . Minor residual pentane present.

Synthesis of (POCOP)Co(Br) (603). **602** (28 mg, 0.064 mmol) was added to a J. Young tube and dissolved in C_6D_6 . Me_3SiBr (10 μL , 0.076 mmol) was added to the sample, resulting in a color change to slightly yellow-green. The reaction was complete after 10 min at RT indicated by complete conversion to a new paramagnetic product and the presence of Me_3SiCl in the ^1H NMR spectrum. The volatiles were removed by vacuum to give a yellow powder. The product was recrystallized from a saturated pentane solution at $-35\text{ }^\circ\text{C}$ to give an orange crystalline solid (22 mg, 72%). ^1H NMR (C_6D_6 , Figure 6-5): δ 45.16 (bs, 4H), 12.75 (bs, 12H), 12.00 (bs, 12H), -17.91 (bs, 2H),

-41.58 (bs, 1H). Elem. Anal. Calc. for $C_{18}H_{31}BrCoO_2P_2$: C, 45.02; H, 6.51. Found: C, 44.95; H, 6.63.

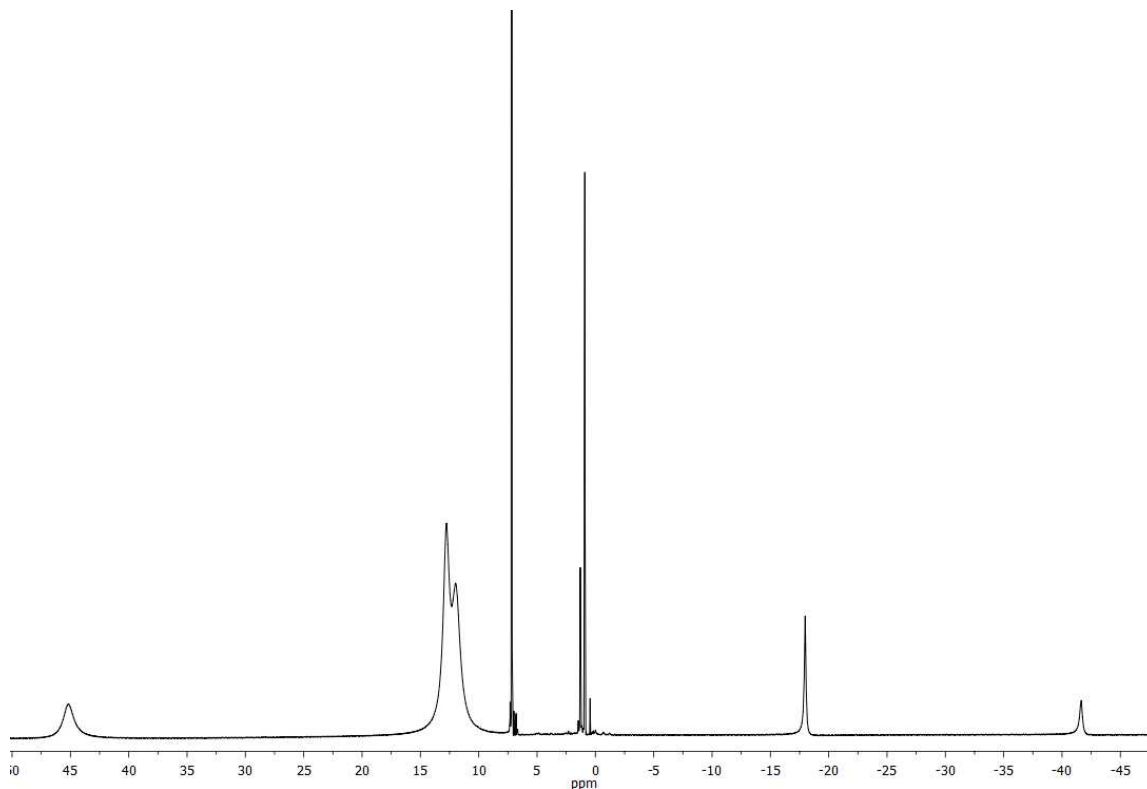


Figure 6-5. 1H NMR spectrum of (POCOP)Co(Br) (**603**) in C_6D_6 . Minor residual pentane present.

Synthesis of (POCOP)Co(I) (604). **602** (30 mg, 0.069 mmol) was added to a J. Young tube and dissolved in C_6D_6 . Me_3SiI (11 μL , 0.078 mmol) was added to the sample, resulting in a color change to yellow-green. The color was slightly darker than that observed with (POCOP)Co(Br). The reaction was complete after 10 min at RT indicated by complete conversion to a new paramagnetic product and the presence of Me_3SiCl in the 1H NMR spectrum. The volatiles were removed by vacuum to give a

yellow powder. The product was recrystallized from a saturated pentane solution at -35 °C to give a dark orange crystalline solid (15 mg, 43%). ^1H NMR (C_6D_6 , Figure 6-6): δ 40.35 (bs, 4H), 12.81 (bs, 12H), 12.01 (bs, 12H), -20.18 (bs, 2H), -27.73 (bs, 1H).

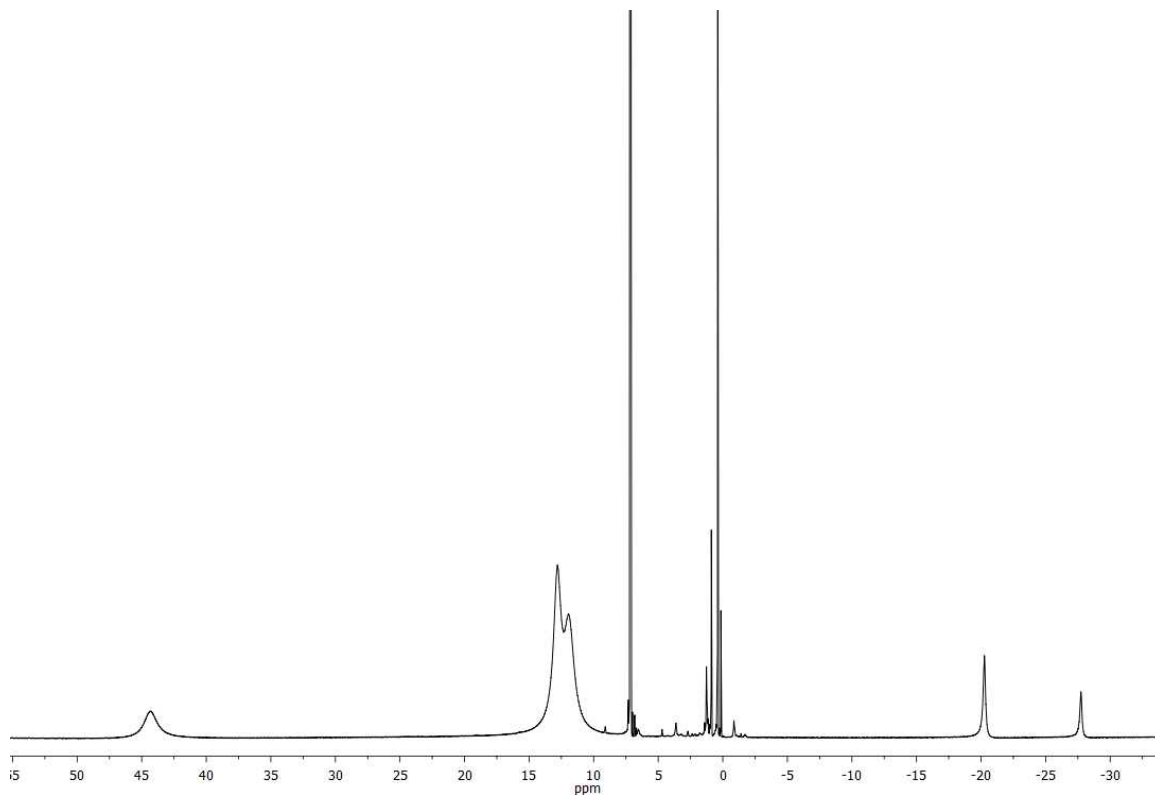


Figure 6-6. ^1H NMR spectrum of (POCOP)Co(I) (**604**) in C_6D_6 . Minor residual pentane and Me_3SiI present.

Synthesis of (POCOP)Co(OTf) (605). **602** (712 mg, 1.64 mmol) was added to a Schlenk flask and dissolved in C_6D_6 . The solution was treated with Me_3SiOTf (592 μL , 3.27 mmol). This led to no noticeable color change; however, the ^1H NMR spectrum of this reaction showed conversion to a new product along with the signal for Me_3SiCl . The volatiles were removed from the reaction by vacuum to give a yellow-orange solid (850

mg, 94%). ^1H NMR (C_6D_6 , Figure 6-7): δ 39.06 (bs, 4H, CHMe_2), 11.26 (bs, 12H, CHMe_2), 9.99 (bs, 12H, CHMe_2), -24.72 (bs, 1H, Ar-H), -26.33 (bs, 2H, Ar-H). Elem. Anal. Calc. for $\text{C}_{19}\text{H}_{31}\text{CoF}_3\text{O}_5\text{P}_2\text{S}$: C, 41.54; H, 5.69. Found: C, 41.37; H, 5.58.

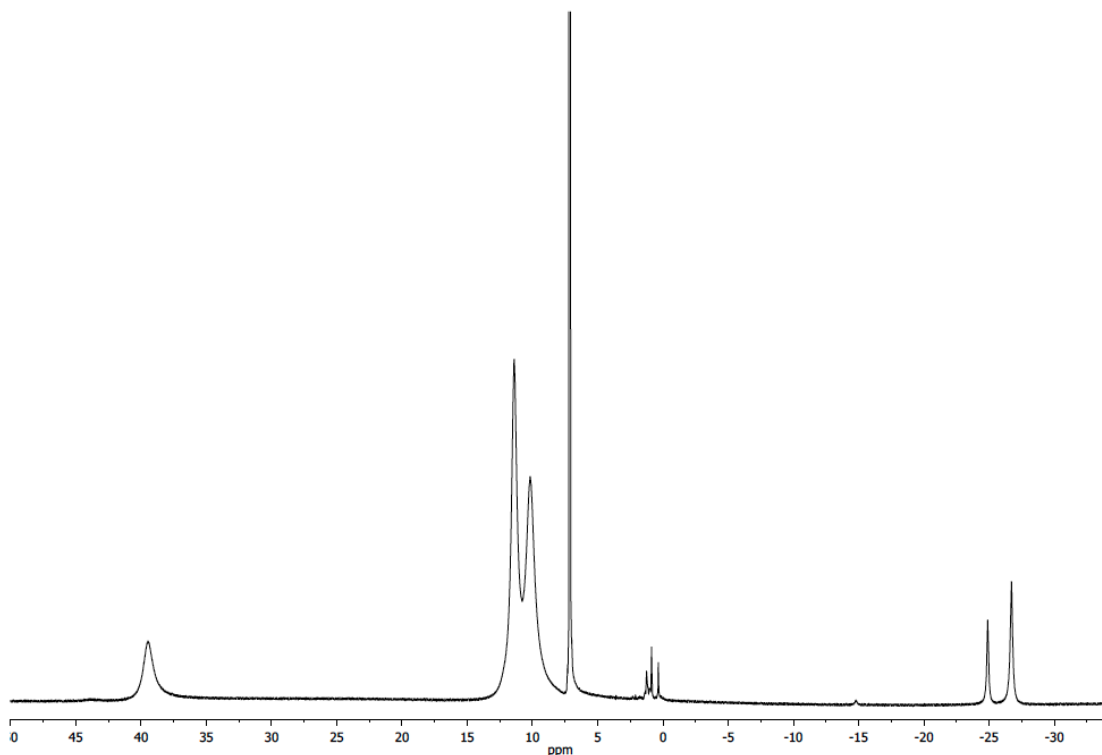


Figure 6-7. ^1H NMR spectrum of $(\text{POCOP})\text{Co}(\text{OTf})$ (**605**) in C_6D_6 . Minor residual pentane present.

Synthesis of $(\text{POCOP})\text{Co}(\text{F})$ (606**).** **605** (840 mg, 1.53 mmol) was added to a Schlenk flask and dissolved in $\text{C}_6\text{H}_5\text{F}$. The solution was treated with CsF (735 mg, 4.83 mmol) and allowed to stir at RT overnight. The solution became a slightly darker orange color. Volatiles were removed by vacuum. The product was extracted with pentane and passed through a pad of Celite to remove CsOTf and excess CsF. The compound was

recrystallized from a minimum of pentane at $-35\text{ }^{\circ}\text{C}$. This gave primarily orange solid with some dark black solid. The recrystallized was washed with cold pentane, which removed the dark solid and left the light orange product. The solid was dried under vacuum to give a light orange solid (399 mg, 63%). ^1H NMR (C_6D_6 , Figure 6-8) -23.38 (bs, 4H, CHMe_2), 8.37 (bs, 12H, CHMe_2), 6.77 (bs, 12H, CHMe_2), 0.38 (bs, 1H, Ar- H), 0.12 (bs, 2H, Ar- H). Elem. Anal. Calc. for $\text{C}_{18}\text{H}_{31}\text{CoFO}_2\text{P}_2$: C, 51.56; H, 7.45. Found: C, 51.39; H, 7.56.

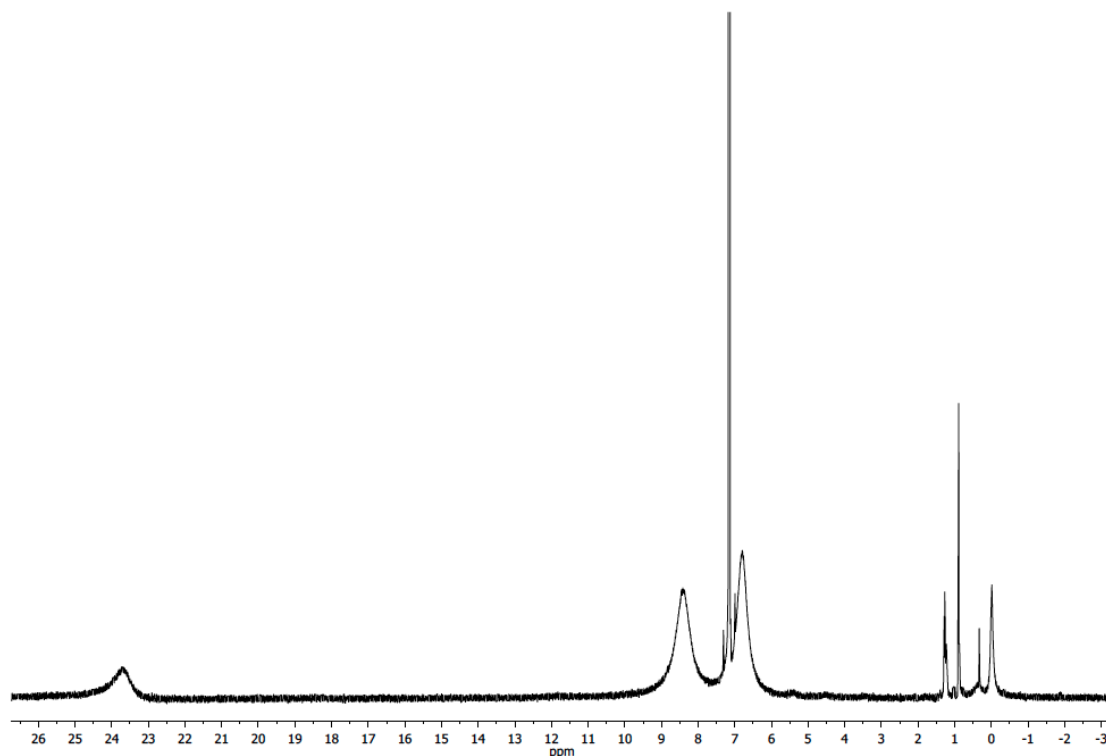


Figure 6-8. ^1H NMR spectrum of $(\text{POCOP})\text{Co}(\text{F})$ (**606**) in C_6D_6 . Minor residual pentane and grease present.

Synthesis of (POCOP)Co(Ph) (607). **602** (91 mg, 0.21 mmol) was added to a Schlenk flask and dissolved in pentane. The solution was treated with PhLi (140 μ L, 1.8 M in OBU₂, 0.25 mmol) leading to an immediate color change from light yellow to dark green. After stirring for 30 min at RT, the solution was passed through a pad of Celite and the volatiles were removed by vacuum to give a green solid. The solid was recrystallized from toluene layered with pentane at -35 °C to give a dark green crystalline solid (81 mg, 81% yield). The compound displayed broad signals outside of the standard diamagnetic range in the ¹H NMR spectrum, indicative of a paramagnetic complex. ¹H NMR (C₆D₆, Figure 6-9): δ 35.99 (bs, 4H), 13.78 (bs, 1H), 11.95 (bs, 12H), 7.31 (bs, 12H), -7.43 (bs, 1H), -15.76 (bs, 2H), -20.04 (bs, 2H), -40.32 (bs, 2H).

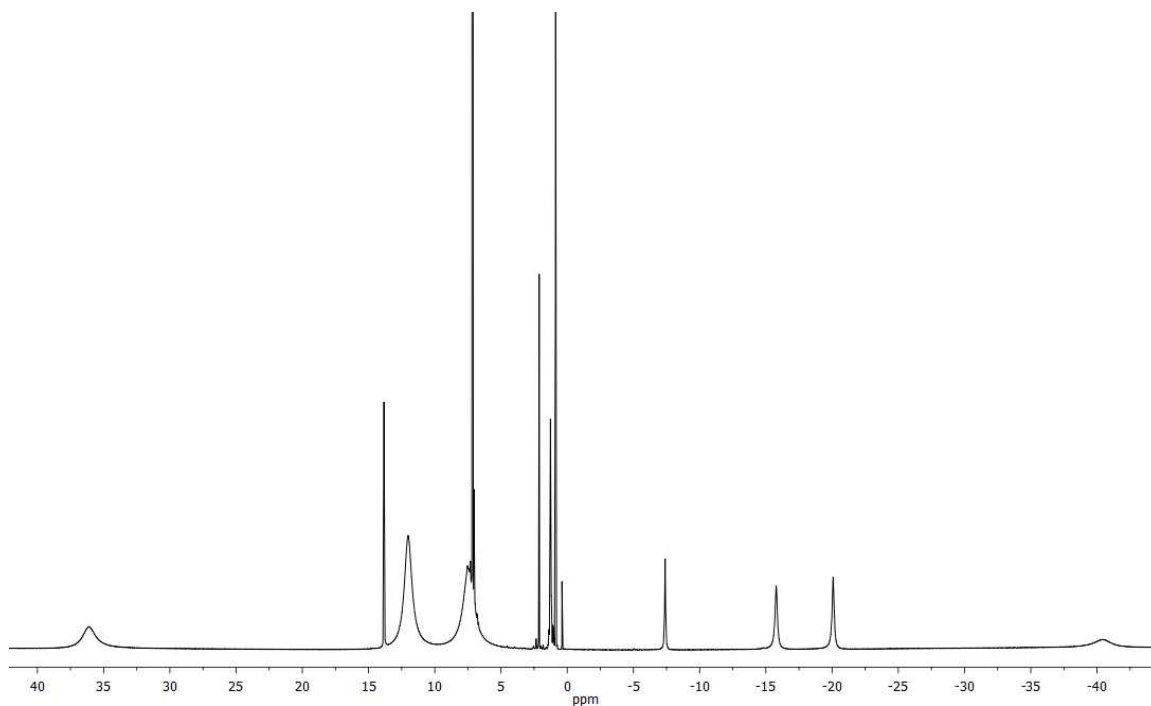


Figure 6-9. ¹H NMR of (POCOP)Co(Ph) (**607**) in C₆D₆. Minor residual pentane, toluene, and grease present.

Synthesis of (POCOP)Co(CH₂Ph) (608). **602** (92 mg, 0.21 mmol) was added to a Schlenk flask and dissolved in pentane. ClMg(CH₂Ph) (232 μ L, 1.0 M in OEt₂, 0.232 mmol) was added to the reaction resulting in an immediate color change to brown orange. The reaction was stirred for 3 h at RT and then passed through a pad of Celite. The volatiles were removed under vacuum to give a dark orange solid. The solid was recrystallized from a concentrated pentane solution at -35 $^{\circ}$ C to give crystalline red-brown solid (57 mg, 55%). ¹H NMR (C₆D₆, Figure 6-10): δ 13.37 (bs, 2H), 15.14 (bs, 4H), 5.95 (bs, 12H), 4.86 (bs, 2H), 3.81 (bs, 12H), 0.21 (bs, 1H), -38.48 (bs, 1H), -47.97 (bs, 2H).

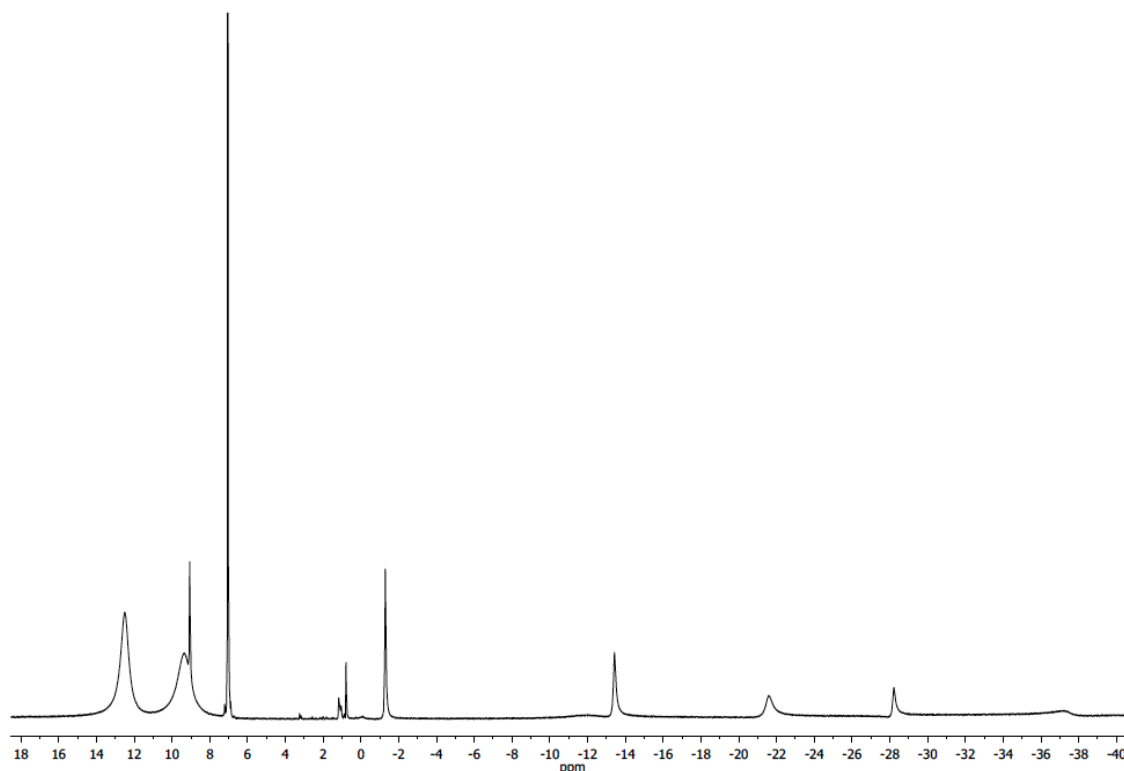


Figure 6-10. ¹H NMR spectrum of (POCOP)Co(CH₂Ph) (**608**) in C₆D₆. Minor residual pentane present.

Synthesis of (POCOP)Co(CCH) (609). **602** (106 mg, 0.244 mmol) was added to a Schlenk flask and dissolved in pentane. ClMg(CCH) (512 μL , 0.5 M in THF, 0.256 mmol) was added to the solution resulting in an immediate color change to dark green. The reaction was stirred at RT for 3 h at RT. The volatiles were removed under vacuum. The product was extracted with pentane and passed over a pad of Celite. The volatiles were removed under vacuum to give a green solid (92 mg, 89%). ^1H NMR (C_6D_6 , Figure 6-11): δ 9.74 (bs, 1H), 7.78 (bs, 12H), 1.47 (bs, 12H), -7.87 (bs, 2H). Two signals integrating to 1H and 4H were unable to be identified.

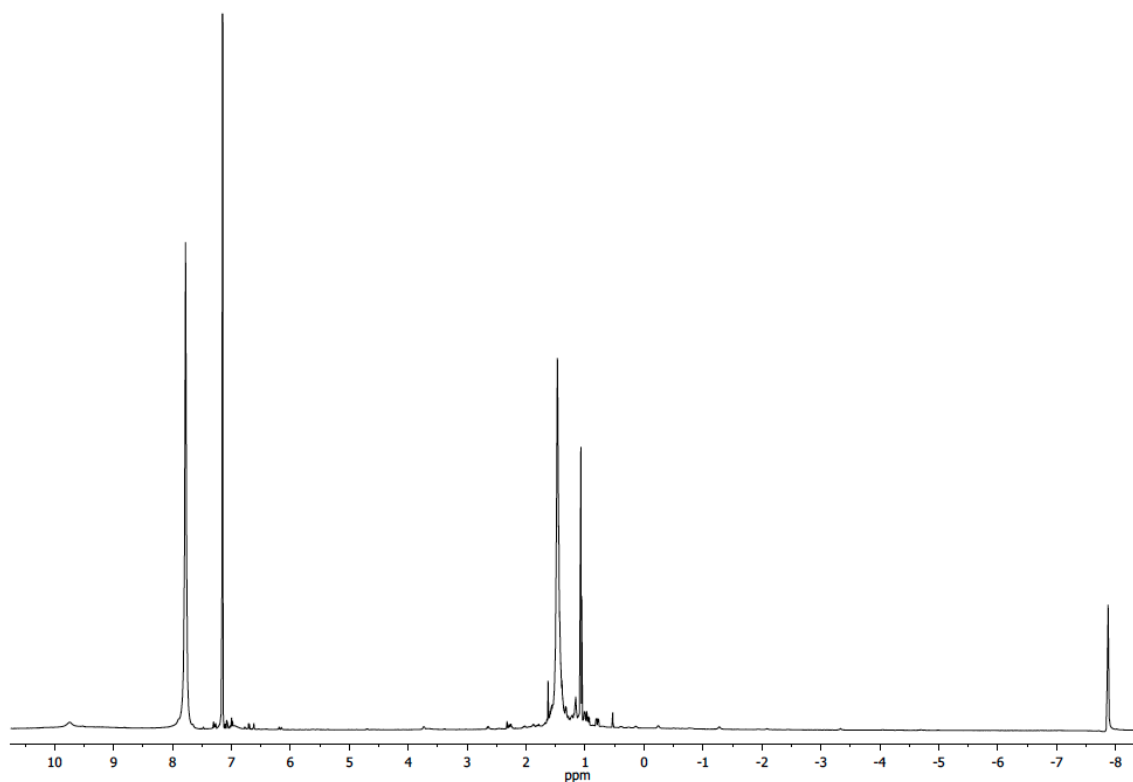


Figure 6-11. ^1H NMR spectrum of (POCOP)Co(CCH) (**609**) in C_6D_6 . Minor impurities including pentane and toluene present.

Treatment of 602 with 1.1 equiv (CH₂CH)MgCl. **602** (217 mg, 0.50 mmol) was added to a Schlenk flask and dissolved in toluene. (CH₂CH)MgCl (343 μL, 1.6 M in THF, 0.55 mmol) was added to the solution resulting in an immediate color change to dark green. After the reaction was stirred for 1 h at RT, the volatiles were removed by vacuum. The residual solid was extracted with pentane and passed over a pad of Celite. The volatiles were removed and the residual green solid was analyzed in C₆D₆ by ¹H NMR spectroscopy. The ¹H NMR spectrum showed primarily unreacted **602** approximately 30% conversion to a new unidentified paramagnetic product, most likely (POCOP)Co(CHCH₂).

Treatment of 602 with 4.0 equiv (CH₂CH)MgCl. **602** (150 mg, 0.35 mmol) was added to a Schlenk flask and dissolved in toluene. (CH₂CH)MgCl (860 μL, 1.6 M in THF, 1.38 mmol) was added to the reaction solution, resulting in an immediate color change to dark brown-green. Analysis of the ¹H NMR and ³¹P{¹H} NMR spectrum after 1 h at RT showed complete conversion of **602** to a complex mixture of products. The volatiles were removed by vacuum. The solid mixture was extracted with pentane and passed over a pad of Celite to give a green solution. The volatiles were removed by vacuum and the solid was recrystallized from a concentrated pentane solution at -35 °C to give a small amount (~15 mg) of green solid. The solid was dissolved in C₆D₆ and analyzed by ¹H and ³¹P NMR spectroscopy. ³¹P{¹H} NMR (C₆D₆): δ 207.7 ppm (bs); ¹H NMR (C₆D₆, Figure 6-12): δ 6.83 (t, 10 Hz, 1H, POCOP), 6.61 (d, 10 Hz, 2H, POCOP), 5.30 (m, 2H), 2.44 (m, 2H, CHMe₂), 2.30 (m, 2H, CHMe₂), 1.90 (d, 5.0 Hz, 2H), 1.14 (m, 18 H, CHMe₂), 1.00 (m, 6H, CHMe₂), 0.22 (m, 2H).

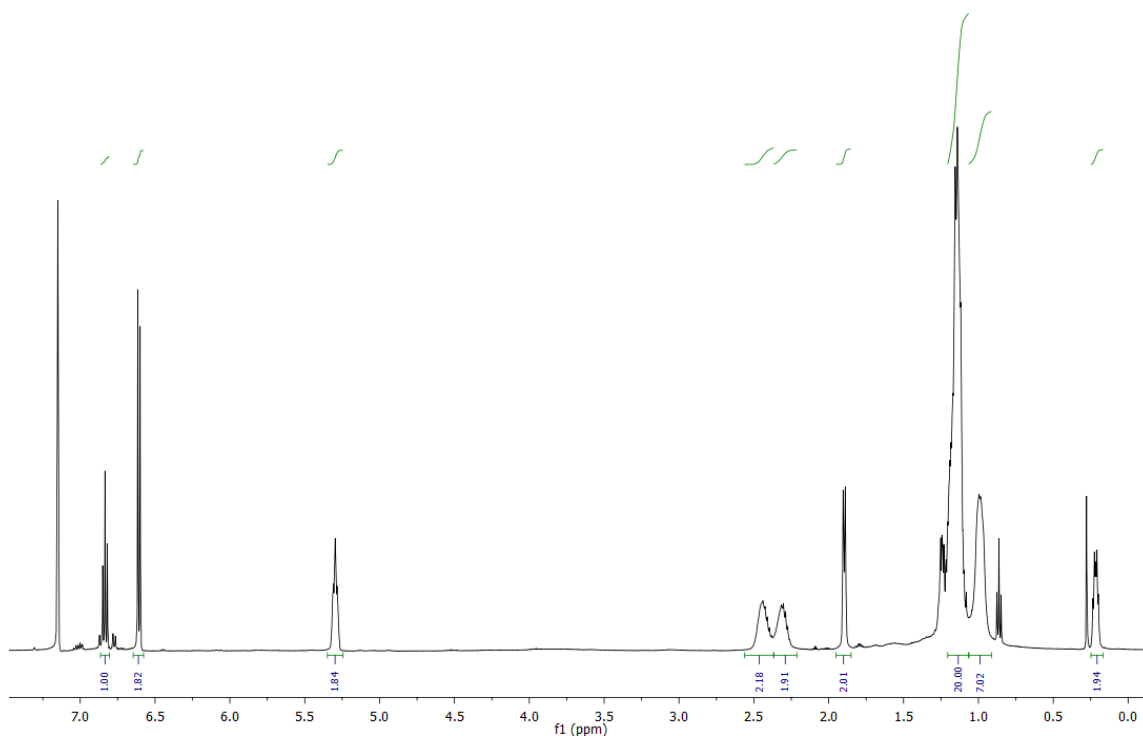


Figure 6-12. ^1H NMR spectrum of isolated green solid from the reaction between **602** with excess $(\text{CH}_2\text{CH})\text{MgCl}$ in C_6D_6 .

A solution of the green solid in C_6D_6 was degassed and filled with 1 atm. CO , resulting an immediate color change to light orange. Analysis of the ^1H NMR spectrum after 30 min at RT showed complete conversion to $(\text{POCOP})\text{Co}(\text{CO})$ (**610**) and the presence of free 1,3-butadiene (Figure 6-13). NMR spectroscopic details for **610**: $^{31}\text{P}\{^1\text{H}\}$ NMR (C_6D_6): δ 227.6 (s); ^1H NMR (C_6D_6): δ 6.79 (t, 5.0 Hz, 1H), 6.68 (d, 10 Hz, 2H), 2.23 (m, 4H, CHMe_2), 1.13 (m, 24H, CHMe_2).

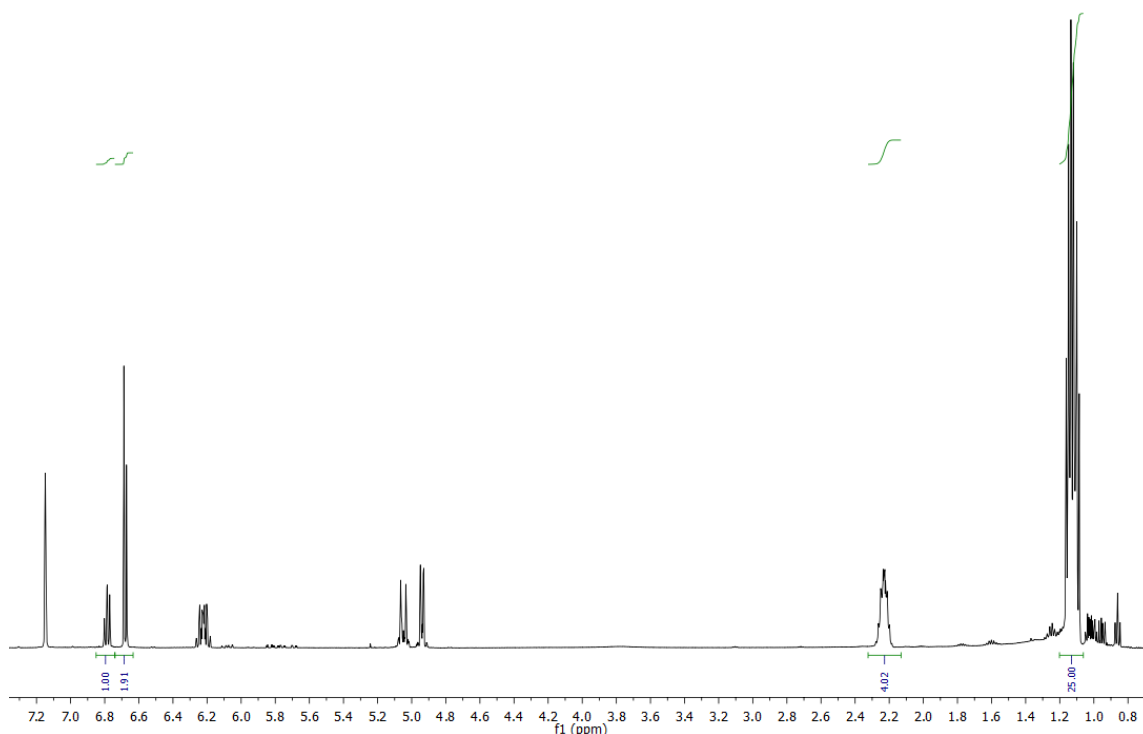


Figure 6-13. ^1H NMR spectrum of $(\text{POCOP})\text{Co}(\text{CO})$ (**610**) in C_6D_6 . Non-integrated signals between 4.8 and 6.3 ppm correspond to free 1,3-butadiene.

Synthesis of $(\text{POCOP})\text{Co}(\text{CF}_3)$ (613**).** **606** (390 mg, 0.93 mmol) was added to a Schlenk flask and dissolved in toluene. The solution was treated with Me_3SiCF_3 (137 μL , 0.93 mmol) and allowed to stir at RT overnight. The volatiles were removed under vacuum leaving a dark orange solid (425 mg, 97%). The overlap of signals made it challenging to assign the peaks and integrate in the ^1H NMR spectrum (Figure 6-14); however, the spectrum indicated the presence of a single paramagnetic product. The methyl resonances of the isopropyl groups appear as two overlapping signals centered at 4.50 ppm in the ^1H NMR spectrum.

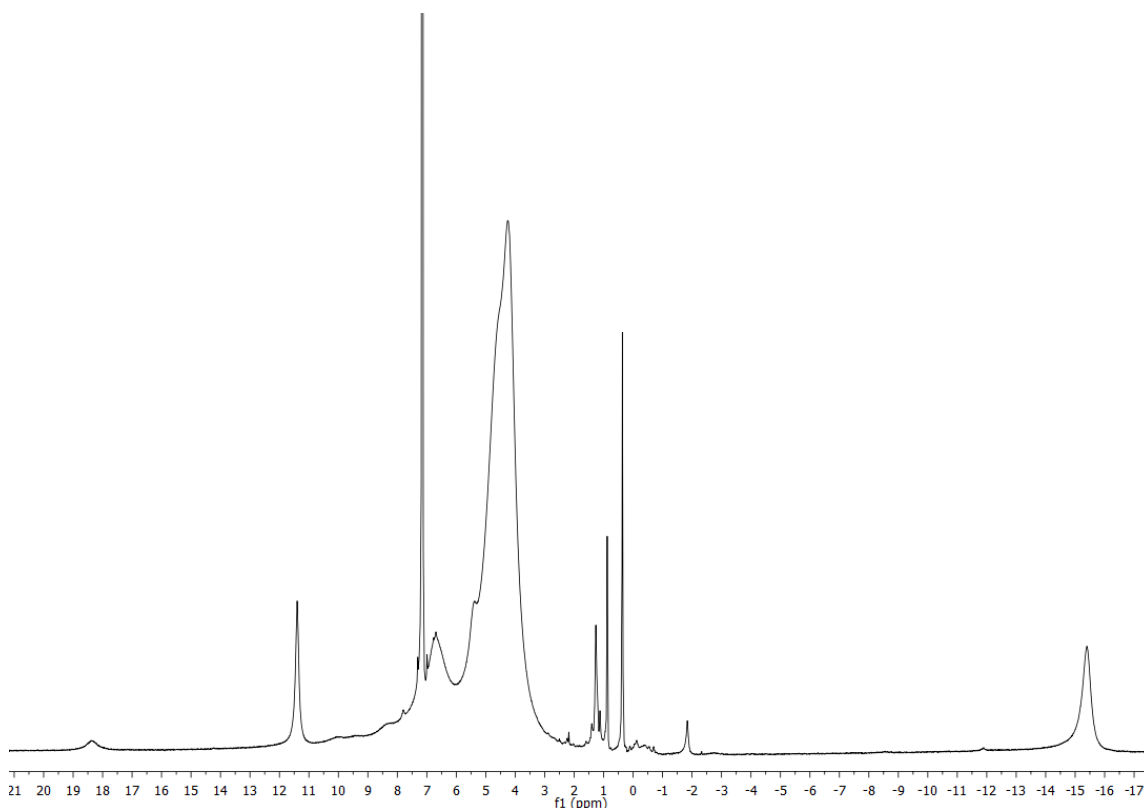


Figure 6-14. ^1H NMR spectrum of $(\text{POCOP})\text{Co}(\text{CF}_3)$ (**613**) in C_6D_6 .

Synthesis of $(\text{POCOP})\text{Co}(\text{O}^t\text{Bu})$ (611**).** **602** (185 mg, 0.42 mmol) was added to a Schlenk flask and dissolved in toluene. NaO^tBu (41 mg, 0.43 mmol) was added to the solution, resulting in an immediate color change to orange. The reaction was stirred at RT for 1 h. The volatiles were removed under vacuum. The product was extracted with pentane, passed through a pad of Celite, and dried under vacuum. The product was recrystallized from a concentrated toluene solution layered with pentane at $-35\text{ }^\circ\text{C}$ to give a brown solid (127 mg, 63%). ^1H NMR (C_6D_6 , Figure 6-15): δ 14.93 (bs, 4H), 4.36 (bs, 26H), -9.88 (bs, 9H), -79.53 (bs, 1H).

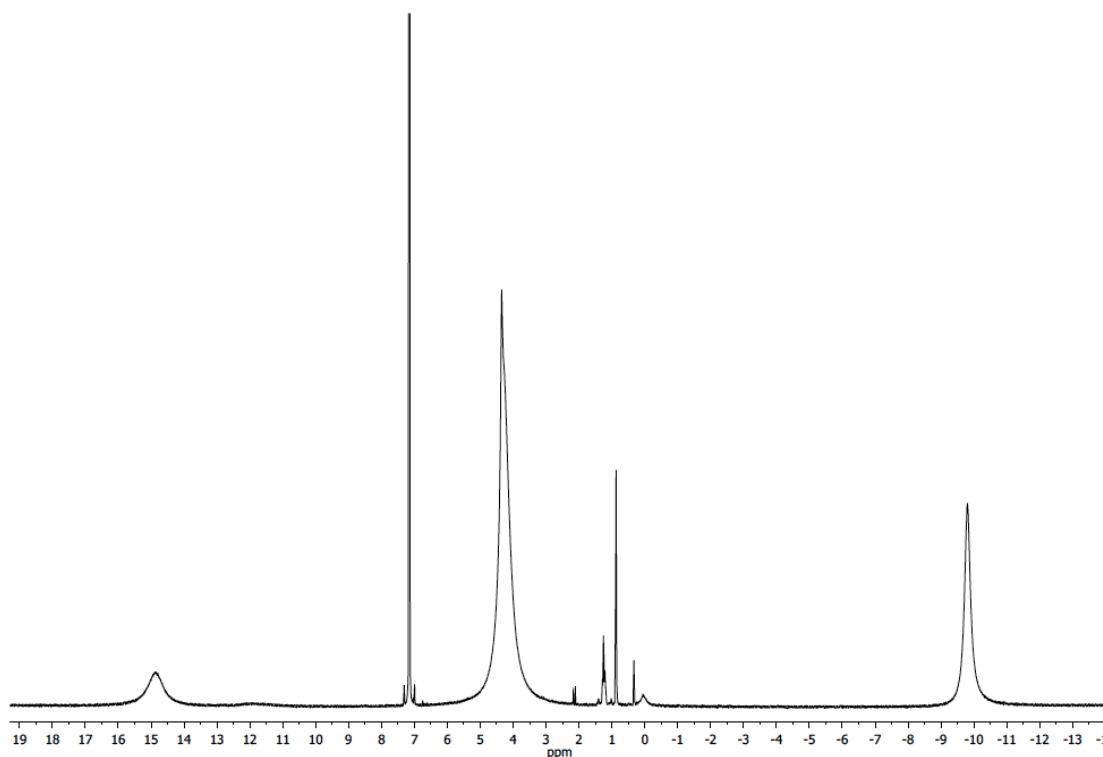


Figure 6-15. ^1H NMR spectrum of $(\text{POCOP})\text{Co}(\text{O}^t\text{Bu})$ (**611**) in C_6D_6 . Minor residual pentane present.

Synthesis of $(\text{POCOP})\text{Co}(\text{NHPh})$ (612**).** **611** (22 mg, 0.048 mmol) was added to a J. Young tube and dissolved in C_6D_6 . NH_2Ph (4.8 μL , 0.053 mmol) was added to the J. Young tube resulting in an immediate color change from orange to purple. Analysis of the *in situ* reaction mixture by ^1H NMR spectroscopy after 30 min at RT indicates conversion to a new paramagnetic compound, *tert*-butanol, and residual NH_2Ph . The reaction was passed through a pad of Celite. The volatiles were removed by vacuum to give a purple solid (13 mg, 59%). ^1H NMR (C_6D_6 , Figure 6-16): δ 19.37 (bs, 2H), 15.14 (bs, 2H), 5.95 (bs, 12H), 4.86 (bs, 4H), 3.81 (bs, 12H), 0.21 (bs, 1H), -38.38 (bs, 1H),

-47.97 (bs, 2H). Unable to locate one resonance corresponding to 1H, which is likely located under one of the broad signals.

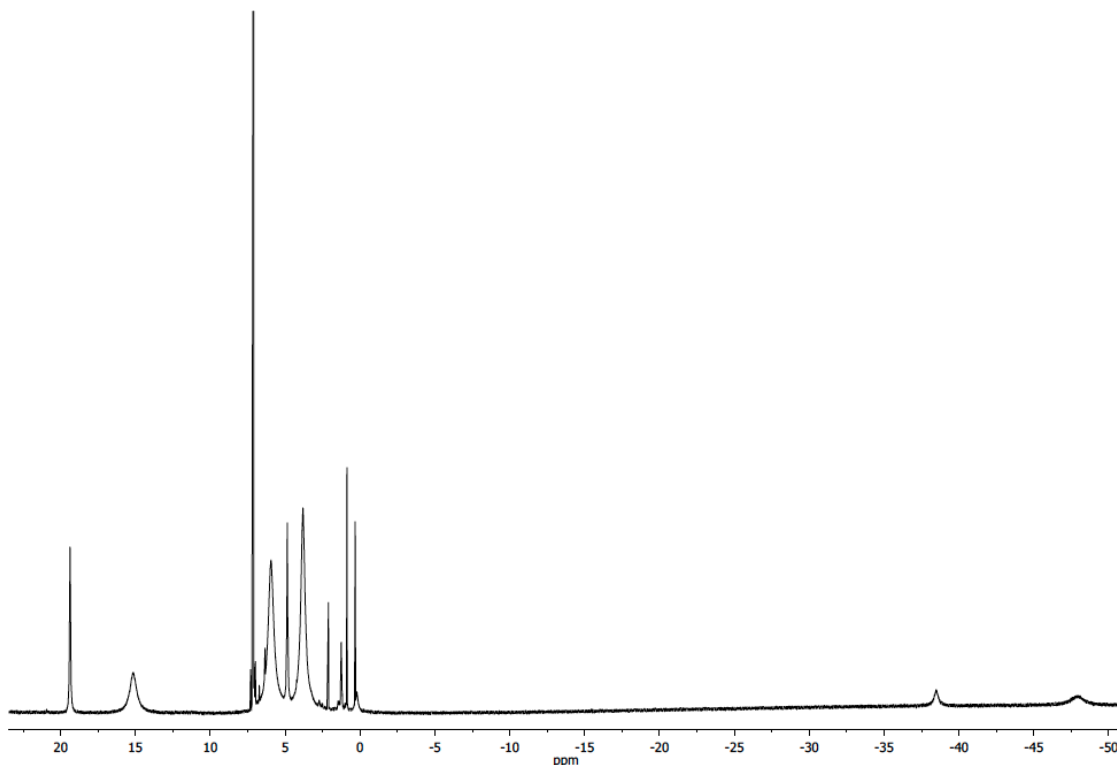


Figure 6-16. ^1H NMR spectrum of (POCOP)Co(NHPh) (**612**) in C_6D_6 . Minor residual pentane and toluene present.

Reaction between 602 with NaO^iPr . **602** (20 mg, 0.046 mmol) and NaO^iPr (8 mg, 0.092 mmol) were combined in a Schlenk flask and dissolved in toluene. Two drops of THF were added to the sample to assist solubility. The reaction was stirred at RT for 2 h with no noticeable color change. The volatiles were removed by vacuum. The product was extracted with pentane and passed through a pad of Celite. The volatiles were removed and the residue was dissolved in C_6D_6 . Analysis of the ^1H NMR spectrum

showed conversion of the starting material to a single product (Figure 6-17). Based on the number of resonances and the integral ratios, the product was assigned as (POCOP)Co(OⁱPr) (**615**). Due to overlap, not all peaks could be assigned, but three large broad resonances at 5.21 ppm, 2.96 ppm, and -10.42 ppm integrating 12:12:6, respectively, were identified in the spectrum, which is consistent with this assignment.

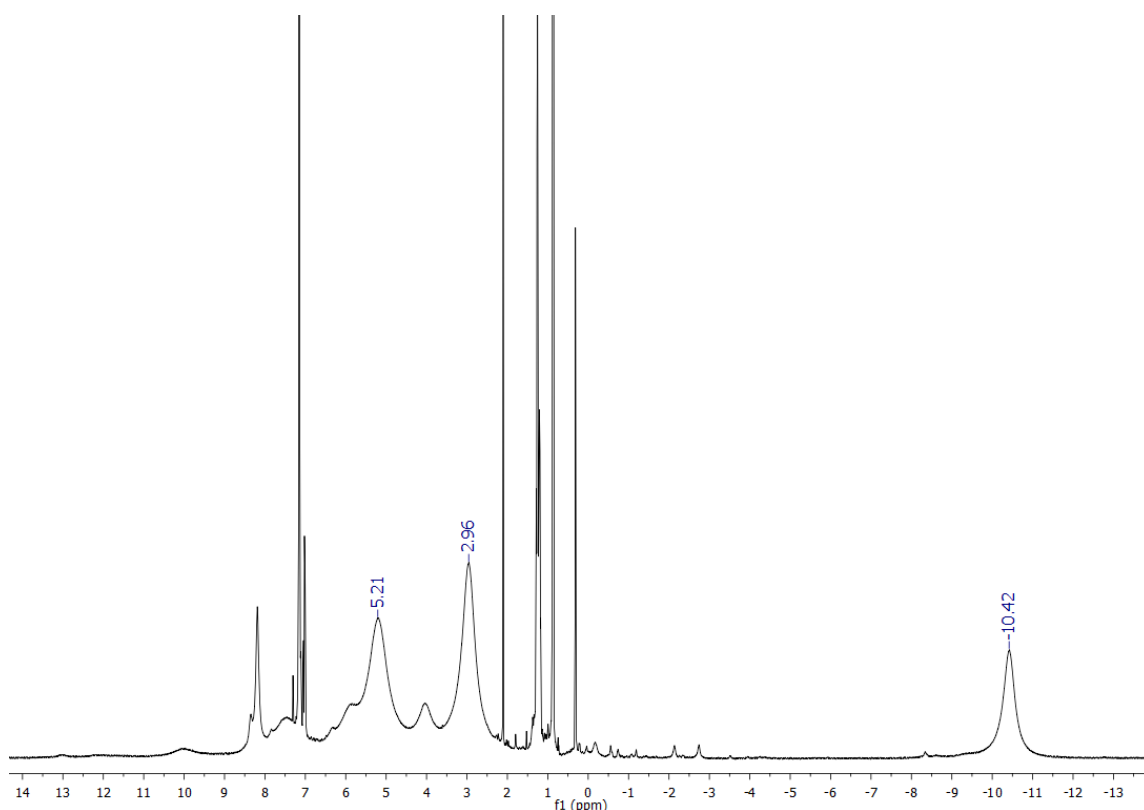


Figure 6-17. ¹H NMR spectrum of (POCOP)Co(OⁱPr) (**615**) in C₆D₆. Minor residual pentane present.

Reaction between 602 with LiEt₃BH. **602**(17 mg, 0.039 mmol) was added to a J. Young tube and dissolved in C₆D₆. LiEt₃BH (39 μL of 1 M solution, 0.039 mmol) was added to the sample, resulting in an immediate color change to blue-green. Analysis of

the ^1H NMR spectrum shows complete conversion of the starting material to a complex mixture of products.

Reaction between 602 with NaBH_4 . **602** (20 mg, 0.047 mmol) and NaBH_4 (12 mg, 0.34 mmol) were combined in a Schlenk and partially dissolved in isopropanol and THF (1:1). The reaction was stirred overnight at RT, resulting in a color change from yellow to orange. The reaction was passed through a pad of Celite. The volatiles were removed under vacuum to give an orange-red solid. Analysis of the solid in C_6D_6 showed signals for a diamagnetic and paramagnetic product, determined to be $(\text{POCOP})\text{Co}(\text{BH}_4)$ (**616**) and $(\text{POCOP})\text{Co}(\text{H})(\text{BH}_4)$ (**617**), respectively. The identity of **617** was determined based on the appearance of three diagnostic hydride signals: a sharp triplet at -22.8 ppm (Co–H) and two broad singlets at -8.4 ppm and -11.8 ppm (Co– BH_4). The identity of **616** was determined from X-ray analysis on a single crystal grown from a saturated pentane solution of the reaction mixture at -35 °C. The NMR sample in C_6D_6 was degassed and refilled with H_2 . After 48 h at RT, no discernible color change occurred and no reaction was evidenced in the ^1H NMR spectrum.

Synthesis of $(\text{POCOP})\text{Co}(\text{Cl})_2$ (618**).** **602** (320 mg, 0.74 mmol) and NCS (98 mg, 0.735 mmol) were combined in a Schlenk flask and dissolved in toluene. The reaction underwent an immediate color change to brown and was stirred at RT for 2 h. The volatiles were removed by vacuum. The product was extracted with pentane and passed through a pad of Celite. The volatiles were removed to yield a brown solid. The solid was recrystallized from a saturated pentane solution at -35 °C to give a crystalline brown solid (250 mg, 72%). X-ray quality crystals of the product were grown from a

saturated toluene solution layered with pentane at -35°C . The compound displayed broad signals outside of the standard diamagnetic range in ^1H NMR spectrum, indicative of a paramagnetic complex. ^1H NMR (C_6D_6 , Figure 6-18): δ 45.77 (bs, 2H), -5.85 (bs, 12H), -7.99 (bs, 12H), -63.22 (bs, 4H). The resonance corresponding to the central proton on the ligand backbone could not be identified and is likely overlapping with one of the other broad signals. Elem. Anal. Calc. for $\text{C}_{18}\text{H}_{31}\text{Cl}_2\text{CoO}_2\text{P}_2$: C, 45.88; H, 6.63. Found: C, 46.26; H, 6.35. The effective magnetic moment was determined to be $2.44 \mu_{\text{B}}$ by Evans method and 2.46 by magnetic susceptibility balance.

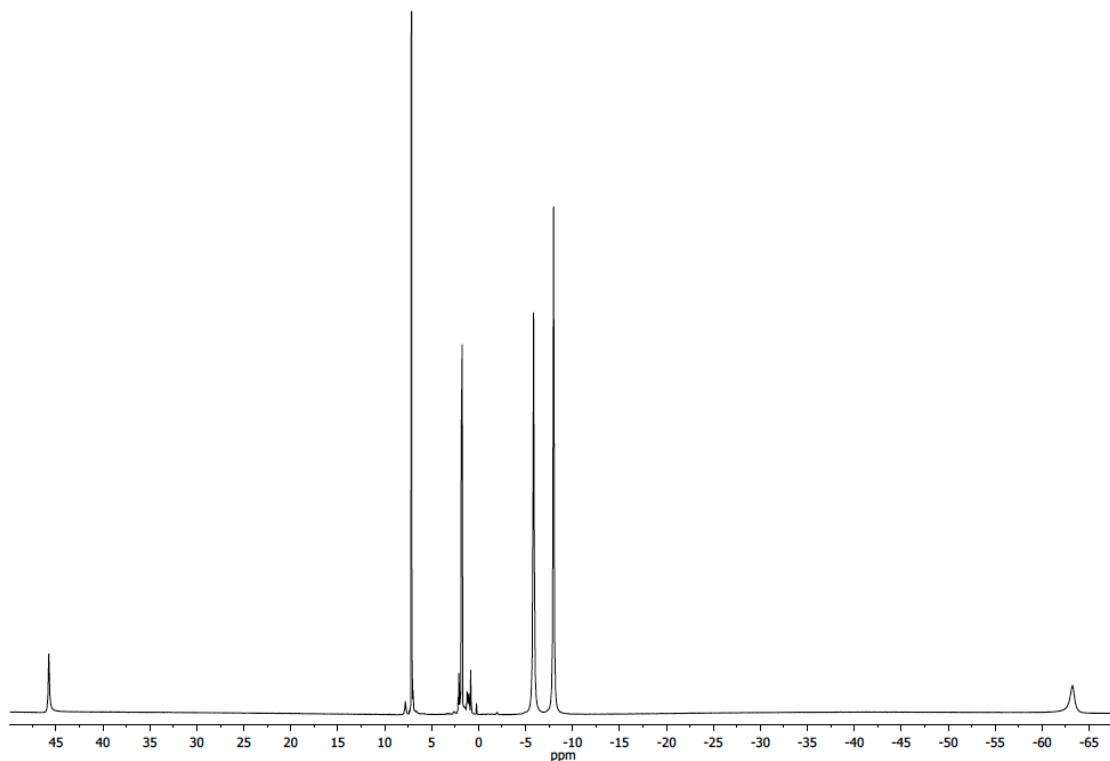


Figure 6-18. ^1H NMR spectrum of $(\text{POCOP})\text{Co}(\text{Cl})_2$ (**618**) in C_6D_6 . Minor residual pentane and toluene present.

Synthesis of (POCOP)Co(Cl)₂(PMe₃) (619). **618** (35 mg, 0.075 mmol) was added to J. Young tube and dissolved in toluene. PMe₃ (7.7 μL, 0.075 mmol) was added to the sample, resulting in an immediate color change from brown to green. After 1 h at RT, the reaction was passed through a pad of Celite and the volatiles were removed by vacuum to give a green solid. The solid was redissolved in C₆D₆ for NMR analysis. ³¹P{¹H} NMR (C₆D₆): δ 178.0 (s), -16.7 (s) (2:1 ratio, respectively); ¹H NMR (C₆D₆, Figure 6-19): δ 7.02 (t, 7.5 Hz, 1H, *Ar*), 6.92 (d, 7.5 Hz, 2H, *Ar*), 3.08 (m, 4H, *CHMe*₂), 1.42 (d, 7.5 Hz, 9H, PMe₃), 1.32 (q, 7.5 Hz, 12H, *CHMe*₂), 1.21 (q, 5.5 Hz, 12H, *CHMe*₂).

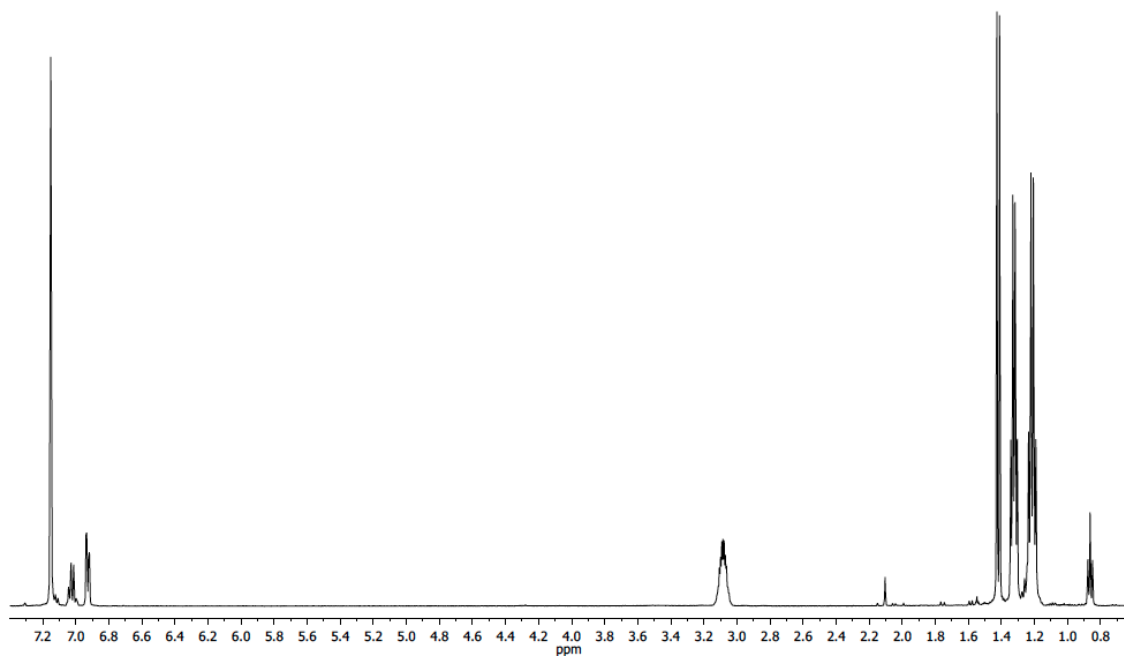


Figure 6-19. ¹H NMR of (POCOP)Co(Cl)₂(PMe₃) (**619**) in C₆D₆. Minor residual pentane and toluene present.

Synthesis of (POCOP)Co(Ph)(Cl) (620). **607** (194 mg, 0.41 mmol) was added to a Schlenk flask and dissolved in pentane. The solution was treated with NCS (58 mg, 0.44 mmol) and stirred at RT for 12 h producing a green-yellow solution. A blue insoluble solid crashed out of the pentane solution and was removed by filtration. The volatiles were removed under vacuum to give a green-yellow solid. The ^1H NMR spectrum of this solid shows paramagnetic signals corresponding to **602** as well as diamagnetic signals corresponding to (POCOP)Co(Ph)(Cl) (**620**). The solid was dissolved in pentane and crystallized at $-35\text{ }^\circ\text{C}$. The recrystallization produced a green crystalline solid and yellow crystalline solid. The yellow solid was determined to be **602** and the green solid was determined to be **620**. Dissolution of the green solid in C_6D_6 showed clean **620** in the ^1H NMR spectrum. After several hours at RT, the same sample showed formation of **602** and biphenyl in addition to **620** in the ^1H NMR spectrum. ^1H NMR (C_6D_6 , Figure 6-20): δ 8.04 (bs, 1H, Ph-*H*), 7.01 (t, 8.5 Hz, 1H, Ar-*H*), 6.69 (d, 8.0 Hz, 2H, Ar-*H*), 6.53 (t, 7.0 Hz, 1H, Ph-*H*), 6.47 (bs, 1H, Ph-*H*), 6.21 (bs, 1H, Ph-*H*), 5.17 (bs, 1H, Ph-*H*), 2.81 (m, 2H, CHMe₂), 2.16 (m, 2H, CHMe₂), 1.21 (q, 7.5 Hz, 6H, CHMe₂), 1.09 (m, 12H CHMe₂), 0.83 (q, 7.5 Hz, 6H, CHMe₂); $^{31}\text{P}\{^1\text{H}\}$ NMR (C_6D_6): δ 176.7 (bs). Unable to obtain $^{13}\text{C}\{^1\text{H}\}$ NMR spectrum or elemental analysis due to the instability of the compound.

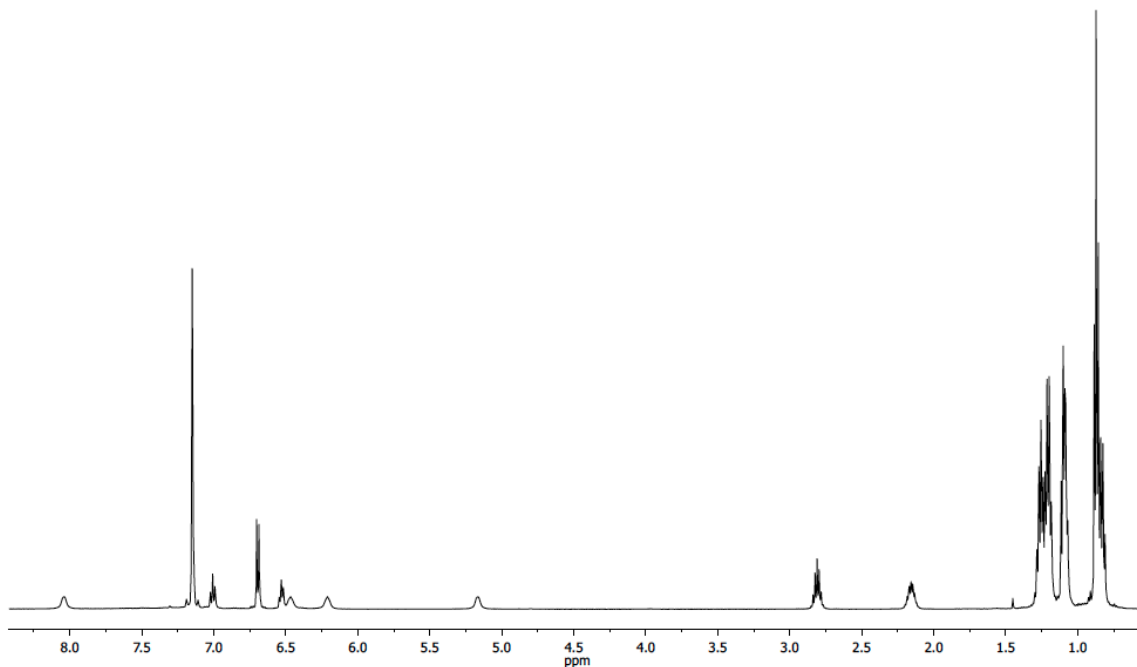


Figure 6-20. ^1H NMR spectrum of $(\text{POCOP})\text{Co}(\text{Ph})(\text{Cl})$ (**620**) in C_6D_6 . Large amount of residual pentane present.

Synthesis of $(\text{POCOP})\text{Co}(\text{Ph})(\text{OAc})$ (621**).** **607** (300 mg, 0.629 mmol) was added to Schlenk flask and dissolved in toluene to give a dark green solution. $\text{PhI}(\text{OAc})_2$ (101 mg, 0.314 mmol) was added to the reaction. The solution quickly became light yellow in color. After stirring overnight at RT, the solution became red in color. The volatiles were removed by vacuum. The product was extracted with pentane and passed through a pad of Celite. The volatiles were removed to give a red-orange solid. The solid was dissolved in a minimum of pentane and left overnight at $-35\text{ }^\circ\text{C}$ to yield a red crystalline solid (270 mg, 80%). ^1H NMR (C_6D_6 , Figure 6-21): δ 8.07 (d, 9.5 Hz, 1H, Ph), 6.99 (t, 6.5 Hz, 1H, Ar), 6.96 (t, 6.5 Hz, 1H, Ph), 6.81 (t, 6.5 Hz, 1H, Ph), 6.68 (d, 6.0 Hz, 2H, Ar), 6.63 (t, 9.5 Hz, 1H, Ph), 5.79 (d, 9.5 Hz, 1H, Ph), 2.58 (bm, 2H,

*CHMe*₂), 1.94 (m, 2H, *CHMe*₂), 1.75 (s, 3H, *CO*₂*Me*), 1.29 (q, 6.5 Hz, 6H, *CHMe*₂), 1.17 (q, 6.5 Hz, 6H, *CHMe*₂), 1.02 (q, 6.5 Hz, 6H, *CHMe*₂), 0.88 (q, 6.5 Hz, 6H, *CHMe*₂); ³¹P{¹H} NMR (C₆D₆): δ 179.3 (bs).

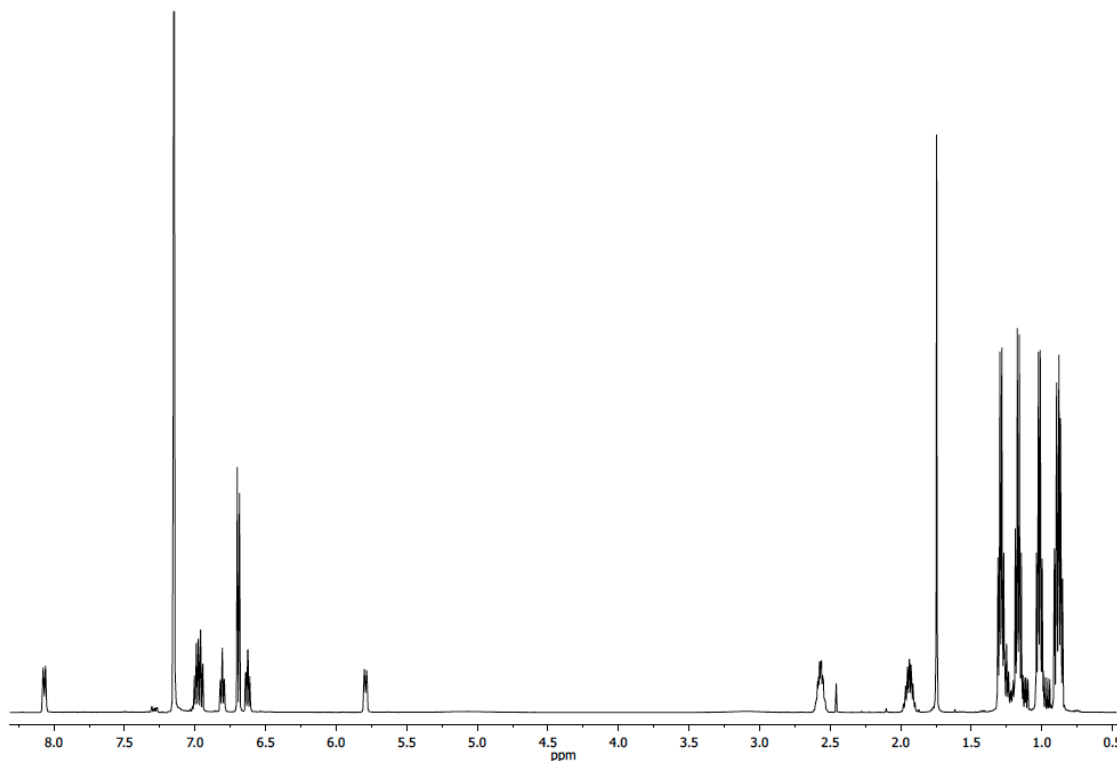


Figure 6-21. ¹H NMR spectrum of (POCOP)Co(Ph)(OAc) (**621**) in C₆D₆. Minor residual pentane and toluene present.

Synthesis of (POCOP)Co(CF₃)(Cl) (622). **613** (330 mg, 0.70 mmol) was added to a Schlenk flask and dissolved in toluene. NCS (99 mg, 0.74 mmol) was added to the solution and the reaction was stirred for 6 h at RT. The reaction was passed through a pad of Celite. The volatiles were removed by vacuum to give a green solid. The solid was recrystallized from a concentrated toluene solution layered with pentane at -35 °C

(170 mg, 48%). ^1H NMR (C_6D_6 , Figure 6-22): δ 6.94 (t, 8.0 Hz, 1H, *Ar*), 6.66 (d, 9.0 Hz, 2H, *Ar*), 2.97 (m, 2H, CHMe_2), 2.38 (m, 2H, CHMe_2), 1.56 (q, 8.0 Hz, 6H, CHMe_2) 1.35 (q, 8.0 Hz, 6H, CHMe_2), 0.98 (q, 8.0 Hz, 6H, CHMe_2), 0.90 (q, 8.0 Hz, 6H, CHMe_2); $^{31}\text{P}\{^1\text{H}\}$ NMR (C_6D_6): δ 181.1 (bs); ^{19}F NMR (C_6D_6): δ 3.9 (t, $J_{\text{P-F}} = 12$ Hz).

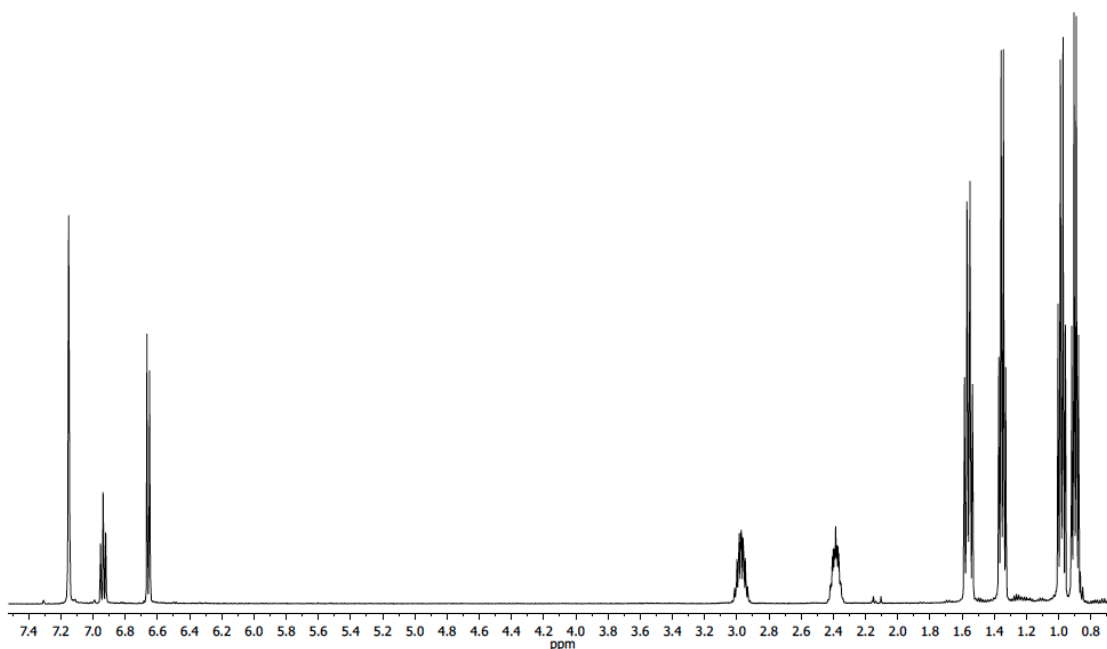


Figure 6-22. ^1H NMR spectrum of $(\text{POCOP})\text{Co}(\text{CF}_3)(\text{Cl})$ (**622**) in C_6D_6 .

Synthesis of $(\text{POCOP})\text{Co}(\text{CF}_3)(\text{OTf})$ (623**).** **622** (13 mg, 0.025 mmol) was added to a J. Young tube and dissolved in C_6D_6 . AgOTf (10 mg, 0.039 mmol) was added to the J. Young tube. No discernible color change occurred. After 1 h at RT, the reaction was passed through a pad of Celite and silica gel. The volatiles were removed to give a green solid (7 mg, 48%). ^1H NMR (C_6D_6 , Figure 6-23): δ 6.84 (t, 7.5 Hz, 1H, *Ar*), 6.50

(d, 8.0 Hz, 2H, *Ar*), 2.88 (m, 2H, *CHMe*₂), 2.50 (m, 2H, *CHMe*₂), 1.38 (q, 7.5 Hz, 6H, *CHMe*₂), 1.32 (q, 7.5 Hz, 6H, *CHMe*₂), 0.85 (q, 7.5 Hz, 6H, *CHMe*₂), 0.66 (q, 7.5 Hz, 6H, *CHMe*₂); ³¹P{¹H} NMR (C₆D₆): δ 184.2 (s); ¹⁹F NMR (C₆D₆): δ 2.5 (t, *J*_{P-F} = 13 Hz, CF₃), -77.8 (s, OTf).

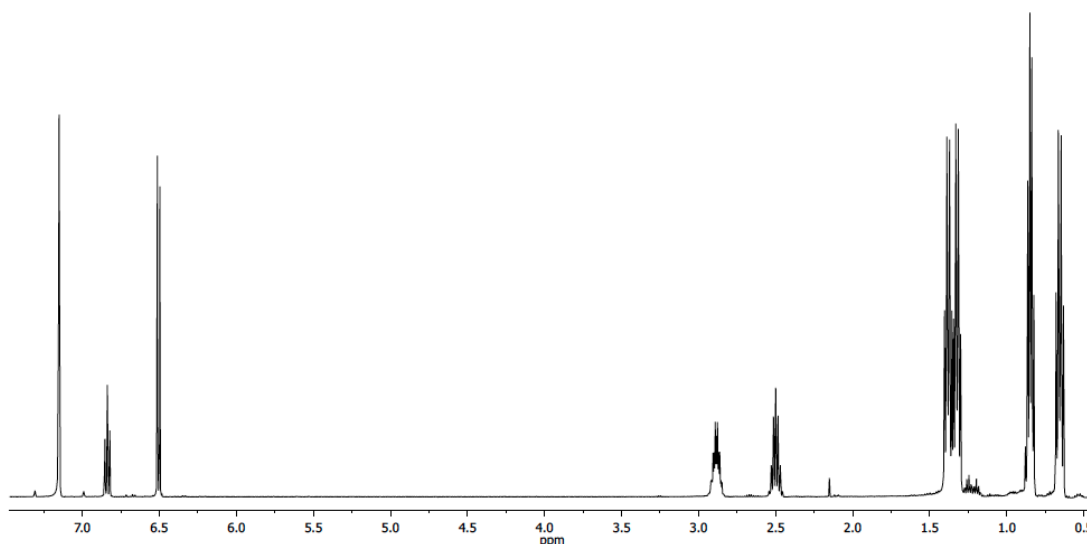


Figure 6-23. ¹H NMR spectrum of (POCOP)Co(CF₃)(OTf) (**623**) in C₆D₆. Minor residual pentane and toluene present.

Reactivity of (POCOP)Co(CF₃)(Cl) (622**) with Grignards and lithium reagents.** (POCOP)Co(CF₃)(Cl) was treated with several lithium reagents (MeLi, ^tBuLi, and PhLi) and PhMgCl. In each of the cases, no reaction occurred. By ¹H, ¹⁹F, ³¹P{¹H} NMR the (POCOP)Co(CF₃)(Cl) remained undisturbed. Heating these samples at temperatures up to 100 °C had no effect.

Reactivity of (POCOP)Co(CF₃)(OTf) (623) with Grignards and lithium reagents. Treatment of (POCOP)Co(CF₃)(OTf) with MeLi, ^tBuLi, and PhLi resulted in no consumption of the (POCOP)Co(CF₃)(OTf). In each of the cases, no reaction occurred by ¹H, ¹⁹F, ³¹P{¹H} NMR spectroscopy. When the (POCOP)Co(CF₃)(OTf) was treated with (CH₂CH)MgCl or (HCC)MgCl, analysis of the ¹H and ³¹P{¹H} NMR spectrum showed complete conversion to (POCOP)Co(CF₃)(Cl).

6.4.3 X-Ray Crystallography

X-Ray data collection, solution, and refinement for (POCOP)Co(BH₄) (616). A single orange crystal of suitable size and quality (0.6 × 0.1 × 0.1 mm) was selected from a representative sample of crystals of the same habit using an optical microscope, mounted onto a nylon loop and placed in a cold stream of nitrogen (110 K). Low-temperature X-ray data were obtained on a Bruker APEXII CCD based diffractometer (Mo sealed X-ray tube, K_α = 0.71073 Å). All diffractometer manipulations, including data collection, integration and scaling were carried out using the Bruker APEXII software.⁸⁸ An absorption correction was applied using SADABS.⁸⁸ The space group was determined on the basis of systematic absences and intensity statistics and the structure was solved by direct methods and refined by full-matrix least squares on F². The structure was solved in the monoclinic P 2₁/c space group using XS⁸⁹ (incorporated in X-Seed). This symmetry was confirmed by PLATON.⁹⁰ With the exception of hydrogen atoms bonded to boron atoms (which were located), all non-hydrogen atoms were refined with anisotropic thermal parameters. Hydrogen atoms were placed in idealized positions and refined using riding model. The structure was refined (weighted

least squares refinement on F^2) to convergence. The check cif report indicates one Level B alert (Hirshfeld Test for atoms C7 – C8). After manual inspection of the thermal ellipsoids, this does not appear to present a problem with the structure.

X-Ray data collection, solution, and refinement for (POCOP)Co(Cl)₂ (618).

A single green crystal of suitable size and quality (0.08 × 0.05 × 0.03 mm) was selected from a representative sample of crystals of the same habit using an optical microscope, mounted onto a nylon loop and placed in a cold stream of nitrogen (110 K). Low-temperature X-ray data were obtained on a Bruker APEXII CCD based diffractometer (Mo sealed X-ray tube, $K_{\alpha} = 0.71073 \text{ \AA}$). All diffractometer manipulations, including data collection, integration and scaling were carried out using the Bruker APEXII software.⁸⁸ An absorption correction was applied using SADABS.⁸⁸ The space group was determined on the basis of systematic absences and intensity statistics and the structure was solved by direct methods and refined by full-matrix least squares on F^2 . The structure was solved in the orthorhombic *Pbca* space group using XS⁸⁹ (incorporated in X-Seed). This symmetry was confirmed by PLATON.⁹⁰ All non-hydrogen atoms were refined with anisotropic thermal parameters. Hydrogen atoms were placed in idealized positions and refined using riding model. The structure was refined (weighted least squares refinement on F^2) to convergence. The check cif report indicates one Level B alert (RINTA01), which is most likely due to the quality of the data or the crystal.

CHAPTER VII

SUMMARY

This dissertation surveyed the stoichiometric and catalytic reactivity of the (POCOP)Rh system related to C-C, C-N, and C-S bond formation. (POCOP)Rh(H)(Cl) (**205**) was demonstrated to be an active precatalyst for C-C, C-N, and C-S coupling reactions with aryl halides with varying degrees of success. For C-C coupling, the coupling of aryl halides with Grignard reagents was fast at RT, but was limited to aryl iodides and Grignard reagents lacking β -hydrogens. The catalytic activity of (POCOP)Rh for the coupling of aryl halides with aryl amines was poor, but formation of the secondary amine products were achieved with both aryl bromides and aryl chlorides. Finally, (POCOP)Rh was very successful for the coupling of aryl halides with thiols. The system was effective for coupling aryl bromides or chlorides with aryl or alkyl thiols, giving high yields and selectivity.

Intermediates involved in the proposed catalytic cycles for C-C, C-N, and C-S coupling were isolated, including Rh(III) aryl/halido complexes and Rh(III) aryl/anilido and aryl/thiolato complexes. Isolation of these complexes allowed for more in depth analysis of the mechanism of the coupling reactions, particularly C-N and C-S coupling. With respect to C-N coupling, the reason for the lack of catalytic function with amines containing β -hydrogens was identified by the stoichiometric formation of Rh(I) imine complexes from reactions with *N*-methylaniline and pyrrolidine. In addition, the kinetics

of C-N RE were analyzed and gave results consistent with first-order RE, the proposed product forming step in Rh catalyzed C-N coupling reactions.

Isolation of a series of (POCOP)Rh aryl/thiolato complexes provided insight into both the steric and electronic properties related to C-S RE from Rh(III). Analogous to Pd systems, more electron-rich Rh thiolates underwent faster reductive elimination ($S^nC_5H_{11}$ vs. SPh). A steric parameter was also established from the decreased rate of reductive coupling from bulky electron donating thiolates compared to less donating sterically unencumbered thiolates (S^tBu vs. $S^nC_5H_{11}$). Aryl chlorides also underwent slower oxidative addition than aryl bromides, consistent with what has been observed with Pd. These results reinforced the observations from the substrate scope of catalytic C-S coupling reactions: increased reactivity with alkyl thiols or aryl bromides and hindered reactivity with sterically demanding aryl thiols.

The propensity for (POCOP)Rh systems to undergo C-F and C-O reductive elimination was also examined; however, neither process was achieved experimentally. Both (POCOP)Rh and (tBu POCOP)Rh suffered from competing lower energy side processes. In the case of (POCOP)Rh, C-C bond formation with the aryl backbone of the ligand was observed, consistent with theoretical predictions. For the (tBu POCOP)Rh system P-F bond formation occurred during the attempted synthesis of Rh(III) vinyl/fluoro complex. The ability for (tBu POCOP)Rh(CHCH₂)(OR) (R = tBu , C₆H₄F) to endure C-O RE elimination was unsuccessful, instead showing decomposition to the divinylacetylene bridged adduct **515**.

Finally, the synthesis and reactivity a series of (POCOP)Co complexes was described. Stable Co(III) complexes were synthesized; however, their reactivity did not provide access to a suitable complex to study RE from Co(III). The (POCOP)Co(Ph)(Cl) complex does provide interesting insight into the potential of this chemistry. This complex appears to be on the border for what is required electronically for a stable Co(III) phenyl/halido complex. It does seem possible that execution with a pincer ligand with a slightly stronger field ligand could provide access to a stable five-coordinate Co(III) phenyl/halido complex and a Co(III) diphenyl complex, which would allow for direct examination of potential C-C RE from Co(III).

REFERENCES

1. de Vries, J. G.; de Vries, A. H. M.; Tucker, C. E.; Miller, J. A. *Innovations Pharm. Technol.* **2001**, *1*, 125.
2. Beller, M.; Zapf, A. Palladium-Catalyzed Coupling Reactions for Industrial Fine Chemical Syntheses In *Handbook of Organopalladium Chemistry for Organic Synthesis*; Negishi, E.-I., Ed.; Wiley: New York, 2002, p 1209.
3. *Handbook of Organopalladium Chemistry for Organic Synthesis*; Negishi, E.-I., Ed.; Wiley: New York, 2002; Vol. 1 & 2.
4. Hartwig, J. F. Cross Coupling In *Organotransition Metal Chemistry: From Bonding to Catalysis*; University Science Books: Sausalito, CA, 2009; Ch. 19.
5. van Leeuwen, P. W. N. M. *Homogeneous Catalysis: Understanding the Art*; Kluwer: Dordrecht, Netherlands, 2004.
6. The Nobel Prize in Chemistry 2010. <http://www.nobelprize.org/> (accessed May 19, 2014).
7. Larsen, R. D.; King, A. O.; Chen, C. Y.; Corley, E. G.; Foster, B. S.; Roberts, F. E.; Yang, C. H.; Lieberman, D. R.; Reamer, R. A.; Tschaen, D. M.; Verhoeven, T. R.; Reider, P. J. *J. Org. Chem.* **1994**, *59*, 6391.
8. Shinkai, I.; King, A. O.; Larsen, R. D. *Pure. Appl. Chem.* **1994**, *66*, 1551.
9. Giordano, C.; Coppi, L.; Minisci, F.; Eur. Pat. Appl.: 1992; Vol. EP 494419.
10. de Vries, J. G. *Can. J. Chem.* **2001**, *79*, 1086.
11. (a) Alsabeh, P. G.; Lundgren, R. J.; McDonald, R.; Johansson Seechurn, C. C. C.; Colacot, T. J.; Stradiotto, M. *Chem. Eur. J.* **2013**, *19*, 2131. (b) Vo, G. D.; Hartwig, J. F. *J. Am. Chem. Soc.* **2009**, *131*, 11049.
12. (a) Lee, H. G.; Milner, P. J.; Buchwald, S. L. *J. Am. Chem. Soc.* **2014**, *136*, 3792. (b) Maimone, T. J.; Milner, P. J.; Kinzel, T.; Zhang, Y.; Takase, M. K.; Buchwald, S. L. *J. Am. Chem. Soc.* **2011**, *133*, 18106. (c) Noël, T.; Maimone, T. J.; Buchwald, S. L. *Angew. Chem. Int. Ed.* **2011**, *50*, 8900. (d) Watson, D. A.; Su, M.; Teverovskiy, G.; Zhang, Y.; Garcia-Fortanet, J.; Kinzel, T.; Buchwald, S. L. *Science* **2009**, *325*, 1661.
13. (a) Ametamey, S. M.; Honer, M.; Schubiger, P. A. *Chem. Rev.* **2008**, *108*, 1501. (b) Lee, E.; Kamlet, A. S.; Powers, D. C.; Neumann, C. N.; Boursalian, G. B.; T., F.;

- Choi, D. C.; Hooker, J. M.; Ritter, T. *Science* **2011**, *334*, 639. (c) Phelps, M. E. *Proc. Natl. Acad. Sci.* **2000**, *97*, 9226.
14. (a) Cho, E. J.; Senecal, T. D.; Kinzel, T.; Zhang, Y.; Watson, D. A.; Buchwald, S. L. *Science* **2010**, *328*, 1679. (b) Fier, P. S.; Hartwig, J. F. *Angew. Chem. Int. Ed.* **2013**, *52*, 2092. (c) Teverovskiy, G.; Surry, D. S.; Buchwald, S. L. *Angew. Chem. Int. Ed.* **2011**, *50*, 7312.
15. McMurry, J. *Organic Chemistry*; 8th ed.; Brooks/Cole: Belmont, CA, 2012; Ch. 19.
16. Rossi, R. A. *Acc. Chem. Res.* **1982**, *15*, 164.
17. Johansson Seechurn, C. C. C.; Kitching, M. O.; Colacot, T. J.; Snieckus, V. *Angew. Chem. Int. Ed.* **2012**, *51*, 5062.
18. Negishi, E.-I.; Fang, L. Palladium- or Nickel-Catalyzed Cross-Coupling with Organometals Containing Zing, Magnesium, Aluminum, and Zirconium In *Metal-Catalyzed Cross-Coupling Reactions*; Diederich, F., Stang, P. J., Eds.; Wiley-VCH: Weinheim, Germany, 1998, p 1.
19. Takahashi, T.; Kanna, K.-I. Nickel-Catalyzed Cross-Coupling Reactions In *Mordern Organonickel Chemistry*; Tamaru, Y., Ed.; Wiley-VCH: Weinheim, Germany, 2005, p 41.
20. (a) Gracias, V.; Iyengar, R. *Chemtracts* **2005**, *18*, 339. (b) Joshi-Pangu, A.; Biscoe, M. R. *Synlett* **2012**, *23*, 1103. (c) Negishi, E.-I. *Acc. Chem. Res.* **1982**, *15*, 340. (d) Wang, Z.-X.; Liu, N. *Eur. J. Inorg. Chem.* **2012**, 901.
21. (a) Beletskaya, I. P.; Cheprakov, A. V. *Coord. Chem. Rev.* **2004**, *248*, 2337. (b) Evana, G.; Blanchard, N.; Toumi, M. *Chem. Rev.* **2008**, *108*, 2054. (c) Thomas, A. W.; Ley, S. V. *Angew. Chem. Int. Ed.* **2003**, *42*, 5400.
22. Monnier, F.; Taillefer, M. *Angew. Chem. Int. Ed.* **2009**, *48*, 6954.
23. (a) Ullman, F. *Dtsch. Chem. Ges.* **1901**, *34*, 2174. (b) Ullman, F. *Dtsch. Chem. Ges.* **1903**, *36*, 2382. (c) Ullman, F. *Dtsch. Chem. Ges.* **1906**, *39*, 1693.
24. Goldberg, I. *Dtsch. Chem. Ges.* **1906**, *39*, 1961.
25. (a) Omar-Amrani, R.; Thomas, A.; Brenner, E.; Schneider, R.; Fort, Y. *Org. Lett.* **2003**, *5*, 2311. (b) Shimasaki, T.; Tobisu, M.; Chatani, N. *Angew. Chem. Int. Ed.* **2010**, *49*, 2929. (c) Wolfe, J. P.; Buchwald, S. L. *J. Am. Chem. Soc.* **1997**, *119*, 6054.

26. (a) Millois, C.; Diaz, P. *Org. Lett.* **2000**, *2*, 1705. (b) Percec, V.; Bae, J.-Y.; Hill, D. H. *J. Org. Chem.* **1995**, *60*, 6895. (c) Taniguchi, N. *J. Org. Chem.* **2004**, *69*, 6904. (d) Zhang, Y.; Ngeow, K. C.; Ying, J. Y. *Org. Lett.* **2007**, *9*, 3495.
27. (a) Lew, S. V.; Thomas, A. W. *Angew. Chem. Int. Ed.* **2003**, *42*, 5400. (b) Surry, D. S.; Buchwald, S. L. *Chem. Sci.* **2010**, *1*, 13.
28. (a) Bates, C. G.; Gujadhur, R. K.; Venkataraman, D. *Org. Lett.* **2002**, *4*, 2803. (b) Kondo, T.; Mitsudo, T.-A. *Chem. Rev.* **2000**, *100*, 3205. (c) Kwong, F. Y.; Buchwald, S. L. *Org. Lett.* **2002**, *4*, 3517.
29. (a) Surry, D. S.; Buchwald, S. L. *Angew. Chem. Int. Ed.* **2008**, *47*, 6338. (b) Wolfe, J. P.; Wagaw, S.; Marcoux, J. F.; Buchwald, S. L. *Acc. Chem. Res.* **1998**, *31*, 805.
30. (a) Hartwig, J. F. *Angew. Chem. Int. Ed.* **1998**, *37*, 2046. (b) Hartwig, J. F. *Nature* **2008**, *455*, 314. (c) Hartwig, J. F. *Acc. Chem. Res.* **2008**, *41*, 1534.
31. (a) Li, G. Y. *Angew. Chem. Int. Ed.* **2001**, *40*, 1513. (b) Murata, M.; Buchwald, S. L. *Tetrahedron* **2004**, *60*, 7397. (c) Schopfer, U.; Schlapbach, A. *Tetrahedron* **2001**, *57*, 3069. (d) Zheng, N.; McWilliams, J. C.; Fleitz, F. J.; Volante, R. P. *J. Org. Chem.* **1998**, *63*, 9606.
32. (a) Fernandez-Rodriguez, M. A.; Shen, Q.; Hartwig, J. F. *Chem. Eur. J.* **2006**, *12*, 7782. (b) Fernandez-Rodriguez, M. A.; Shen, Q.; Hartwig, J. F. *J. Am. Chem. Soc.* **2006**, *128*, 2180.
33. Guram, A. S.; Rennels, R. A.; Buchwald, S. L. *Angew. Chem. Int. Ed.* **1995**, *34*, 1348.
34. Louie, J.; Hartwig, J. F. *Tetrahedron Lett.* **1995**, *36*, 3609.
35. (a) Crawford, S. M.; Lavery, C. B.; Stradiotto, M. *Chem. Eur. J.* **2013**, *19*, 16760. (b) Lundren, R. J.; Hesp, K. D.; Stradiotto, M. *Synlett* **2011**, 2443. (c) Lundren, R. J.; Stradiotto, M. *Aldrichimica Acta* **2012**, *45*, 59.
36. (a) Gilbertson, S. R.; Starkey, G. W. *J. Org. Chem.* **1996**, *61*, 2922. (b) Herd, O.; Hessler, A.; Hingst, M.; Tepper, M.; Stelzer, O. *J. Organomet. Chem.* **1996**, *522*, 69. (c) Vyskocil, S.; Smrcina, M.; Hanus, V.; Polasek, M.; Kocovsky, P. *J. Org. Chem.* **1998**, *63*, 7738.
37. (a) Ding, S.; Gray, N. S.; Wu, X.; Ding, Q.; Schultz, P. G. *J. Am. Chem. Soc.* **2002**, *124*, 1594. (b) Kuwabe, S.; Torraca, K. E.; Buchwald, S. L. *J. Am. Chem. Soc.* **2001**, *123*, 12202. (c) Palucki, M.; Wolfe, J. P.; Buchwald, S. L. *J. Am. Chem. Soc.* **1997**, *119*, 3395. (d) Vorogushin, A. V.; Huang, X. H.; Buchwald, S. L. *J. Am. Chem. Soc.* **2005**, *127*, 8146.

38. Hartwig, J. F. Oxidative Addition In *Organotransition Metal Chemistry: From Bonding to Catalysis*; University Science Books: Sausalito, 2009; Ch. 6.
39. Hartwig, J. F. Reductive Elimination In *Organotransition Metal Chemistry: From Bonding to Catalysis*; University Science Books: Sausalito, 2009; Ch. 8.
40. Crabtree, R. H. *The Organometallic Chemistry of the Transition Metals*; 5th ed.; Wiley: Hoboken, 2005; Ch. 6.
41. (a) Hayashi, T.; Konishi, M.; Kobori, Y.; Kumada, M.; Higuchi, T.; Hirotsu, K. *J. Am. Chem. Soc.* **1984**, *106*, 158. (b) Hayashi, T.; Konishi, M.; Kumada, M. *Tetrahedron Lett.* **1979**, *20*, 1871.
42. (a) Littke, A. F.; Dai, C.; Fu, G. C. *J. Am. Chem. Soc.* **2000**, *122*, 4020. (b) Steffen, W. L.; Palenik, G. J. *Inorg. Chem.* **1976**, *15*, 2432.
43. Grushin, V. V.; Alper, H. *Chem. Rev.* **1994**, *94*, 1047.
44. Littke, A. F.; Fu, G. C. *Angew. Chem. Int. Ed.* **2002**, *41*, 4176.
45. Littke, A. F.; Fu, G. C. *Angew. Chem. Int. Ed.* **1998**, *110*, 3586.
46. Schoenebeck, F.; Houk, K. N. *J. Am. Chem. Soc.* **2010**, *132*, 2496.
47. Dicosimo, R.; Whitesides, G. M. *J. Am. Chem. Soc.* **1982**, *104*, 3601.
48. (a) Driver, M. S.; Hartwig, J. F. *J. Am. Chem. Soc.* **1995**, *117*, 4708. (b) Driver, M. S.; Hartwig, J. F. *J. Am. Chem. Soc.* **1997**, *119*, 8232.
49. Mann, G.; Shelby, Q.; Roy, A. H.; Hartwig, J. F. *Organometallics* **2003**, *22*, 2775.
50. Jones, W. D.; Kuykendall, V. L. *Inorg. Chem.* **1991**, *30*, 2615.
51. (a) Aranyos, A.; Old, D. W.; Kiyomori, A.; Wolfe, J. P.; Sadighi, J. P.; Buchwald, S. L. *J. Am. Chem. Soc.* **1999**, *121*, 4369. (b) Wolfe, J. P.; Buchwald, S. L. *Angew. Chem. Int. Ed.* **1999**, *111*, 2570. (c) Wolfe, J. P.; Singer, R. A.; Yang, B. H.; Buchwald, S. L. *J. Am. Chem. Soc.* **1999**, *121*, 9950.
52. Shelby, Q.; Nataoka, N.; Mann, G.; Hartwig, J. F. *J. Am. Chem. Soc.* **2000**, *122*, 10718.
53. (a) Grasa, G. A.; Viciu, M. S.; Huang, J.; Nolan, S. P. *J. Org. Chem.* **2001**, *66*, 7729. (b) Viciu, M. S.; Kelly III, R. A.; Stevens, E. D.; Naud, F.; Studer, M.; Nolan, S. P. *Org. Lett.* **2003**, *5*, 1479. (c) Viciu, M. S.; Kissling, R. M.; Stevens, E. D.; Nolan, S. P. *Org. Lett.* **2002**, *4*, 2229.

54. Christmann, U.; Vilar, R. *Angew. Chem. Int. Ed.* **2005**, *44*, 366.
55. (a) Dong, J.; Long, Z.; Song, F.; Wu, N.; Guo, Q.; Lan, J.; You, J. *Angew. Chem. Int. Ed.* **2013**, *52*, 580. (b) Qin, X.; Liu, H.; Qin, D.; Wu, Q.; You, J.; Zhao, D.; Guo, Q.; Huang, X. H.; Lan, J. *Chem. Sci.* **2013**, *4*, 1964. (c) Roy, I. D.; Burns, A. R.; Pattison, G.; Michel, B.; Parker, A. J.; Lam, H. W. *Chem. Commun.* **2014**, *50*, 2865. (d) Saxena, A.; Lam, H. W. *Chem. Sci.* **2011**, *2*, 2326. (e) Sezen, B.; Sames, D. *J. Am. Chem. Soc.* **2004**, *126*, 13244. (f) Shintani, R.; Yamagami, T.; Hayashi, T. *Org. Lett.* **2006**, *8*, 4799. (g) Wang, X.; Lane, B. S.; Sames, D. *J. Am. Chem. Soc.* **2005**, *127*, 4996. (h) Zhang, L.; Wu, J. *Adv. Synth. Catal.* **2008**, *350*, 2409.
56. Ueura, K.; Satoh, T.; Miura, M. *Org. Lett.* **2005**, *7*, 2229.
57. Ishiyama, T.; Hartwig, J. F. *J. Am. Chem. Soc.* **2000**, *122*, 12043.
58. Lewis, J. C.; Wiedemann, S. H.; Bergman, R. G.; Ellman, J. A. *Org. Lett.* **2004**, *6*, 35.
59. Yanagisawa, S.; Sudo, T.; Noyori, R.; Itami, K. *J. Am. Chem. Soc.* **2006**, *128*, 11748.
60. Murata, M.; Ishikura, M.; Nagata, M.; Watanabe, S.; Masuda, Y. *Org. Lett.* **2002**, *4*, 1843.
61. Kim, M.; Chang, S. *Org. Lett.* **2010**, *12*, 1640.
62. (a) Abeysekera, A. M.; Grigg, R.; Trocha-Grimshaw, J.; Wiswanatha, V. *J. Chem. Soc., Perkin. Trans.* **1977**, *1*, 1395. (b) Chen, S.; Li, Y.; Zhao, J.; Li, D. *Inorg. Chem.* **2009**, *48*, 1198. (c) Grushin, V. V.; Marshall, W. J. *J. Am. Chem. Soc.* **2004**, *126*, 3068. (d) Hoogervorst, W. J.; Goubitz, K.; Fraanje, J.; Lutz, M.; Spek, A. L.; Ernsting, J. M.; Elsevier, C. J. *Organometallics* **2004**, *23*, 4550. (e) Macgregor, S. A.; Roe, D. C.; Marshal, W. J.; Bloch, K. M.; Bakhmutov, V. I.; Grushin, V. V. *J. Am. Chem. Soc.* **2005**, *127*, 15304. (f) Semmelhack, M. F.; Ryono, L. *Tetrahedron Lett.* **1973**, *31*, 2967.
63. Puri, M.; Gatard, S.; Smith, D. A.; Ozerov, O. V. *Organometallics* **2011**, *30*, 2472.
64. Gatard, S.; Guo, C.; Foxman, B. M.; Ozerov, O. V. *Organometallics* **2007**, *26*, 6066.
65. Gatard, S.; Çelenligil-Çetin, C.; Guo, C.; Foxman, B. M.; Ozerov, O. V. *J. Am. Chem. Soc.* **2006**, *128*, 2808.
66. de Pater, B. C.; Zipp, E. J.; Frühauf, H.-W.; Ernsting, J. M.; Budzelaar, P. H. M.; Gal, A. W. *Organometallics* **2004**, *23*, 269.

67. Willems, S. T. H.; Budzelaar, P. H. M.; Moonen, N. N. P.; de Gelder, R.; Smits, J. M. M.; Gal, A. W. *Chem. Eur. J.* **2002**, *8*, 1310.
68. Douglas, T. M.; Chaplin, A. B.; Weller, A. S. *Organometallics* **2008**, *27*, 2918.
69. (a) Lam, H. W.; Shimada, S.; Batsanov, A. S.; Lin, Z.; Marder, T. B.; Cowan, J. A.; Howard, J. A. K.; Mason, S. A.; McIntyre, G. J. *Organometallics* **2003**, *22*, 4557. (b) Olivan, M.; Eisenstein, O.; Caulton, K. G. *Organometallics* **1997**, *16*, 2227. (c) Rachidi, I. E.-I.; Eisenstein, O.; Jean, Y. *New J. Chem.* **1990**, *14*, 671. (d) Riehl, J.-F.; Jean, Y.; Eisenstein, O.; Pelissier, M. *Organometallics* **1992**, *11*, 729.
70. Morales-Morales, D.; Jensen, C. G. M. *The Chemistry of Pincer Compounds*; Elsevier: Amsterdam, 2007.
71. (a) Roddick, D. M. *Top. Organomet. Chem.* **2013**, *40*, 49. (b) van der Boom, M. E.; Milstein, D. *Chem. Rev.* **2003**, *103*, 1759. (c) van Koten, G. *J. Organomet. Chem.* **2013**, *730*, 156.
72. Nemeš, S.; Jensen, C.; Binamira-Soriaga, E.; Kaska, W. C. *Organometallics* **1983**, *2*, 1442.
73. (a) Gozin, M.; Alzenberg, M.; Liou, S.-Y.; Weisman, A.; Ben-David, Y.; Milstein, D. *Nature* **1994**, *370*, 42. (b) Gozin, M.; Weisman, A.; Ben-David, Y.; Milstein, D. *Nature* **1993**, *364*, 699. (c) Liou, S.-Y.; Gozin, M.; Milstein, D. *J. Chem. Soc., Chem. Commun.* **1995**, 1965. (d) Liou, S.-Y.; Gozin, M.; Milstein, D. *J. Am. Chem. Soc.* **1995**, *117*, 9774.
74. van der Boom, M. E.; Liou, S.-Y.; Ben-David, Y.; Shimon, L. J. W.; Milstein, D. *J. Am. Chem. Soc.* **1998**, *120*, 6531.
75. Salem, H.; Ben-David, Y.; Shimon, L. J. W.; Milstein, D. *Organometallics* **2006**, *25*, 2292.
76. Ghosh, R.; Emge, T. J.; Krogh-Hespersen, K.; Goldman, A. S. *J. Am. Chem. Soc.* **2008**, *130*, 11317.
77. (a) Molnár, Á. *Palladium Catalyzed Coupling Reactions*; Wiley: Somerset, 2013. (b) Tsuji, J. *Palladium Reagents and Catalysts: New Perspectives for the 21st Century*; 2nd ed.; Wiley: New York, 2004.
78. Corbet, J.-P.; Mignani, G. *Chem. Rev.* **2006**, *106*, 2651.
79. Tamao, K. *J. Organomet. Chem.* **2002**, *653*, 23.

80. Liu, W.; Cao, H.; Lei, A. *Angew. Chem. Int. Ed.* **2010**, *49*, 2004.
81. Gatard, S.; Chen, C.-H.; Foxman, B. M.; Ozerov, O. V. *Organometallics* **2008**, *27*, 6257.
82. Weng, W.; Guo, C.; Çelenligil-Çetin, C.; Foxman, B. M.; Ozerov, O. V. *Organometallics* **2008**, *27*, 6257.
83. Salem, H.; Shimon, L. J. W.; Leitus, G.; Weiner, L.; Milstein, D. *Organometallics* **2008**, *27*, 2293.
84. Farugia, L. J. *J. Appl. Cryst.* **1997**, *30*, 565.
85. (a) Heravi, M. M.; Hajiabbasi, P. *Monatsh. Chem.* **2012**, *143*, 1575. (b) Jin, Z.; Gu, X.-P.; Qiu, L.-L.; Wu, G.-P.; Song, H.-B.; Fang, J.-X. *J. Organomet. Chem.* **2011**, *696*, 859. (c) Li, G. Y. *J. Organomet. Chem.* **2002**, *653*, 63. (d) Prim, D.; Campagne, J.-M.; Joseph, D.; Andrioletti, B. *Tetrahedron Lett.* **2002**, *58*, 2041.
86. Morales-Morales, D.; Redon, R.; Yung, C.; Jensen, C. M. *Inorg. Chem. Acta.* **2004**, *357*, 2953.
87. Bedford, R. S.; Hazelwood, S. L.; Norton, P. N.; Hursthouse, M. B. *Dalton Trans.* **2003**, 4164.
88. APEX2, Version 2 User Manual, M86-E01078, Bruker Analytical X-ray Systems, Madison, WI, June 2006.
89. Sheldrick, G. M. *Acta. Cryst.* **2008**, *A64*, 112.
90. Spek, A. L. *Acta. Cryst.* **1990**, *A46*, C34.
91. de Meijere, A.; Diederich, F. *Metal Catalyzed Cross-Coupling Reactions*; Wiley-VCH: New York, 2004; Vol. 1 & 2.
92. Hartwig, J. F. *Acc. Chem. Res.* **1998**, *31*, 852.
93. Ley, S. V.; Thomas, A. W. *Angew. Chem. Int. Ed.* **2003**, *42*, 5400.
94. (a) Huffman, L. M.; Stahl, S. S. *J. Am. Chem. Soc.* **2008**, *130*, 9196. (b) Huffman, L. M.; Stahl, S. S. *Dalton Trans.* **2011**, *40*, 8959.
95. (a) Fors, B. P.; Dooleweerd, K.; Zeng, Q.; Buchwald, S. L. *J. Am. Chem. Soc.* **2009**, *131*, 5766. (b) Fors, B. P.; Watson, D. A.; Biscoe, M. R.; Buchwald, S. L. *J. Am. Chem. Soc.* **2008**, *130*, 13552.

96. (a) Ogata, T.; Hartwig, J. F. *J. Am. Chem. Soc.* **2008**, *130*, 13848. (b) Shen, Q.; Ogata, T.; Hartwig, J. F. *J. Am. Chem. Soc.* **2008**, *130*, 6586.
97. Mann, G.; Hartwig, J. F.; Driver, M. S.; Fernández-Rivas, C. *J. Am. Chem. Soc.* **1998**, *120*, 827.
98. (a) Fan, L.; Foxman, B. M.; Ozerov, O. V. *Organometallics* **2004**, *23*, 326. (b) Liang, L.-C.; Lin, J.-M.; Hung, C.-H. *Organometallics* **2003**, *22*, 3007. (c) Winter, A. M.; Eichele, K.; Mach, H.-G.; Potuznik, S.; Mayer, H. A.; Kaska, W. *C. J. Organomet. Chem.* **2003**, 682, 142.
99. (a) Liang, L.-C. *Coord. Chem. Rev.* **2006**, *250*, 1152. (b) Mindiola, D. J. *Acc. Chem. Res.* **2006**, *39*, 813.
100. Timpa, S. D.; Fafard, C. M.; Herbert, D. E.; Ozerov, O. V. *Dalton Trans.* **2011**, *40*, 5426.
101. (a) Bedford, R. B.; Limmert, M. E. *J. Org. Chem.* **2003**, *68*, 8669. (b) Ito, J.-I.; Miyakawa, T.; Nishiyama, H. *Organometallics* **2008**, *27*, 3312. (c) Yamanoi, Y.; Nishihara, H. *J. Org. Chem.* **2008**, *73*, 6671.
102. Lewis, J. C.; Bergman, R. G.; Ellman, J. A. *Acc. Chem. Res.* **2008**, *41*, 1013.
103. Chapter II of this dissertation.
104. Weng, W.; Guo, C.; Çelenligil-Çetin, C.; Foxman, B. M.; Ozerov, O. V. *Chem. Commun.* **2006**, 197.
105. Choy, S. W. S.; Page, M. J.; Bhadhade, M.; Messerle, B. A. *Organometallics* **2013**, *32*, 4726.
106. Hartwig, J. F. *Inorg. Chem.* **2007**, *46*, 1936.
107. Scalmani, G.; Frisch, M. J. *J. Chem. Phys.* **2010**, *132*, 114110.
108. Zhao, Y.; Truhlar, D. *Theor. Chem. Acc.* **2008**, *119*, 525.
109. Morse, P. M.; Spencer, M. D.; Wilson, S. R.; Girolami, G. S. *Organometallics* **1994**, *13*, 11317.
110. (a) Dvorak, C. A.; Schmitz, W. D.; Poon, D. J.; Pryde, D. C.; Lawson, J. P.; Amos, R. A.; Meyers, A. I. *Angew. Chem. Int. Ed.* **2000**, *39*, 1664. (b) Grand, B. L.; Pignier, C.; Letienne, R.; Cuisiat, F.; Rolland, F.; Mad, A.; Vacher, B. *J. Med. Chem.* **2008**, *51*, 3856. (c) Kemperman, G. J.; Zhu, J.; Klunder, A. J. H.; Zwaneburg, B. *Eur. J. Org. Chem.* **2001**, 1817. (d) Liu, G.; Link, J. T.; Pei, Z.; Reilly, E. B.; Leitza, S.; Nguyen, B.; Marsh, K. C.; Okasinski, G. F.; Geldern, T.

- W. V.; Ormes, M.; Fowler, K.; Gallatin, M. *J. Med. Chem.* **2000**, *43*, 4025. (e) Thomas, G. L.; Spandl, R. J.; Glansdorp, F. G.; Welch, M.; Bender, A.; Cockfield, J.; Lindsay, J. A.; Bryant, C.; Brown, D. F. J.; Loiseleur, O.; Rudyk, H.; Ladlow, M.; Spring, D. R. *Angew. Chem. Int. Ed.* **2008**, *47*, 2808.
111. Cristau, H. J.; Chabaud, B.; Chene, A.; Christol, H. *Synthesis* **1981**, 892.
112. (a) Chang, J.-R.; Chang, S.-L.; Lin, T.-B. *J. Catal.* **1997**, *169*, 338. (b) Paal, Z.; Matussek, K.; Muhler, M. *Appl. Catal. A.* **1997**, *149*, 113.
113. Bastug, G.; Nolan, S. P. *J. Org. Chem.* **2013**, *78*, 9303.
114. Wong, Y.-C.; Jayanth, T. T.; Cheng, C.-H. *Org. Lett.* **2006**, *8*, 5613.
115. Alvaro, E.; Hartwig, J. F. *J. Am. Chem. Soc.* **2009**, *131*, 7858.
116. Arisawa, M.; Suzuki, T.; Ishikawa, T.; Yamaguchi, M. *J. Am. Chem. Soc.* **2008**, *130*, 12214.
117. Ajiki, K.; Hirano, M.; Tanaka, K. *Org. Lett.* **2005**, *7*, 4193.
118. Ozerov, O. V.; Guo, C.; Papkov, V. A.; Foxman, B. M. *J. Am. Chem. Soc.* **2004**, *126*, 4792.
119. Fryzuk, M. D.; MacNeil, P. A. *J. Am. Chem. Soc.* **1981**, *103*, 3592.
120. (a) English, U.; Chandwick, S.; Ruhlandt-Senge, K. *Inorg. Chem.* **1998**, *37*, 283. (b) Jeigel, E.; Bock, H.; Krenzel, V.; Sievert, M. *Acta. Cryst.* **2001**, *C57*, 154.
121. Purser, S.; Moore, P. R.; Swallow, S.; Gouverneur, V. *Chem. Rev.* **2008**, *37*, 320.
122. (a) Jeschke, P. *ChemBioChem* **2004**, *5*, 570. (b) Theodoridis, G. Fluorine-Containing Agrochemicals: An Overview of Recent Developments In *Advances in Fluorine Science*; Alain, T., Ed.; Elsevier: Amsterdam, 2006; Vol. 2; Ch. 2.
123. (a) Okazoe, T. *Proc. Jpn. Acad. Ser. B* **2009**, *85*, 276. (b) Shimizu, M.; Hiyama, T. *Angew. Chem. Int. Ed.* **2005**, *44*, 214.
124. Sanford, G. *J. Fluor. Chem.* **2007**, *128*, 90.
125. (a) Adams, D. J.; Clark, J. H. *Chem. Soc. Rev.* **1999**, *28*, 225. (b) Finger, G. C.; Kruse, C. W. *J. Am. Chem. Soc.* **1956**, *78*, 6034.
126. Pike, V. W.; Aigbirhio, F. I. *J. Chem. Soc., Chem. Commun.* **1995**, 2215.

127. Casitas, A.; Canta, M.; Sola, M.; Costas, M.; Ribas, X. *J. Am. Chem. Soc.* **2011**, *133*, 19386.
128. (a) Furuya, T.; Klein, J. E. M. N.; Ritter, T. *Synthesis* **2010**, 1804. (b) Hollingworth, C.; Gouverneur, V. *Chem. Commun.* **2012**, *48*, 2929.
129. (a) Engle, K. M.; Mei, T.-S.; Wang, X.; Yu, J. *Angew. Chem. Int. Ed.* **2011**, *50*, 1478. (b) Hull, K. L.; Anani, W. Q.; Sanford, M. S. *J. Am. Chem. Soc.* **2006**, *128*, 7134. (c) Liang, T.; Neumann, C. N.; Ritter, T. *Angew. Chem. Int. Ed.* **2013**, *52*, 8214.
130. (a) Kaspi, A. W.; Goldberg, I.; Vigalok, A. *J. Am. Chem. Soc.* **2010**, *132*, 10626. (b) Vigalok, A. *Organometallics* **2011**, *30*, 1275.
131. (a) Katcher, M. H.; Doyle, A. G. *J. Am. Chem. Soc.* **2010**, *132*, 17402. (b) Lee, H. G.; Milner, P. J.; Buchwald, S. L. *Org. Lett.* **2013**, *15*, 5602.
132. (a) Brandt, J. R.; Lee, E.; Boursalian, G. B.; Ritter, T. *Chem. Sci.* **2014**, *5*, 169. (b) Furuya, T.; Benitez, D.; Tkatchouk, E.; Strom, A. E.; Tang, P.; Goddard, W. A.; Ritter, T. *J. Am. Chem. Soc.* **2010**, *132*, 3793.
133. Cui, L.; Saeys, M. *ChemCatChem* **2011**, *3*, 1060.
134. (a) Grushin, V. V. *Chem. Eur. J.* **2002**, *8*, 1007. (b) Grushin, V. V. *Acc. Chem. Res.* **2010**, *43*, 160. (c) Grushin, V. V.; Marshall, W. J. *Organometallics* **2008**, *27*, 4825. (d) Grushin, V. V.; Marshall, W. J. *J. Am. Chem. Soc.* **2009**, *131*, 918.
135. Yandulov, D. V.; Tran, N. T. *J. Am. Chem. Soc.* **2007**, *129*, 1342.
136. (a) Bruno, N. C.; Buchwald, S. L. *Org. Lett.* **2013**, *15*, 2876. (b) Wu, X.; Fors, B. P.; Buchwald, S. L. *Angew. Chem. Int. Ed.* **2011**, *50*, 9943.
137. Hartwig, J. F.; Paul, F. *J. Am. Chem. Soc.* **1995**, *117*, 4708.
138. Weng, W.; Guo, C.; Moura, C.; Yang, L.; Foxman, B. M.; Ozerov, O. V. *Organometallics* **2005**, *24*, 3487.
139. Hartwig, J. F. *Structure and Bonding In Organotransition Metal Chemistry: From Bonding to Catalysis*; University Science Books: Sausalito, 2009; Ch. 1.
140. FRAMBO v. 4.1.05 "Program for Data Collection on Area Detectors" BRUKER-Nonius Inc., 5465 East Cheryl Parkway, Madison, WI 53711-5373 USA.
141. Sheldrick, G. M. "Cell_Now (version 2008/1): Program for Obtaining Unit Cell Constants from Single Crystal Data": University of Göttingen, Germany.

142. APEX2 “Program for Data Collection and Integration on Area Detectors”
BRUKER AXS Inc., 5465 East Cheryl Parkway, Madison, WI 53711-5373 USA.
143. (a) Old, D. W.; Wolfe, J. P.; Buchwald, S. L. *J. Am. Chem. Soc.* **1998**, *120*, 9722.
(b) Trost, B. M.; Vranken, D. L. V.; Bingel, C. *J. Am. Chem. Soc.* **1992**, *114*, 9327.
144. Wu, J.; Zhang, L.; Gao, K. *Eur. J. Org. Chem.* **2006**, 5260.
145. (a) Atienza, C. C. H.; Milsmann, C.; Lobkovsky, E.; Chirik, P. J. *Angew. Chem. Int. Ed.* **2011**, *50*, 8143. (b) Atienza, C. C. H.; Milsmann, C.; Semproni, S. P.; Turner, Z. R.; Chirik, P. J. *Inorg. Chem.* **2013**, *52*, 5403. (c) Bowman, A. C.; Milsmann, C.; Bill, E.; Lobkovsky, E.; Weyhermüller, T.; Wieghardt, K.; Chirik, P. J. *Inorg. Chem.* **2010**, *49*, 6110. (d) Obligacion, J. V.; Chirik, P. J. *J. Am. Chem. Soc.* **2013**, *135*, 19107. (e) Yu, R. P.; Darmon, J. M.; Milsmann, C.; Margulieux, G. W.; Stieber, S. C. E.; DeBeer, S.; Chirik, P. J. *J. Am. Chem. Soc.* **2013**, *135*, 13168.
146. (a) Hulley, E. B.; Wolczanski, P. T.; Lobkovsky, E. B. *J. Am. Chem. Soc.* **2011**, *133*, 18058. (b) Volpe, E. C.; Wolczanski, P. T.; Lobkovsky, E. B. *Organometallics* **2010**, *29*, 364.
147. (a) Amatore, M.; Gosmini, C. *Angew. Chem. Int. Ed.* **2008**, *47*, 2089. (b) Hess, W.; Treutwein, J.; Hilt, G. *Synthesis* **2008**, *22*, 3537. (c) Smith, A. L.; Hardcastle, K. I.; Soper, J. D. *J. Am. Chem. Soc.* **2010**, *132*, 14358.
148. Ingleson, M.; Fan, H.; Pink, M.; Tomaszewski, J.; Caulton, K. G. *J. Am. Chem. Soc.* **2006**, *128*, 1804.
149. Semproni, S. P.; Atienza, C. C. H.; Chirik, P. J. *Chem. Sci.* **2014**, *5*, 1956.
150. Obligacion, J. V.; Semproni, S. P.; Chirik, P. J. *J. Am. Chem. Soc.* **2014**, *136*, 4133.
151. (a) Enthaler, S.; Junge, K.; Beller, M. *Angew. Chem. Int. Ed.* **2008**, *47*, 3317. (b) Hill, D. H.; Parvez, M. A.; Sen, A. *J. Am. Chem. Soc.* **1994**, *116*, 2889. (c) Sherry, B. D.; Fuerstner, A. *Acc. Chem. Res.* **2008**, *41*, 1500. (d) Yamamoto, A.; Ikariya, T. *J. Organomet. Chem.* **1976**, *120*, 257.
152. (a) Dolphin, D. *B12*; John Wiley & Sons: New York, 1982. (b) Toscano, P. J.; Marzilli, L. G. *Prog. Inorg. Chem.* **1984**, *31*, 105.
153. (a) Bresciani-Pahor, N.; Forcolin, M.; Marzilli, L. G.; Randaccio, L.; Summers, M. F.; Toscano, P. J. *Coord. Chem. Rev.* **1985**, *63*, 1. (b) Ng, F. T. T.; Rempel, D. L. *J. Am. Chem. Soc.* **1982**, *104*, 621. (c) Tsou, T.-T.; Loots, M.; Halpern, J. *J. Am. Chem. Soc.* **1982**, *104*, 623.

154. Fryzuk, M. D.; Leznoff, D. B.; Thompson, R. C.; Rettig, S. J. *J. Am. Chem. Soc.* **1998**, *120*, 10126.
155. Xu, H.; Bernskoetter, W. H. *J. Am. Chem. Soc.* **2011**, *133*, 14956.
156. Liebeskind, L. S.; Baysdon, S. L.; South, M. S. *J. Organomet. Chem.* **1980**, *202*, C73.
157. (a) Jaynes, B. S.; Ren, T.; Liu, S.; Lippard, S. J. *J. Am. Chem. Soc.* **1992**, *114*, 9670. (b) Jaynes, B. S.; Ren, T.; Masschelein, A.; Lippard, S. J. *J. Am. Chem. Soc.* **1993**, *115*, 5589.
158. Hebden, T. J.; St. John, A. J.; Gusev, D. G.; Kaminsky, W.; Goldberg, K. I.; Heinekey, D. M. *Angew. Chem. Int. Ed.* **2011**, *50*, 1873.
159. Theofanis, P. L.; Goddard, W. A. *Organometallics* **2011**, *30*, 4941.
160. Denney, M. C.; Pons, V.; Hebden, T. J.; Heinekey, D. M.; Goldberg, K. I. *J. Am. Chem. Soc.* **2006**, *128*, 12048.
161. (a) Godfrey, S. M.; McAuliffe, C. A.; Pritchard, R. G. *J. Chem. Soc., Chem. Commun.* **1994**, 45. (b) McAuliffe, C. A.; Godfrey, S. M.; Mackie, A. G.; Pritchard, R. G. *Angew. Chem. Int. Ed.* **1992**, *31*, 919. (c) van Enkevort, W. K. P.; Hendricks, H. M.; Beurskens, P. T. *Cryst. Struct. Commun.* **1977**, *6*, 531.
162. Cini, R.; Cavaglioni, A. *Inorg. Chem.* **1999**, *38*, 3751.
163. (a) Hughes, R. P. *Adv. Organomet. Chem.* **1990**, *31*, 183. (b) Morrison, J. A. *Adv. Organomet. Chem.* **1993**, *35*, 3398.

APPENDIX A
X-RAY STRUCTURES SUBMITTED TO CAMBRIDGE CRYSTALLOGRAPHIC
DATA CENTER

| <i>Compound #</i> | <i>Compound Name</i> | <i>CCDC #</i> |
|-------------------|------------------------------|---------------|
| 205 | (POCOP)Rh(H)(Cl) | 807206 |
| 221 | (POCOP)Rh(Ph)(I) | 807205 |
| 406 | (POCOP)Rh(Ph)(SPh) | 999151 |
| 407 | (POCOP)Rh(SPh ₂) | 999152 |
| 418 | (POCOP)Rh(H)(SPh) | 999153 |
| 421 | (POCOP)Rh(NaSPh) | 999154 |

Address:

Cambridge Crystallographic Data Centre

12 Union Road

Cambridge

CB2 1EZ

United Kingdom